UNITED STATES DEPARTMENT OF COMMERCE
DANIEL C. ROPER, Secretary
NATIONAL BUREAU OF STANDARDS
Lyman J. Briggs, Director

✦

Journal of Research

of the

National Bureau of Standards

✦

Volume 20, No. 2
February 1938

[Published with approval of the Director of the Budget]

UNITED STATES
GOVERNMENT PRINTING OFFICE
WASHINGTON : 1938

For sale by the Superintendent of Documents, Washington, D. C. - - - - - - Price 25 cents
$2.50 per year on subscription

The prices of the separate Research Papers appearing in this JOURNAL are given on the front cover page. If 100 or more copies of any separate are ordered, a discount of 25 percent is allowed. Those who desire copies of separate Research Papers should send their orders and remittances without delay to the Superintendent of Documents, U. S. Government Printing Office, Washington, D. C. This will aid him to determine the number of copies to be printed for sale. Research Papers are not printed from electrotypes, and usually no more reprints can be had when the first and only printing is exhausted.

U. S. Department of Commerce National Bureau of Standards

RESEARCH PAPER RP1069

Part of Journal of Research of the National Bureau of Standards, Volume 20, February 1938

BROMINE OXIDATION AND MUTAROTATION MEASUREMENTS WITH α-*d*-β-MANNOHEPTOSE AND α-*d*-α-GULOHEPTOSE

By Horace S. Isbell

ABSTRACT

The lead salts of *d*-α-mannoheptonic acid and *d*-β-mannoheptonic acid were made and used for the separation of the corresponding free acids. The gamma lactone of *d*-β-mannoheptonic acid was prepared and reduced with sodium amalgam to give *d*-β-mannoheptose which was separated in the crystalline alpha modification. This new sugar is structurally related to α-*d*-talose and exhibits similar properties. Its mutarotation is complex, consisting in a fast change followed or accompanied by a smaller slow change. The proportions of the constitutents involved in the rapid reaction vary with temperature so that a change in temperature results in a rapid mutarotation. The temperature coefficient for the rapid mutarotation reaction corresponds to that for the rapid mutarotation reactions of galactose, arabinose, talose, ribose, and *d*-β-glucoheptose, whereas the temperature coefficient for the slow change agrees with the temperature coefficients for the mutarotations of glucose, mannose, gulose, and other reactions which consist in the interconversion of the alpha and beta pyranoses. The parallelism between the properties of *d*-talose, *d*-α-guloheptose, and *d*-β-mannoheptose is evidence that the configurations of the five carbon atoms comprising the pyranose ring determine in large measure the composition of the equilibrium solutions of the sugar. Measurements of the rates of oxidation with bromine water show that α-*d*-β-mannoheptose and α-*d*-α-guloheptose are oxidized at rates comparable to that previously found for the oxidation of α-*d*-talose and that the equilibrium solutions contain substantial quantities of rapidly oxidizable material.

CONTENTS

	Page
I. Mutarotation of α-*d*-β-mannoheptose	97
II. Bromine oxidation measurements with *d*-α-guloheptose and *d*-β-mannoheptose	102
III. Experimental details	104
1. Separation of *d*-α-mannoheptonic and *d*-β-mannoheptonic acids	104
2. *d*-β-Mannoheptonic acid	104
3. α-*d*-β-Mannoheptose hydrate	106
4. *d*-α-Mannoheptonic acid	106
5. α-*d*-α-Mannoheptose hydrate	106
6. β-*d*-α-Mannoheptose hydrate	107
IV. General summary	107
V. References	108

I. MUTAROTATION OF α-*d*-β-MANNOHEPTOSE

The mutarotations of many sugars reveal that when the sugar is dissolved in water, at least two fundamentally different reactions occur [1, 2, 3].[1] One of these consists in the interconversion of the

[1] The numbers in brackets throughout this paper relate to the literature citations on page 108.

alpha and beta pyranose modifications, while the other involves labile modifications of unknown structure. The interconversion of the alpha and beta pyranoses occurs relatively slowly and the equilibrium state is not influenced markedly by temperature changes. The other reaction involving the labile modification is more rapid and is characterized by variation of the equilibrium position with temperature [4]. Mutarotation and bromine oxidation measurements [3] with sugars containing the glucose, mannose, and gulose structures show that the equilibrium solutions of these sugars consist almost exclusively of the alpha and beta pyranose modifications. On the other hand, the mutarotation and oxidation measurements [3, 5] with sugars containing the galactose, talose, and idose structures show that the equilibrium solutions of these sugars contain substantial proportions of modifications other than the alpha and beta pyranoses. The changes in optical rotation caused by the formation of the labile constituents in the solutions of galactose, arabinose, and related sugars are small and therefore it is difficult to study these interesting reactions by observations on these readily available sugars. The changes in optical rotation caused by the formation of the labile constituents in solutions of talose are much larger and therefore this sugar is more suitable for use in investigating this subject. However, talose is difficult to prepare [6] and therefore its application is restricted. In a previous paper [7], the author reported the preparation of *d*-α-guloheptose, which has the talose structure and is also suitable for investigating these labile reactions. This sugar, however, is prepared from the synthetic sugar, *d*-gulose, so that its preparation represents a long and tedious process. A second heptose, *d*-β-mannoheptose, containing the talose structure, can be made from mannose. The preparation of this sugar was undertaken with the hope that it would provide a more readily available sugar for the investigation of the character of the labile modification of the sugars and the rapid mutarotation reactions.

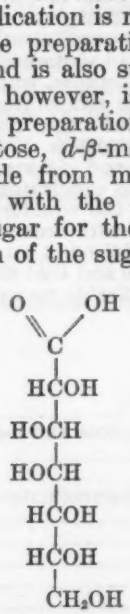

I. *d*-α-Mannoheptonic acid

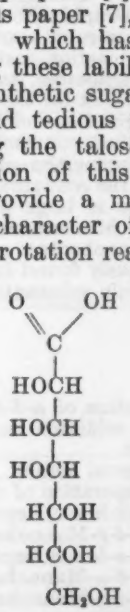

II. *d*-β-Mannoheptonic acid

III. α-d-β-Mannoheptose

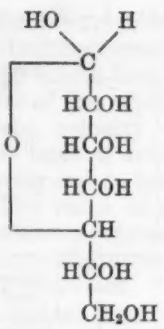

IV. α-d-α-Guloheptose

Application of the cyanhydrin synthesis to mannose [8] gives a large quantity of d-α-mannoheptonic acid, I, and a small quantity of d-β-mannoheptonic acid, II. But since d-α-mannoheptonic acid can be converted to d-β-mannoheptonic acid, by rearrangement in pyridine solution, considerable quantities of d-β-mannoheptonic acid can be prepared without much difficulty. The most tedious part of the process is the separation of the two acids. Several salts of these acids have been studied as a possible means for accomplishing this separation. The purification of d-α-mannoheptonic acid is not laborious because it forms difficultly soluble barium [9] and calcium [10] salts. On the other hand, d-β-mannoheptonic acid forms a difficultly soluble lead salt from which the free acid can be prepared. The free acid forms a crystalline γ-lactone, which, on reduction with sodium amalgam, gives α-d-β-mannoheptose, III. This sugar separates in long, thin, wedge-shaped crystals which melt at 83° C and give $[\alpha]_D^{20}=+45.7$. The analysis reveals that the new sugar is a monohydrate, and since the oxygen ring lies to the right [11] and it is the more dextrorotatory member of the alpha-beta pair, it is designated α-d-β-mannoheptose monohydrate.

When dissolved in water, α-d-β-mannoheptose exhibits the complex mutarotation given in table 1. This mutarotation can be represented by the following equations:

$$[\alpha]_D^{20}=+14.5+8.3\times10^{-.0141t}+22.9\times10^{-.0916t}$$

$$[\alpha]_D^{0.1}=+16.5+9.3\times10^{-.00181t}+19.3\times10^{-.0159t}$$

in which t is the time measured in minutes after the sugar is dissolved in water. The complex mutarotation shows that the equilibrium is established between certain modifications more rapidly than between the others, and that the solution contains at least three modifications of the sugar in dynamic equilibrium. Inspection of the data and equations representing the mutarotation at 20° C reveals that the rapid reaction, m_2, is responsible for a change of 22.9°, whereas the slow reaction, m_1, is responsible for a change of 8.3°. Obviously, the rapid reaction comprises a large part of the mutarotation, in which respect the mutarotation of α-d-β-mannoheptose resembles the mutarotations of the structurally related sugars, α-d-talose [3] and α-d-α-guloheptose [7].

TABLE 1.—*Mutarotation of α-d-β-mannoheptose in distilled water* [1]

0.9981 g in 25 ml at 20.0° C read in a 4-dm tube

$°S = +6.71 + 3.85 \times 10^{-.0141t} + 10.58 \times 10^{-.0916t}$

$[\alpha]_D^{20} = +14.5 + 8.3 \times 10^{-.0141t} + 22.9 \times 10^{-.0916t}$

Initial rotation, $[\alpha]_D^{20} = +45.7$

Equilibrium rotation, $[\alpha]_D^{20} = +14.5$

Time	Observed reading	$(k_1+k_2)\times10^3$	$m_1\times10^3$	Deviation	$m_2\times10^3$
Minutes	°S				
2.55	+16.44			6.18	
5.16	+13.55	58.6		3.58	90.8
7.57	+11.88	54.7		2.16	90.9
9.97	+10.79	50.9		1.29	91.7
13.20	+9.85	46.1		0.63	93.1
19.89	+8.86	37.8		.13	(96.7)
30.10	+8.16	30.0			
41.00	+7.74	25.4	13.7		
50.49	+7.44	23.5	14.6		
60.50	+7.25	21.7	14.1		
75.06	+7.05	20.1	14.0		
93.09	+6.92	18.4	(13.3)		
∞	+6.71				
Average			14.1		91.6

1.013 g in 25.3 ml at 0.1° C in a 4-dm tube

$°S = +7.65 + 4.32 \times 10^{-.0181t} + 8.95 \times 10^{-.0139t}$

$[\alpha]_D^{0.1} = +16.5 + 9.3 \times 10^{-.0181t} + 19.3 \times 10^{-.0139t}$

Initial rotation, $[\alpha]_D^{0.1} = +45.1$

Equilibrium rotation, $[\alpha]_D^{0.1} = +16.5$

3.96	+19.64			7.74	
8.99	+18.21	10.95		6.40	16.4
14.61	+16.93	10.45		5.21	16.1
19.73	+15.99	9.99		4.36	15.8
24.73	+15.21	9.64		3.66	15.7
29.81	+14.52	9.35		3.05	15.6
39.96	+13.41	8.84		2.10	15.7
50.04	+12.62	8.30		1.46	15.7
60.11	+12.00	7.84		0.99	15.9
75.21	+11.37	7.13		.56	16.0
90.64	+10.91	6.53		.30	16.3
147.25	+9.99	4.95			
209.89	+9.45	4.00	1.82		
265.39	+9.09	3.52	1.78		
339.57	+8.69	3.16	1.83		
∞	+7.65				
Average			1.81		15.9

[1] The equations and values for the mutarotation constants, m_1 and m_2, were determined by the method described by Isbell and Pigman, J. Research NBS 18, 156 (1937) RP969. The distilled water contained carbon dioxide and read pH=5.4.

Previous measurements with various sugars have revealed that the temperature coefficients for the interconversion of the alpha and beta

pyranoses are consistently larger than the temperature coefficients for the rapid reactions involving the labile modifications.[2] This is evidence that the heat of activation, Q, for the alpha-beta pyranose interconversion is larger than that characteristic of the rapid reaction. Application of the Arrhenius equation [3] to the velocity constants, m_1 and m_2, of α-d-β-mannoheptose gives for the heat of activation, Q, values of 16,408 and 13,200. These values correspond to temperature coefficients [4] of 2.46 and 2.15, respectively. The value of Q from m_1 is close to the values of Q obtained from the constants representing the interconversion of the alpha and beta modifications of glucose (17,200), mannose (16,900), xylose (16,800), and other pyranoses. The value obtained from m_2 is close to the values obtained from the rapid mutarotations of arabinose (14,700), ribose (11,700), galactose (14,100) talose (12,800), and d-α-guloheptose (12,610). Since the value obtained from m_1 is 16,408, while that from m_2 is only 13,200, the results are in accord with those obtained for other sugars and support the generalization that the heat of activation for the rapid reaction is less than the heat of activation for the slow reaction.

The effect of temperature on the equilibrium state is illustrated further by the thermal mutarotation given in table 2. After a solution of d-β-mannoheptose is cooled, the optical rotation increases in the dextro direction at a rate comparable to that of the rapid reaction (m_2). This increase in optical rotation which comprises the larger part of the mutarotation shows that the change in temperature causes a disturbance in the equilibrium proportions of the labile constituents. This initial equilibrium disturbance is followed by a readjustment of the proportions of the normal alpha and beta isomers which causes a small decrease in the optical rotation. The large alteration in the equilibrium proportions of the labile modifications with temperature, as shown by the thermal mutarotation, shows that the rapid reaction involves a change in energy. This observation is in accord with the generalization that the rapid reactions involving the labile modifications result in the liberation or absorption of heat, whereas the heat of reaction for the interconversion of the alpha and beta pyranoses is small. In this respect the large alteration in the equilibrium proportions of levulose at various temperatures might appear exceptional. It seems probable, however, that the mutarotation of levulose is like the rapid mutarotation reaction of galactose and differs from a normal alpha-beta reversible interconversion.

The mutarotations of α-d-β-mannoheptose, α-d-α-guloheptose, and α-d-talose resemble one another in striking manner and therefore support the generalization that the configurations of the carbon atoms comprising the pyranose ring largely determine the proportions of the various stereomeric modifications in the equilibrium solutions and the rates at which these constituents change from one to another. This similarity, which is obvious by comparing the structural formulas, is responsible in large measure for the similarity in the chemical properties of the structurally related sugars, which will be considered in the next section of this paper.

[1] Page 165 of [3] and page 643 of [7].

[2] $2.3026 \log \frac{k_1}{k_2} = \frac{Q}{1.9864}\left(\frac{1}{T_2} - \frac{1}{T_1}\right)$.

[4] The temperature coefficient is the ratio of the rate at 35° C to that at 25° C and its logarithm equals Q/2,011.

TABLE 2.—*Mutarotation of a 3.3-percent aqueous solution of d-β-mannoheptose after cooling from 25° C to 0.1° C.*

$°S=+0.21\times10^{-.021t}-1.34\times10^{-.013t}+6.29$			
Time	Saccharimeterreading	Deviation	$m_1\times10^3$
Minutes	°S		
3.57	+5.31	−1.18	
6.90	+5.47	−1.02	19.0
9.99	+5.55	−0.94	15.4
15.17	+5.68	−.80	14.6
19.96	+5.79	−.69	14.2
30.30	+5.96	−.51	13.6
40.22	+6.10	−.36	14.1
49.95	+6.18	−.28	14.3
60.05	+6.27	−.18	14.5
151.26	+6.40		
∞	+6.29		
Average			15.0

II. BROMINE OXIDATION MEASUREMENTS WITH *d*-α-GULOHEPTOSE AND *d*-β-MANNOHEPTOSE

Bromine oxidation measurements [3, 5, 12] made with many sugars, under controlled conditions in which the change of one modification to another is slow, have shown that the alpha and beta aldopyranoses are oxidized at widely different rates, and that the rates of oxidation can be correlated with the configuration of the first carbon in relation to the ring oxygen [11]. The aldose sugars (beta) in which the hydrogen of the first carbon is represented, in the conventional manner, as *cis* to the ring oxygen are oxidized more rapidly than the sugars (alpha) in which the hydrogen of the first carbon is represented as *trans* to the ring oxygen. The results given in tables 3 and 4 reveal that the rates of oxidation for the alpha and beta modifications of *d*-α-guloheptose and *d*-β-mannoheptose are in complete agreement with the correlation between the configuration of the first carbon and its rate of oxidation. As might be anticipated from their structures, α-*d*-β-mannoheptose (III) and α-*d*-α-guloheptose (IV) are oxidized at relatively slow rates. The equilibrium solutions of these sugars contain more rapidly oxidizable modifications, which are probably the corresponding beta sugars. The rates of reaction for α-*d*-β-mannoheptose (0.111) and for α-*d*-α-guloheptose (0.094) are comparable to the rate (0.078) previously found for α-*d*-talose. The more easily oxidizable substance in the solution of *d*-β-mannoheptose is oxidized 10 times as fast as the freshly dissolved alpha modification, whereas the more reactive substance in the solution of *d*-α-guloheptose is oxidized 13.6 times as fast as the freshly dissolved alpha form. Presumably the easily oxidizable fractions are largely the beta pyranose modifications, in which respect it is noted that β-*d*-talose is oxidized about 10 times as rapidly as α-*d*-talose and that the equilibrium solution of *d*-talose contains approximately 44 percent of the rapidly oxidizable fraction, whereas the equilibrium solution of *d*-β-mannoheptose contains 38 percent and that of *d*-α-guloheptose 33 percent of the rapidly oxidizable material.

TABLE 3.—*Bromine oxidations of freshly dissolved crystalline sugars at 0°C*[1]

Time after beginning oxidation	Unoxidized sugar	Averages for oxidation period			Velocity constants $ak=\frac{1}{t}\log\frac{A}{A-X}$	
		Bromide (Br)	Bromine (Br_2)	Free bromine (a)	$ak\times10^3$	$k\times10^3$
		α-d-β-MANNOHEPTOSE MONOHYDRATE				
Minutes	mg/ml	*Moles/liter*	*Moles/liter*	*Moles/liter*		
0.5	11.50	0.360	0.380	0.093		
7.5	9.82	.368	.372	.087	9.80	113
15.0	8.36	.374	.366	.084	9.55	114
30.0	6.42	.384	.356	.078	8.58	110
60.0	4.14	.397	.343	.070	7.46	107
Average						111
		α-d-α-GULOHEPTOSE				
0.5	10.29	0.360	0.381	0.094		
7.5	8.87	.367	.374	.088	9.21	105
15.0	7.78	.373	.368	.085	8.37	98
30.0	6.42	.380	.361	.080	6.95	87
60.0	4.31	.393	.348	.073	6.35	87
Average						94.2

[1] Samples of the crystalline sugar (0.01 mole) with 1.2 g of barium carbonate were placed in 100-ml long-neck flasks and cooled to 0°C in an ice bath. To each flask 20 ml of a cold solution containing 60 g of $Ba(Br)_2.2H_2O$, 20 ml of bromine, and 4 ml of *N* hydrobromic acid per liter were added and the mixture was shaken continuously. After definite time intervals the oxidation was stopped by the addition of 5 ml of linseed oil dissolved in 10 ml of benzene, and the reducing sugar in the aqueous solution was determined by the use of alkaline copper sulphate in the usual manner. The bromine (Br_2) in the oxidizing solution was determined by thiosulphate titration, and the concentration of the oxidant (free bromine) and the velocity constants were calculated as described on page 168 of [3].

TABLE 4.—*Bromine oxidations at 0° C in aqueous sugar solutions in equilibrium at the beginning of the oxidation* [1]

Time after mixing solutions	Unoxidized sugar			Averages for the oxidation period			Velocity constants			
	Total	More reactive fraction	Less reactive fraction	Bromide (Br)	Bromine (Br_2)	Free bromine (a)	More reactive fraction		Less reactive fraction	
							$ak_B\times10^3$	$k_B\times10^3$	$ak_A\times10^3$	$k_A\times10^3$
				d-β-MANNOHEPTOSE (HYDRATE)						
Minutes	mg/ml	mg/ml	mg/ml	*Moles/liter*	*Moles/liter*	*Moles/liter*				
0	11.88	4.44	7.44							
.5	11.30	3.95	7.35	0.360	0.386	0.095				
7.5	7.32	0.95	6.37	.379	.367	.083	88.4	1,065		
15.0	5.58	.0	5.58	.388	.358	.077				
15.0	5.58		5.58							
30.0	4.40		4.40	.417	.331	.062			6.87	111
60.0	3.00		3.00	.423	.324	.059			5.99	102
Average								1,065		107

[1] The oxidations were conducted like the oxidations of the freshly dissolved crystalline sugars, except that a solution of the sugar in 10 ml of water was mixed with 10 ml of the oxidation solution adjusted to give the same concentrations of the reactants as those used for the oxidations reported in table 3. The proportions of the more reactive and less reactive fractions were calculated as described on page 177 of [3].

TABLE 4.—*Bromine oxidations at 0° C in aqueous sugar solutions in equilibrium at the beginning of the oxidation*—Continued

Time after mixing solutions	Unoxidized sugar			Averages for the oxidation period			Velocity constants			
	Total	More reactive fraction	Less reactive fraction	Bromide (Br)	Bromine (Br_2)	Free bromine (a)	More reactive fraction		Less reactive fraction	
							$ak_B \times 10^3$	$k_B \times 10^3$	$ak_A \times 10^3$	$k_A \times 10^3$
				d-α-GULOHEPTOSE						
Minutes	*mg/ml*	*mg/ml*	*mg/ml*	*Moles/liter*	*Moles/liter*	*Moles/liter*				
0	11.98	4.05	7.93							
.5	11.37	3.52	7.85	0.360	0.380	0.093				
10.0	7.06	0.43	6.63	.381	.359	.080				
15.0	6.15		6.15	.386	.354	.086	104.3	1,304		
15.0	6.15		6.15							
30.0	4.95		4.95	.412	.328	.062			6.29	101
60.0	3.56		3.56	.421	.321	.058			5.28	91
Average								1,304		96

III. EXPERIMENTAL DETAILS

1. SEPARATION OF *d*-α-MANNOHEPTONIC AND *d*-β-MANNOHEPTONIC ACIDS

The nitriles of *d*-α- and *d*-β-mannoheptonic acids were formed in the usual manner by treating 600 g of mannose in a 10-percent aqueous solution with equivalent quantities of sodium cyanide and calcium chloride [13]. Hydrolysis of the product with an excess of lime gave a precipitate of basic calcium salts which was collected on a filter and washed with limewater. These salts were decomposed by carbonation in a large volume of hot water to give the normal calcium salts. The aqueous solution was evaporated and about 250 g of crystalline calcium *d*-α-mannoheptonate was separated. The residual liquor contained a small quantity of calcium *d*-β-mannoheptonate mixed with calcium *d*-α-mannoheptonate. To separate the constituent acids, the calcium was removed with aqueous sulphuric acid and the resulting heptonic acids were converted to difficultly soluble normal lead salts by reaction with an equivalent quantity of lead oxide. The resulting lead salts were dissolved in hot water and fractionally crystallized in the following manner. The hot aqueous solution of the salts was seeded with lead *d*-α-mannoheptonate and allowed to cool slowly. Considerable lead *d*-α-mannoheptonate separated from the solution in slender needle-like prisms before lead *d*-β-mannoheptonate began to crystallize in rhomb-shaped plates. The needle-like crystals were collected in one fraction and the rhombic plates in another. By repeated fractionation and recrystallization about 50 g of pure lead *d*-β-mannoheptonate and 100 g of lead *d*-α-mannoheptonate were separated from the preparation which began with 600 g of mannose.

2. *d*-β-MANNOHEPTONIC ACID

The preparation of this acid in the crystalline state was reported previously by V. Ettel [14]. It resembles talonic acid in that it is relatively difficultly soluble and crystallizes readily. The acid ob-

tained from lead *d*-β-mannoheptonate by treatment with sulphuric acid was recrystallized from aqueous isopropyl alcohol. The product so obtained is dextrorotatory and exhibits the mutarotation given in table 5. The changes in optical rotation indicate that a dextrorotatory delta lactone and a levorotatory gamma lactone are formed and that the delta lactone is formed more rapidly than the gamma lactone.

TABLE 5.—*Mutarotation of d-β-mannoheptonic acid in 4-percent aqueous solution*

Time	$[\alpha]_D^{20}$	Time	$[\alpha]_D^{20}$
Minutes		*Minutes*	
5	+4.0	240	+6.1
20	+5.4	1,510	−3.2
30	+5.7	2,885	−8.8
60	+6.2	5,765	−17.1
123	+6.7	30 days	−25.0

d-β-Mannoheptonic γ-lactone was prepared by evaporating and heating an aqueous solution of *d*-β-mannoheptonic acid in the presence of a few drops of hydrochloric acid. The resulting thick sirup was dissolved in ethyl alcohol and allowed to stand in a desiccator over sodium hydroxide. Crystallization occurred in the course of several weeks. The crude product was recrystallized from hot absolute ethyl alcohol. The new substance separates in concentric clusters of long, thin crystals which melt at 130° C and give $[\alpha]_D^{20}=-35.7$ The product corresponds to the following analysis: Calculated for $C_7H_{12}O_7$: C, 40.39; H, 5.81. Found: C, 40.45; H, 5.82. The direction of the optical rotation and the rate of hydrolysis as indicated by the slow mutarotation given in table 6 show that the product is the gamma rather than the delta lactone. It is slightly sweet and requires one equivalent of alkali for saponification.

TABLE 6.—*Mutarotation of d-β-mannoheptonic γ-lactone in water at 20° C*

[4.0152 g per 100 ml in a 4-dm tube]

Time	Observed rotation	$[\alpha]_D^{20}$	Time	Observed rotation	$[\alpha]_D^{20}$
Minutes	°S		*Days*	°S	
4.0	−8.29	−35.7	1	−8.10	−34.9
10.1	−8.27	−35.7	3	−7.91	−34.1
20.1	−8.29	−35.7	31	−6.64	−28.6
372.0	−8.25	−35.6	105	−6.48	−27.9

Potassium d-β-mannoheptonate was prepared in aqueous alcoholic solution from equivalent quantities of *d*-β-mannoheptonic acid and potassium hydroxide. The salt gives triangular crystals which form readily and can be used for purification. After drying at 40° C in vacuo the new salt gives $[\alpha]_D^{20}=+0.3$ (in 4-percent aqueous solution) and corresponds to the following analysis: Calculated for $KC_7H_{13}O_8$: C, 31.81; H, 4.96; K, 14.79. Found: C, 32.06; H, 4.97; K, 14.6.

Lead d-β-mannoheptonate was separated from the lead-salt mixture which resulted from the cyanhydrin synthesis. The salt crystallizes in laminated clusters of rhomb-shaped plates which are slightly soluble in hot water and very difficultly soluble in cold water; at 20° C

0.255 g dissolves in 100 ml of water. One gram of the crystals dissolved in 100 ml of hot water and then cooled to 20° C gives $[\alpha]_D^{20}=+2.16$. The salt is anhydrous as shown by the following analysis: Calculated for Pb $(C_7H_{13}O_8)_2$: C, 25.57; H, 3.98; Pb, 31.51. Found: C, 25.7; H, 3.9; Pb, 31.5.

3. *α-d-β*-MANNOHEPTOSE HYDRATE

Fifty grams of *d-β*-mannoheptonic *γ*-lactone was reduced in the usual manner [15] with 1,500 g of 3-percent sodium amalgam, after which an analysis showed the presence of 35 g of sugar. Following the removal of the sodium sulphate and excess *d-β*-mannoheptonate by alcohol precipitation, the reduced solution was concentrated to a thick sirup, which was dissolved in aqueous isopropyl alcohol. After several days, crystals of *α-d-β*-mannoheptose monohydrate formed. The crystals were separated and recrystallized from aqueous isopropyl alcohol. The new sugar separates in long thin wedge-shaped crystals which melt at 83° C and correspond to the following analysis: Calculated for $C_7H_{14}O_7.H_2O$: C, 36.84; H, 7.07. Found: C, 36.9; H, 6.9. The sugar exhibits the complex mutarotation given in table 1. The final specific rotation of the hydrated sugar at 20° C is +14.5 and the initial rotation is +45.7.

The relative copper-reducing value measured with Benedict's solution, using 4 minutes to bring to boiling and boiling 6 minutes, and based on the weight of the anhydrous sugar, is 83 percent of that of glucose. This value is the same as that obtained for the epimeric sugar, *d-α*-mannoheptose, and is close to the values obtained for the structurally related sugars, *d-α*-guloheptose and *d-β*-guloheptose.

A crystalline modification of *d-β*-mannoheptose which melts at 140° C and gives $[\alpha]_D=7.6$ was described by Ettel [14] but unfortunately the physical and chemical properties are not reported in sufficient detail to permit classification of the sugar. Since the optical rotation differs markedly from that of *α-d-β*-mannoheptose, Ettel's product represents either another modification of the sugar or an entirely different substance.

4. *d-α*-MANNOHEPTONIC ACID

This acid has been investigated by previous workers [9,10,15] who prepared the crystalline acid, its gamma lactone, and the sodium, ammonium, calcium, barium, strontium, and cadmium salts. The lead and potassium salts are reported in this paper. *Lead d-α-mannoheptonate* crystallizes in slender prisms which are slightly soluble in hot water and difficultly soluble in cold water; at 20° C 0.046 g dissolves in 100 ml of water. The air-dried salt contains one molecule of water of crystallization and corresponds to the following analysis: Calculated for $Pb(C_7H_{13}O_8)_2.H_2O$: C, 24.89; H, 4.18; Pb, 30.67. Found: C, 25.2; H, 4.3; Pb, 30.65. *Potassium d-α-mannoheptonate* crystallizes in needles which are very soluble in water and give $[\alpha]_D^{20}=+5.4$ in 4-percent aqueous solution. The salt corresponds to the following analysis: Calculated for $KC_7H_{13}O_8$: C, 31.81; H, 4.96; K, 14.79. Found: C, 31.64; H, 5.08; K, 14.7.

5. *α-d-α*-MANNOHEPTOSE HYDRATE

Crude *d-α*-mannoheptose prepared by the method of Fischer and Passmore [15] was recrystallized in the following manner: An aqueous

solution containing 50 g of sugar was dehydrated by evaporation to a thick sirup followed by the addition of absolute alcohol and a second evaporation. The residue was taken up in absolute alcohol and brought to crystallization. The product which was probably the anhydrous alpha form melted at 140° C. On recrystallization from cold aqueous alcohol this product was converted to a monohydrate which melts at 107° C and gave the following analysis: Calculated for $C_7H_{14}O_7.H_2O$: C, 36.84; H, 7.07. Found: C, 36.96; H, 7.26. As reported on page 517 of reference [5], the mutarotation at 20° C is represented by the following equation: $[\alpha]_D^{20} = +3.4 \times 10^{-.0485t} + 51.9 \times 10^{-.00391t} + 64.7$.

6. β-d-α-MANNOHEPTOSE HYDRATE

This sugar was prepared in the following manner: Sixty grams of crude *d*-α-mannoheptose was dissolved in 40 ml of hot water. After the lapse of sufficient time for the sugar to reach equilibrium the solution was filtered and mixed with 200 ml of acetic acid. Upon cooling, rectangular prismatic crystals of β-*d*-α-mannoheptose hydrate separated. The new sugar melts at 104° C and corresponds to the following analysis: Calculated for $C_7H_{14}O_7.H_2O$: C, 36.84; H, 7.07. Found: C, 37.04; H, 7.19. The final specific rotation at 20° C is +64.5 and the initial rotation is +42.3. The mutarotation at 20° C and bromine-oxidation measurements were reported previously [5].

IV. GENERAL SUMMARY

By treating mannose with sodium cyanide followed by lime, basic calcium salts of the epimeric mannoheptonic acids were precipitated. Decomposition of the basic salts by treatment with carbon dioxide gave a mixture of the normal salts from which crystalline calcium *d*-α-mannoheptonate was separated. The salts in the mother liquor were converted to lead salts which were separated by fractional crystallization. *Lead d-α-mannoheptonate*, $Pb(C_7H_{13}O_8)_2.H_2O$, forms slender prisms which are very difficultly soluble in water. *Potassium d-α-mannoheptonate*, $KC_7H_{13}O_8$, crystallizes in needles which are very soluble in water and gives $[\alpha]_D^{20} = +5.4$ in 4-percent aqueous solution. *Lead d-β-mannoheptonate*, $Pb(C_7H_{13}O_8)_2$, crystallizes in rhomb-shaped plates which give $[\alpha]_D^{20} = +2.16$ in 1-percent aqueous solution. *Potassium d-β-mannoheptonate*, $KC_7H_{13}O_8$, crystallizes in triangular plates which give $[\alpha]_D^{20} = +0.3$. *d-β-Mannoheptonic* γ-lactone, $C_7H_{12}O_7$, forms long thin crystals which melt at 130°C and give $[\alpha]_D^{20} = -35.7$. Reduction of *d*-β-mannoheptonic γ-lactone gives α-*d*-β-mannoheptose hydrate, $C_7H_{14}O_7.H_2O$, which melts at 83°C and gives $[\alpha]_D^{20} = +45.7$ with mutarotation. The mutarotations at 20° and 0.1°C are represented by the following equations:

$$[\alpha]_D^{20} = +14.5 + 8.3 \times 10^{-.0141t} + 22.9 \times 10^{-.0916t}$$

$$[\alpha]_D^{1} = +16.5 + 9.3 \times 10^{-.00181t} + 19.3 \times 10^{-.0159t}$$

The mutarotation, which resembles that of α-*d*-talose, reveals a fast and a slow reaction. The proportions of the constituents involved in the fast reaction vary with temperature so that the equilibrium rotation also varies with temperature. The temperature coefficient for the rapid reaction corresponds with the coefficients previously obtained for the rapid reactions found in other complex mutarota-

tions and for the mutarotation of levulose, whereas the temperature coefficient for the slow reaction corresponds with the values previously obtained for the reversible interconversion of the alpha and beta pyranoses.

Bromine oxidations of α-*d*-α-guloheptose and of α-*d*-β-mannoheptose take place slowly at rates comparable to the oxidation of α-*d*-talose. The oxidations of equilibrium solutions of the sugars proceed rapidly until a portion of the sugar is used up and then more slowly as the remaining sugar continues to be oxidized. The results show that equilibrium solution of *d*-α-guloheptose contains 33 percent of some substance which is oxidized about 13.6 times as fast as α-*d*-α-guloheptose; and that the equilibrium solution of *d*-β-mannoheptose contains 38 percent of some substance which is oxidized about 10 times as fast as α-*d*-β-mannoheptose

The marked resemblance of α-*d*-α-guloheptose and α-*d*-β-mannoheptose to α-*d*-talose and other alpha sugars illustrates clearly the advantages of classifying the alpha and beta sugars according to the configuration of the first carbon in relation to the pyranose ring. The results furnish additional evidence to show that the configurations of the five carbon atoms comprising the pyranose ring determine in large measure the peculiarities found in the mutarotations of sugars which contain the galactose, talose, and idose structures.

The author expresses his appreciation to Clement J. Rodden of this Bureau who made the microanalyses, and to William A. Stanton and Robert E. Barnett, student assistants, who prepared the mannoheptonic acids and assisted in the preparation of the sugars.

V. REFERENCES

[1] C. N. Riiber and J. Minsaas. Ber. deut. chem. Ges. **59,** 2266 (1926).
[2] G. F. Smith and T. M. Lowry. J. Chem. Soc. **1928,** 666.
[3] H. S. Isbell and W. W. Pigman. J. Research NBS **18,** 141 (1937) RP969.
[4] H. S. Isbell and W. W. Pigman. J. Research NBS **16,** 553 (1936) RP892.
[5] H. S. Isbell. J. Research NBS **18,** 505 (1937) RP990.
[6] W. W. Pigman and H. S. Isbell. J. Research NBS **19,** 189 (1937) RP1021.
[7] H. S. Isbell. J. Research NBS **19,** 639 (1937) RP1052.
[8] G. Pierce. J. Biol. Chem. **23,** 333 (1916).
[9] E. Fischer and J. Hirshberger. Ber. deut. chem. Ges. **22,** 370 (1889).
[10] G. Hartmann. Liebigs Ann. Chem. **272,** 190 (1892).
[11] H. S. Isbell. J. Chem. Education **12,** 96 (1935).
[12] H. S. Isbell and W. W. Pigman. BS J. Research **10,** 337 (1933) RP534.
[13] C. S. Hudson, O. Hartley, and C. B. Purves. J. Am. Chem. Soc. **56,** 1248 (1934).
[14] V. Ettel. Collection Czechoslov. Chem. Communications **4,** 504 (1932).
[15] E. Fischer and F. Passmore. Ber. deut. chem. Ges. **23,** 2226 (1890).

WASHINGTON, December 17, 1937.

U. S. DEPARTMENT OF COMMERCE NATIONAL BUREAU OF STANDARDS

RESEARCH PAPER RP1070

Part of Journal of Research of the National Bureau of Standards, Volume 20, February 1938

SOME EXPERIMENTS AT RADIO FREQUENCIES ON SUPERCONDUCTORS

By Francis B. Silsbee, Ferdinand G. Brickwedde, and Russell B. Scott

ABSTRACT

Measurements were made in the temperature range 2.5 to 4.2° K on wires of tin and of tantalum. A tin wire in the superconducting transition range carrying an alternating current of frequency 200,000 c/s (cycles per second) superposed on a direct current was found to exhibit a potential drop having a strong component of double the applied frequency. This indicates that the superconducting state can be destroyed by a magnetic field and re-created in a time interval of less than 10^{-6} sec. For each substance the transition temperature from the normal resisting to the superconducting state was found to be the same for alternating currents of radio frequency as for direct currents. The effective resistance of the specimens when below their transition temperatures was found to be too small to detect at radio frequencies by the calorimetric and electrical methods tried (i. e., less than 4 percent of that above the transition temperature in the case of tin and less than 1 percent in the case of tantalum).

CONTENTS

	Page
I. Introduction	109
II. Time required for the establishment and destruction of the superconducting state	110
III. Transition temperature	116
IV. Microresidual resistance	120
V. Conclusions	123

I. INTRODUCTION

Since our communication in 1931[1] reporting on some experiments on the superconductivity of tin for alternating currents, we have carried on intermittently, as other work permitted, a series of experiments comparing for alternating and for direct currents the performances of the superconductors tin and tantalum in the form of solid wires. Three different phases of the problem were investigated: (1) the time required for the establishment and for the destruction of the superconducting state by changes in the magnetic field; (2) the relation between the temperatures at which the superconducting transition occurs for high-frequency current and for direct current; and (3) the resistance to the flow of high-frequency currents at temperatures below the transition.

[1] Silsbee, Scott, Cook, and Brickwedde. Phys. Rev. **39**, 379 (1932).

The tin specimens were made from NBS Standard Sample material, 99.99 percent pure, which was extruded at an elevated temperature into wire 0.022 cm in diameter. The tantalum wire, 0.0075 cm diameter, was in the hard-drawn condition as purchased from the Fansteel Co. Spectrochemical analysis of the tantalum showed only small amounts of Sn and Si (not over a few tenths percent) and traces of Fe, Ca, Al, and Cb. This tantalum showed an abnormally high resistance (0.26 times its resistance at 0° C) at 4.0° K and a low transition temperature, 3.94° K, as compared with 4.4° K for the tantalum reported by Meissner.[2] The variation of the critical magnetic field with temperature (dH_c/dT) was 150 oersteds [3] per degree for the tin and 1,250 oersteds per degree for the tantalum. This high value of dH_c/dT for tantalum and its comparatively large R/R_0 at low temperatures would class our specimen, like many alloys, in the category of anomalous superconductors. It was also found, as seems to be a characteristic of alloys, that the magnetic field produced at the surface of the wire by the critical current is much smaller than the critical value of an externally applied magnetic field, the magnetic field of the critical current for the alloy being of the same order as the critical magnetic field for pure metals. The magnetic field of the critical current was found to increase at a rate of only 50 oersteds per degree as the temperature was decreased.

The specimens were formed by winding the wire bifilarly on glass or paper forms, and were provided with current and potential terminals at both ends. The d-c resistances of the two tin and one tantalum specimens, on which most of the data were obtained, were 65, 15, and 95 ohms, respectively, at room temperature, and 0.06, 0.012, and 25 ohms, respectively, at 4.0° K. For small currents, the transition temperatures were 3.738 and 3.961° K for the tin and tantalum specimens, respectively. The temperature at which the resistivity of a specimen is half its value in the normal resisting state was taken as its transition temperature. Temperatures were calculated from the observed vapor pressures of the liquid-helium bath in which the specimens were immersed, using the vapor-pressure equation reported by Keesom, Weber, and Norgaard.[4] In the range of temperatures of this investigation, a change in temperature of 0.001° K corresponds to a change in the vapor pressure of helium of about 0.5 mm of Hg.

II. TIME REQUIRED FOR THE ESTABLISHMENT AND DESTRUCTION OF THE SUPERCONDUCTING STATE

The fact that a conductor in the superconducting state offers no measurable resistance to a high-frequency alternating current affords no direct evidence that the times required for the establishment and destruction of the superconducting state are short. With the aid of high-frequency currents, however, it is possible to investigate this question.

Suppose a specimen is subjected to a rapidly pulsating magnetic field, such as might be produced by the superposition of a direct and an alternating component; suppose the magnitudes are such that at

[2] Z. Physik 61, 191 (1930).

[3] In accordance with the formal action of the International Electrotechnical Commission in 1930 and of the International Union of Pure and Applied Physics in 1932, we here use the name "oersted" for the cgs unit of magnetic-field intensity in place of the name "gauss," which is still frequently used for both this unit and that of magnetic-flux density.

[4] Keesom, Weber, and Norgaard. Leiden Communication 202b (1929).

sustained values of the field equal to the maxima, the specimen has normal resistance; but suppose the temperature is such that in the continued absence of the field, the specimen is superconducting. If, now, the time required for the establishment or for the destruction of the superconducting state is long as compared with the period of the pulsations, the specimen would be expected to have a nearly constant resistance. If the times required are short, the specimen would oscillate between the superconducting and normal resisting conditions with each cycle of the pulsation. Let, now, a single-frequency alternating current, synchronous and in phase with the alternating component of the magnetic field, be sent through the specimen. If then, the times required for the establishment and destruction of the superconducting state are short, the wave form of the (IR) potential drop across the specimen will differ from the simple sine-form of the current and have a strong double-frequency component. Such a distortion of wave form would not be expected if the time required for the establishment or the destruction of the superconducting state were long as compared with the period of the pulsations.

The requisite conditions were met most simply by superposing direct and alternating currents of appropriate values in a wire of circular cross section. For any particular value of the direct current there is a range of temperatures in which the magnetic field of the direct current at the surface of the wire is only slightly less than the magnetic field of the critical current for the specimen. If a sufficient alternating current is superposed, then during most of one-half of the cycle when the fields are aiding, the total field in the outer regions of the wire exceeds the critical value and, if the material can follow the pulsations, it has resistance. During the other half of the cycle, when the fields are opposing, the total field is less than the critical value and the resistance is zero. The potential difference at the terminals of a wire having such a cyclically varying resistance and being traversed by a single-frequency alternating current would be expected to have a component of double the fundamental frequency. It may be noted that by reason of the skin effect the high-frequency current is confined to the outer regions of the wire.

A double-frequency component originating in the way described can be distinguished from spurious effects, such as harmonics in the current source, by the following criteria: (1) When the temperature is so low that the magnetic field is less than the critical magnetic field, even at that crest of the a-c wave which adds to the direct current, the expected double-frequency component should be absent; (2) when as a result of either (a) high temperature or (b) high direct current, the magnetic field is greater than the critical magnetic field even at the crest of the a-c wave that is opposed to the direct current, the double-frequency component should be absent; and (3) when the direct current is zero, and the crest value of the magnetic field of the alternating current exceeds the critical value, the wave form of the (IR)-potential drop, while distorted, should be symmetrical and, hence, contain only odd harmonics so that the double-frequency component would not be observed.

The experimental arrangement shown in figure 1 was used. Specimen S was supplied with direct current from battery B through ammeter A_0 and adjustable rheostat R_0. The d-c potential across the

ends of the specimen was measured by the deflection of the galvanometer G_0, which was connected to the potential leads at the ends of the specimen. This galvanometer, G_0, was calibrated with a potentiometer not shown in the figure. The radio-frequency oscillator was coupled magnetically with coil L_1, and induced the main alternating current through the circuit $L_1R_1A_1SC_1$. The detecting circuit L_2C_2S was connected to the potential leads and tuned to double the oscillator frequency. To still further reduce the fundamental current flowing in L_2C_2, the auxiliary circuit $L'C'R'M$, tuned to the oscillator frequency, was provided and so adjusted as to insert at M an emf

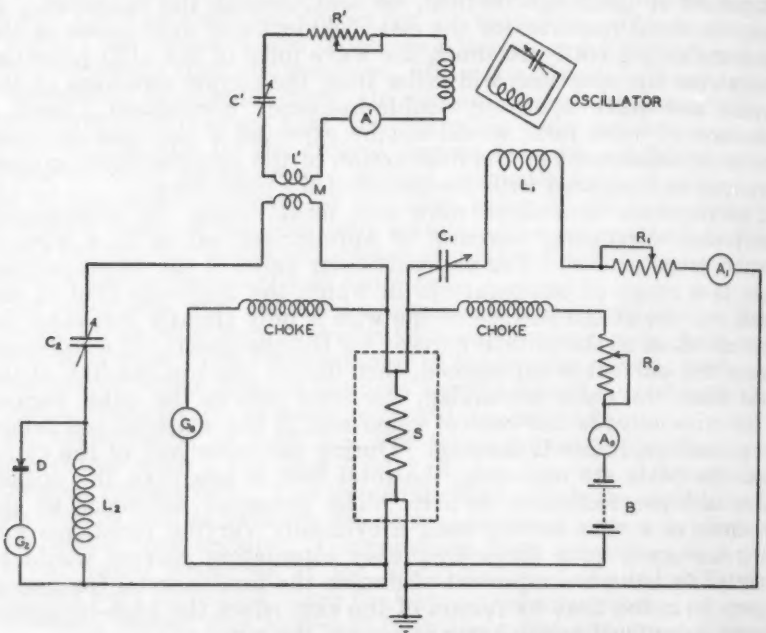

FIGURE 1.—*Circuits used to detect pulsation in resistance.*

S, tin specimen; *B*, battery supplying d-c component of current; $L_1R_1A_1C_1$, tuned circuit supplying a-c component of current; L_2C_2, detecting circuit tuned to double frequency; $L'C'R'A'$, circuit compensating fundamental frequency; and *D*, crystal detector.

opposed as closely as possible in magnitude and phase to the fundamental component of the potential drop in the specimen. The crystal detector D, with galvanometer G_2, indicates the potential drop in coil L_2. To correlate this with the double-frequency component of potential drop in S, the detector was calibrated roughly by adjusting the oscillator to give double frequency and noting the deflection for known values of M and of current in A', the main circuit through L_1C_1 being opened.

With these circuits, observations were made at 200 and 290 kc/s on the 65-ohm tin specimen. The procedure for any one measurement was to hold the temperature as constant as possible, and for given values of direct and alternating current, as read by milliammeters A_0 and A_1, respectively, to tune circuit L_2C_2 by adjustment of condenser C_2 until a maximum deflection of G_2 was obtained. This reading was recorded and also the readings when C_2 was thrown off on each side

sufficiently to destroy the tuning and yield a reading which was almost independent of the setting of C_2. This false zero arose, presumably, from lack of perfect neutralization of the fundamental component of the drop by the auxiliary emf of M.

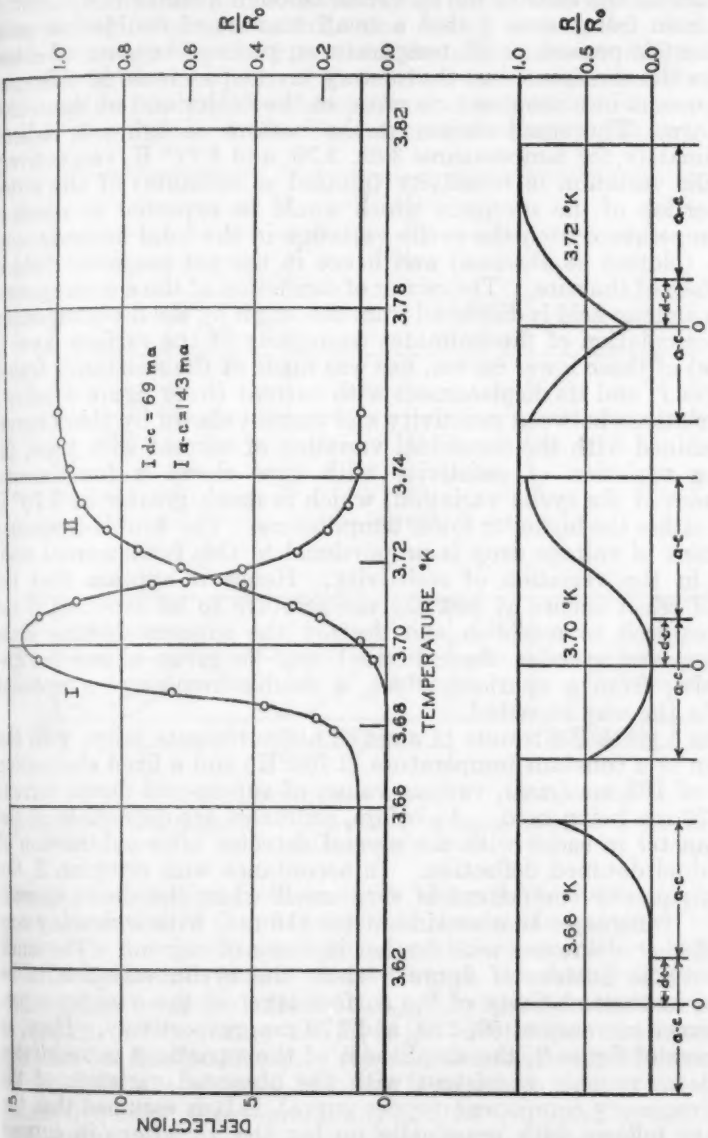

FIGURE 2.—*Double-frequency component of potential drop as a function of temperature.*

Figure 2 gives the results of a typical set of measurements made at a succession of different temperatures held constant during each measurement, the superposed direct and alternating currents being the same for the entire set. The values plotted in figure 2 are for a run in which the direct current was 69 ma, and the root-mean-square value of the alternating current 143 ma and its frequency 200 kc/s.

The ordinates of curve *I* are the deflections of the galvanometer in series with the crystal detector after subtraction of the residual detuned deflection. Curve *II* is the d-c resistance transition curve derived from the simultaneous deflections of the galvanometer connected across the ends of the specimen through a choke coil.

It is seen from curve *I* that a small amount of double-frequency component is present at all temperatures, perhaps because of a harmonic in the oscillator, but that a very marked increase in this component occurs in a temperature range at the colder end of the transition range. The small curves at the bottom of figure 2 indicate approximately, for temperatures 3.68, 3.70, and 3.72° K, respectively, the cyclic variation in resistivity (plotted as ordinate) of the outermost portion of the specimen which would be expected to result at each temperature from the cyclic variation in the total instantaneous current (plotted as abscissa) and hence in the net magnetic field at the surface of the wire. The center of oscillation of the a-c component of the magnetic field is displaced from the origin by the d-c component. In the calculation of the ordinates (resistivity of the surface layer of the wire) of these lower curves, use was made of the resistance transition curve *II* and its displacement with current (from figure 5 below). If the relations between resistivity and current shown by these curves are combined with the sinusoidal variation of current with time, the resulting variation of resistivity with time shows a fundamental component of the cyclic variation, which is much greater at 3.70° K than at either the higher or lower temperature. The double-frequency component of voltage drop is proportional to this fundamental component in the variation of resistivity. Hence it appears that the observed effect occurs at just the temperature to be expected if the times required to establish and destroy the superconducting state are short, and satisfies the criteria 1 and 2a given above for distinguishing from a spurious effect, a double-frequency component arising in the way expected.

Figure 3 gives the results of a set of measurements taken with the specimen at a constant temperature (3.706°K) and a fixed alternating current of 102 ma (rms), various values of superposed direct current up to 170 ma being used. As before, ordinates are deflections of the galvanometer in series with the crystal detector after subtraction of the residual detuned deflection. In accordance with criterion 3, the double-frequency component is very small when the direct current is zero. It increases to a maximum (at 118 ma) with increasing current and then decreases with further increase of current. The small curves at the bottom of figure 3 show the cyclic variation to be expected in the resistivity of the surface layer of the wire for superposed direct currents of 50, 120, and 170 ma, respectively. Here, as in the case of figure 2, the amplitudes of the variations in resistivity are at least roughly consistent with the observed variation of the double-frequency component (upper curve), if it is assumed that the resistivity follows with practically no lag the variations in current and magnetic field.

A quantitative check based on the magnitude of the double-frequency component is rendered difficult both by the complexity introduced by skin effect and the experimental difficulty of avoiding stray coupling while calibrating the detector by the emf induced in

the mutual inductance M, (figure 1.) Of the 12 sets of measurements made at successively different temperatures while the currents were held constant, 8 were secured with reasonably good calibrations. All eight sets corresponded to fairly large current values, so that at the optimum temperature the resistivity of the surface layer should have been carried from zero to full value during each cycle. Taking the current through the detector (and the galvanometer deflections) as proportional to the square of the emf across the detector, the double-frequency emf induced by the specimen was found to be proportional to the magnitude of the fundamental-frequency current flowing

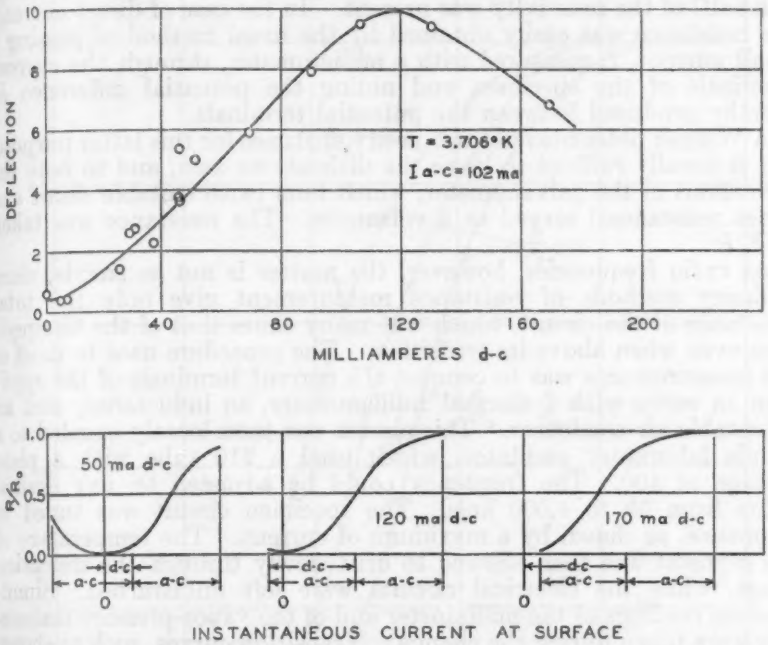

FIGURE 3.—*Double-frequency component of potential drop as a function of d-c component of current.*

through the specimen, their ratio being 0.08 ± 0.008 mv/ma. An exact calculation of the magnitude of the double-frequency emf to be expected is not feasible but an approximate calculation shows that with the optimum value of direct current, the double-frequency emf (rms) should be of the order of $I_1 R_1/\sqrt{8}$, where I_1 is the current (rms) of fundamental frequency and R_1 is the effective a-c resistance of the specimen for this frequency. The effective resistance of the specimen for 200 kc/s was about 0.36 ohm, from which one would expect a double-frequency effect amounting to $0.36/\sqrt{8}$ equal to 0.13 mv/ma. This is of the same order of magnitude as that observed. The difference in value is no greater than can be attributed to the uncertainties either in experiment or in theory.

We conclude, that if any time at all is required for the establishment and for the destruction of the superconducting state it is short compared with 5×10^{-6} sec and is probably less than 1×10^{-6} sec.

III. TRANSITION TEMPERATURE

The transition from the normal resisting to the superconducting state of the polycrystalline specimens here used, while occurring within a narrow temperature range, occupied a finite interval of about 0.02° K in tin and 0.05° K in tantalum. The obvious procedure for determining whether there is a difference between the transition temperatures for direct and high-frequency currents is to observe the resistance of the specimen at various temperatures through the transition range using (a) direct current and (b) radio-frequency current, and to compare the temperatures at which a given fraction (say, one-half) of the resistivity was present. In the case of direct current, the resistance was easily obtained by the usual method of passing a small current, I, measured with a milliammeter, through the current terminals of the specimen and noting the potential difference E, thereby produced between the potential terminals.

A Wenner potentiometer was used sometimes for this latter purpose, but it usually sufficed to leave the dials set on zero, and to note the deflections of the galvanometer, which thus (with suitable shunt and series resistances) served as a voltmeter. The resistance was taken as E/I.

At radio frequencies, however, the matter is not so simple, since ordinary methods of resistance measurement give only the total resistance of the circuit, which was many times that of the tin specimen even when above its transition. The procedure used in most of the measurements was to connect the current terminals of the specimen in series with a thermal milliammeter, an inductance, and an adjustable air condenser. This circuit was then loosely coupled to a simple laboratory oscillator, which used a 210 tube with a plate voltage of 400. The frequency could be adjusted to any desired value from 50 to 4,000 kc/s. The specimen circuit was tuned to resonance, as shown by a maximum of current. The temperature of the cryostat was then allowed to drift slowly through the transition range, while the electrical circuits were left undisturbed. Simultaneous readings of the milliameter and of the vapor-pressure manometer were taken during the change. Transition curves, such as shown in fig. 4, could be plotted from these data, using also the change in current observed when a known resistance was added, and the assumption that the specimen had zero resistance at the cold end of the transition range.[5]

The frequency which could be used effectively was limited to about 1,000 kc/s with the tin specimens and to 3,500 kc/s with the tantalum specimen, because of the unavoidable capacitance of the specimen and its leads to the metallic walls of the liquefier. It is probable that the apparent resistance of the specimen was considerably enhanced by such capacitance effects even below these limits, but the procedure of plotting the transition curves on a percentage basis prevents any such error from appreciably affecting the curves.

A more serious difficulty arose from the lag of the temperature of the specimen behind that of the helium bath in which it was immersed. This was largely avoided by taking the mean of pairs of transitions, one heating and the other cooling. Slight differences in the rate at which the temperature drifted in the two transitions of each pair are probably the main cause of the scattering shown in the results.

[5] For details of the resistance variation method, see NBS Circular C74, p. 180 (1924).

A further complication arises from the magnetic and thermal effects of the current used in making the measurement. The maximum currents used (200 ma for the tin specimens and 30 ma for the tantalum specimen) would be expected to depress the transition by 0.029 and 0.032° K, respectively. The specimens were wound bifilarly but with rather close spacing, so that the mutual action of neighboring

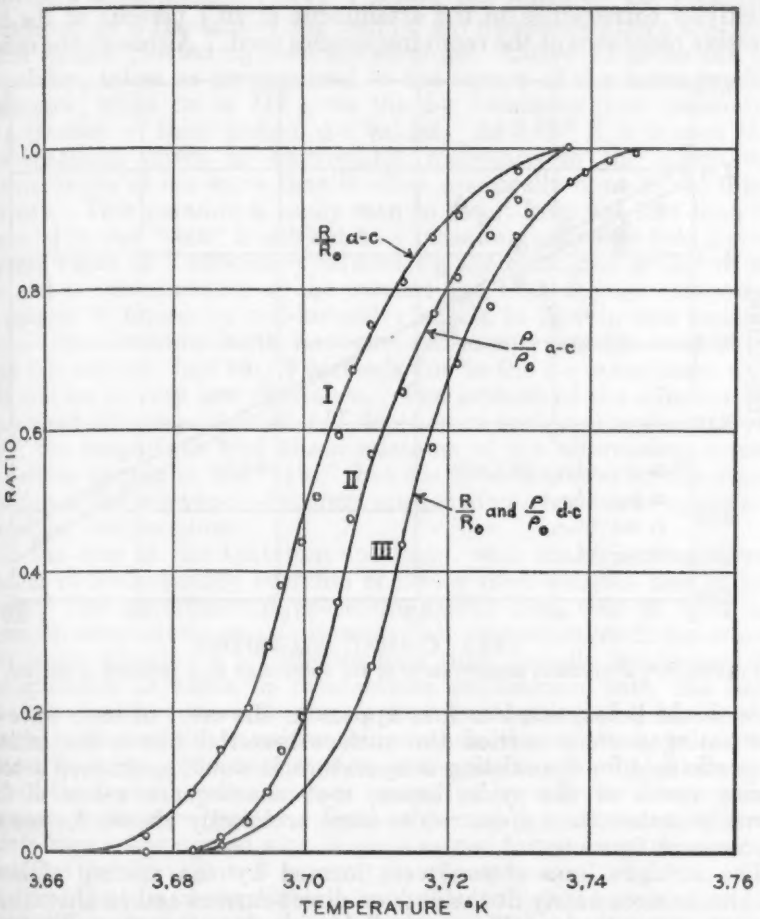

FIGURE 4.—*Transition curves with alternating and direct current superposed.*

I. Alternating-current resistance as a fraction of the a-c resistance above the transition.
II. Alternating-current resistivity as a fraction of the a-c resistivity above the transition.
III. Direct-current resistance and d-c resistivity as fractions of their values above the transition.

wires may have appreciably increased the effect as estimated above for a straight wire. A heating effect of the current, while absent at the cold end of the transition, might be present at the hot end. In the case of the tin wire, the great skin effect would make such heating more pronounced at the higher frequencies and might introduce an apparent shift in transition temperature with frequency. Because of the smaller diameter and much larger resistivity of the tantalum specimen, the skin effect in it was negligible.

To minimize these effects in the final comparison, the data on the two tin samples were plotted as shown in figure 5, in which the ordinates are the temperature of the helium bath at which the specimen showed one-half of its normal resistivity, while the abscissas are the values of the measuring current. The different markings of the points correspond to different frequencies and specimens. It is to be noted that by reason of the great skin effect the attainment of half of normal resistivity corresponds to the attainment of 70.7 percent of the full effective resistance at the radio frequencies used. Although the resist-

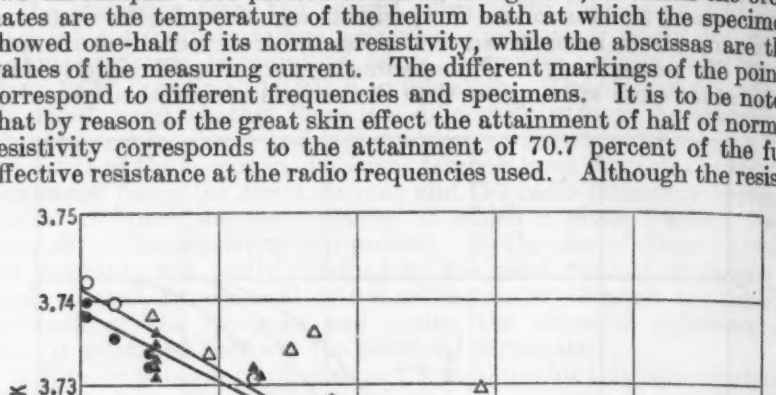

FIGURE 5.—*Transition temperatures of tin specimens as a function of current.*

ance would be expected to first appear as the crest of each wave of alternating current carried the surface material above the critical magnetic field for the existing temperature, it would again drop to zero during much of the cycle, hence, root-mean-square values of the currents rather than crest values were arbitrarily chosen for use as abscissas in figure 5.

The straight lines shown were located by the method of least squares to most nearly fit the data on direct current and on alternating current, respectively. Points at all frequencies other than zero were taken as of equal weight. The intercepts of the two lines are the best available indication of the midpoint of the transition when magnetic and heating effects of the currents are eliminated. These values are 3.738° K for direct current and 3.740° K for alternating current. The difference, 0.002° K, somewhat exceeds the mean-square deviation, which is 0.0007° K for either intercept, but is probably not significant.

The slope of the direct current curve, 2.0×10^{-4} °K/ma, is somewhat larger than the value 1.2×10^{-4}, calculated from Tuyn's [6] data, for the case of a single straight wire, presumably because of the mutual magnetic effects of adjacent wires.

[6] J. Franklin Inst. 201, 379 (1926).

The device of superposing direct and radio-frequency currents in the specimen simultaneously, offered some promise as a means for making sure that both sets of measurements corresponded to exactly the same temperature. Figure 4 shows a typical pair of transition curves obtained with the longer tin specimen when a direct current of 69 ma and a current of 136 ma (rms value) at a frequency of 200 kc/s were superposed. Curve I shows the effective a-c resistance (expressed as a fraction of the normal a-c resistance above the transition range) plotted against temperature. Curve *II* gives the a-c resistivity, taken as proportional to the square of the corresponding resistance; while curve *III* gives the d-c resistance (and resistivity) as a fraction of their normal d-c values. At 3.68° K it is seen that the specimen offers an appreciable resistance to the alternating current while at the same time it offers practically none to the direct current. This paradox is easily seen to result from the fact that the material in the "skin" is subject to a pulsating magnetic field having a crest value of 5 oersteds produced by the combined action of the d-c and a-c components of the current and that the a-c component of current is forced by self-inductive effects to flow in this resisting skin. The d-c component, however, can escape into the core which, with a maximum field of 1.3 oersteds due to the d-c component only, will still be of very low resistance. The amount of the effective displacement of curves *II* and *III* depends in such a complicated way upon the magnitude and phase relations of the alternating current at various depths in the "skin" that the data obtained by the superposition of the two types of current are not of much value in comparing transition temperatures.

In the case of the tantalum specimen, with its higher resistance, smaller radio-frequency currents could be used without loss of precision. The experimental procedure found best was to hold the specimen successively at two intermediate temperatures in the transition range, allowing a sufficiently long time (usually 4 minutes) for the specimen to come to temperature equilibrium with the bath. The temperatures were so chosen that both points fell within the central portion of the transition range where the resistance is varying almost linearly. The temperature corresponding to the attainment of half the normal resistance was computed by a linear interpolation between these two points. Data obtained by approaching both points from below agreed with those obtained from above, the average deviation being about 2 percent in resistance or 0.001° K. The results of the two most reliable sets of data are given in table 1. The mean difference between the d-c value and those at 3,500 kc/s is 0.010° K. These results were obtained with direct currents of 5 ma and with alternating currents which were 6 ma (rms) when the specimen was cold but which fell off to 4 ma when the resistance was fully restored. The effects of current should therefore have been nearly equal in the two cases except as the cyclic variation by carrying the alternating current to crest values higher than the d-c or root-mean-square values may have produced an effect. The total observed change in resistance through the transition at 3,500 kc/s was 35.7 ohms which is 43 percent more than the d-c resistance change. This may have been due in part to dielectric losses in the insulation of the leads, to a local circulation of current between the specimen and the capacitance of the leads, thus increasing the current in the former, and to

other extraneous effects. Also, if an appreciable part of the excess resistance was the result of a skin effect greater than the small amount calculated on the basis of an isolated straight wire, the temperature for the restoration of one-half the resistivity would be higher, and hence nearer to the d-c value, than the temperature for the restoration of one-half the resistance. In view of these possibilities the observed difference in transition temperature, while greater than the accidental errors of measurement, is perhaps not larger than can be accounted for by some factor such as those mentioned above.

TABLE 1.—*Temperature at which tantalum specimen had one-half normal resistance*

Date	Transition temperature for—		Frequency
	Direct current	Alternating current	
	°K	°K	kc/sec
8/14/34	3.948	3.945	1,000
		3.939	3,500
9/13/34	3.947	3.935	3,500

We conclude that there is no effect of frequency per se in the superconducting transition temperature up to the frequencies here used, 3×10^6 c/s. This is in accord with the conclusion of Burton.[7] It is, of course, possible that there may be an effect at higher frequencies.[8]

IV. MICRORESIDUAL RESISTANCE

The electrical methods described above for measuring effective resistance at radio frequencies gave directly only the total resistance of a complete circuit. The metal-clad construction of the liquefier prevented us from inducing currents in a complete superconducting circuit, as had been done by the workers at Toronto. The resistance, 0.7 ohm, of the longest tin specimen was so small compared to the minimum workable value of about 6 ohms in the external circuit, that there was little hope of obtaining satisfactory measurements by any method of differences. In view of this situation, an attempt was made to apply calorimetric methods which could separate the heating and hence the resistance in the specimen proper from that in the rest of the circuit.

The very low specific heat of metals at low temperatures and the high sensitivity in temperature measurement obtainable with a helium vapor-pressure thermometer in this range were favorable factors. However, difficulty in securing sufficiently good thermal insulation of the specimen and the long time required for thermal equalization to be attained throughout the specimen reduced our precision so seriously that the method was finally abandoned. The following paragraphs, however, summarize the meager results obtained.

The specimen consisted of 0.6 g of tin which had been extruded into wire 0.022 cm in diameter and 2.25 m long. This was wound into a

[7] E. F. Burton. The Phenomenon of Superconductivity, p. 73, University of Toronto Press (1934).
[8] See McLennan, Burton, Pitt, and Wilhelm. Proc. Roy. Soc. (London) [A] 136, 52 (1932).

coil about 3 cm in diameter made in two sections, so connected that their magnetic fields were in opposition, to minimize induction effects in the walls of the liquefier. Adjacent wires were separated by a silk thread and successive layers by cigarette paper, the whole structure being cemented with collodion. A resistance thermometer consisting of 400 cm of phosphor-bronze wire 0.013 cm in diameter wound bifilarly and having a resistance at room temperature of about 44 ohms was embedded between the two sections of tin wire. A few centimeters of lead (Pb) wire were used between the main specimen and the copper wires running out of the liquefier. As lead is superconducting up to 7.7° K, it was expected that there would be no heating in these connecting wires, even during the check runs made with the temperature slightly above the transition temperature of tin.

The flow of heat down the copper wires into the liquefier proper was so great, however, that, in spite of repeated efforts to get good thermal contact between these wires and the upper chamber of the liquefier, the junction of the lead and the copper wires was appreciably warmer than the walls of the liquefier. When the space surrounding the specimen was pumped down to a vacuum sufficient to give moderate thermal insulation, the specimen took on an appreciable fraction of this temperature difference and was about 0.22° K warmer than the bulb of the vapor-pressure thermometer. When current was flowing in the specimen the heating in the copper wires could cause a change in this temperature difference. This effect, together with possible dielectric loss in the insulation between the layers of the specimen and the currents which may have been induced in the phosphor-bronze winding, in spite of its bifilar arrangement, constituted possible sources of heat, even if the specimen itself had zero resistance.

Some 75 calorimetric runs were made on three different days and with two different specimens. When the thermal insulation was good enough, the rise in resistance of the bronze thermometer wire produced by a measured current of radio frequency flowing in the specimen for a measured short time (10 to 15 sec.) was taken as measuring the heat developed in the specimens under the conditions of temperature, frequency, etc., then existing. This tacitly assumes that the specific heat is constant. The known variations of specific heat in this range are not such as to seriously affect the conclusion. When the thermal insulation was not so high the current was allowed to flow until the bronze had come to a steady temperature and the calculations of rate of generation of heat were based on comparisons of these ultimate temperature rises (usually less than 1° K). Runs were made below (at about 2.5° K) and above (at about 3.9° K) the transition temperature of tin. In all cases some heating was observed and it is impossible to estimate precisely how much may have been due to the sources listed above. Table 2 gives the ratio of the effective resistance below the critical temperature to that observed at the same frequency above the transition. These figures are the average of a number of observations and indicate that the greater part at least of the resistance of tin vanishes below the transition even at radio frequencies.

TABLE 2.—*Ratio of heating observed at temperature below the transition temperature to that observed above the transition, tin sample*

Frequency	Ratio [1]
Direct current	0.004
120 kc/s	.02
220 kc/s	.03
514 kc/s	.04
800 kc/s	.04

[1] These figures for the high-frequency currents are larger than the ratio of about 0.01 reported to the American Physical Society at its meeting in April 1933 because of the inclusion of additional data.

It may be noted that the ratio of a-c to d-c heating above the transition temperature was about 10:1 at 514 kc/s, which is in reasonable agreement with the value 8.5:1 calculated from the skin effect in a straight wire of the same diameter at this frequency.

The much greater resistance of the tantalum specimen made possible the use at radio frequency of a method of differences which served to separate the resistance of the specimen proper from that of the rest of the circuit. The total resistance of the circuit containing specimen, leads and milliammeter was measured by the resistance-variation method,[9] by noting the value, I_1, of the current at resonance with the circuit in normal condition, and the value I_2 when a resistance ΔR had been added, and the circuit again tuned. The original resistance of the circuit is then given by

$$R=\Delta R I_2/(I_1-I_2)$$

Let the resistances of the two leads running to one end of the specimen be denoted by A and B, respectively, and those of the two leads to the other end by C and D, the resistance of the specimen being X. By connecting in succession each of the six possible pairs of terminals to the tuned radio-frequency circuit, the external part of which has the resistance Y, six values of total circuit resistance can be determined. If there is no mutual action between the various leads these six values will be

$$R_1=A+B+Y$$
$$R_2=A+C+Y+X$$
$$R_3=A+D+Y+X$$
$$R_4=B+C+Y+X$$
$$R_5=B+D+Y+X$$
$$R_6=C+D+Y$$

Eliminating the lead and external-circuit resistances from these equations gives

$$2X=R_2+R_5-R_1-R_6, \text{ or}$$
$$2X=R_3+R_4-R_1-R_6$$

as two partially independent determinations of X.

[9] NBS Circular C 74, p. 180 (1924).

By this method 48 such determinations were made of the resistance of the tantalum specimen at temperatures from 2.9 to 3.6° K, well below its transition of 3.9° K. Three of the measurements were discarded as they differed from a tentative mean value in which they were included by more than 6 times the average deviation of a single observation from this mean. The results from the remaining 45 determinations are shown in table 3. The second column gives the number of determinations made at each frequency; the third column, the algebraic mean of these results; and the fourth column, a measure of the precision of the items in the third column, this measure being obtained by dividing the mean value without regard to sign of the several determinations by the square root of the number of determinations. It happens that the mean of all the values of resistance in the superconducting state comes out to be only −0.02 ohm, but the measurements should be considered as indicating merely that the microresidual resistance is less than 0.2 ohm, or 0.8 percent of the resistance just above the transition.

TABLE 3.—*Resistance of tantalum specimen below transition*

[Resistance just above transition=25 ohms]

Frequency	Number of measurements	Mean resistance	Avg. deviation $\sqrt{n}$
kc/s		*Ohms*	*Ohms*
500	2	−0.25	±0.18
1,000	4	+.27	±.18
1,500	7	−.37	±.22
2,000	7	−.29	±.12
2,500	7	−.11	±.11
3,000	7	+.02	±.25
3,500	11	+.59	±.28
Mean		−.02	±.20

V. CONCLUSIONS

In view of the foregoing results, the answers to the three major questions seem to be as follows:

1. The transition from the normally resisting to the superconducting state and back again, under the influence of a pulsating magnetic field, can take place with sufficient rapidity [10] to follow pulsations having a frequency of 200,000 c/s.

2. The change in transition temperature with frequency is probably zero up to 3×10^6 c/s, the small observed shifts being in opposite directions in the two materials tried.

3. The microresidual resistance for high-frequency currents of a superconductor when well below its transition temperature is probably zero. If any resistance exists, these experiments show that it is less than 4 percent of the resistance just above the transition in the case of tin, and less than 1 percent, in the case of tantalum. In terms of the resistance at room temperature these limits are 4×10^{-5} for tin and 2×10^{-3} for tantalum. These limits are unfortunately much larger than the corresponding limits for d-c measurements because of the experimental difficulties met in high-frequency work.

WASHINGTON, September 30, 1937.

[10] Other experiments (NBS J. Research 18, 295 (1937)) RP977, indicate that, at least in tantalum under certain rather limited conditions, a special type of transition may occur at a relatively very slow speed.

U. S. DEPARTMENT OF COMMERCE NATIONAL BUREAU OF STANDARDS

RESEARCH PAPER RP1071

Part of Journal of Research of the National Bureau of Standards, Volume 20, February 1938

SPECTRUM OF LUTECIUM MONOXIDE

By William W. Watson[1] and William F. Meggers

ABSTRACT

A vibrational quantum analysis is given for the most conspicuous band system of the LuO spectrum. The wave numbers of band heads in this system are represented by the equation:

$$\nu = 21471.8 + 791.60(v' + \tfrac{1}{2}) - 3.12(v' + \tfrac{1}{2})^2 - 841.66(v'' + \tfrac{1}{2}) + 4.07(v'' + \tfrac{1}{2})^2 - 2.07v'v''.$$

The unexpected singlet character of the spectrum and the value of the vibrational frequency are discussed.

Spectra of the monoxides of a large number of the elements are known, and for many of these, quantum analyses, at least for the measurements of the band heads, have been made. For the rare-earth group, however, but one analysis has so far been reported, that of two apparently unrelated band systems of GdO observed in the oxyhydrogen flame by Piccardi,[2] who states that many of the bands appear very bright at flame temperature but disappear completely at arc temperature. Instability at arc temperature may account for the general lack of data on the band spectra of the rare earths, although it may be attributed in part to the same difficulties hindering the analysis of their atomic spectra (scarcity of pure materials, complexity of spectra, high multiplicities, low ionization potentials, etc.). Because of their probable low multiplicity, the molecular spectra of the first (cerium) and the last (lutecium) of the rare-earth group might be expected to be more amenable to vibrational quantum analysis than the others. Particularly is this true for lutecium, the ground-state configuration of which is similar to that of lanthanum but with the addition of the completed shell of 14 *f*-type electrons. Lutecium is, indeed, outstanding among the rare earths in showing a sequence of intense bands in the conventional arc spectrum.

A new description of the conventional arc and spark spectra of lutecium was recently published by Meggers and Scribner.[3] Using a 220-volt d-c arc carrying 5 amperes between pure-silver electrodes on to which some lutecium oxide was fused, it was found that in the entire range from 2000 to 11 000 A the only bands attributable to lutecium com-

[1] Associate Professor of Physics, Yale University.

[2] G. Piccardi. Gazz. chim. ital. **63**, 887 (1933). Although Piccardi displays 10 systems of bands only 2, in our opinion, can be ascribed to GdO molecules. Two systems with 0,0 bands at 17597.3 and 16931.8 cm^{-1} and vibrational frequencies of 276.1 and 303.1, respectively, for the lower states are suggestive of a fairly heavy monochloride; they may be due to GdCl. The remaining systems are isolated sequences, two of which, with 0,0 heads at 16169.1 and 16093.1 cm^{-1}, are most probably identified as CaCl, while the rest may be fragmentary chloride systems of Gd or of impurities.

[3] W. F. Meggers and B. F. Scribner. J. Research NBS **19**, 31 (1937) RP1008.

pounds occur in the blue portion of the spectrum. These bands degrade to the red, are apparently single-headed, and fall principally into two groups or sequences, one quite intense with principal head at 4662 A, the other much weaker and beginning with a band at 4509 A. That this spectrum is emitted by the LuO molecule is indicated by structural resemblance with other monoxide spectra. Although the observed bands, about 35 in number, may not constitute the entire spectrum of LuO, it seems probable that no other band sequences of comparable intensity or length exist. And since further experimental study of the LuO spectrum is at present impossible because of the scarcity of material, we feel that the analysis of these bands should be presented as a contribution to the limited knowledge of the spectra of rare-earth molecules. A reproduction of the principal bands of this spectrum is shown in figure 1.

The more intense group of bands starting at 4662 A forms the $\Delta v=0$ sequence of the system, while the less intense group on the shorter wave length side of this is the $\Delta v=-1$ sequence. Placing these band head frequencies in a $v'v''$ array in such a fashion as to give plausible values for $\Delta G''(1/2)$, the frequencies of a possible $\Delta v=+1$ sequence were computed. These were found to agree quite closely with "hazy" lines of low intensity in the wave-length tables of Meggers and Scribner, who assumed them to be characteristic of neutral Lu atoms. However, none of these lines have been found essential in the Lu I analysis, and inspection of the spectograms shows that they are weak band heads.

Two additional weak band heads needed to complete the -1 sequence were found on the most intense spectrogram. The $v'v''$ array of LuO bands in table 1 shows the wave numbers corresponding to band heads, whose wave lengths and estimated intensities appear in table 2.

The wave numbers of these heads are given by the equation:

$$\nu=21471.8+791.60(v'+1/2)-3.12(v'+1/2)^2-841.66(v''+1/2)$$
$$+4.07(v''+1/2)^2-2.07\ v'v''$$

Allowance for the variation in the interval $\nu_{head}-\nu_0$ with v is made with the final $v'v''$ term. The coefficient 2.07 for this term is unusually large, indicating that there is but a very small change in the moment of inertia of the molecule in its transition from one electronic state to the other. One would also expect this from the relatively small change (6 percent) in the vibrational frequency, which apparently causes the Condon parabola for the distribution of the most intense bands to be so narrow as to give only the $\Delta v=0$ sequence good intensity. There is some indication of the necessity of a cubic term in v', but random fluctuations in the course of the few $\Delta G(v'+1/2)$ intervals make its evaluation uncertain. The magnitude of the $\nu_{obs}-\nu_{calc.}$ differences, as well as the low intensities for the bands involving the $v'=5$ level, indicate a perturbation of this level.

Research Paper 1071
Journal of Research of the National Bureau of Standards

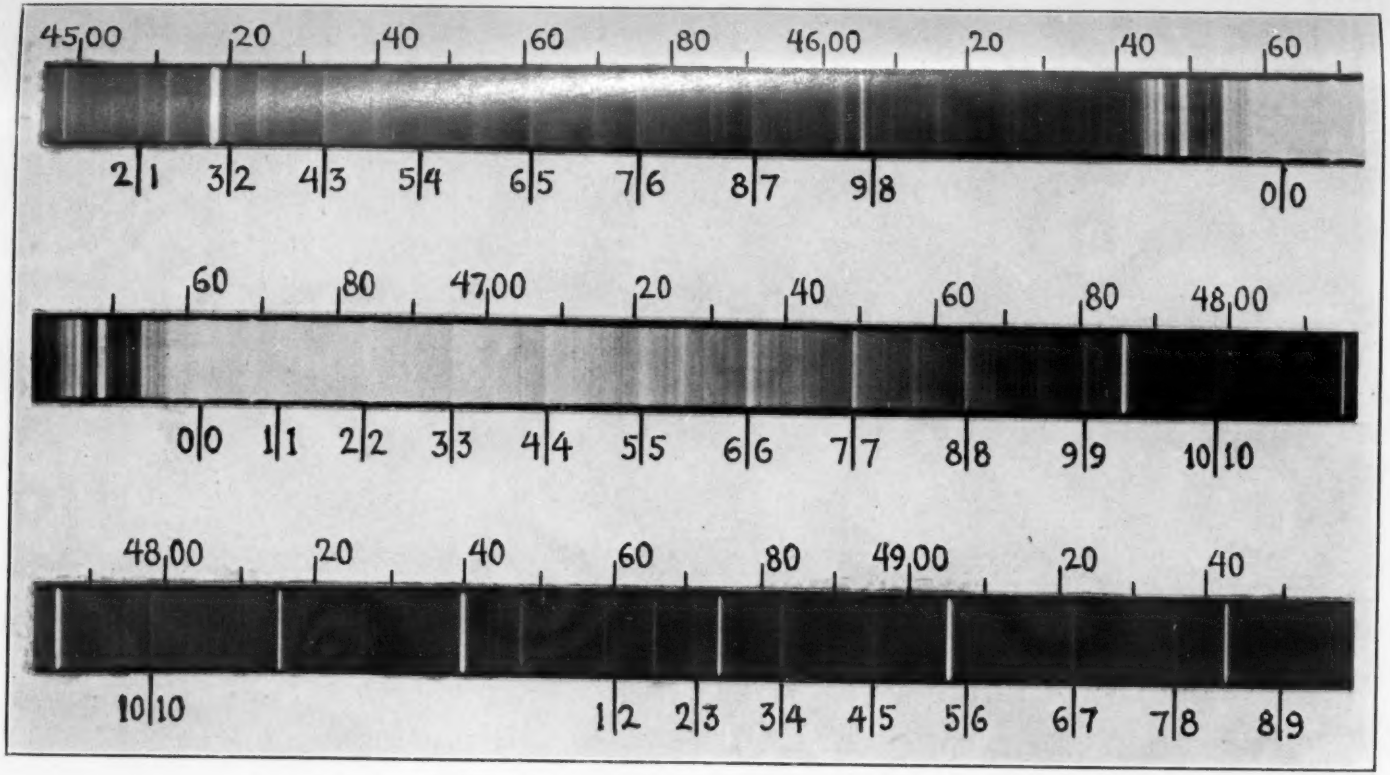

FIGURE 1.—*Spectrum of lutecium monoxide* (LuO).

Wavelengths marked above, band heads below.

TABLE 1.—*Wave numbers and differences between progressions of* LuO *bands*

TABLE 1.—*Wave numbers and differences between progressions of* LuO *bands*

v'' \ v'	0	1	2	3	4	5	6	7	8	9	10
0	21445.2										
1		21396.7 *827.0* *775.4*	20569.7 *772.9*								
2		22172.1 *829.5*	21342.6 *817.7* *762.8*	20524.9 *766.8*							
3			22112.4 *821.2*	21291.2 *815.2* *761.2*	20476.0 *758.5*						
4				22052.4 *817.9*	21234.5 *811.2* *755.7*	20423.3 *763.4*					
5					21990.2 *813.5*	21176.7 *804.0* *742.4*	20372.7 *740.7*				
6						21919.1 *805.7*	21113.4 *800.9* *736.9*	20312.5 *738.2*			
7							21850.3 *799.6*	21050.7 *795.1* *726.5*	20255.6 *728.4*		
8								21777.2 *793.2*	20984.0 *786.8* *717.0*	20197.2 *717.0*	
9									21701.0 *786.8*	20914.2	
10											20836.2

TABLE 2.—*Band heads in the spectrum of lutecium monoxide* (LuO)

v', v''	λ_{air} A	Intensity	$\nu_{vac.}$ cm^{-1}	$\nu_{obs.}-\nu_{calc.}$
2, 1	4508.91	5	22172.1	−1.7
3, 2	4521.08	2	22112.4	−0.5
4, 3	4533.39	5	22052.4	+2.4
5, 4	4546.2	1	21990.2	+5.4
6, 5	4560.95	8	21919.1	+1.8
7, 6	4575.31	5	21850.3	+2.8
8, 7	4590.68	3	21777.2	+1.7
9, 8	4606.8	1	21701.0	−0.3
0, 0	4661.75	150	21445.2	−1.8
1, 1	4672.31	120	21396.7	−0.1
2, 2	4684.16	100	21342.6	−1.7
3, 3	4695.46	80	21291.2	+1.6
4, 4	4708.00	60	21234.5	+1.0
5, 5	4720.86	5	21176.7	+3.3
6, 6	4735.00	25	21113.4	+1.4
7, 7	4749.11	10	21050.7	+2.3
8, 8	4764.22	7	20984.0	+1.6
9, 9	4780.11	5	20914.2	−0.1
10, 10	4798.00	3	20836.2	−7.7
1, 2	4860.15	1	20569.7	+0.4
2, 3	4870.78	1	20524.9	+2.0
3, 4	4882.40	3	20476.0	+1.7
4, 5	4895.00	1	20423.3	−0.1
5, 6	4907.16	1	20372.7	+2.4
6, 7	4921.70	3 (+Lu II)	20312.5	−2.4
7, 8	4935.53	2 (+Yb II)	20255.6	−1.7
8, 9	4949.8	1	20197.2	−0.3

One would expect a multiplicity of two for the terms of the neutral LuO molecule, with considerable resemblance between the spectra of LuO and LaO molecules because of the similarity in their electron configurations. Seven or more band systems due to LaO have been described [4] and the doublet character of the LaO levels has been reported for at least five of these systems. The LuO bands, although more or less diffuse, are apparently single-headed. The most plausible explanation of the appearance of just this singlet band spectrum would seem to be that it constitutes say a $^2\Delta_{2½}\rightarrow{}^2\Delta_{2½}$ or a $^2\phi_{3½}\rightarrow{}^2\phi_{3½}$ transition (possible types for LuO), with the other multiplet component, $^2\Delta_{½}\rightarrow{}^2\Delta_{½}$ or $^2\phi_{2½}\rightarrow{}^2\phi_{2½}$, respectively, practically eliminated by predissociation in the upper state. Such registration of just one component of the complete multiplet transition has been noted in other cases (NiH,[5] CoH).[6] Some of the unassigned bands (4094, 4096, 4239, 4242, 4569, 4654, 5161, 5170 A) may represent a trace of the missing transition (or of other systems).

The vibrational frequency $\omega''=841.66$ differs but little from the value 841.00 for one of the GdO systems analyzed by Piccardi. This is not surprising, for in view of the nearly identical chemical behavior of all the rare earths the force constants for the vibrations of homologous molecules for all of these elements should be nearly the same. There should be but a 1 percent change in the vibration frequency due to the change in the *reduced mass* of the molecule in passing from CeO to LuO. It would seem then that all of the rare-earth monoxides should have one lower state vibrational frequency in the range 840 to 850 cm^{-1}.

WASHINGTON, November 15, 1937.

[4] W. Jevons. Proc. Phys. Soc. (London) **41**, 520 (1929). W. F. Meggers and J. A. Wheeler. BS J. Research **6**, 239 (1931) RP273.
[5] A. G. Gaydon and R. W. B. Pearse, Proc. Roy. Soc. (London) [A] **148**, 312 (1935). A. Heimer, Z. Phys. **105**, 56 (1937). ($^3\Delta_{3½}\rightarrow{}^3\Delta_{3½}$ transition.)
[6] A. Heimer, Z. Phys. **104**, 448 (1937). ($^3\phi_4\rightarrow{}^3\phi_4$ transition.)

U. S. DEPARTMENT OF COMMERCE NATIONAL BUREAU OF STANDARDS

RESEARCH PAPER RP1072

Part of Journal of Research of the National Bureau of Standards, Volume 20, February 1938

QUANTITATIVE ANALYSIS, WITH RESPECT TO THE COMPONENT STRUCTURAL GROUPS, OF THE INFRARED (1 TO 2 μ) MOLAL ABSORPTIVE INDICES OF 55 HYDROCARBONS [1]

By Frank W. Rose, Jr.[2]

ABSTRACT

Data from previous studies on the infrared absorption spectra between 1.2 and 1.8 μ (5400 to 8900 cm^{-1}) for 54 hydrocarbons have been analyzed mathematically. The total molal absorptive index, K, at any wave length, is shown to follow, within the limits necessary to define the number of groups, the formula

$$K = n_a\alpha + n_b\beta \qquad \text{(a)}$$

for the normal paraffin hydrocarbons, and the formula

$$K = n_a\alpha' + n_b\beta + n_c\gamma + n_d\delta \qquad \text{(b)}$$

for other classes of hydrocarbons, where n_a, n_b, n_c, n_d are the number of $-CH_3$, $>CH_2$, $\gtrless CH$, and $>CH$ (aromatic) groups and α (or α'), β, γ, δ, are the values respectively, of the absorptive index for the respective unit group. Equation b is demonstrated to hold for branched-chain paraffins, cycloparaffins (naphthenes) and aromatic hydrocarbons, including 10 of high molecular weight (C_{24} to C_{32}). The accuracy of the method as well as restrictions on its application are given. Possible extensions in order to distinguish between paraffins and cycloparaffins are indicated. Its use is demonstrated by an example of the identification of an unknown isomeric nonane.

CONTENTS

	Page
I. Introduction	130
II. Discussion of concepts	130
III. Calculation of unit absorption coefficients	134
IV. Results	144
V. Discussion	148
1. Normal paraffins	148
2. Isoparaffins	148
3. Naphthene and aromatic hydrocarbons	150
4. Hydrocarbons of high molecular weight	151
VI. Determination of the number and kind of structural groups in unknown hydrocarbons	152
1. General procedure	152
2. Example: Determination of the structure of an unknown isomeric nonane	153
3. Limitations of the method	156
VII. References	156

[1] Financial assistance has been received from the research fund of the American Petroleum Institute. This work is part of Project 6, The Separation, Identification, and Determination of the Constituents of Petroleum.

[2] Research Associate at the National Bureau of Standards, representing the American Petroleum Institute.

I. INTRODUCTION

In connection with the work of the American Petroleum Institute Research Project 6 on the separation and identification of hydrocarbons from petroleum, the property of infrared absorption between 1.2 and 1.8 μ (5400 to 8900 cm^{-1}) was first used to "fingerprint" the hydrocarbons isolated [1] [3] and later, in a qualitative way, to aid in the identification [2]. For the hydrocarbons of low molecular weight, most of which have been synthesized and subjected to measurement, the identification can be definitely made by comparison with the synthetic hydrocarbons, using such physical properties as molecular weight, carbon-hydrogen content, boiling point, freezing point, density, and refractive index, as discussed by Washburn [3], and leaving the infrared-absorption spectra as a corroborating "fingerprint." In the case of hydrocarbons of higher molecular weight, however, relatively few have been synthesized, and it often becomes impossible to identify the hydrocarbons isolated from petroleum because of the absence of data on the corresponding synthetic hydrocarbons of known structure.

In this latter case, recourse must be had to methods of identification that will yield a knowledge of the class or type of the given unknown molecule and of the nature and number of its structural units. A number of effective methods for classifying unknown hydrocarbons and their mixtures according to the general or average type of molecule have been developed and used extensively in recent years. These methods include the use of the molecular volume [4], the viscosity index [4, 5, 6, 7, 8], the specific refraction [9], the specific dispersion [9, 10, 11, 12, 13, 14], the viscosity-gravity index [15], refractivity intercept [16], etc. But known properties which yield information concerning the actual structural units of hydrocarbon molecules are rare. It has been known for several years that the infrared absorption due to vibrations between carbon and hydrogen atoms in the region of the spectrum from 1.2 to 1.8 μ is different in both wave length and intensity for $-CH_3$, $>CH_2$, $\gtrless CH$, and $>CH$ (aromatic) groups [17, 2].[4] It seemed desirable, therefore, to extend the method of Wulf and Liddel [36] so that this property might yield quantitative, as well as qualitative, information concerning the structural units of an unknown hydrocarbon molecule.

The present report gives the results of a quantitative mathematical analysis of the infrared-absorption curves for 54 hydrocarbons that have already been published by the Project [2, 18], with the purpose of yielding the numerical values for the number of structural groups in a given unknown hydrocarbon molecule whose molecular weight and carbon-hydrogen composition are known. The method proposed is neither absolute nor independent, but reliable results can be obtained by the use of this property in conjunction with a judicious consideration of certain other properties of the unknown hydrocarbon.

II. DISCUSSION OF CONCEPTS

Although W. Herschel [19], in 1800, demonstrated the existence of radiation having wave lengths longer than those of the visible spectrum, the infrared-absorption spectra of organic compounds were not

[3] Figures in brackets here and throughout the text refer to the references at the end of the paper.

[4] Hereafter an incomplete valence bond indicates the attachment to the remainder of the molecule through another C atom.

studied until 1881, when Abney and Festing [20] investigated a series of typical organic liquids in the near infrared (0.7 to 1.2 μ) by photographic means. These authors correctly stated (for this region) "that the foundation of all absorptions in these bodies is the hydrogen," and furthermore advanced the hypothesis that absorption at specific wave lengths can be attributed to certain radicals. These authors also made a distinction between paraffinic and aromatic bonds. Using a bolometer, Julius [21] extended the range of measurements to 10 μ, and concluded that the absorption spectrum is a function not only of the elementary composition but also of the structure of the compound. Julius assigned the maxima at 3.45 μ and 6 to 7 μ[5] in the curves of percentage absorption plotted against wave length to the presence of methyl ($-CH_3$) groups in the molecule. Later Donath [23], from work on essential oils, found maxima at 1.69 and 2.2 μ and concluded that the action is intermolecular and not intramolecular, because the absorption bands were not as sharp as those in the visible spectra. Coblentz [22] stated that Ransohoff [24] measured the absorption spectra of six alcohols, finding maxima at 7.71, 3.0, and 3.43 μ, the absorption at 3.0 μ being assumed to be characteristic of the hydroxyl group. Puccianti [25] investigated a series of benzene derivatives, and found that all compounds which had carbon bound to hydrogen showed a maximum at 1.71 μ, while all molecules containing a benzene nucleus had additional maxima at 2.18 and 2.49 μ. From this evidence Puccianti concluded that the groups in the molecule are the governing influence in infrared absorption in this region. In 1905, Coblentz [22] published an extensive work on 135 compounds (solids, liquids, and gases, mainly organic) with the principal conclusions that:

1. The arrangement (bonding) of the atoms has a great influence on the resulting absorption spectrum.
2. No shifting of the maximum of absorption is observed with increase in molecular weight (except for gases).
3. A distinction must be made between a true shifting of the maximum and a shift which, on the introduction of a new adjacent band, occurs because the center of gravity is changed.
4. Certain absorbing groups preserve their identity in compounds containing other groups.

Later workers tended to confirm these results by Coblentz.[6] In recent papers Barnes [27, 28], Bloch and Errera [44], and others have presented the modern conceptions of the relation of absorbing groups to infrared spectra, while Mecke [45, 46] has reviewed the use of the photographic infrared in the determination of constitutional formulas. Bartholomé and Teller [47] have made theoretical calculations relating the infrared spectra to the constitution of organic compounds.

The region, 6 to 15 μ, in which the infrared absorption is determined mainly by the carbon skeleton, has been the subject of much investigation by Lecomte and coworkers [26]. Thus Lambert and Lecomte [29] were able to make certain deductions concerning the nature of petroleum distillates by measurements in this region.

[5] As corrected by Coblentz [22].
[6] An excellent review of the development of this field is found in the recent treatise by Lecomte [26].

In 1919, Henri [30][7] attempted to correlate the intensity of absorption with molecular structure by assuming that the maximum at 3.4 μ in the absorption curves of alcohols was a linear function of the number of C—H bonds. Bonino [31], on the other hand, expressed the molal absorptive index as various functions (logarithmic, parabolic, and linear) of the number of such bonds, depending on the class of compound. Bonino's conclusions were in discord with those of Bell [32], who found that di-*n*-butyl and diisobutyl carbonates had different absorptive power although containing the same number of C—H bonds. However, the justification for this distinction became apparent when Brackett [17], using a high dispersion, resolved into its components the band occurring at 1.2 μ in the absorption spectra of hydrocarbons. Thus Brackett's work showed definitely that a distinction must be made between the $-CH_3$, $>CH_2$, and $\gtrdot CH$ groups. Later, Liddel and Kasper [2] not only confirmed these findings but also showed that "aromatic" absorption could be distinguished. In the same report of Liddel and Kasper, similar results were obtained for the bands at 1.8 and 1.4 μ. Freymann [33] found analogous behavior at 0.9 and 1 μ. A previous paper [18] by the author extended the scope of the compounds measured to hydrocarbons of high molecular weight. It is these units, $-CH_3$, $>CH_2$, $\gtrdot CH$, and $>CH$ (aromatic), which are the variables in terms of which the intensity of absorption must be expressed.

Meanwhile, Liddel and Wulf [34] stated that "First, the absorption coefficient for the N—H bond in its absorption at 1.5 μ throughout a very considerable range in the character of the compounds . . . remains the same order of magnitude. Second, there are measurable differences in this absorption coefficient from class to class; i. e., primary aliphatic, secondary aliphatic, primary aromatic, etc., as well as differences in the position of the maximum of absorption. Third, when a normal paraffin greater than two carbon atoms long is attached to the amine group,[8] the absorption coefficient and maximum of absorption vary very little." In a later paper, Wulf and Liddel [36] use the area under the molal absorptive index curve in a given region as a quantitative measure of the number of bonds which give rise to the absorption at that place.

If, for various compounds, the form of the absorption curve is identical, the ordinate of the curve of the molal absorptive index at a given wave length is directly proportional to the total area under the curve for a given region [36]. It follows, under these conditions, that the ordinate at a given wave length, preferably near the maximum of a given "hump", will be proportional to the number of groups giving rise to the absorption at that place.[9] To test the Wulf and Liddel assumption that the area is proportional to the number of groups, and also to check, in part, the assumed similarity in the

[7] The insistence of Henri upon the use of the molal absorption index instead of the percentage absorption or transmission led to more readily apparent relationships with molecular structure. The molal absorption index, K, is defined [48] thus:

$$K=\frac{-\log_{10} I/I_0}{cd},$$

where I is the intensity of the transmitted light, I_0 the incident light, c the concentration in moles per liter, and d the cell depth in centimeters.

[8] Confirmation of this fact is given by the work of Rossini [35] on the heats of combustion of normal paraffins and alcohols where it is shown that intramolecular action is minor beyond two carbon atoms.

[9] For the present purpose it is unnecessary to resolve the curve of an ideal group into components which can be associated with different modes of vibration, as Wulf [37] has done. It suffices to develop a value of the molal absorptive index for an average unit group at a fixed wave length.

form of the curve, a plot was made from the data on the normal paraffin hydrocarbons, of the value of the ordinate of the molal absorptive index curve at 8160, 8254, 8400, and 8750 cm^{-1}, against the number of $>CH_2$ groups in the molecule.[10]

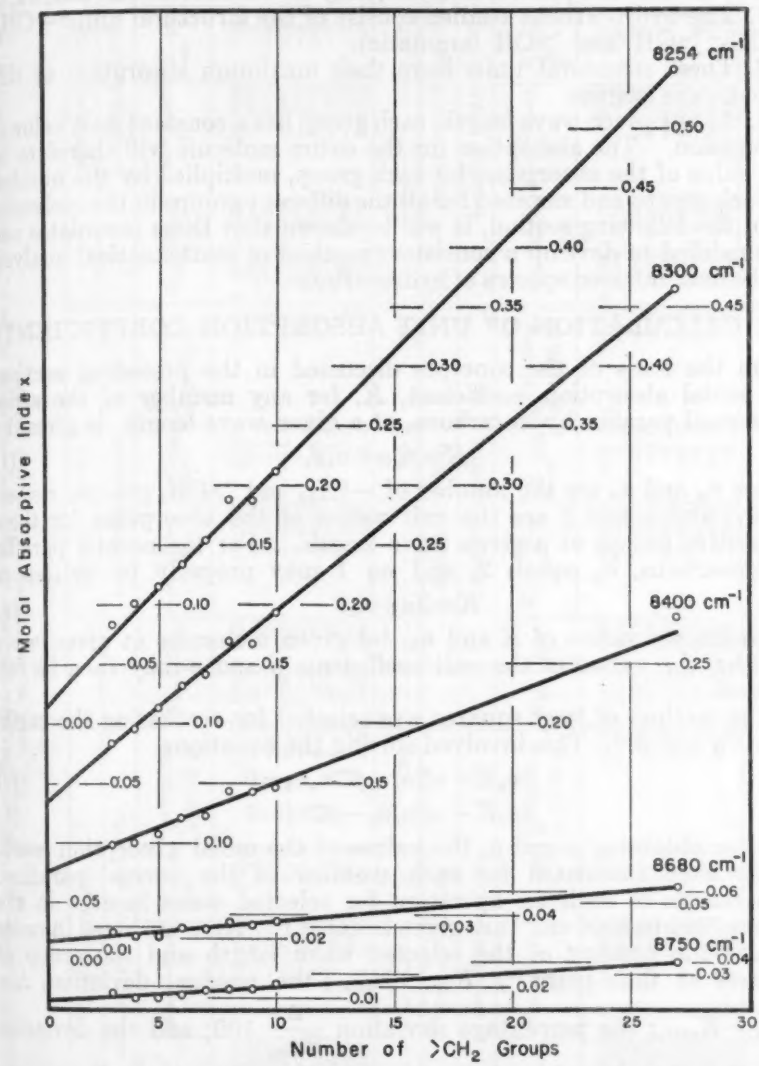

FIGURE 1.—*Plot of the data on the absorption of the normal paraffin hydrocarbons at various wave numbers.*

The scale of ordinates gives K, the molal absorption index, of the given normal paraffin at the wave length indicated at the right-hand side of the plot. The scale of abscissas gives n_3, the number of methylene ($>CH_2$) groups in the molecule.

Figure 1 shows that the given ordinate at the respective wave numbers is substantially linear with the number of $>CH_2$ groups

[10] In the previous paper [18], a table is given showing the wave number at which maxima occur for the various structural groups.

in the molecule.[11] The positive intercept at zero number of $>CH_2$ groups represents the substantially constant absorption due to the two $-CH_3$ groups in each of the molecules.

The concepts, which have been discussed above and which form the initial basis of the present analysis, may be summarized as follows:

1. The hydrocarbons studied consist of the structural units $-CH_3$, $>CH_2$, $>CH$, and $>CH$ (aromatic).
2. These structural units have their maximum absorption at different wave lengths.
3. At any given wave length, each group has a constant unit value of absorption. The absorption for the entire molecule will therefore be the value of the absorption for each group, multiplied by the number of such groups and summed for all the different groups in the molecule.

In the following section, it will be shown that these postulates can be modified to develop a consistent method of mathematical analysis of the near-infrared spectra of hydrocarbons.

III. CALCULATION OF UNIT ABSORPTION COEFFICIENTS

On the basis of the concepts discussed in the preceding section, the molal absorption coefficient, K, for any member of the series of normal paraffin hydrocarbons, at a given wave length, is given by

$$K=n_a\alpha+n_b\beta, \tag{1}$$

where n_a and n_b are the number of $-CH_3$ and $>CH_2$ groups, respectively, and α and β are the unit values of the absorption for these respective groups at a given wave length. For the normal paraffin hydrocarbons, n_a equals 2, and eq 1 may properly be written as

$$K=2\alpha+n_b\beta \tag{1a}$$

With known values of K and n_b, for given molecules at given wave lengths, the values of the unit coefficients α and β may then be calculated.

The method of least squares was selected for evaluating the coefficients α and β.[12] This involved solving the equations

$$\Sigma n_aK-\alpha\Sigma n_a^2-\beta\Sigma n_an_b=0 \tag{2}$$

$$\Sigma n_bK-\alpha\Sigma n_an_b-\beta\Sigma n_b^2=0 \tag{3}$$

After obtaining α and β, the values of the molal absorption coefficients were calculated for each member of the normal paraffins. The results of such an operation for selected wave lengths in the region 7900 to 8900 cm^{-1} are given in table 1. Here are listed in order (under the heading of the selected wave length and the group of interest at that point [13]): $K_{obs.}$; $K_{calc.}$; the residual deviation, $\Delta=K_{obs.}-K_{calc.}$; the percentage deviation $\frac{\Delta}{K_{obs.}}100$; and the deviation in terms of the number of the group sought at that point.[14]

[11] After this work was completed, a paper by Williams [38] appeared in which the data of Coblentz [22] on the transmission at 3.4 μ for a series of fractions isolated from petroleum were converted to molal absorption coefficients and plotted as a function of the number of C—H bonds.

[12] The simpler method of averages (Lipka [39], p. 126) was not used since it involves division of the data into two groups. Experience has shown that different groupings often lead to inconsistent results. Thus complications might result if it be true, as suggested by Liddel and Kasper [2], that maxima at certain wave lengths show an alternation in wave length or position with the number of carbon antoms in the chain.

[13] The wave numbers at which data were taken were so selected that some one of the various types of structural groups possessed a maximum of absorption at or near such wave numbers. As a result, the numerical value for the group of interest could be calculated with accuracy.

[14] The derivations of unit coefficients γ and δ for $>CH$ and $>CH$ (aromatic) are explained below. Deviations in terms of such groups are included in table 1 to show that an analysis would not falsely indicate the presence of such groups.

TABLE 1.—*Results of representing, for the normal paraffins, the total molal absorption coefficient, K, as a function of the number*

TABLE 1.—*Results of representing, for the normal paraffins, the total molal absorption coefficient, K, as a function of the number, n_a, of primary ($-CH_3$), and, n_b, of secondary ($>CH_2$) groups*

$$K = n_a\alpha + n_b\beta$$

Compound	Number of groups, $>CH_2$	8160 cm^{-1} ($\geqslant CH$) $\alpha=0.00295$ $\beta=0.00992$ $\gamma=0.01132$					8254 cm^{-1} ($>CH_2$) $\alpha=0.00629$ $\beta=0.01989$					8400 cm^{-1} ($-CH_3$) $\alpha=0.03770$ $\beta=0.00735$				
	n_b	$K_{obs.}$	$K_{calc.}$	$\frac{K_{obs.}-K_{calc.}}{\Delta}$	$\frac{\Delta}{K_{obs.}}100$	$\frac{\Delta}{\alpha}$=Number of $\geqslant CH$ gr.	$K_{obs.}$	$K_{calc.}$	$\frac{K_{obs.}-K_{calc.}}{\Delta}$	$\frac{\Delta}{K_{obs.}}100$	$\frac{\Delta}{\beta}$=Number of $>CH_2$ gr.	$K_{obs.}$	$K_{calc.}$	$\frac{K_{obs.}-K_{calc.}}{\Delta}$	$\frac{\Delta}{K_{obs.}}100$	$\frac{\Delta}{\alpha}$=Number of $-CH_3$ gr.
n-Pentane	3	0.0469	0.0357	+0.0113	+31.7	+1.2	0.0822	0.0723	+0.0099	+12.1	+0.5	0.0978	0.0974	+0.0004	+0.4	0.0
n-Hexane	4	.0443	.0456	−.0013	−2.9	−.1	.0991	.0921	+.0070	+7.1	+.3	.0992	.1048	−.0056	−5.7	−.1
n-Heptane	5	.0490	.0555	−.0065	−11.7	−.7	.1147	.1120	+.0027	+2.4	+.1	.1072	.1121	−.0049	−4.6	−.1
n-Octane	6	.0667	.0654	+.0013	+2.0	+.1	.1338	.1319	+.0019	+1.4	+.1	.1217	.1195	+.0022	+1.8	+.1
n-Nonane	7	.0691	.0753	−.0062	−8.2	−.7	.1534	.1518	+.0016	+1.1	+.1	.1225	.1268	−.0043	−3.5	−.1
n-Decane	8	.0886	.0853	+.0033	+3.9	+.4	.1877	.1717	+.0160	+8.5	+.8	.1430	.1342	+.0088	+6.2	+.2
n-Undecane	9	.0985	.0952	+.0033	+3.5	+.4	.1875	.1916	−.0041	−2.1	−.2	.1430	.1415	−.0090	−6.3	−.2
n-Dodecane	10	.0995	.1051	−.0056	−5.3	−.6	.2115	.2115	.0000	0.0	.0	.1460	.1489	−.0029	−2.0	−.1
n-Nonacosane	27	.2763	.2737	+.0026	+0.9	+.3	.5500	.5495	+.0005	+.1	.0	.2893	.2739	+.0155	+5.4	+.4
Average deviation					±7.8	±0.5				±3.9	±0.2				±4.0	±0.1

Compound	Number of groups, $>CH_2$	8300 cm^{-1} ($>CH_2$) $\alpha=0.01681$ $\beta=0.01585$					8680 cm^{-1} ($-CH_3$) $\alpha=0.00811$ $\beta=0.00176$					8750 cm^{-1} ($>CH$) (aromatic) $\alpha=0.00327$ $\beta=0.00126$ $\delta=0.01121$				
	n_b	$K_{obs.}$	$K_{calc.}$	$\frac{K_{obs.}-K_{calc.}}{\Delta}$	$\frac{\Delta}{K_{obs.}}100$	$\frac{\Delta}{\beta}$=Number of $>CH_2$ gr.	$K_{obs.}$	$K_{calc.}$	$\frac{K_{obs.}-K_{calc.}}{\Delta}$	$\frac{\Delta}{K_{obs.}}100$	$\frac{\Delta}{\alpha}$=Number of $-CH_3$ gr.	$K_{obs.}$	$K_{calc.}$	$\frac{K_{obs.}-K_{calc.}}{\Delta}$	$\frac{\Delta}{K_{obs.}}100$	$\frac{\Delta}{\delta}$=Number of $>CH$ (arom.) gr.
n-Pentane	3	0.0836	0.0812	+0.0024	+2.9	+0.2	0.0241	0.0215	+0.0026	+10.8	+0.3	0.0138	0.0103	+0.0035	+25.4	+0.3
n-Hexane	4	.0948	.0970	−.0022	−2.3	−.1	0218	.0233	−.0015	−6.9	−.2	.0094	.0116	−.0022	−23.4	−.2
n-Heptane	5	.1122	.1128	−.0006	−0.5	.0	.0204	.0251	−.0047	−23.0	−.6	.0095	.0128	−.0033	−34.8	−.3
n-Octane	6	.1318	.1287	+.0031	+2.4	+.2	.0287	.0268	+.0019	+6.6	+.2	.0130	.0141	−.0010	−7.7	−.1
n-Nonane	7	.1405	.1445	−.0040	−2.8	−.3	.0276	.0285	−.0009	−3.2	−.1	.0147	.0154	−.0007	−4.7	−.1
n-Decane	8	.1691	.1604	+.0087	+5.4	+.6	.0339	.0302	+.0037	+10.9	+.5	.0167	.0166	+.0001	+.6	.0
n-Undecane	9	.1670	.1762	−.0092	−5.5	−.6	.0302	.0320	−.0018	−5.6	−.2	.0175	.0179	−.0004	−2.3	.0
n-Dodecane	10	.1934	.1921	+.0013	+0.1	+.1	.0348	.0338	+.0010	+2.9	+.1	.0216	.0191	+.0025	+11.6	+.2
n-Nonacosane	27	.4620	.4615	+.0005	+.1	.0	.0633	.0636	−.0003	−0.5	.0	.0402	.0406	−.0004	−1.0	.0
Average deviation					±2.4	±0.2				±7.8	±0.2				±12.4	±0.1

At 8254 cm^{-1}, only the values for *n*-octane to *n*-nonacosane were used (omitting that for *n*-decane, which is probably in error). This necessary modification of the basic concept 3, p. 134, was introduced because the residuals (excluding *n*-decane) manifest an increasing positive trend as the length of the chain is decreased.[15] A possible explanation for this fact is given in the next section. Exclusion of the values of K for *n*-pentane, *n*-hexane, *n*-heptane, and *n*-decane altered α, while β remained relatively unchanged. Thus, the entire series yielded $\alpha=0.0095, \beta=0.0196$, while the selected points gave $\alpha=0.0063$, $\beta=0.0199$. It is important to note that, though the residual for *n*-pentane at 8254 cm^{-1} is high, the error in terms of the number of the groups sought is not large.

At 8750 cm^{-1}, the large deviations of *n*-pentane, *n*-hexane, and *n*-heptane caused their exclusion, though the values of the coefficients were not greatly altered by the omission. The use of the entire series yielded $\alpha=0.00307$, $\beta=0.00128$, while the use of the higher members gave $\alpha=0.00327$, $\beta=0.00126$.

With the exception of the values at 8254 and 8750 cm^{-1}, the values of the coefficients, α and β, were derived from the entire series of normal paraffins. Since the deviations of the lower members at all other wave numbers are for the most part random, this portion of the data confirms the simple concepts 1 to 3, as stated in section II.

The other regions, 5400 to 6400 and 6400 to 7400 cm^{-1} were similarly treated using all data, and yielded results similar to those in table 1. The values of α derived for these regions are as follows: 5668 cm^{-1}, 0.1056; 5781 cm^{-1}, 0.1078; 5800 cm^{-1}, 0.1624; 5860 cm^{-1}, 0.1970; 5870 cm^{-1}, 0.1914; 5900 cm^{-1}, 0.1574; 6950 cm^{-1}, 0.00909; 6975 cm^{-1}, 0.01133; 7064 cm^{-1}, 0.01253; 7185 cm^{-1}, 0.02138; and 7350 cm^{-1}, 0.01025. The corresponding values of β are those given in table 5. For consistency in calculation, the values of the unit coefficients given throughout the paper are expressed in more significant figures than are warranted by the data. An optimistic estimate of the inaccuracy of these coefficients would be 3 to 4 percent, while the conservative value used here in analysis for the experimental error of the total molal absorption coefficient is ± 8 percent.

The coefficients, α and β, were next applied to the branched-chain paraffins, as shown in the first portion of table 2 for the wave numbers 8400 and 5860 cm^{-1}. Consistently negative deviations increasing in magnitude with the increase in number of methyl groups indicate that the value for α is too large. On inspection, no simple variation in these residuals as a function of the number of secondary ($>CH_2$) groups was apparent. Hence although the basic concept 3, p. 134 (section II) does not seem usefully valid for the methyl groups, the simplifying assumption that the value of β remains unchanged for the isoparaffins was retained.[16] It is shown later that a value, α', modified to fit the data on the isoparaffins is applicable to all the classes of hydrocarbons considered, with few exceptions. Since the identity of

[15] An equation containing three constants,

$$K=\alpha'' n_a+\beta'' n_b+\frac{\gamma''}{n_b} \tag{4}$$

was also tested for representation of the data on normal paraffins at 8254 cm^{-1}. Here the last term might be expected to eliminate the deviation for small values of n_b. But the residuals were practically unchanged.

[16] That even this is not strictly true is demonstrated when a least-squares solution is applied to the isoparaffins alone. At 8400 cm^{-1}, the coefficients thus developed were $\alpha'''=0.0260$, $\beta'''=0.0106$. In this series, the value for the unit methyl group is probably more accurately evaluated than was the case for the normal series.

the normal paraffins need never be in doubt, the efficacy of this method for the determination of the structure of hydrocarbons is not impaired and the derivation of α may be considered as merely a step in the process of obtaining the more general coefficient, α'.

It was possible, at certain wave lengths, to use α unchanged, since the residuals manifested no trends. In the event that α, from the normal paraffins, seemed unsuitable for the calculations of the total molal-absorption index, the method adopted (except at 8160 and 6950 cm^{-1}) for deriving a new unit coefficient, α', for a methyl group in the isoparaffins was as follows: After the effect of the secondary ($> CH_2$) linkages (as determined from the normal paraffins) was deducted, the sum of the remainders was divided by the total number of methyl groups, to yield a mean value for a single methyl group, α', thus

$$\alpha' = \frac{\Sigma(K_{(obs.)} - n_b)}{\Sigma n_a} \tag{5}$$

This simple method yielded residuals for the isoparaffins that were not significantly larger than those obtained by the least-squares solution (see footnote 16, p. 136). The result of applying α' and β to the isoparaffins at 8400 and 5860 cm^{-1} is found in the second or revised portion of table 2.

TABLE 2.—*Results of representing, for the branched-chain paraffins, the total molal absorption coefficient, K, as a function of the number, n_a, of primary ($-CH_3$), and, n_b, of secondary groups*

$K = n_a\alpha + n_b\beta$

Compound	Number of groups		8400 cm^{-1}					5860 cm^{-1}				
	$-CH_3$	$>CH_2$	$\alpha=0.03770$ $\beta=0.00735$					$\alpha=0.1970$ $\beta=0.0194$				
	n_a	n_b	$K_{obs.}$	$K_{calc.}$	$\frac{K_{obs.}-K_{calc.}}{\Delta}$	$\frac{\Delta}{K_{obs.}}100$	$\frac{\Delta}{\alpha}$=Number of $-CH_3$ gr.	$K_{obs.}$	$K_{calc.}$	$\frac{K_{obs.}-K_{calc.}}{\Delta}$	$\frac{\Delta}{K_{obs.}}100$	$\frac{\Delta}{\alpha}$=Number of $-CH_3$ gr.
2-Methylbutane	3	1	0.0891	0.1204	−0.0313	−35.1	−0.8	0.396	0.610	−0.214	−54.3	−1.1
2-Methylpentane	3	2	.1180	.1278	−.0098	−8.3	−.3	.524	.630	−.106	−20.3	−.6
2-Methylhexane	3	3	.1150	.1351	−.0201	−17.5	−.5	.494	.649	−.155	−31.4	−.8
2-Methylnonane	3	6	.1341	.1572	−.0231	−17.2	−.6	.550	.707	−.157	−28.6	−.8
3-Methylpentane	3	2	.1058	.1278	−.0220	−20.8	−.6	.490	.630	−.140	−28.6	−.7
3-Methylhexane	3	3	.1140	.1351	−.0211	−18.5	−.6	.512	.649	−.137	−26.8	−.7
3-Methylnonane	3	6	.1346	.1572	−.0226	−16.8	−.6	.580	.707	−.127	−21.9	−.6
4-Methylnonane	3	6	.1362	.1572	−.0210	−15.4	−.6	.557	.707	−.150	−26.9	−.8
5-Methylnonane	3	6	.1177	.1572	−.0395	−33.6	−1.0	.578	.707	−.129	−22.3	−.7
3-Ethylpentane	3	3	.1219	.1351	−.0132	−10.8	−.4	.513	.649	−.136	−26.5	−.7
3,3-Dimethylpentane	4	2	.1227	.1655	−.0431	−36.0	−1.1	.545	.827	−.282	−51.7	−1.4
2,3-Dimethybutane	4	0	.1108	.1508	−.0400	−36.1	−1.0	.517	.789	−.272	−52.6	−1.4
2,3-Dimethylpentane	4	1	.1162	.1581	−.0420	−36.1	−1.1	.551	.807	−.256	−46.5	−1.3
2,4-Dimethylpentane	4	1	.1100	.1581	−.0481	−43.7	−1.3	.602	.807	−.205	−34.1	−1.0
2,2,3-Trimethylbutane	5	0	.1195	.1885	−.0653	−54.7	−1.7	.446	.985	−.539	−120.6	−2.7
2,2,4-Trimethylpentane	5	1	.1346	.1958	−.0612	−45.5	−1.6	.611	1.004	−.393	−64.3	−2.0
3,5,5-Trimethylheptane	5	3	.1522	.2106	−.0584	−38.3	−1.5	.752	1.043	−.291	−38.7	−1.5
3,4,5,5-Tetramethylhexane	6	1	.1502	.2335	−.0833	−55.5	−2.3	.765	1.201	−.436	−57.0	−2.2
Average deviation						−30.0	−1.0				−41.8	−1.2

(Revised) $K = n_a\alpha' + n_b\beta$

(Revised) $K = n_a\alpha' + n_b\beta$

Compound	Number of groups		8400 cm⁻¹					5860 cm⁻¹				
	$-CH_3$	$>CH_2$	$\alpha'=0.02705$ $\beta=0.00735$					$\alpha'=0.1363$ $\beta=0.0194$				
	n_a	n_b	$K_{obs.}$	$K_{calc.}$	$\frac{K_{obs.}-K_{calc.}}{\Delta}$	$\frac{\Delta}{K_{obs.}}100$	$\frac{\Delta}{\alpha}$=Number of $-CH_3$ gr.	$K_{obs.}$	$K_{calc.}$	$\frac{K_{obs.}-K_{calc.}}{\Delta}$	$\frac{\Delta}{K_{obs.}}100$	$\frac{\Delta}{\alpha}$=Number of $-CH_3$ gr.
2-Methylbutane	3	1	0.0891	0.0886	+0.0005	+0.6	0.0	0.396	0.428	−0.032	−8.1	−0.2
2-Methylpentane	3	2	.1180	.0959	+.0221	+18.7	+.8	.524	.448	+.076	+14.5	+.6
2-Methylhexane	3	3	.1150	.1033	+.0117	+10.2	+.4	.494	.467	+.027	+4.9	+.2
2-Methylnonane	3	6	.1341	.1253	+.0088	+6.6	+.3	.550	.525	+.025	+4.5	+.2
3-Methylpentane	3	2	.1058	.0959	+.0099	+9.4	+.4	.490	.448	+.043	+8.8	+.3
3-Methylhexane	3	3	.1140	.1033	+.0107	+9.4	+.4	.512	.467	+.045	+8.8	+.3
3-Methylnonane	3	6	.1346	.1253	+.0093	+6.9	+.3	.580	.525	+.055	+9.5	+.4
4-Methylnonane	3	6	.1362	.1253	+.0109	+8.0	+.4	.557	.525	+.032	+5.7	+.2
5-Methylnonane	3	6	.1177	.1253	−.0077	−6.6	−.3	.578	.525	+.053	+9.2	+.4
3-Ethylpentane	3	3	.1219	.1033	+.0186	+15.3	+.7	.513	.467	+.046	+9.0	+.3
3,3-Dimethylpentane	4	2	.1227	.1229	−.0002	−.2	.0	.545	.583	−.038	−7.0	−.3
2,3-Dimethylbutane	4	0	.1108	.1086	+.0026	+2.3	+.1	.517	.545	−.028	−5.4	−.2
2,3-Dimethylpentane	4	1	.1162	.1156	+.0006	+.5	.0	.551	.564	−.013	−2.4	−.1
2,4-Dimethylpentane	4	1	.1100	.1156	−.0056	−5.1	−.2	.602	.564	+.038	+6.3	+.3
2,2,3-Trimethylbutane	5	0	.1195	.1353	−.0158	−13.2	−.6	.446	.682	−.304	(−68.2)	(−2.2)
2,2,4-Trimethylpentane	5	1	.1346	.1426	−.0080	−6.0	−.3	.611	.701	−.099	−16.2	−.7
3,5,5-Trimethylheptane	5	3	.1522	.1573	−.0051	−3.4	−.2	.752	.740	+.012	+1.6	+.1
3,4,5,5-Tetramethylhexane	6	1	.1502	.1696	−.0194	−12.9	−.7	.765	.837	−.072	−9.4	−.5
Average deviation						±7.5	±.3				±7.7	±.3

Consideration of the tertiary (>CH) groups present in the isoparaffins as absorbing entities extends the equation analogous to eq 1 to the form

$$K=n_a\alpha'+n_b\beta+n_c\gamma, \tag{6}$$

where K, n_a, n_b, α', and β follow the previous notation, and n_c represents the number of tertiary groups having the unit coefficient of absorption, γ. The coefficient, γ, was evaluated only at 8160 cm^{-1} and 6950 cm^{-1}; at all other wave numbers it was assumed to be zero.

The disregard of >CH as an absorbing group is justified by the weak absorption of the group at most wave numbers. Furthermore, the residuals at all wave numbers, examined with regard to a systematic variation of the residuals as a function of the number of >CH groups, showed no significant trends. Indeed, this group has only a weak absorption, even at its maxima (8160 and 6950 cm^{-1}), since it involves only one C—H bond, and hence, at other wave numbers, becomes very small.

At 8160 cm^{-1}, a preliminary value for the unit coefficient, γ, was obtained by subtracting from the observed molal absorption coefficient the absorption due to $-CH_3$ and $>CH_2$, using α and β, the unrevised unit coefficients derived from the normal paraffins. The remainders were, in all but a few cases, positive, and varied in magnitude with the number of >CH groups in the molecule. The sum of these remainders divided by the sum of the tertiary >CH groups yields the unit coefficient, γ.

Another value was obtained by subtracting from each observed molal absorption coefficient only the absorption attributable to secondary ($>CH_2$) groups (assuming β to be unchanged, as was done in the development of α') and applying a least-squares solution for α' and γ to the remainders. Thus, in the equation

$$K_{(obs.)}-\beta n_b=n_a\alpha'+n_c\gamma, \tag{7}$$

only α' and γ are unknown. Better agreement between observed and calculated values was obtained by the latter method, although the constant, γ, was not radically different. In the former method, using $\alpha=0.00295$ and $\beta=0.00992$, γ became 0.00921; while in the latter, with β remaining unchanged, and $\alpha'=0.00197$, γ became 0.01132.

Application of the first method to the data for 6950 cm^{-1} yielded only slightly negative residuals, which indicated that the change in the unit coefficient for methyl ($-CH_3$) was sufficient to cloak the effect of the tertiary group. However, the second method yielded reasonable unit coefficients (see table 5) and these were adopted.

Before developing δ, the unit coefficient for >CH (aromatic) absorption, it is necessary to define clearly the group to which it refers. Since, in the region 5400 to 8900 cm^{-1}, the absorption is due solely to the vibration of the C—H bonds, a benzene derivative will not show the same strength attributable to "aromatic" bonds as does the unsubstituted benzene nucleus if the absorption per >CH (aromatic) bond remains substantially constant. Furthermore, the magnitude of the absorption decreases with the number of nuclear substitutions. Hence δ is the unit coefficient for one >CH (aromatic) bond, of which benzene possesses six, toluene five, xylene four, etc. In this report, the possible consequences of the symmetry of benzene in rendering the absorption spectra unique are disregarded.

The numerical value of δ is deduced, in general, in a similar fashion to α' and γ, by deducting the absorption caused by the aliphatic groups ($-CH_3$, $>CH_2$) in the molecule and dividing the sum of the remainder by the sum of the $>CH$ (aromatic) bonds.

At all wave numbers, values of δ and δ' using α and α' were computed. The selection of the value for the unit coefficient of the $>CH$ (aromatic) bond was based on the randomness of the deviations, the value having the least trend in the residuals being considered superior. However, α' generally gave the best fit. The points at which α was used to develop δ are indicated in table 5. The effect of neglecting the unit coefficient δ (i. e., assuming that the aromatic nucleus did not contribute to the absorption) was tried at several wave numbers far removed from the maximum for aromatic absorption. Finally, the value of δ selected was that one conforming most closely with the observed data. In table 3 are given some results of using both α and α' on the series of aromatic hydrocarbons. Incidentally, the naphthenes shown were not included in the derivation of the coefficient, β.

TABLE 3.—*Results of representing, for the cycloparaffins and aromatic hydrocarbons, the total molal absorption coefficient, as a function of the number n_a, of primary ($-CH_3$), n_b, of secondary ($>CH_2$) and, n_d, of $>CH$ (aromatic) groups (unrevised coefficients also given)*

$$K = n_a\alpha' + n_b\beta + n_d\delta$$

Compound	Number of groups				8750 cm⁻¹					5900 cm⁻¹ (unrevised)					5900 cm⁻¹				
	$-CH_3$	$>CH_2$	$>CH$	Arom.	$\alpha=0.00327^a$ $\beta=0.00126$ $\delta=0.01121$					$\alpha=0.1574$ $\beta=0.0057$ $\delta=0.0651$					$\alpha'=0.1256$ $\beta=0.0057$ $\delta'=0.0764$				
	n_a	n_b	n_c	n_d	$K_{obs.}$	$K_{calc.}$	$K_{obs.}-K_{calc.}=\Delta$	$\frac{\Delta}{K_{obs.}}100$	$\frac{\Delta}{\delta}$=Number of $>CH$ (arom.) gr.	$K_{obs.}$	$K_{calc.}$	$K_{obs.}-K_{calc.}=\Delta$	$\frac{\Delta}{K_{obs.}}100$	$\frac{\Delta}{\delta}$=Number of $>CH$ (arom.) gr.	$K_{obs.}$	$K_{calc.}$	$K_{obs.}-K_{calc.}=\Delta$	$\frac{\Delta}{K_{obs.}}100$	$\frac{\Delta}{\delta}$=Number of $>CH$ (arom.) gr.
Benzene	0	0	0	6	0.0692	0.0672	+0.0020	+2.9	+0.2	0.516	0.391	+0.125	+23.2	+1.9	0.516	0.458	+0.058	+11.2	+0.8
Toluene	1	0	0	5	.0670	.0593	+.0070	+1.0	+.6	.541	.483	+.058	+10.7	+0.9	.541	.508	+.033	+6.1	+.4
Ethylbenzene	1	1	0	5	.0634	.0606	+.0029	+4.6	+.3	.524	.489	+.035	+6.7	+.5	.524	.514	+.010	+1.9	+.1
n-Propylbenzene	1	2	0	5	.0702	.0618	+.0084	+11.9	+.8	.507	.495	+.012	+23.7	+.2	.507	.519	−.012	−2.4	−.2
Isopropylbenzene	2	0	1	5	.0675	.0625	+.0050	+7.4	+.4	.569	.641	−.072	−12.7	−1.1	.569	.633	−.064	−11.2	−.8
m-Xylene	2	0	0	4	.0390	.0513	−.0123	−32.4	−1.1	.448	.576	−.128	−28.6	−2.0	.448	.557	−.109	−24.3	−1.4
o-Xylene	2	0	0	4	.0551	.0513	+.0038	+6.9	+0.3	.570	.576	−.006	−1.1	−0.1	.570	.557	−.013	−2.3	−0.1
p-Xylene	2	0	0	4	.0482	.0513	−.0031	−6.4	−0.3	.678	.576	+.102	+15.1	+1.6	.678	.557	+.121	+17.9	+1.6
Mesitylene	3	0	0	3	.0297	.0434	−.0137	−46.2	−1.2	.516	.667	−.151	−29.2	−2.3	.516	.606	−.090	−17.5	−1.2
Hemimellitene	3	0	0	3	.0494	.0434	+.0060	+12.2	+0.5	.601	.667	−.066	−11.0	−1.0	.601	.606	−.005	−0.8	−0.1
Pseudocumene	3	0	0	3	.0372	.0434	−.0062	−16.7	−0.6	.605	.667	−.062	−10.2	−1.0	.605	.606	−.001	−0.2	.0
Average deviation								±13.5	±0.6				±15.7	±1.1				±8.7	±0.6

[a] $\alpha=\alpha'$ at this point.

Compound	Number of groups			5781 cm^{-1} (unrevised)				5781 cm^{-1}			
	$-CH_3$	$>CH_2$	$\geqslant CH$	$\alpha=0.1008\ \beta=0.0908$				$\alpha'=0.0708\ \beta=0.0908$			
	n_a	n_b	n_c	$K_{obs.}$	$K_{calc.}$	$\frac{K_{obs.}-K_{calc.}}{\Delta}$	$\frac{\Delta}{K_{obs.}}100$	$K_{obs.}$	$K_{calc.}$	$\frac{K_{obs.}-K_{calc.}}{\Delta}$	$\frac{\Delta}{K_{obs.}}100$	$\frac{\Delta}{\beta}$=Number of $>CH_2$ gr.
Cyclohexane	0	6	0	0.736	0.545	+0.191	+25.9	0.736	0.545	+0.191	+25.9	+2.1
Methylcyclohexane	1	5	1	.662	.555	+.107	+16.2	.662	.525	+.137	+20.7	+1.5
Ethylcyclohexane	1	6	1	.623	.645	−.023	−3.7	.623	.616	+.007	+1.1	+0.1
Average deviation							±15.3				+15.9	+1.2
1, 2-Dimethylcyclopentane (bp 99.3°)	2	3	2	.363	.474	−.111	−30.6	.363	.414	−.051	−14.2	−0.6
1, 2-Dimethylcyclopentane (bp 91.8°)	2	3	2	.358	.474	−.116	−32.4	.358	.414	−.056	−15.7	−.6
Methylcyclopentane	1	4	1	.274	.464	−.190	−69.4	.274	.434	−.160	−58.4	−1.6
Average deviation							−44.1				−29.4	−1.0

IV. RESULTS

The results, listed under the names of the compounds, are summarized in table 4. The formulas and numbers of structural units comprising the molecule are listed in appropriate columns. The values given in this table in the columns headed primary, secondary, etc., indicate the deviations between calculated and observed ordinates of the molal absorption curves in terms of the structural units of particular interest at the wave number under which these values appear. The average deviation is shown for each series of compounds (such as isoparaffins, cycloparaffins, etc.) and is calculated as the arithmetical mean of the individual deviations. Values in parentheses have been omitted from the averages by assuming that they are mistakes.

The unit coefficients of the several groups (α', β, γ, and δ) are found in table 5, where they are arranged in order of increasing wave number.

TABLE 4.—*Summary of deviations of calculated values of the molal absorption coefficient from the observed*

TABLE 4.—*Summary of deviations of calculated values of the molal absorption coefficient from the observed values; these residuals being expressed in terms of group sought*

Compound	Formula	Number of groups				Primary $-CH_3$							Secondary $>CH_2$						Tertiary $>CH$		Aromatic ($>CH$)		
		$-CH_3$	$>CH_2$	$\gg CH$	Arom.	*5800	5860	5900	6975	7350	8400	8680	5668	5781	7064	7185	8254	8300	6950	8160	5900	8680	8750
		n_a	n_b	n_c	n_d																		
2-Methylbutane	C_5H_{12}	3	1	1	----	−0.2	−0.2	−0.3	−0.8	−0.3	0.0	−0.4	0.0	+0.3	−0.7	+0.3	+0.1	+0.2	−1.5	+0.1	−0.5	−0.5	−0.2
2-Methylpentane	C_6H_{14}	3	2	1	----	+.4	+.6	+.2	+.2	−.3	+.8	+.2	+.1	+.2	−.1	−.4	+.2	+.3	+.8	+.3	+.3	+.2	−.2
2-Methylhexane	C_7H_{16}	3	3	1	----	+.2	+.2	+.7	+.4	+.1	+.4	+.5	.0	+.2	+1.2	+.9	+.3	+.7	+.2	+.2	+1.2	+.5	+.2
2-Methylnonane	$C_{10}H_{22}$	3	6	1	----	+.3	+.2	+.1	.0	−.3	+.3	.0	+.3	−.6	+.2	−.3	+.3	+.7	.0	+1.1	+.1	.0	−.3
3-Methylpentane	C_6H_{14}	3	2	1	----	+.8	+.3	−.1	+.9	−.1	+.4	+.4	+1.4	+.9	+1.0	+.7	+.8	+1.2	−2.1	+.7	−.2	+.5	+.1
3-Methylhexane	C_7H_{16}	3	3	1	----	+.4	+.3	+.1	+.1	+.1	+.4	−.1	.0	+.1	−.7	+.5	−.1	−1.5	−.2	−.2	+.2	−.1	+.1
3-Methylnonane	$C_{10}H_{22}$	3	6	1	----	+1.0	+.4	+.6	−.2	−.2	+.3	+.1	+.2	.0	−.3	−.1	−.2	+.4	−.9	+.1	+1.0	+.1	.0
4-Methylnonane	$C_{10}H_{22}$	3	6	1	----	−.1	+.2	+.4	−.1	.0	+.4	+.8	−.6	−1.1	−.5	−.1	−.2	+.5	−1.0	+.4	+.6	+.8	−.1
5-Methylnonane	$C_{10}H_{22}$	3	6	1	----	−.5	+.4	+.3	−.2	−.5	−.3	−1.4	−.2	−.9	.0	−.2	−.6	−.5	−.4	+.4	+.5	−1.4	−1.1
3-Ethylpentane	C_7H_{16}	3	3	1	----	+.3	+.3	.0	−.7	−.1	+.7	+.4	−.2	−.4	−1.3	+.3	−.5	+.2	−2.0	−1.2	.0	+.4	+.3
3,3-Dimethylpentane	C_7H_{16}	4	2	0	----	−.9	−.3	.0	−.4	−.2	.0	−.3	−.3	−.4	−.8	.0	−.7	−1.1	+1.0	−.7	.0	−.4	.0
2,3-Dimethylbutane	C_6H_{14}	4	0	2	----	+.4	−.2	−.7	(+2.2)	−.7	+.1	−.2	(+2.8)	+1.1	+1.1	+.1	+1.7	+1.8	+2.2	+.8	−1.2	−.2	−.1
2,3-Dimethylpentane	C_7H_{16}	4	1	2	----	.0	−.1	+.3	+.4	+.4	.0	−.1	+.3	+.3	+.1	+.6	−.1	−.3	+.6	−.4	+.5	−.1	+.2
2,4-Dimethylpentane	C_7H_{16}	4	1	2	----	−.2	+.3	+.1	+.5	−.2	−.2	−.3	+.1	+.4	+.6	−.1	−.2	−1.0	+.2	−.7	+.2	−.3	−.2
2,2,3-Trimethylbutane	C_7H_{16}	5	0	1	----	−1.3	(−2.2)	−.6	−.4	−.1	−.6	.0	−1.4	−.1	−1.7	−1.4	−.6	−1.0	+1.1	−.1	−1.0	.0	+.4
2,2,4-Trimethylpentane	C_8H_{18}	5	1	1	----	−1.7	−.7	−1.1	.0	+.6	−.3	+.4	−1.8	−.7	−.1	−.2	+.1	−.3	+1.5	−.2	−1.8	+.4	+.2
3,5,5-Trimethylheptane	$C_{10}H_{22}$	5	3	1	----	−.9	+.1	+.9	−1.2	+.7	−.2	+.3	−.7	−.4	−1.7	−.2	−1.3	−1.4	−1.1	−1.0	−1.5	+.3	+.3
3,4,5,5-Tetramethylhexane	$C_{10}H_{22}$	6	1	2	----	−1.1	−.5	−.2	−.5	+.5	−.7	.0	−.7	−.1	−1.3	−.2	−.2	−.5	−.4	−1.1	−.4	.0	+.3
Average deviation						±.6	±.3	±.4	±.4	±.3	±.3	±.3	±.5	±.5	±.7	±.4	±.5	±.8	±1.0	±.5	±.6	±.3	±.2
Cyclohexane	C_6H_{12}	0	6	0	----	+1.6	+.2	+.2	−.6	−.4	+1.0	−.1	−.2	+2.1	−.8	+.1	−.2	+2.0	−1.0	−.2	+.4	−.1	−.3
Methylcyclohexane	C_7H_{14}	1	5	1	----	+.5	−.3	−.1	+.1	−.2	+.3	−.3	+1.2	+1.5	−1.5	+.2	−.2	+1.2	−.8	+.3	−.1	−.3	−.4
Ethylcyclohexane	C_8H_{16}	1	6	1	----	+1.2	+.4	+.7	−.6	−.4	+.5	−.4	−.9	+.1	−.4	+.2	−.5	+.9	−1.9	+.2	+1.2	−.4	−.3
Average deviation						+1.1	±.3	±.3	±.4	−.3	+.6	−.3	±.8	+1.2	−.9	+.2	−.3	+1.4	−1.2	±.2	±.6	−.3	−.3
1,2-Dimethylcyclopentane (bp. 99.3°)	C_7H_{14}	2	3	2	----	−.2	+.4	+1.0	−.7	.0	+.8	−.4	+.8	−.6	−1.4	−1.6	−.8	.0	−2.1	−1.4	+1.6	−.5	−.1
1,2-Dimethylcyclopentane (bp. 91.8°)	C_7H_{14}	2	3	2	----	.0	+.1	+.7	−.2	−.1	+.4	−.2	−.5	−.6	−.2	−1.2	−1.2	−.9	−1.7	−2.0	+1.1	−.2	−.4
Methylcyclopentane	C_6H_{12}	1	4	1	----	−.3	+.9	+1.4	−.5	+.7	+1.2	−1.6	−.1	−1.8	−.7	−1.4	−1.4	−.5	−1.5	−1.5	+2.3	−1.5	+.2
Average deviation						−.2	+.5	+1.0	−.5	±.3	+.8	−.3	±.5	−1.0	−.8	−1.4	−1.1	−.5	−1.8	−1.6	+1.7	−.7	±.2

* Wave number values in cm^{-1}

TABLE 4.—*Summary of deviations of calculated values of the molal absorption coefficient from the observed values; these residuals being expressed in terms of group sought*—Continued

Compound	Formula	Number of groups				Primary $-CH_3$					Secondary $>CH_2$					Tertiary $\geq CH$	Aromatic ($>CH$)		
		$-CH_3$	$>CH_2$	$\geq CH$	Atom.	*5800	5860	5900	6975	7350	8400	8680	5668	5781	7064	7185	8254	8300	6950	8160	5900	8680	8750
		n_a	n_b	n_c	n_d																		
Benzene	C_6H_6	0	0	---	6																		
Toluene	C_7H_8	1	0	---	8	+2.3	+.4	+.3	+.8	-.3	+.1	-3.2	-.9	-.2	.0	+.7	+.2	+.1	.0	+.2	+.8	-3.4	+.2
Ethylbenzene	C_8H_{10}	1	1	---	5	-.3	+.4	+.3	+.5	.0	+.1	-.8	-.1	+.5	+.4	+.4	.0	+.1	+1.1	+.1	+.4	-.8	+.6
n-Propylbenzene	C_9H_{12}	1	2	---	5	-.3	-.2	+.1	-.4	-.6	+.5	-2.0	+.2	-.8	----	-.5	-.3	+.5	----	-.2	-2.1	+.6	+.3
Isopropylbenzene	C_9H_{12}	2	0	---	5	-.6	-.3	-.1	-.7	-.3	+.7	+.6	-.7	-.9	-.5	+.1	-.1	+.7	-1.0	-.1	-.2	-.8	+.8
m-Xylene	C_8H_{10}	2	0	---	4	-.6	-.3	-.5	-.3	-.3	+.4	-1.0	+.7	-.8	-.2	-.4	-.1	+.4	-1.1	+.3	-1.4	-.3	+.4
o-Xylene	C_8H_{10}	2	0	---	4	-.6	-.3	-.1	.0	.0	.0	-1.0	-.2	+.8	+.4	.0	+.3	.0	-1.4	+.3	-1.1	-1.1	+.8
p-Xylene	C_8H_{10}	2	0	---	4	+.3	-.1	+1.0	+.1	.0	-.1	+2.7	+.1	+.6	+.1	+.4	-.3	-.1	+.1	-.1	+1.6	+2.9	-.3
Mesitylene	C_9H_{12}	3	0	---	3	+.6	+.6	+.7	+.7	+.4	+.4	+2.2	+.9	-1.2	.0	-.1	+.1	+.4	-.1	-.2	-1.2	+2.4	-1.2
Hemimellitene	C_9H_{12}	3	0	---	3	-.5	-.6	.0	-.3	+.3	-.6	+.3	+.5	+.3	+.4	-.7	+.2	-.6	-.5	-.3	-.1	+.4	+.5
Pseudocumene	C_9H_{12}	3	0	---	3	-.1	+.1	.0	-.6	-.5	-.1	+1.3	+.9	-.1	+.9	-.1	+.3	-.1	+.3	+.4	.0	+1.4	-.6
Average deviation	----------	---	---	---	---	±.5	±.4	±.4	±.4	±.3	±.3	±1.3	±.5	±.6	±.2	±.4	±.2	±.3	±.5	±.2	±.6	±1.4	±.6
1-Phenyl-*n*-octadecane	$C_{24}H_{44}$	1	17	0	5	+1.3	+.4	+.4	-.6	-1.5	+.1	-2.0	+.6	+.3	-.3	-1.1	-1.3	-.3	-1.6	-.9	+1.0	-2.6	-1.8
1-Cyclohexyl-*n*-octadecane	$C_{24}H_{46}$	1	22	1	0	+1.6	+.6	+.6	-.9	-1.5	+.5	-1.8	+1.3	-.4	-2.1	-1.8	+.4	+.8	-2.6	+.8	+1.4	-2.0	-1.3
5-Cyclohexyl-*n*-docosane	$C_{28}H_{56}$	2	24	2	0	+2.5	+.6	+.6	-.1	-1.4	+.5	-1.3	-2.3	+3.7	-1.6	-1.9	+.3	-1.0	-3.9	-1.0	+1.5	-1.7	-1.0
1-(7-Tetrahydronaphthyl)-*n*-octadecane	$C_{24}H_{44}$	1	21	0	5	+1.6	+.7	+.7	-.8	-1.4	+.8	+.7	+3.7	-.2	+1.1	-1.9	-1.4	+.6	-1.8	+2.3	+1.8	+.9	-1.9
5-(7-Tetrahydronaphthyl)-*n*-docosane	$C_{32}H_{56}$	2	23	1	5	+1.5	+.6	+.6	-1.2	-1.5	+1.2	+.8	+1.3	-.1	-1.1	-1.1	-1.0	+1.2	-3.8	-.2	+1.6	+1.1	-2.4
5-(7-Tetrahydronaphthyl)-*n*-docosene-5	$C_{32}H_{54}$	2	22	(1)	3	+1.8	+.9	+.9	.0	-1.0	+1.0	+.2	+2.0	-1.2	+.5	-1.4	-1.7	+.7	-1.1	+.6	+2.3	+.2	-2.1
5-(2-Decahydronaphthyl)-*n*-docosane	$C_{32}H_{66}$	2	26	4	0	+3.8	+.5	+.5	-.6	-3.0	+.8	-1.4	+4.1	(+5.8)	+.7	-.9	+.1	+2.4	-5.3	+.4	+1.1	-1.9	-1.4
1-(*p*-Diphenyl)-*n*-octadecane	$C_{36}H_{44}$	1	17	0	9	+1.6	-1.0	-1.0	-.7	-1.6	+.3	-2.0	-.4	+.2	+.7	-1.0	-.9	-.2	-2.3	+.2	-2.4	-2.6	-.3
5-(*p*-Diphenyl)-*n*-docosene-5	$C_{40}H_{62}$	2	18	(1)	9	+.7	-.9	-.9	(+4.2)	-.9	+.2	-2.4	-1.3	-.9	(+11.1)	+.7	-1.7	-.6	(+6.1)	-.6	+.4	-3.1	+.4
Average deviation	----------	---	---	---	---	±1.5	±.7	±.7	-.6	-1.5	+.5	±1.4	±1.8	±.6	±1.1	1.3	1.3	±.8	-2.8	±.8	±1.7	±1.8	±1.4

* Wave number values in cm^{-1}

TABLE 5.—*Values of unit coefficients of the various groups at the indicated wave numbers*

Wave number	Group sought	$-CH_3$	$>CH_2$	$\geqslant CH$	$>CH$ (aromatic)
cm^{-1}		α'	β	γ	δ
5668	$>CH_2$	0.0529	0.0638		0.0216
5781	$>CH_2$	.0708	.0908		.0137
5800	$-CH_3$	.1052	.0674		.0138
5860	$-CH_3$	.1363	.0194		[b].0314
5870	$-CH_3$	.1426	.0130		.0376
5900	$-CH_3$, $>CH$ (aromatic)	.1256	.0057		.0764
6950	$\geqslant CH$	.00718	.00748	0.00532	.00175
6975	$-CH_3$	.00948	.00776		[b].00136
7064	$>CH_2$	.01253	.00956		.00134
7185	$>CH_2$	.01791	.00978		.00118
7350	$-CH_3$	.01025	.00164		.00184
8160	$\geqslant CH$	.00197	.00992	.01132	
8254	$>CH_2$	.00629	[a].01989		
8300	$>CH_2$, $-CH_3$	.00948	.01585		
8400	$-CH_3$	.02705	.00735		
8680	$-CH_3$	.00663	[a].00176		.00622
8750	$>CH$ (aromatic)	.00327	.00126		.01121

[a] Developed using C_8 to C_{20} (omitting C_{10}).
[b] Developed by using α.

The method used in table 4 for expressing the correspondence between the observed and calculated data is best suited to the present purpose. The principal factor that fixes the accuracy is the percentage transmission. Since there are optimum values for the ratio I/I_0, the concentration of a compound under investigation is adjusted so that its maximum of absorption lies within certain limits. Consequently, a homologous series such as the normal paraffins, for which the maximum does not shift appreciably, has the same percentage error for the various members at any specific wave number. However, the error for one compound at different wave numbers within a single region is more nearly absolute than relative, and comparisons at the same wave number between compounds having maxima at different wave numbers can not be made on a basis of percentage error.

It should be noted that several effects combine to give less accuracy in the regions 5400 to 6400 cm^{-1} and 6400 to 7400 cm^{-1} than in the region 7900 to 8900 cm^{-1}. These are as follows: (1) The steepness of the curves that causes large errors if, when reading the photographic plate of the automatically recorded transmission curve, the proper position with respect to the fiducial point is not maintained; (2) the greater complexity of the regions 5400 to 6400 cm^{-1} and 6400 to 7400 cm^{-1}; (3) the proximity of the points at which maxima of absorption for the various groups appear; and (4) the absorption of atmospheric water in the region 6400 to 7400 cm^{-1}.

TABLE 6.—*List of wave numbers*

[Arranged according to groups for which used; with comments.]

Group sought	Wave number	Remarks
$-CH_3$	8400	Maximum for $-CH_3$; best point.
$-CH_3$, $>CH_2$	8300	Excellent check point.
$-CH_3$	5900	Maximum for $-CH_3$; strong absorption by $>CH$ (aromatic).
$-CH_3$	5860	Maximum for $-CH_3$.
$-CH_3$	5870	Check point.
$-CH_3$	6975	Do.
$-CH_3$	7350	Do.
$>CH_2$	8254	Maximum for $>CH_2$; best point.
$>CH_2$	5781	Maximum for $>CH_2$.
$>CH_2$	5668	Naphthenes different at this point.
$>CH_2$	5800	Do.
$>CH_2$	7185	Check point.
$>CH_2$	7075	Affected by substitution; check point.
$>CH$	8160	Maximum for $>CH$; best point.
$>CH$	6950	Check point.
$>CH$ (aromatic)	8750	Maximum for $>CH$ (aromatic); best point.
$>CH$ (aromatic)	8680	Check point. Second maximum of $-CH_3$.
$>CH$ (aromatic)	5900	Check point; strong absorption by $-CH_3$.

The region 5,400 to 6,400 cm^{-1} does have the advantage that the proper concentration is one-fifth that of the other regions. This reduces the opportunity for departures from Beer's law [31, 34].

In table 6 the wave numbers are listed in order of importance with respect to the various groups, together with appropriate remarks concerning conditions at that particular wave number.

V. DISCUSSION

1. NORMAL PARAFFINS

The normal paraffins show, in general, excellent agreement with the calculated results (see table 1). The average deviations are less than one structural group. However, the lower members (*n*-pentane to *n*-heptane) exhibit, in most cases, an anomalous behavior. The occurrence of larger deviations in the case of the smaller molecules rather than of the larger ones is to be expected because the latter are composed mainly of "average" $>CH_2$ groups, in the sense that these units may be considered equivalent to each other and unaffected by lengthening of the chain (i. e., the intramolecular environment is more constant on the average). The remainder of the variations, excepting those for *n*-decane, are well within the experimental precision. No alternating effects (caused by an odd or even number of carbon atoms in the chain) are noticeable.

2. ISOPARAFFINS

The data for the isoparaffins do not agree, in general, as well as those for the normal paraffins. The values appearing in table 5 as α' were used in all cases tabulated in table 4. However, comparison of these values with the values of α listed in section III reveals that at 7064, 7350, 8254, and 8750 cm^{-1}, α' is identical with α. In these instances, the algebraic sums of the residuals resulting from the application to the isoparaffins of the coefficients, α and β, developed for the normal paraffins were almost zero. The equality of α and α'

at these points may be explained either by saying that the decrease usually encountered in α by passing from a normal paraffin to an isoparaffin is offset by an increase in the coefficient for some other group (see next paragraph), or that the mode of vibration associated with absorption at these wave lengths is unchanged when the methyl ($-CH_3$) group is shifted from the end of the chain to some intermediate position.[16a]

The true hybrid nature of α' should be emphasized. Some of the methyl groups used in its derivation probably have the same value as those in the normal paraffins. It is reasonable to suppose that the single methyl group at the extremity of 2-methylnonane is the same as a methyl group in *n*-nonane. Actually, a differentiation can be made between "normal" methyl groups ($-CH_2-CH_3$) and "iso" methyl groups ($-CH\langle^{CH_3}_{CH_3}$). This effect may explain the fact that there is a negative trend of the residuals in the revised data on the isoparaffins as the proportion of methyl groups increases, showing that the average coefficient is too great when the ratio of "iso" to "normal" methyl groups becomes large. Thus, strictly, there can be at least two types of methyl groups with their respective coefficients.[17]

Practically, the simplification attained by the retention of a single average coefficient for any group is necessary where unknowns are to be analyzed. Due regard for the deviations in the data on similar structures previously studied permits a comparison to be made between an unknown compound of low molecular weight and an assumed structure. The author believes that as additional data are accumulated distinctions can logically be made between the types of methyl groups. However, the present data do not furnish justification for these refinements. The series of methylnonanes should furnish opportunity for the discrimination between the two types of methyl groups. For example, 2-methylnonane contains two "iso" and one "normal" methyl groups, while 5-methylnonane has one "iso" and two "normal" methyl groups. The other isomers are intermediate and conceivably might be a means of evaluating the distance over which interaction between two methyl groups can be exerted. Inspection of table 4 conclusively shows that the variations between the methylnonanes are of the order of the experimental error.

Theoretical considerations would also demand an investigation concerning the change of value for $>CH_2$ groups with respect to the relative position of the nearest $-CH_3$ group. The method employed for the derivation of α' takes no cognizance of such corresponding possible variations in β but imposes the effects on α'. Moreover, included in α' is the absorption, if any, due to $\gtrless CH$ groups (except at 6950 and 8160 cm^{-1}). Thus, owing to the structure of the majority of the compounds studied, α' may represent more nearly the value for the group $HC(-CH_3)$. The presence of the various types of methyl groups will modify the composite value of α'.

The analysis for tertiary ($\gtrless CH$) groups is poor in contrast with the other groups. This is to be expected since the group contains only one C—H bond, and its absorption is therefore relatively weak.

[16a] See Wulf [37] for a discussion of this point.

[17] A third type would be that in which two methyl groups are joined to the same carbon atom of a chain. Minor effects might also be noticed due to the proximity of other methyl groups (i. e., a 2,3-dimethyl compound).

Even at its maximum, the majority of the absorption is due to other groups and inaccuracies in the total molal absorption coefficient cause considerable errors in the analysis for tertiary groups. Fair results are obtained at the wave number 8160 cm^{-1}.

3. NAPHTHENE AND AROMATIC HYDROCARBONS

The results for the naphthenes indicate a slight departure from the values of the unit coefficients developed for the paraffin hydrocarbons. It has been previously noted by Liddel and Kasper [2] that naphthenic secondary ($>CH_2$) groups are not exactly equivalent to similar paraffinic groups.

A critical source of error in the results for the naphthenic as well as the aromatic hydrocarbons lies in the inadequate number of compounds available for study. Unsubstituted rings, such as benzene and cyclohexane, do not necessarily furnish a basis for unit coefficients, since substitution, by destroying their symmetry, may lead to different behavior. Furthermore, the unit coefficient for a $-CH_3$ group joined directly to the ring is not necessarily the same as that found in aliphatic compounds. This obviates the possibility of any study of the ring if the absorption of the $-CH_3$ groups is proportionately large. It was observed in a previous paper [18] and substantiated in this paper (see table 3) that the mono-substituted alkyl benzene derivatives have absorption spectra that are more constant as to position and magnitude of the maxima arising from the aromatic bonds than do the polysubstituted derivatives.[18] Consequently, data are needed on a greater number of mono-substituted derivatives of both the naphthenes and aromatics before the analysis of such structures can be as satisfactory as that for the paraffin hydrocarbons.

An additional factor complicating the investigation of the polysubstituted derivatives of the cyclic hydrocarbons is the dissimilarity between the spectra of isomers obtained by varying the positions of the substituents on the nucleus. The existence of interaction with mutual alterations may be demonstrated by studying the absorption spectra of compounds in regions where either the nucleus or the substituent groups do not absorb. Thus Barnes [40] found that the absorption of benzene is modified not only by the replacement of a hydrogen atom by halogen but also by a variation in halogen (chlorine to bromine). Wulf and coworkers [36, 41], in a study of OH and NH bonds, have recorded absorption spectra which vary with the spatial distribution of the absorbing groups on the inactive nucleus (i. e., catechol, resorcinol, and hydroquinone; the *o*-,*m*-, and *p*-phenylenediamines; and the benzidines). A theoretical explanation for such effects has been furnished by Pauling [43]. No doubt similar effects of lesser magnitude are manifested in the cyclic hydrocarbons and influence the absorption of both the nucleus and the substituent groups.

Notwithstanding such theoretical possibilities, the criterion for the validity of the method given in this paper lies in the degree of concordance obtained by the practical application. Inspection of table 4

[18] This fact has also been observed by Barnes [40] for the region of the fundamental. Using the very high resolving power of an echelette grating, he recorded the percentage transmission of benzene and some of its derivatives for the region 3.0 to 3.6 μ. Only a small shift (0.007 μ) was noted in the benzene bands of mono-substituted alkyl derivatives while the relative intensities of these bands were not greatly changed. The xylenes, however, showed dissimilarities not only from benzene but among themselves.

reveals that a correct analysis for most of the aromatic hydrocarbons and a nearly correct analysis for the naphthenes can be expected after careful selection of the proper wave lengths. Some uncertainty is, however, attached to the method in the case of naphthenes of low molecular weight. Further data on longer chain derivatives would, the author believes, permit removal of the present discrepancies.

4. HYDROCARBONS OF HIGH MOLECULAR WEIGHT

The hydrocarbons of high molecular weight are an excellent test of the agreement of experimental with calculated molal absorption coefficients. Since these compounds were not used in the development of the unit coefficients, the agreement of the values cannot be ascribed to the manner in which the constants were evaluated. From table 4 it is apparent that the number of groups is accurate in the more favorable instances to ± 1 group. The average percentage deviations (not shown) are generally ± 8 percent, which is roughly the experimental error. A more exact analysis of such large molecules can be expected with improved experimental technique.

The hydrocarbons studied include several structural groups concerning which there is no available information from the present data. The olefin bonds in two of the compounds are of minor importance as only one C—H is involved, unless the unsaturated bond affects adjacent groups. These bonds are indicated in the column for $>CH$ groups and are italicized since they were neglected in the computations. As observed in the previous paper [18], the C—H bonds in the benzenoid ring of tetrahydronaphthalene are not necessarily equivalent to similar bonds in benzene. The fact that the tetrahydronaphthyl derivatives alone show positive deviations at 8680 cm^{-1}, and, in general have higher negative deviations at 8750 cm^{-1}, substantiates the hypothesis [18] that the maximum of absorption for the "aromatic" portion of the tetrahydronaphthyl nucleus has shifted to lower wave numbers.

The consistently negative deviations for almost all the compounds at 7185 and 8254 cm^{-1} can be explained as a modification of the absorption coefficients for the $>CH_2$ groups,[19] owing to the proximity of the cyclic nuclei. Although these deviations are still within the experimental error, the fact that they are not random is significant. Their virtually constant value precludes the possibility of their dependence upon structural variables other than one common to all.

At the wave numbers 5668 and 5800 cm^{-1}, the deviations of the partially and totally hydrogenated ring structures can be correlated with the number of secondary ($>CH_2$) groups included in the ring. Possibly in the other regions there are similar wave numbers at which data were not calculated. This behavior might furnish a method for distinguishing between paraffinic and naphthenic secondary groups. It would, however, first be necessary to establish that the two types of bonding are equivalent at one wave length and different at another.

[19] See footnote 8, p. 132.

VI. DETERMINATION OF THE NUMBER AND KIND OF STRUCTURAL GROUPS IN UNKNOWN HYDROCARBONS

1. GENERAL PROCEDURE

In utilizing the present analytical method to determine the number and kind of structural groups in unknown hydrocarbons, the following procedure is used:

1. Measurement is made of the transmission of the given hydrocarbon in solution in carbon tetrachloride in the regions 6400 to 7400 cm^{-1}, 7900 to 8900 cm^{-1}, and 5400 to 6400 cm^{-1}, with the concentration so adjusted that the transmission lies in the limits 40 to 60 percent [2, 34].

2. The transmission curves are reduced to curves of total molal absorptive index, K, [2, 34].

3. For the given wave numbers selected for determining the various structural groups, values of the total molal absorptive index, K, are recorded.

4. Combination of these experimental values of K with the values of the unit coefficients, α', β, γ, δ at the appropriate wave numbers, yields a series of simultaneous equations, of the general form,

$$K=n_a\alpha'+n_b\beta+n_c\gamma+n_d\delta \tag{8}$$

5. These simultaneous equations are solved to obtain values for n_a, n_b, n_c, and n_d, the number of $-CH_3$, $>CH_2$, $\geqslant CH$, and $>CH$ (aromatic) groups respectively. To each value so obtained an estimated uncertainty is assigned.

6. These values of the various structural groups are checked by calculating the total molal absorption index at wave numbers where the use of simultaneous equations is not feasible because of physical indeterminacy.

In practice, a simplification of rule 5 may be effected. A visual inspection can be made of the molal absorption curve to determine if absorption due to aromatic bonds in the molecule is evident. In the absence of significant absorption in the region near 8750 cm^{-1}, the series of simultaneous equations except those for 8160 and 6950 cm^{-1} may be reduced to two unknowns, the number of methyl ($-CH_3$) groups, n_a, and of methylene ($>CH_2$) groups, n_b. After properly evaluating n_a and n_b, the number of tertiary ($\geqslant CH$) groups may be calculated from data on K at 8160 and 6950 cm^{-1}. The assumed absence of aromatic bonds in the molecule should be verified by a comparison at 8750 cm^{-1} of the observed total molal absorption coefficient with the value calculated from the various aliphatic bonds.

When, however, "aromatic" absorption appears to be present, a series of simultaneous equations involving α', β, γ, and δ should be set up and solved.

The accuracy of the final result is determined by assigning to the total molal absorption index an error of ± 8 percent. This error is carried through the equations in absolute value and finally converted into terms of the group sought.

When all the desired values for n_a, n_b, n_c, and n_d have been calculated, they are carefully considered in connection with the following

expressions, which can be written from a knowledge of the molecular weight and the carbon-hydrogen content of the unknown hydrocarbon:

$$C_nH_{(2n+x)} \tag{9}$$

$$n_a+n_b+n_c+n_d \leq n \tag{10}$$

$$3n_a+2n_b+n_c+n_d=2n+x \tag{11}$$

If there are present carbon atoms to which no hydrogen atoms are joined, the total number of carbon atoms calculated from the infrared spectra will be less than the number, n, from the molecular weight. Obviously, the total number of carbon atoms can never be greater than the number fixed by the molecular weight. Under any conditions, eq 11 must hold. These equations are essentially "material" balances, eq 10 relating to carbon and eq 11 to hydrogen.

2. EXAMPLE: DETERMINATION OF THE STRUCTURE OF AN UNKNOWN ISOMERIC NONANE

The foregoing procedure is illustrated by its application to the determination of the number and kind of structural groups in an unknown "isononane" which was recently isolated from a midcontinent petroleum by White and Rose [42].

Figure 2 shows the curves of the molal absorptive index for the given unknown "isononane" for the regions

5400 to 6400 cm^{-1}, 6400 to 7400 cm^{-1}, and 7900 to 8900 cm^{-1}.

From the values of the molal absorptive index, K, obtained from these curves and values of the unit coefficients, α', β, γ, given in table 5, the following system of equations may be written

At 5668 cm^{-1}	0.465	$=0.0529$	$n_a+0.0638$	n_b		(11a)
5781	.608	$=$ .0708	n_a+ .0908	n_b		(11b)
5800	.632	$=$ .1052	n_a+ .0674	n_b		(11c)
5860	.599	$=$ .1363	n_a+ .0194	n_b		(11d)
5900	.535	$=$ .1256	n_a+ .0057	n_b		(11e)
6975	.0595	$=$ .00948	n_a+ .00776	n_b		(11f)
7064	.0793	$=$ .01253	n_a+ .00956	n_b		(11g)
7185	.0960	$=$ .01791	n_a+ .00978	n_b		(11h)
7350	.0411	$=$ .01025	n_a+ .00164	n_b		(11i)
8254	.0808	$=$ .00629	n_a+ .01989	n_b		(11j)
8400	.1230	$=$ .02705	n_a+ .00735	n_b		(11k)

In solving, the equations have been paired as follows for methyl ($-CH_3$): 11d, 11e; 11e, 11a; 11e, 11b; 11f, 11k; 11j, 11k; 11c, 11d; 11c, 11i; 11f, 11i; for methylene ($>CH_2$) 11e, 11b; 11e, 11a; 11h, 11j; 11e, 11j; 11j, 11k; 11c, 11d; 11c, 11j. The above pairings were found to be the most favorable combinations of the unit coefficients to yield accurate values of the group sought. Other pairings either gave indeterminate solutions or included wave numbers where the analysis was not accurate.

In table 7 are given the results of the solution of the above simultaneous equations. The values of the groups are given in the order of decreasing reliability as judged by the error. The error is expressed in terms of unit groups and is found as explained in the preceding section. Under "wave numbers used" are listed the points at which data were taken to furnish the two equations whose solution yielded

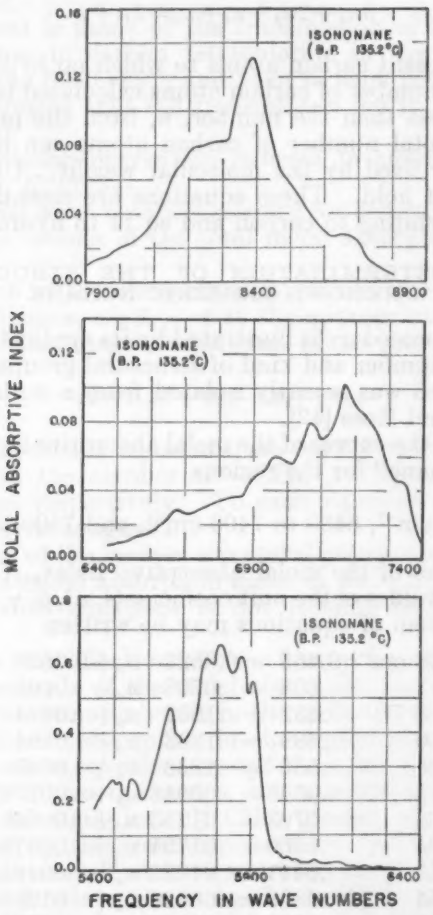

FIGURE 2.

the value shown. In only a few instances was a single pair of equations favorable to the determination of both methyl ($-CH_3$) and methylene ($>CH_2$) groups. Where indeterminate results were obtained, the values have been omitted from consideration. From table 7, the number of $-CH_3$ groups, n_a, is fixed as four and the number of $>CH_2$ groups as three.

In table 8, the same data are treated in a different manner. Where methyl ($-CH_3$) groups are to be determined, the integral value of methylene ($>CH_2$) groups is assumed (as determined from table 7) and vice versa. Both $-CH_3$ and $>CH_2$ groups are assumed to find the number of tertiary ($\gtrless CH$) groups.

TABLE 7.—*Results of solution of the simultaneous equations 11a to 11k*

Calculated number of groups	Wave numbers used
METHYL ($-CH_3$)	
4.10±0.35	5900, 5781
3.77± .40	8254, 8400
4.20± .50	5860, 5900
3.94± .47	5800, 5860
3.69± .55	6975, 8400
4.08± .35	5900, 5668
3.35± .51	5800, 7350
3.46± .42	6975, 7350
METHYLENE ($>CH_2$)	
2.87±0.36	8254, 8400
2.76± .33	8254, 5900
2.86± .43	8254, 7185
2.71± .45	8254, 5800
3.50± .63	5900, 5781
3.91± .67	5900, 5668
3.23±1.19	5800, 5860

TABLE 8.—*Results of application of integral values of groups sought to data at all available wave numbers*

Wave number	Molal absorptive index			Calculated number of groups
	$K_{obs.}$	$K_{calc.}$	% Error	
METHYL ($-CH_3$)				
5800	0.632	0.623	+1.4	4.1 ±0.48
5860	.599	.603	−0.7	4.0 ± .35
5900	.535	.520	+2.8	4.1 ± .34
6975	.0595	.0612	−1.2	3.9 ± .50
7350	.0411	.0459	−11.7	3.5 ± .32
8400	.1230	.1302	−5.9	3.8 ± .36
8680	.0263	.0318	----------	(3.2) ±(.6)
METHYLENE ($>CH_2$)				
5668	0.465	0.403	+13.3	4.0 ±0.58
5781	.608	.556	+8.6	3.6 ± .54
7064	.0793	.0788	+0.6	3.1 ± .66
7185	.0960	.1009	−5.1	2.5 ± .79
8254	.0808	.0848	−5.0	2.8 ± .33
8300	.0824	.0869	−5.5	2.7 ± .42
TERTIARY (>CH)				
6950	0.0571	0.0618	−8.2	1.1 ±0.86
8160	.0643	.0603	+6.2	2.4 ± .45
AROMATIC (>CH)				
5900	0.535	0.520	----------	----------
8680	.0263	.0318	----------	----------
8750	.0097	.0169	----------	----------

The results are in excellent agreement for a compound having these values: $n_a=4$, $n_b=3$, $n_c=2$. The compound is therefore an isononane having two branches not joined to the same carbon atom. The first conclusion is reached from the number of methyl ($-CH_3$) groups, while the latter is concluded from the number of secondary ($>CH_2$) and tertiary ($\geqslant CH$) groups. The unknown must thereby be a dimethylheptane or a methylethylhexane where the two substitutions are on different carbon atoms.

Actually, the given isononane has been lately identified as 2,6-dimethylheptane, on the basis of a comparison of its boiling point, freezing point, density, and refractive index with those of a synthetic sample of 2,6-dimethylheptane prepared by Calingaert and Soroos in the laboratories of the Ethyl Gasoline Corporation.[20]

3. LIMITATIONS OF THE METHOD

In connection with the application of the present method to unknown hydrocarbons, the following limitations should be pointed out: (a) Because of the assumed experimental uncertainty of about ± 8 percent, the uncertainty in the deduced value for the number of a given kind of group may be more than one if the number of the given kind of group is large or if the group is of low absorbing power. (b) The assumption of the equivalence of various isomeric structures known to differ somewhat in their absorption is a weakness of the method. However, unless a compound is an extreme example of such a type with the consequent multiplication of a minor effect, a correct analysis can still be made. (c) The possibility always exists that a compound of radically different structure not yet measured would reproduce the absorption curve of one of the substances included in or extrapolated from this study. Although the use of "check" points minimizes this possibility, the further accumulation of data on different types of hydrocarbons will materially increase the reliability of this method.

The development of the ideas presented in this paper was materially aided by the suggestions and guidance of O. R. Wulf, Bureau of Chemistry and Soils, United States Department of Agriculture, and of F. D. Rossini, Director of the American Petroleum Institute Research Project 6.

The author acknowledges the aid of F. W. Melpolder and P. Schoonover in many of the calculations.

VII. REFERENCES

[1] E. W. Washburn. Ind. Eng. Chem. **25,** 891 (1933).
[2] U. Liddel and C. Kasper. BS J. Research **11,** 599–618 (1933) RP610.
[3] E. W. Washburn. Ind. End. Chem. **22,** 985–8 (1930).
[4] G. H. B. Davis and E. N. McAllister. Ind. Eng. Chem. **22,** 1326 (1930).
[5] L. A. Mikeska. Ind. Eng. Chem. **28,** 970–983 (1936).
[6] G. Hugel. Chimie & industrie **26,** 1282 (1931).
[7] E. W. Dean and G. H. B. Davis. Chem. Met. Eng. **36,** 618 (1929).
[8] G. H. B. Davis, M. Lapeyrouse, and E. W. Dean. Oil & Gas J. **30,** 46, 92 (1932).

[20] The description of the synthetic compound and the identification of the isononane from petroleum will appear in a forthcoming paper in the Journal of Research of the National Bureau of Standards, by White and Rose, in collaboration with Calingaert and Soroos.

[9] J. C. Vlugter, H. I. Waterman, and H. A. Van Westen. J. Inst. Petroleum Tech. **18,** 735 (1932); **21,** 661 (1935); **21,** 707 (1935).
[10] J. C. Vlugter. Dissertation, Delft (1932).
[11] H. I. Waterman. Proc. World Petroleum Cong. **2,** 332 (1933).
[12] H. I. Waterman, P. C. Kruijff, W. J. K. Schönlau, and A. J. Tulleners. J. Inst. Petroleum Tech. **20,** 159 (1934).
[13] G. H. Fuchs and A. P. Anderson. Ind. Eng. Chem. **29,** 319 (1936).
[14] A. L. Ward and W. H. Fulweiler. Ind. Eng. Chem., Anal. Ed. **6,** 396 (1934).
[15] J. B. Hill and H. B. Coates. Ind. Eng. Chem. **20,** 641 (1928).
[16] S. S. Kurtz, Jr., and A. Q. Ward. J. Franklin Inst. **222,** 563 (1936).
[17] F. S. Brackett. Proc. Nat. Acad. Sci. **14,** 857–864 (1928).
[18] F. W. Rose, Jr. J. Research NBS **19,** 143–161 (1937) RP1017.
[19] W. Herschel. Phil. Trans. **90,** 225, 293, 437 (1800).
[20] W. Abney and B. Festing. Phil. Trans. **172,** 887 (1881).
[21] H. Julius. Verhandl. Akad. Wetenschappen Amsterdam **1,** 1 (1892).
[22] W. W. Coblentz. Investigations of Infrared Spectra, Carnegie Inst., Wash. Pub. 35 (1905).
[23] B. Donath. Ann. Physik [3] **58,** 609 (1896).
[24] Ransohoff. Inaug. Dissertation, Berlin (1896).
[25] L. Puccianti. Nuovo Cimento **11,** 241 (1900); Physik. Z. **1,** 49, 494 (1899–1900).
[26] M. J. Lecomte. *Structure des molécules et spectres d'absorption dans l'infrarouge,* Traité de Chimie Organique, **II** (Masson et Cie., Paris, 1936).
[27] R. B. Barnes. Rev. Sci. Inst. **7,** 265 (1936).
[28] R. B. Barnes, L. G. Bonner, and E. U. Condon. J. Chem. Phys. **4,** 772 (1936).
[29] M. P. Lambert and M. J. Lecomte. Ann. Comb. Liquides, 1001–1084 (1931); 979–993 (1934); 1077–1092 (1935).
[30] V. Henri. Etudes de Photochimie (Gauthier-Villars et Cie, Paris, 1919).
[31] G. B. Bonino. Trans. Faraday Soc. **25,** 876 (1929).
[32] F. K. Bell. J. Am. Chem. Soc. **50,** 2940 (1928).
[33] M. R. Freymann. Compt. rend. **193,** 657 (1931).
[34] U. Liddel and O. R. Wulf. J. Am. Chem. Soc. **55,** 3574 (1933).
[35] F. D. Rossini. J. Research NBS **13,** 21 (1934) RP692; **13,** 189 (1934) RP701.
[36] O. R. Wulf and U. Liddel. J. Am. Chem. Soc. **57,** 1464 (1935).
[37] O. R. Wulf. Paper 28 (Division of Physical and Inorganic Chemistry), Rochester, N. Y., meeting of the American Chemical Society, Sept. 6, 1937.
[38] D. Williams and R. Taschek. J. Applied Phys. **8,** 497 (1937).
[39] J. Lipka. Graphical and Mechanical Computation (John Wiley and Sons, Inc., New York, N. Y., 1918).
[40] R. B. Barnes. Phys. Rev. **35,** 1524 (1930); **36,** 296 (1930).
[41] O. R. Wulf, U. Liddel, and S. B. Hendricks. J. Am. Chem. Soc. **58,** 2287 (1936).
[42] J. D. White and F. W. Rose, Jr. J. Research NBS **17,** 943 (1936) RP955.
[43] L. Pauling. J. Am. Chem. Soc. **58,** 94 (1936).
[44] B. M. Bloch and J. Errera. J. phys. radium **6,** 154 (1935).
[45] R. Mecke, P. Gänswein, O. Vierling. Z. Electrochem. **40,** 474 (1934).
[46] R. Mecke. Angew. Chem. **48,** 320 (1935).
[47] E. Bartholomé and E. Teller. Z. physik. Chem. [B] **19,** 366 (1932).
[48] R. Davis and K. S. Gibson. NBS Misc. Pub. M114 (1931).

WASHINGTON, September 28, 1937.

U. S. Department of Commerce National Bureau of Standards

RESEARCH PAPER RP1073

Part of Journal of Research of the National Bureau of Standards, Volume 20, February 1938

WEATHERING TESTS ON FILLED COATING ASPHALTS[1]

By O. G. Strieter [2]

ABSTRACT

The durabilities of filled and unfilled coating asphalts were determined both in outdoor and in accelerated exposures. The results show that, in general, the durability of coating asphalt to weathering can be improved by the addition of mineral fillers, and that there is a difference in the effectiveness of various sizes and types of fillers. The data demonstrate the similarity between outdoor and accelerated weathering.

CONTENTS

	Page
I. Introduction	159
II. Preparation, compositions, and mode of exposure of panels	160
III. Physical properties of the fillers	162
IV. Outdoor exposures and accelerated tests	164
1. Outdoor exposures	164
(a) Surface oxidation	164
(b) Cracking	164
(c) Classification of outdoor exposures	165
2. Accelerated-weathering tests	166
V. Discussion of results	170
VI. Summary	171

I. INTRODUCTION

Asphalt shingles and roll-roofings are made by impregnating felt with a relatively soft asphalt and then surfacing with a harder asphalt known as a coating asphalt. Early in the manufacture of these roofings, unfilled coatings were considered superior to those containing mineral filler, but, because of the favorable results obtained in accelerated weathering tests on filled coatings, it has become general practice in recent years to mix finely ground slate, limestone, and similar mineral fillers with the asphalt coatings. Filled coatings, in general, are less affected by sunlight and less subject to plastic flow. However, as no data were available to show the serviceability of filled coatings the present investigation was undertaken to determine the effect of various kinds and grades of commercial fillers on the weather-resisting properties of coating asphalt. Various asphalt-filler mixtures were prepared and tested. Specific gravities, compacting weights, sieve analyses of the mineral fillers, and softening points and penetrations on the asphalt-filler mixtures were determined.

[1] A paper reporting the results up to 1¼ years of outdoor exposure was published in the Proc. Am. Soc. Testing Materials 36, pt. II, 486 (1936).

[2] Research Associate at the National Bureau of Standards, representing the Asphalt Shingle and Roofing Institute.

The weather-resisting properties of the asphalt-filler mixtures were determined by exposing them outdoors in various localities, and to accelerated weathering. Comparisons were made of the durabilities of the various coatings, and also between the effects of accelerated and outdoor exposures.

II. PREPARATION, COMPOSITIONS, AND MODE OF EXPOSURE OF PANELS

Two asphalts of different softening points were used for preparing the asphalt-filler mixtures. Both were made from the same crude

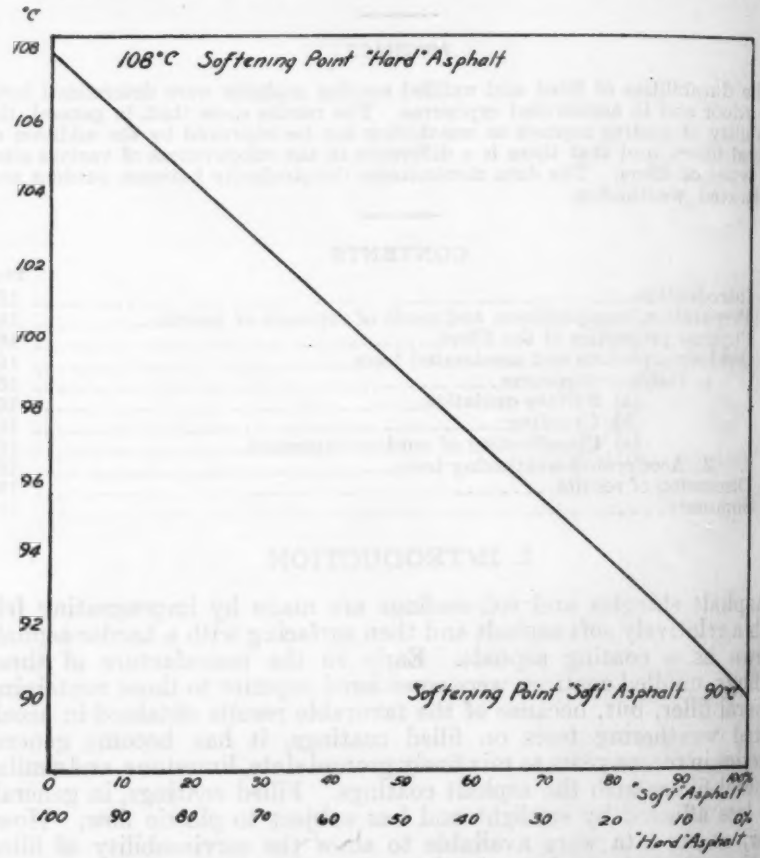

FIGURE 1.—*Ratio of hard and soft asphalts to obtain an asphalt of definite softening point.*

petroleum in a single operation, and their preparation differed only in the duration of the blowing.

The "soft" and "hard" asphalts were so blended that when combined with 15, 25, and 35 percent by weight of various mineral fillers, the softening points of the resulting mixtures were all approximately the same as that of the original "hard" asphalt, namely, 108° C. The proper blend of the two asphalts was determined graphically by

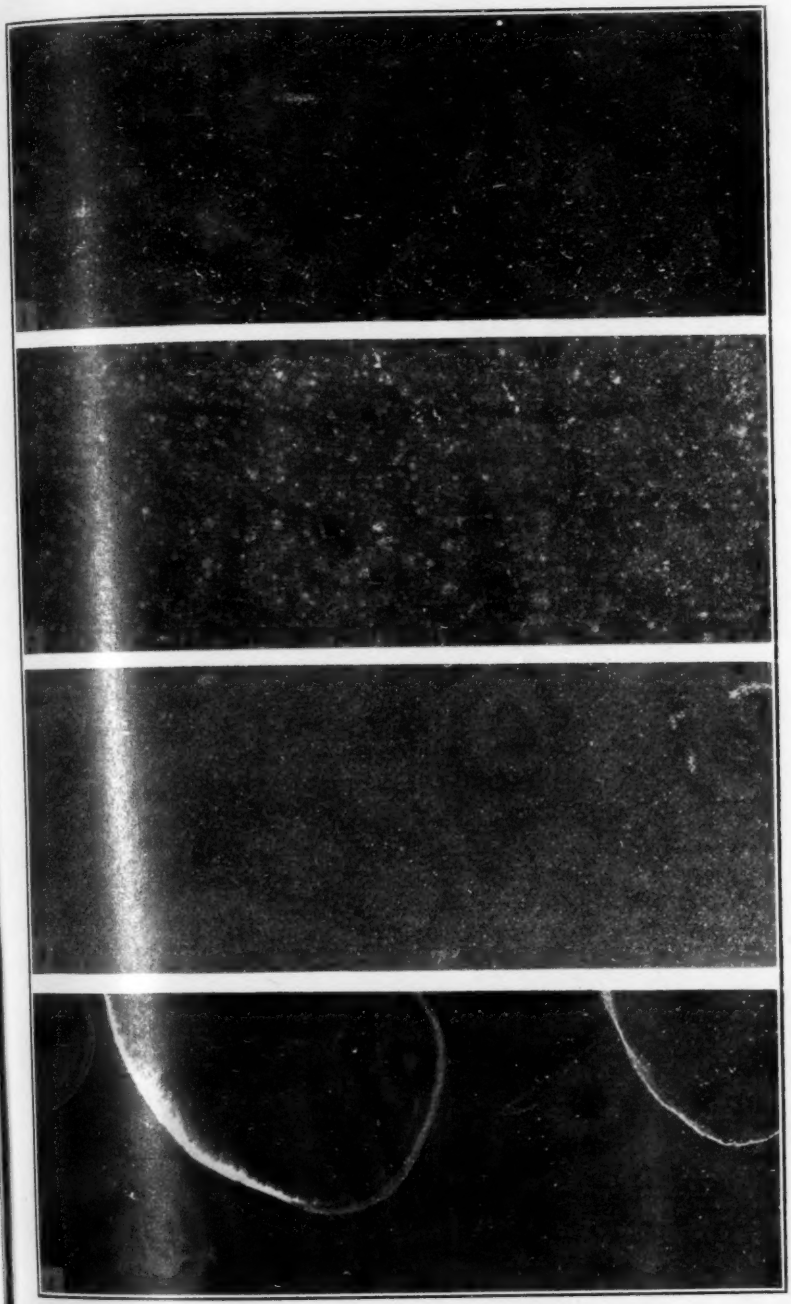

FIGURE 2.—*Specimens of group I (table 4).*

Comparisen of specimens 30 (table 1) in their outdoor- and accelerated-weathering exposures. The specimens contain 35 percent of talc (filler 12). Exposures: 1, accelerated weathering; 2, Los Angeles; 3, Washington; and 4, Manville.

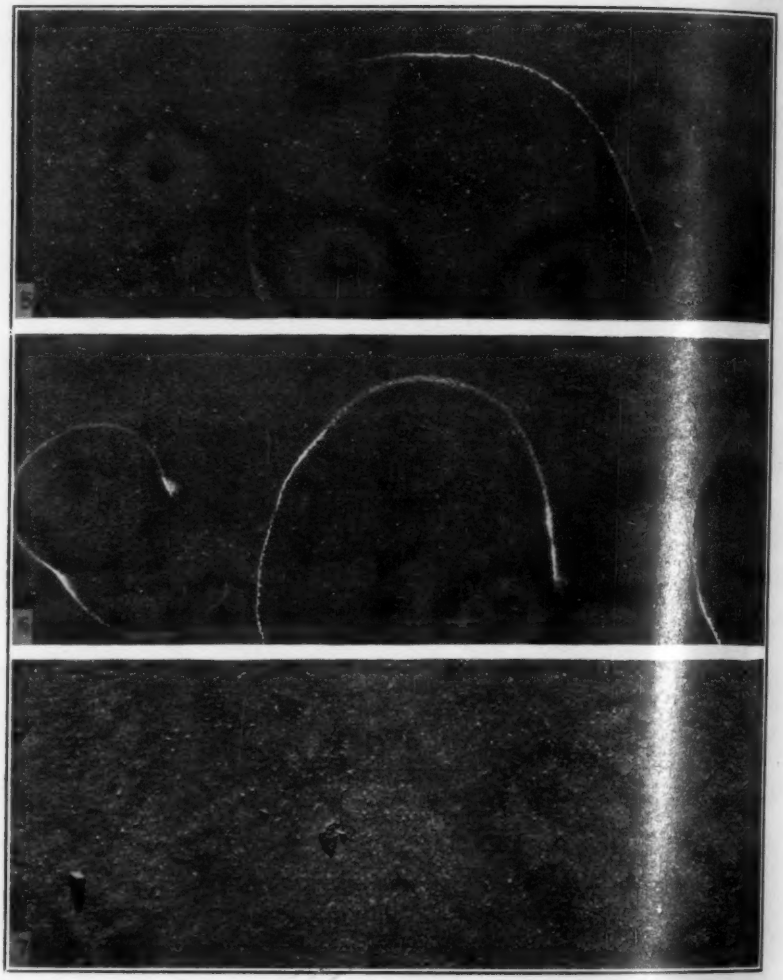

FIGURE 3.—*Specimens of group I.*

Comparison of specimens 30 (table 1) in their outdoor- and accelerated-weathering exposures. The specimens contain 35 percent of talc (filler 12). Exposures: 5, Chicago; 6, Buffalo; and 7, New Orleans.

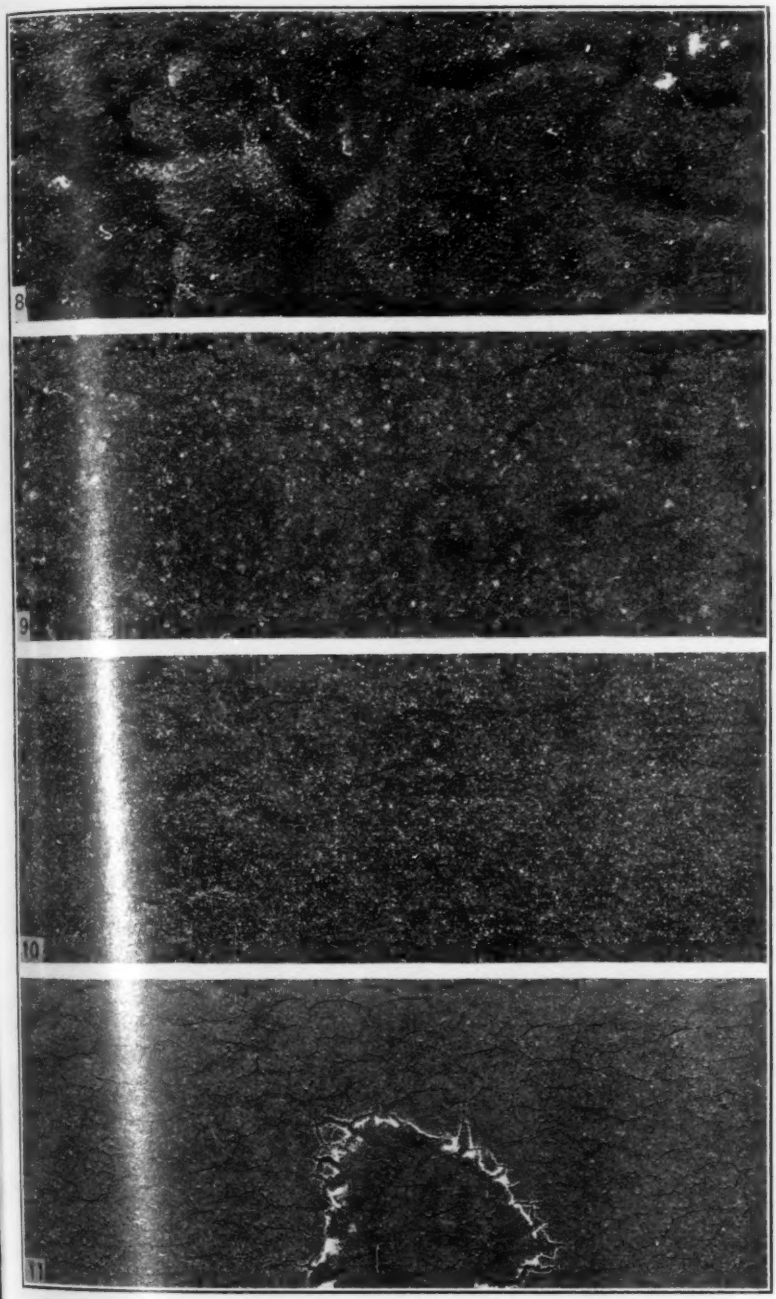

FIGURE 4.—*Durable specimens of group II (table 4).*

Comparison of specimens 19 (table 1) in the outdoor- and accelerated-weathering exposures. The specimens contain 35 percent of greenstone (filler 7). Exposures: 8, accelerated weathering; 9, Los Angeles; 10, Washington; and 11, Manville.

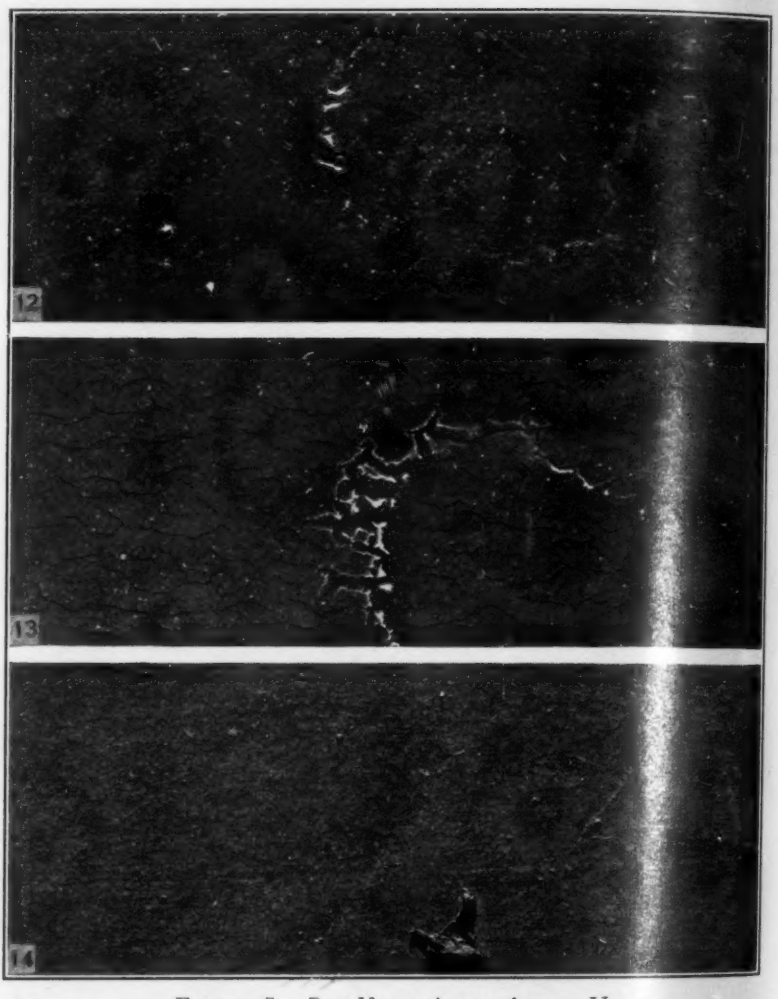

FIGURE 5.—*Durable specimens of group II.*

Comparison of specimens 19 (table 1) in the outdoor- and accelerated-weathering exposures. The specimens contain 35 percent of greenstone (filler 7). Exposures: 12, Chicago; 13, Buffalo; and 14, New Orleans.

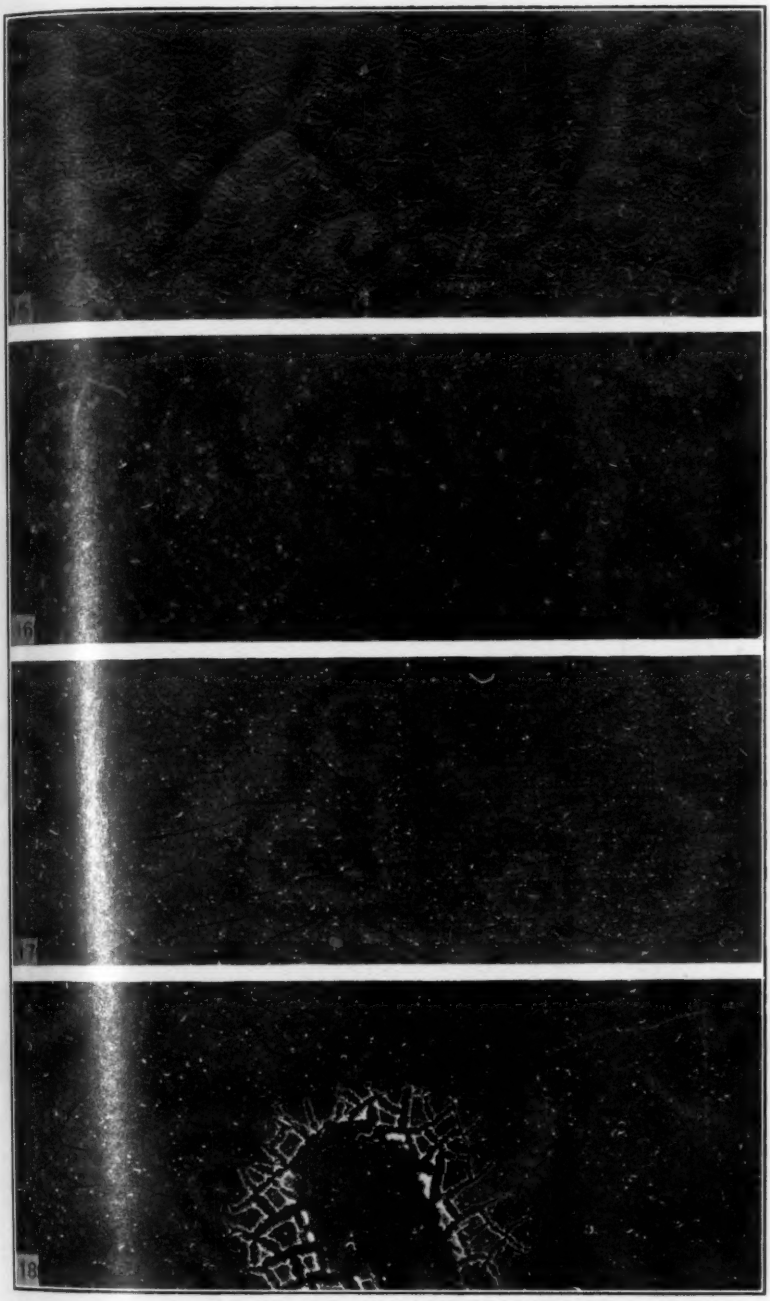

FIGURE 6.—*Less durable specimens of group II (table 4).*

Comparison of specimens 21 (table 1) in the outdoor- and accelerated-weathering exposures. The specimens contain 15 percent of greenstone (filler 7). Exposures: 15, accelerated weathering; 16, Los Angeles; 17, Washington; and 18, Manville.

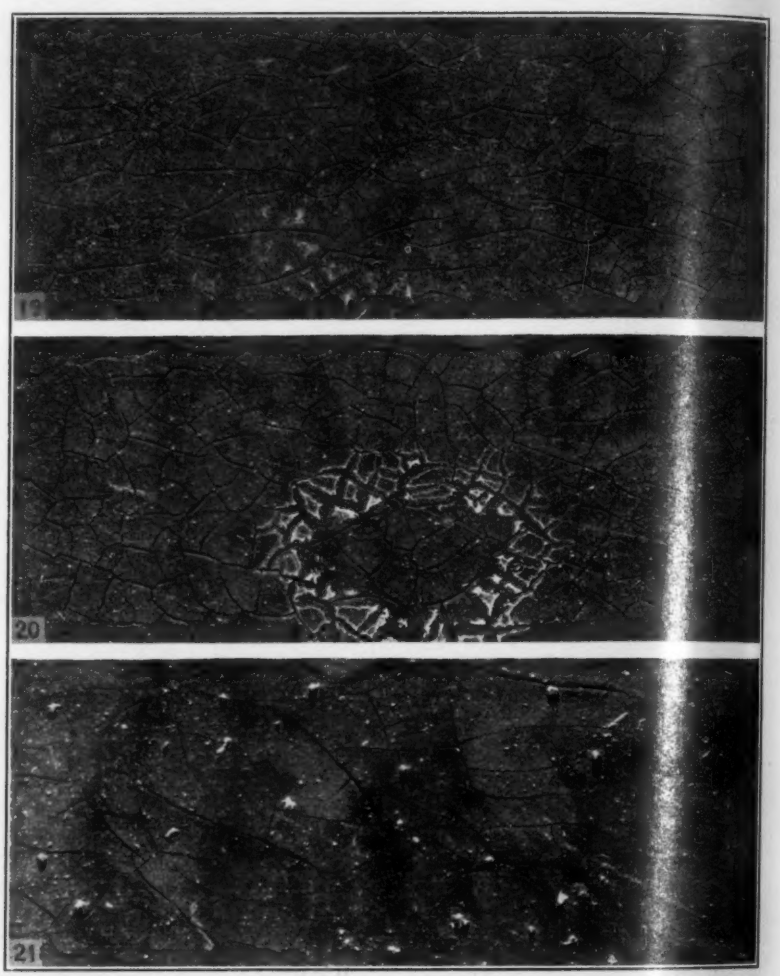

FIGURE 7.—*Less durable specimens of group II.*

Comparison of specimens 21 (table 1) in the outdoor- and accelerated-weathering exposures. The specimens contain 15 percent of greenstone (filler 7). Exposures: 19, Chicago; 20, Buffalo; and 21, New Orleans.

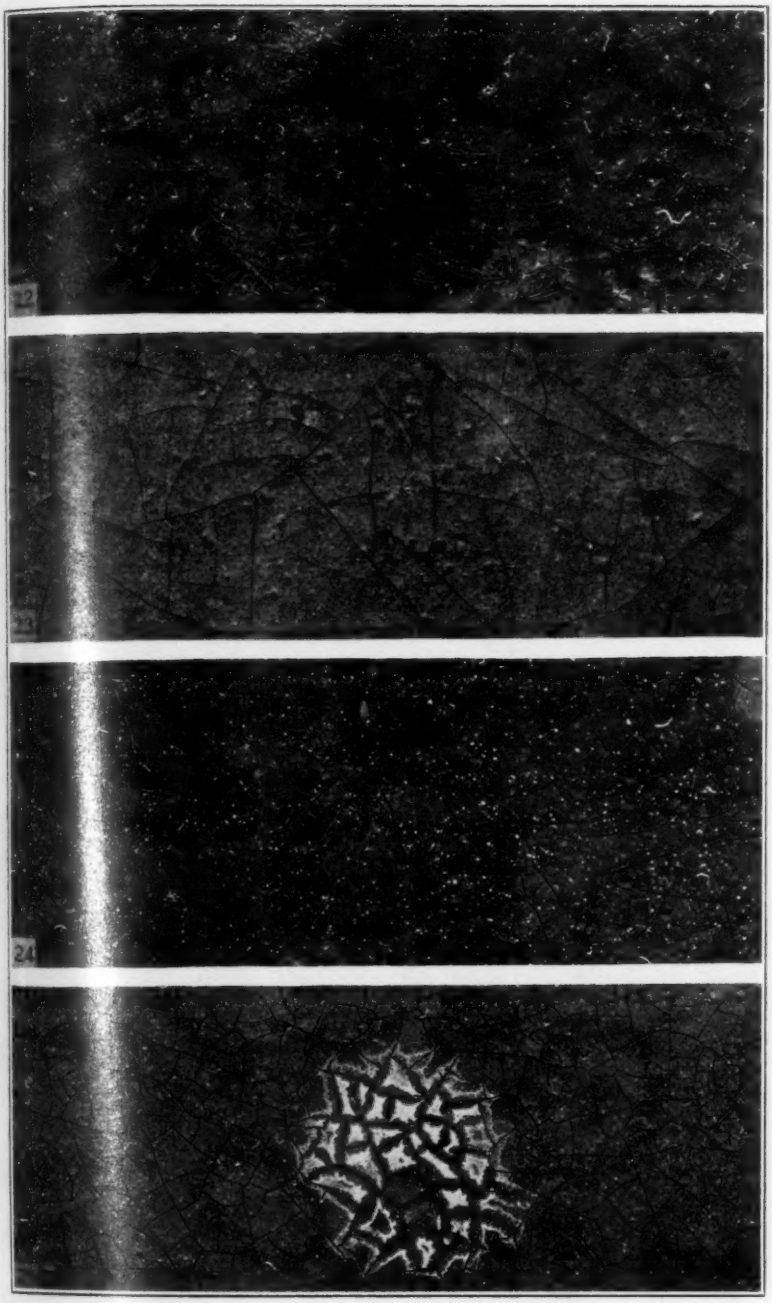

FIGURE 8.—*Specimens of group III (table 4).*

Comparison of specimens 24 (table 1) in the outdoor- and accelerated-weathering exposures. The specimens contain 15 percent of hydrated lime (filler 8). Exposures: 22, accelerated weathering; 23, Los Angeles; 24, Washington; and 25, Manville.

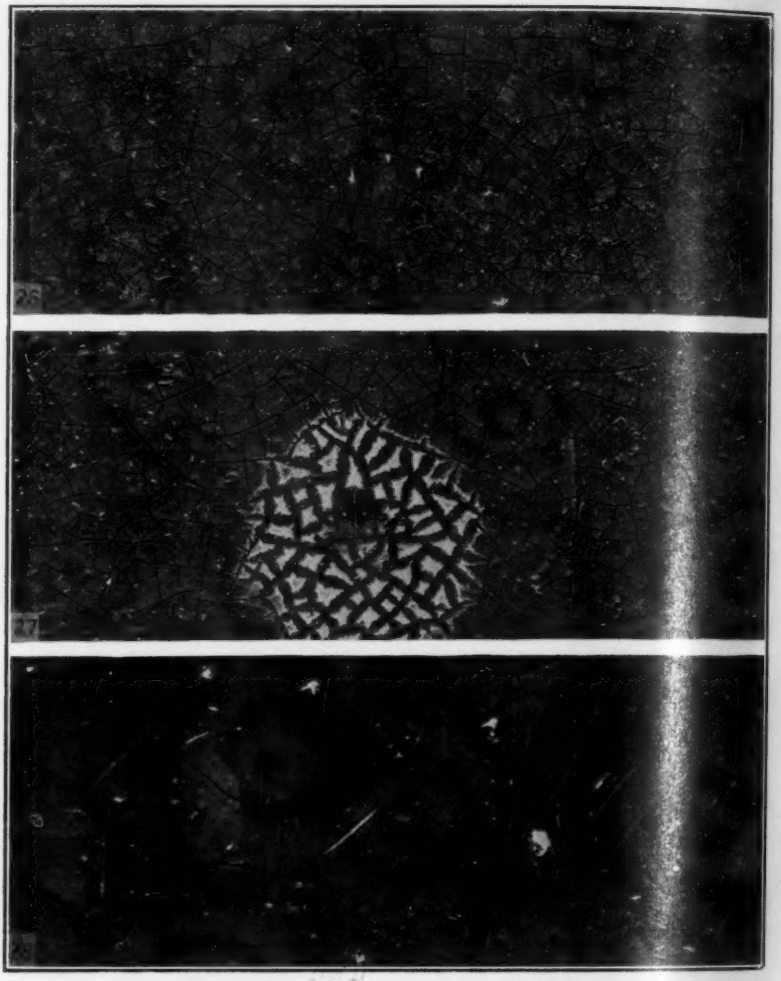

FIGURE 9.—*Specimens of group III.*

Comparison of specimens 24 (table 1) in the outdoor- and accelerated-weathering exposures. The specimens contain 15 percent of hydrated lime (filler 8). Exposures: 26, Chicago; 27, Buffalo; and 28, New Orleans.

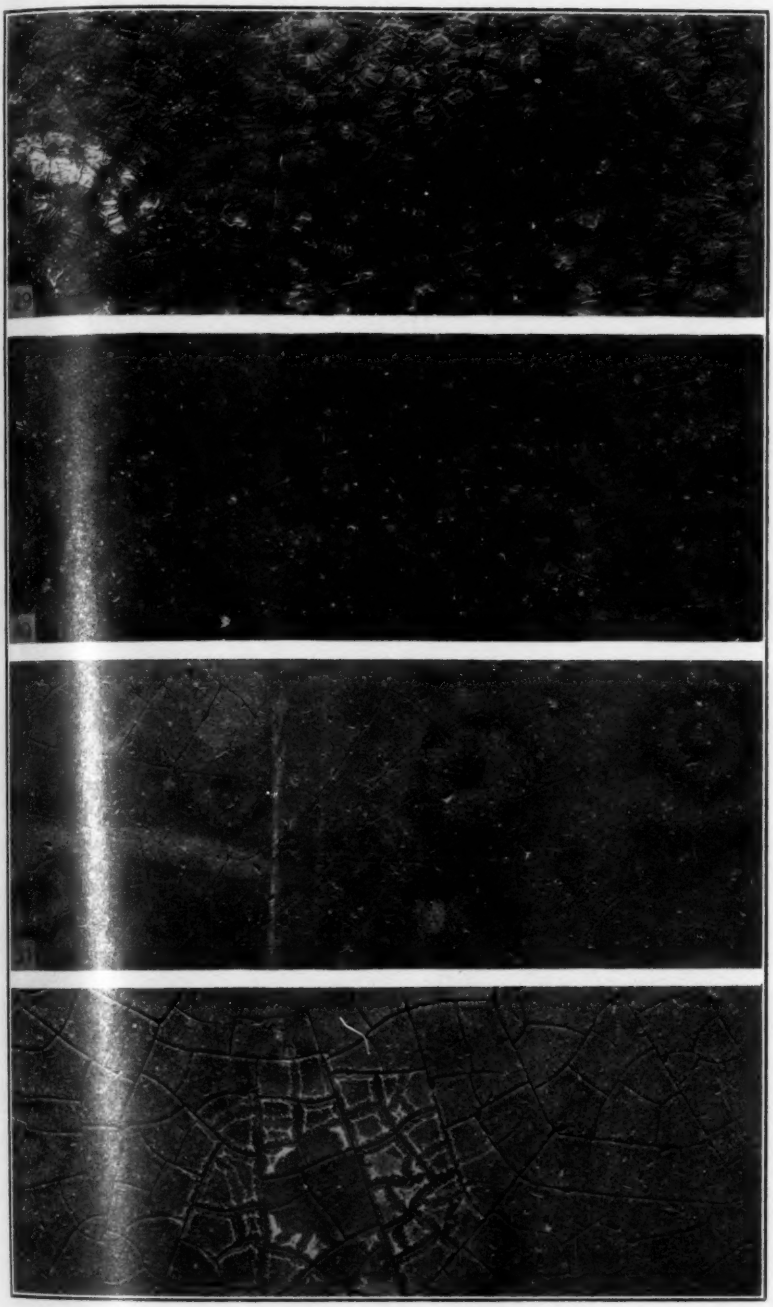

FIGURE 10.—*Unfilled-coating asphalt (specimens 55, table 1) in the outdoor- and accelerated-weathering exposures.*

Exposures: 29, accelerated weathering; 30, Los Angeles; 31, Washington; and 32, Manville.

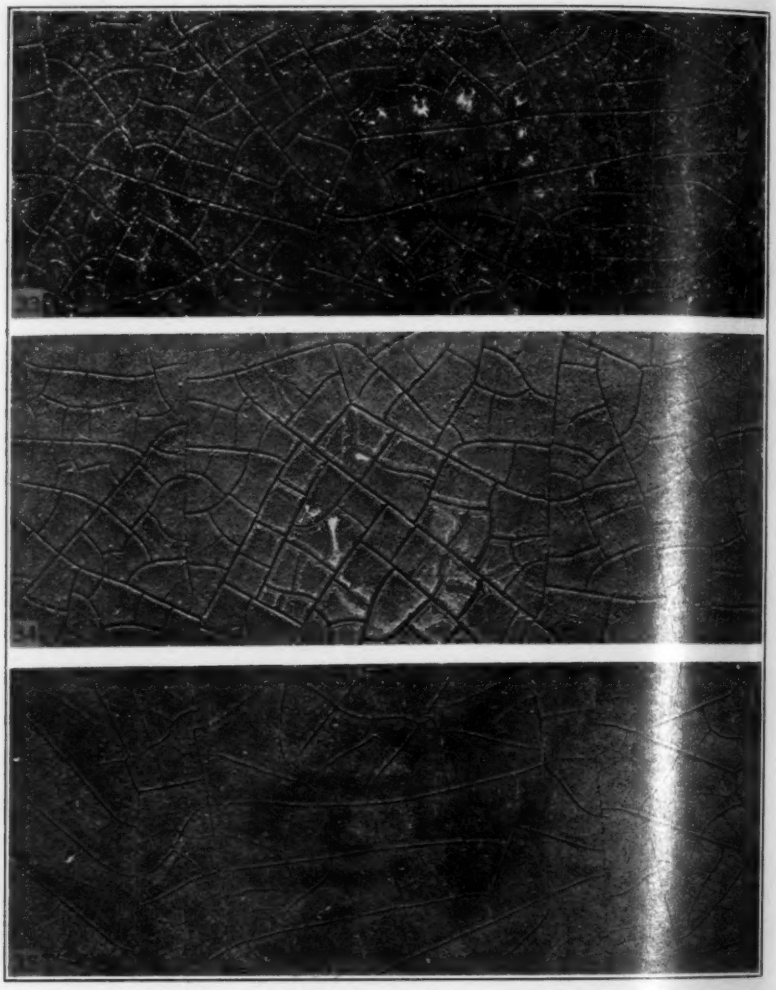

FIGURE 11.—*Unfilled-coating asphalt (specimens 55, table 1) in the outdoor- and accelerated-weathering exposures.*

Exposures: 33, Chicago; 34, Buffalo; and 35, New Orleans.

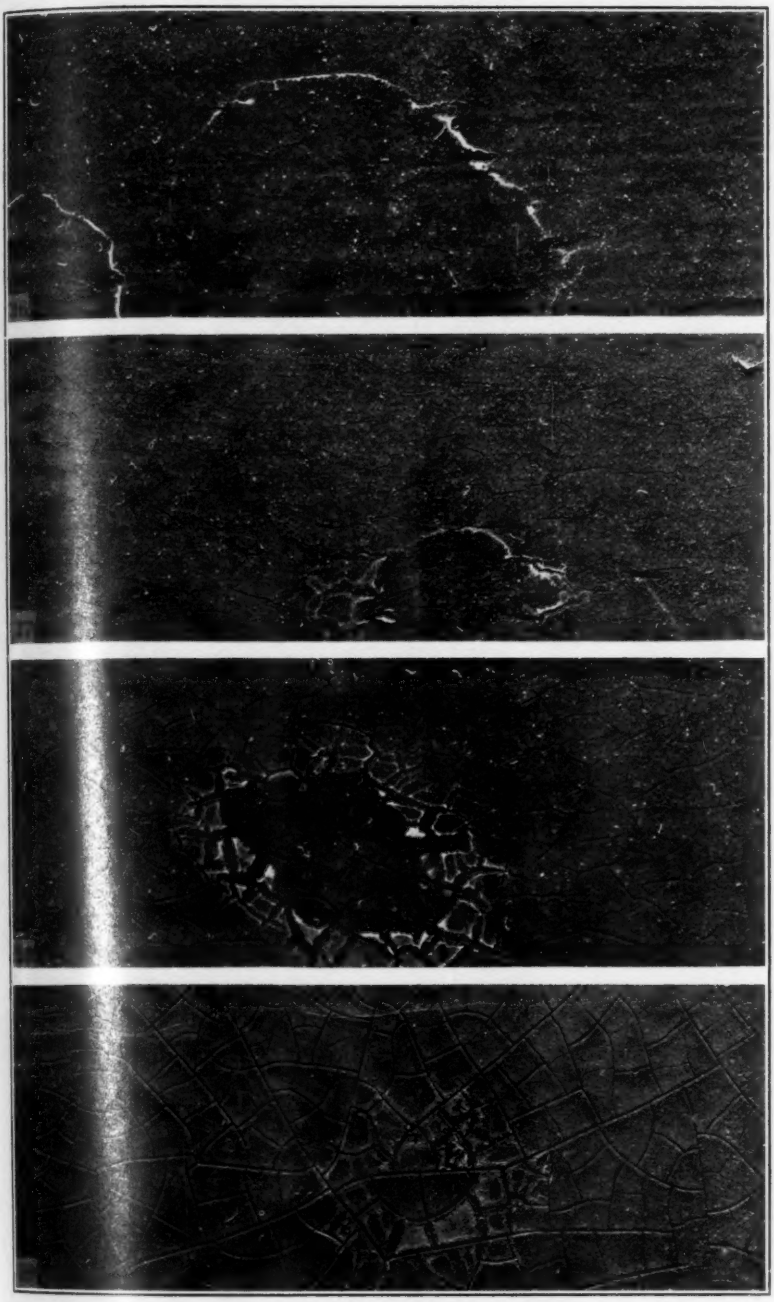

FIGURE 12.—*Comparison of specimens containing 35, 25, and 15 percent of slate, respectively, with the unfilled-coating asphalt.*

All specimens exposed at Buffalo.

Compositions: 36. Specimen 13 (table 1) containing 35 percent of slate, filler 5.
37. Specimen 14 (table 1) containing 25 percent of slate, filler 5.
38. Specimen 15 (table 1) containing 15 percent of slate, filler 5.
39. Specimen 54 (table 1) coating asphalt, without filler.

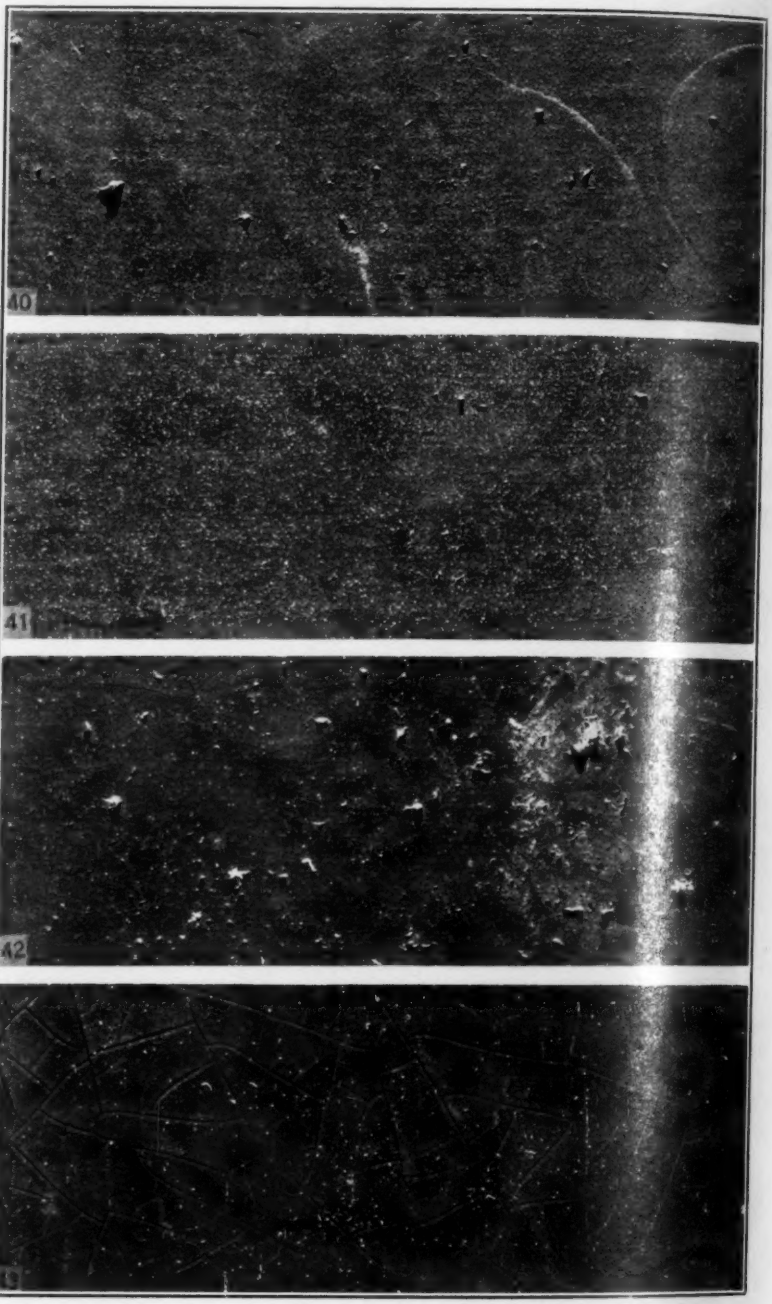

FIGURE 13.—*Comparison of specimens containing 35, 25, and 15 percent of slate, respectively, with the unfilled-coating asphalt.*

All specimens exposed at New Orleans.

Compositions: 40. Specimen 13 (table 1) containing 35 percent of slate, filler 5.
41. Specimen 14 (table 1) containing 25 percent of slate, filler 5.
42. Specimen 15 (table 1) containing 15 percent of slate, filler 5.
43. Specimen 54 (table 1) coating asphalt, without filler.

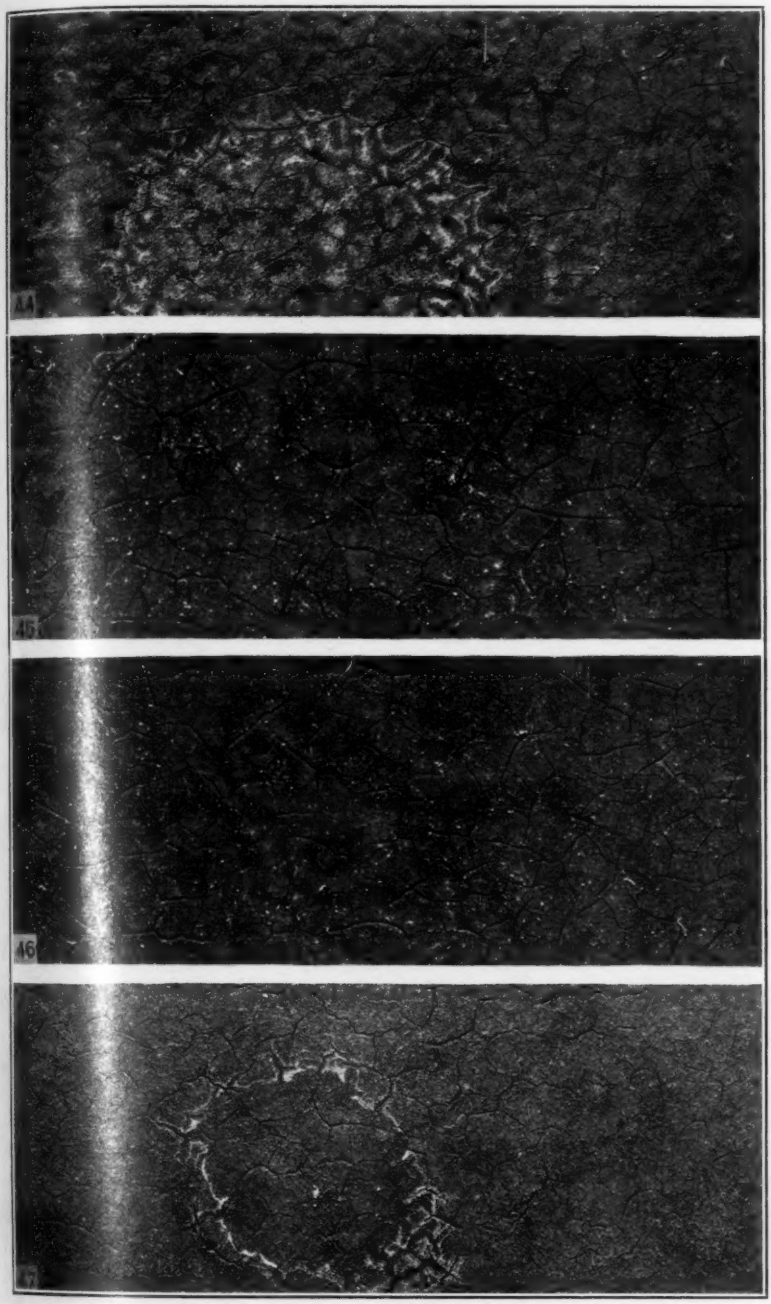

FIGURE 14.—*Comparison of specimens containing various fillers.*

All specimens exposed at Buffalo.

Compositions: 44. Specimen 25 (table 1) containing 35 percent of trap rock, filler 9.
45. Specimen 4 (table 1) containing 35 percent of dolomite, filler 2.
46. Specimen 10 (table 1) containing 35 percent of limestone, filler 4.
47. Specimen 33 (table 1) containing 35 percent of silica, filler 13.

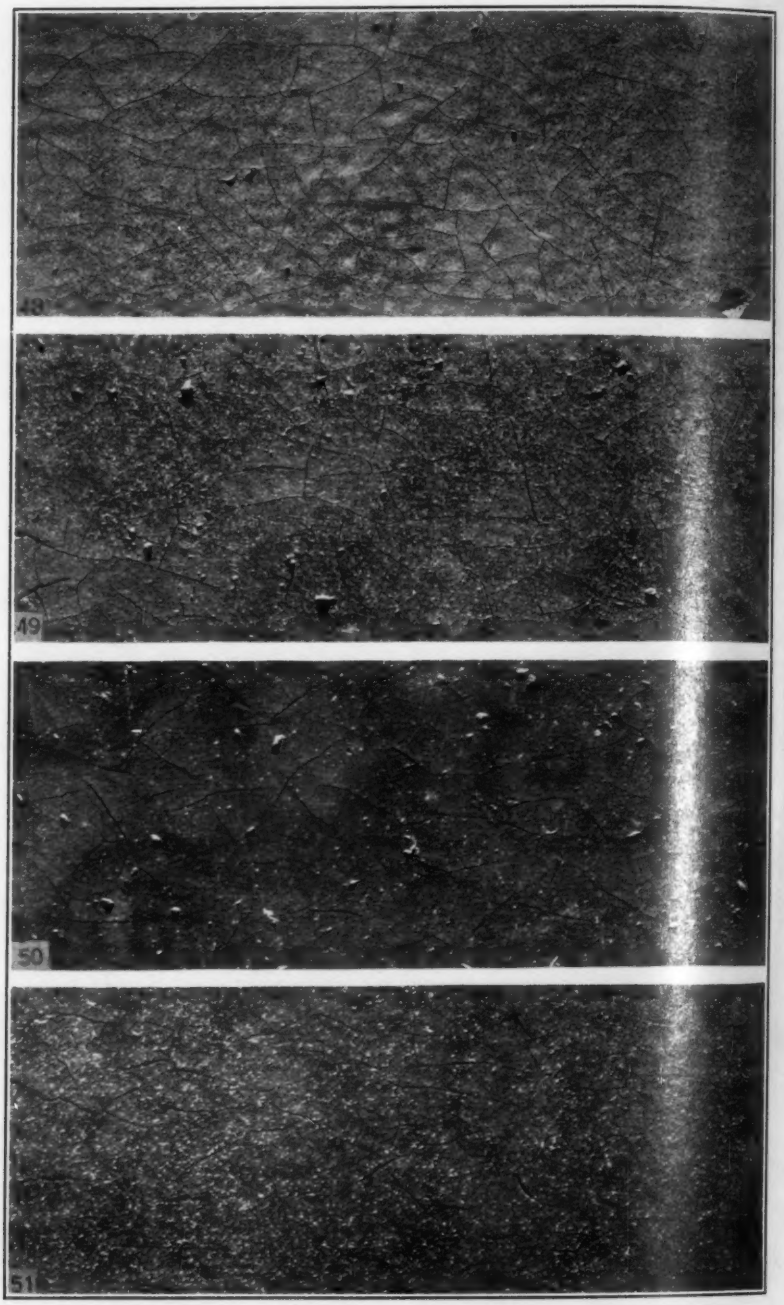

FIGURE 15.—*Comparison of specimens containing various fillers.*

All specimens exposed at New Orleans.

Compositions: 48. Specimen 25 (table 1) containing 35 percent of trap rock, filler 9.
49. Specimen 4 (table 1) containing 35 percent of dolomite, filler 2.
50. Specimen 10 (table 1) containing 35 percent of limestone, filler 4.
51. Specimen 33 (table 1) containing 35 percent of silica, filler 13.

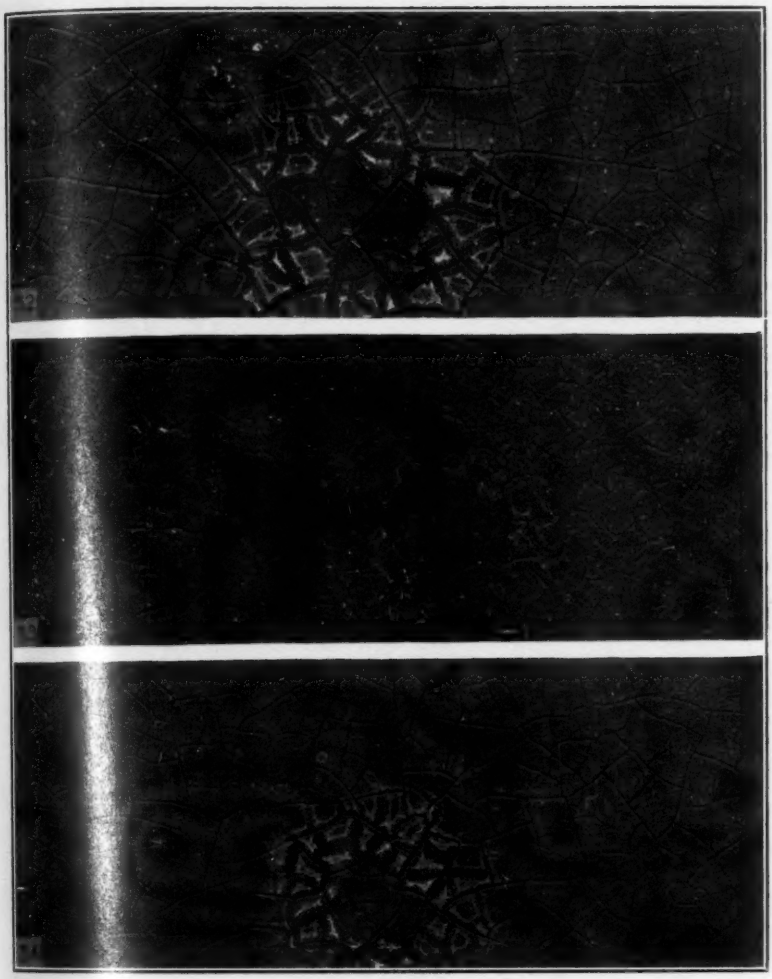

FIGURE 16.—*Comparison of specimens containing limestone filler of various particle sizes.*

All specimens exposed at Buffalo.

Compositions: 52. Specimen 49 (table 1) containing 25 percent of limestone, filler 18, passing No. 200 sieve.
53. Specimen 52 (table 1) containing 25 percent of limestone, filler 19, passing No. 100 but retained on No. 200 sieve.
54. Specimen 11 (table 1) containing 25 percent of limestone, filler 4, 91 percent passing No. 200 sieve.

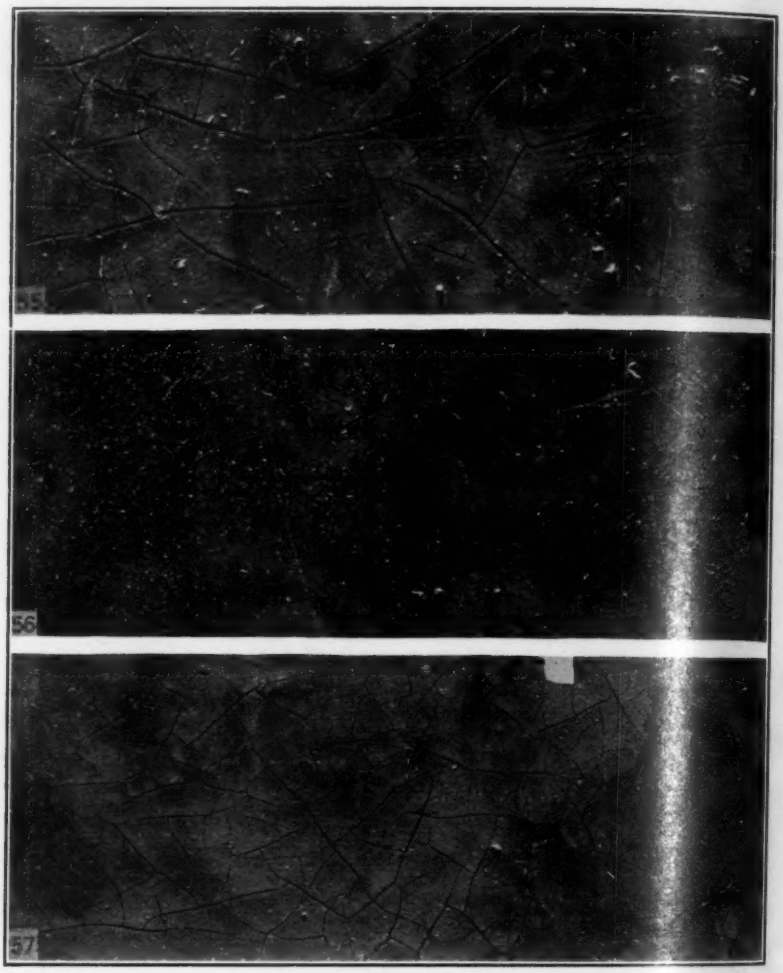

FIGURE 17.—*Comparison of specimens containing limestone filler of various particle sizes.*

All specimens exposed at New Orleans.

Compositions: 55. Specimen 49 (table 1) containing 25 percent of limestone, filler 18, passing No. 200 sieve.
56. Specimen 52 (table 1) containing 25 percent of limestone, filler 19, passing No. 100 but retained on No. 200 sieve.
57. Specimen 11 (table 1) containing 25 percent of limestone, filler 4, 91 percent passing No. 200 sieve.

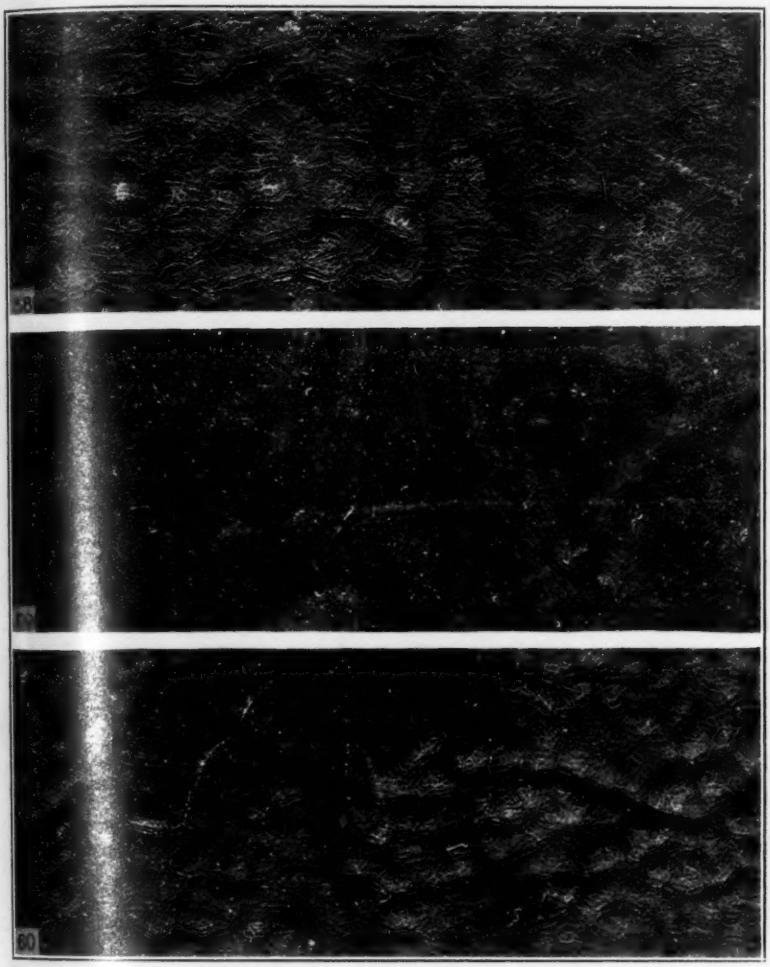

FIGURE 18.—*Comparison of specimens containing limestone filler of various particle sizes.*

All specimens exposed to accelerated weathering.

Compositions: 58. Specimen 49 (table 1) containing 25 percent of limestone, filler 18, passing No. 200 sieve.
59. Specimen 52 (table 1) containing 25 percent of limestone, filler 19, passing No. 100 but retained on No. 200 sieve.
60. Specimen 11 (table 1) containing 25 percent of limestone, filler 4, 91 percent passing No. 200 sieve.

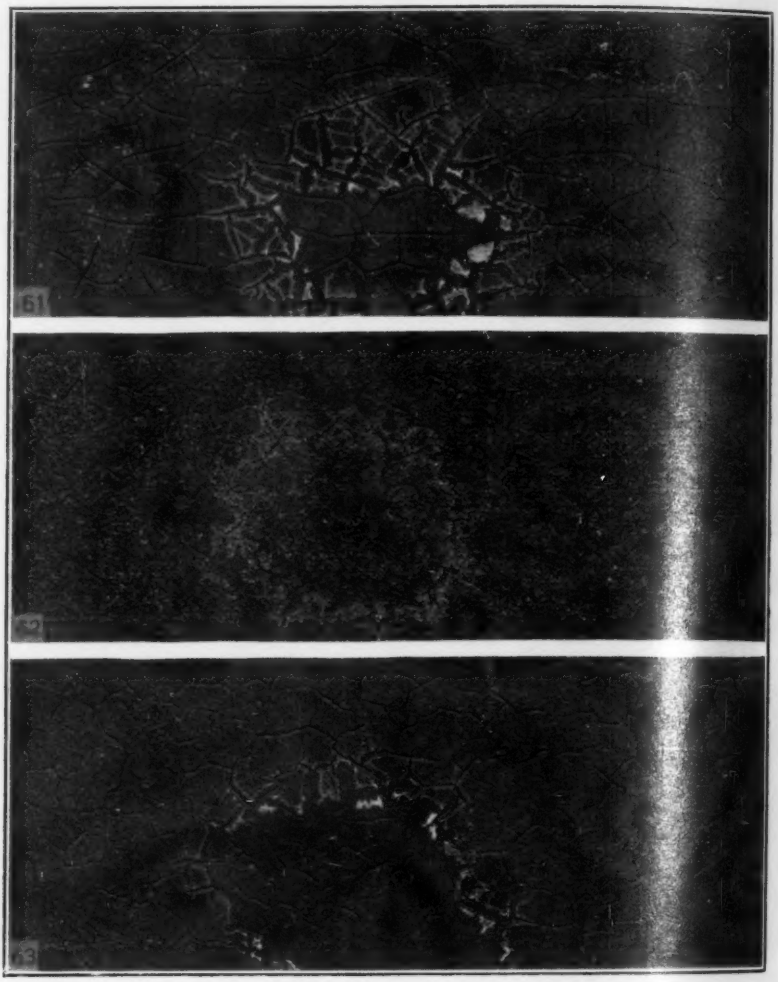

FIGURE 19.—*Comparison of specimens containing silica of various particle sizes as filler.*

All specimens exposed at Buffalo.

Compositions: 61. Specimen 37 (table 1) containing 25 percent of silica, filler 14, passing No. 200 sieve.
62. Specimen 40 (table 1) containing 25 percent of silica, filler 15, passing No. 100 but retained on No. 200 sieve.
63. Specimen 34 (table 1) containing 25 percent of silica, filler 13, 67 percent passing No. 200 sieve.

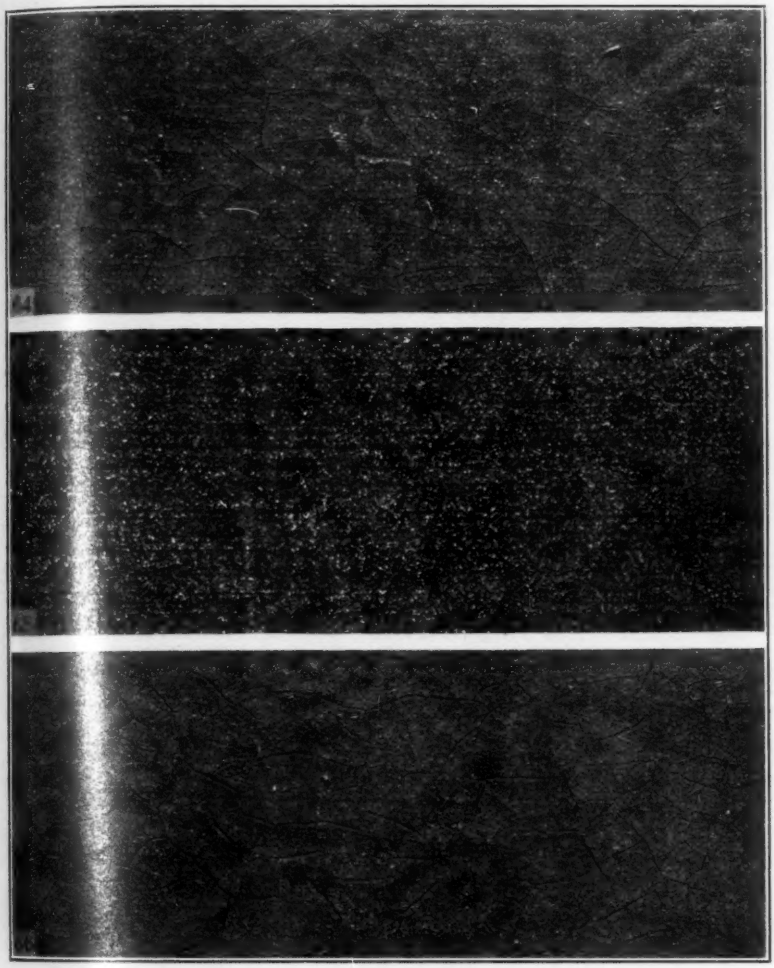

FIGURE 20.—*Comparison of specimens containing silica of various particle sizes as filler.*

All specimens exposed at New Orleans.

Compositions: 64. Specimen 37 (table 1) containing 25 percent of silica, filler 14, passing No. 200 sieve.
65. Specimen 40 (table 1) containing 25 percent of silica, filler 15, passing No. 100 but retained on No. 200 sieve.
66. Specimen 34 (table 1) containing 25 percent of silica, filler 13, 67 percent passing No. 200 sieve.

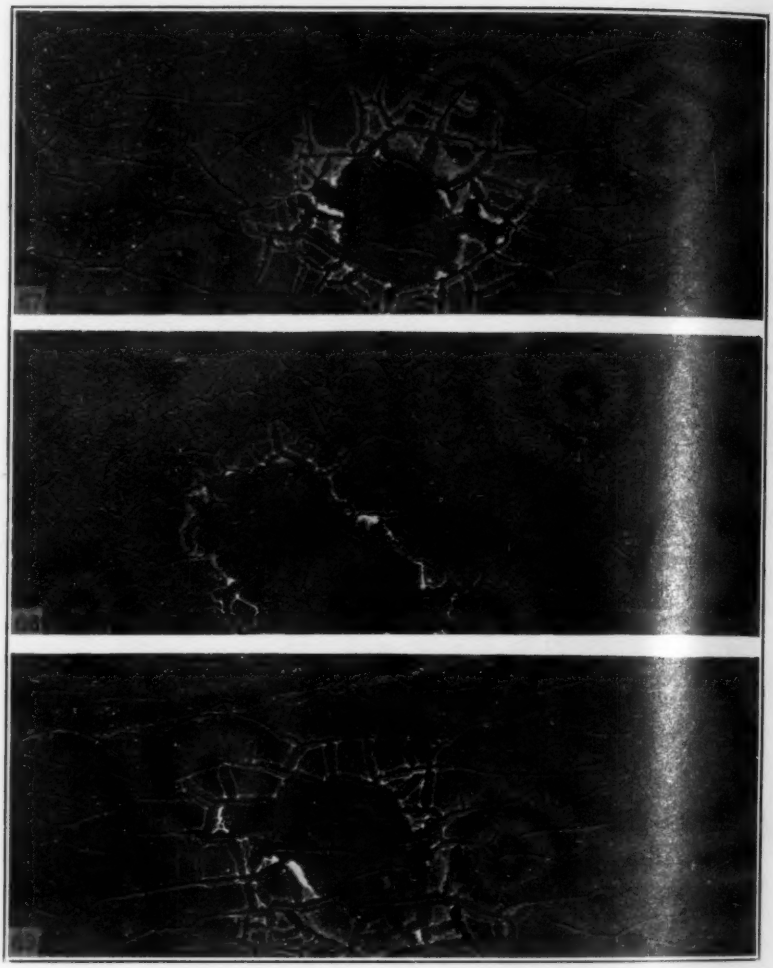

FIGURE 21.—*Comparison of specimens containing slate of various particle sizes as filler.*

All specimens exposed at Buffalo.

Compositions: 67. Specimen 44 (table 1) containing 15 percent of slate, filler 16, passing No. 200 sieve.
68. Specimen 47 (table 1) containing 15 percent of slate, filler 17, passing No. 100 but retained on No. 200 sieve.
69. Specimen 15 (table 1) containing 15 percent of slate, filler 5, 79 percent passing No. 200 sieve.

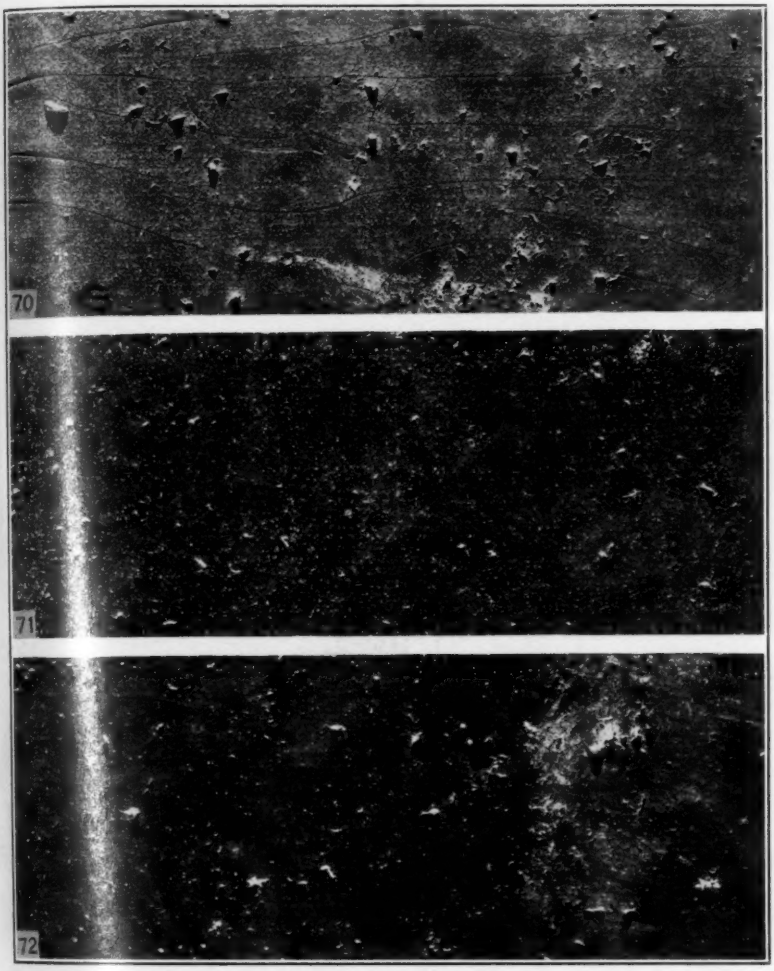

FIGURE 22.— *Comparison of specimens containing slate of various particle sizes as filler.*

All specimens exposed at New Orleans.

Compositions: 70. Specimen 44 (table 1) containing 15 percent of slate, filler 16, passing No. 200 sieve.
71. Specimen 47 (table 1) containing 15 percent of slate, filler 17, passing No. 100 but retained on No. 200 sieve.
72. Specimen 15 (table 1) containing 15 percent of slate, filler 5, 79 percent passing No. 200 sieve.

plotting the softening points [3] in a system of coordinates, using the ordinate as the temperature scale and the abscissa as the percentage scale, as shown in figure 1. With such a system of coordinates, the percentage composition of "hard" and "soft" asphalt for a blend of a desired softening point was readily determined by inspection. The effect of filler on the softening point of the asphalt was determined by trial.

Table 1 shows the compositions and penetrations [4] of the asphalt-filler mixtures.

TABLE 1.—*Compositions, physical properties, and durabilities of asphalt-filler mixtures*

Specimen number	Asphalt-filler mixture				Kind of filler	Filler No.	Penetrations in 0.01-cm units			Durability	
	Hard asphalt	Soft asphalt	Filler	Hard asphalt in total asphalt			At 32° F, 200 g, 60 sec	At 77° F, 100 g, 5 sec	At 115° F, 50 g, 5 sec	3-yr outdoor exposure, group number [a]	Life in accelerated test
	%	%	%	%							*Cycles*
1	47	18	35	72	Green-slate flour	1	6	9	13	I	62
2	62	13	25	83			6	9	16	II	45
3	73	12	15	86			7	9	17	II	37
4	47	18	35	72	Dolomite	2	6	10	18	II	37
5	60	15	25	80			6	10	17	II	28
6	73	12	15	86			7	10	17	III	28
7	47	18	35	72	do	3	6	9	15	II	40
8	60	15	25	80			8	11	18	II	37
9	73	12	15	86			7	10	17	III	28
10	47	18	35	72	Limestone	4	6	9	16	II	43
11	60	15	25	80			6	10	17	II	37
12	73	12	15	86			6	9	18	III	33
13	47	18	35	72	Peach Bottom slate	5	6	8	15	I	65
14	60	15	25	80			7	10	16	I	62
15	73	12	15	86			7	8	18	II	43
16	47	18	35	72	Silica sand	6	8	12	18	II	28
17	68	7	25	90			6	11	15	II	28
18	80	5	15	94			8	11	14	III	28
19	47	18	35	72	Greenstone	7	7	11	14	II	65
20	60	15	25	80			7	10	16	II	46
21	73	12	15	86			7	10	17	II	40
22	------	65	35	0	Hydrated lime	8	6	8	14	III	28
23	------	75	25	0			8	11	21	III	28
24	37	48	15	56			7	11	21	III	28
25	30	29	35	55	Trap rock	9	6	9	15	II	43
26	53	22	25	70			7	9	17	II	37
27	72	13	15	85			7	9	16	III	28
28	13	72	15	15	Supercel	10	8	10	22	II	40
29	41	44	15	48	Mica	11	7	10	17	I	65+
30	23	42	35	36	Foliated talc	12	6	10	16	I	65
31	44	31	25	58			7	9	18	I	65
32	66	19	15	78			7	9	18	I	48
33	49	16	35	75	Silica dust	13	7	8	16	II	35
34	62	13	25	83			7	8	16	II	33
35	78	7	15	92			7	9	17	III	28

[a] See p. 166 of text for identification of groups.

[3] The softening points were determined by the ring-and-ball method described by Herbert Abraham in Asphalts and Allied Substances, 3d edition (D. Van Nostrand Co., New York, N. Y.).

[4] The method of test is fully described in *Standard method of test for penetration of bituminous materials*, A. S. T. M. Designation: *D 5–25* Book of Standards, Am. Soc. Testing Materials, pt. II, 971 (1933).

TABLE 1.—*Compositions, physical properties, and durabilities of asphalt-filler mixtures*—Continued

Specimen number	Asphalt-filler mixture				Kind of filler	Filler No.	Penetrations in 0.01-cm units			Durability	
	Hard asphalt	Soft asphalt	Filler	Hard asphalt in total asphalt			At 32° F, 200 g, 60 sec	At 77° F, 100 g, 5 sec	At 115° F, 50 g, 5 sec	3-yr outdoor exposure, group number	Life in accelerated test
	%	%	%	%							Cycles
36	40	25	35	62	Silica dust	14	7	9	18	II	35
37	54	21	25	72			6	9	16	II	30
38	72	13	15	85			6	9	16	III	28
39	49	16	35	75	do	15	7	9	17	II	35
40	64	11	25	85			7	10	17	II	35
41	77	8	15	91			7	9	17	II	28
42	33	32	35	51	Slate flour	16	7	10	17	I	65
43	50	25	25	67			7	10	17	I	51
44	68	17	15	80			7	10	17	II	43
45	44	21	35	68	do	17	7	10	14	I	65
46	58	17	25	78			7	10	15	I	65
47	75	10	15	88			7	10	18	II	43
48	43	22	35	66	Limestone	18	7	10	18	II	45
49	56	19	25	75			7	10	18	III	33
50	75	10	15	88			7	10	19	III	28
51	49	16	35	75	do	19	7	10	18	II	53
52	64	11	25	85			8	10	17	II	48
53	81	4	15	95			6	10	19	III	28
54	100	------	------	100	----------	----	7	10	17	III	28
55	75	25	------	75	----------	----	9	11	17	III	28
56	50	50	------	50	----------	----	8	12	21	III	28
57	25	75	------	25	----------	----	9	15	27	III	28

Fifty-seven different combinations of asphalts and asphalt-filler mixtures, including nearly all of the fillers in commercial use, were prepared and surfaced to a thickness of 0.025 in.[5] on aluminum sheet panels (3 by 6 in.). Seven sets of such panels were prepared in duplicate, making 114 panels for each set. Single sets were exposed outdoors at Buffalo, N. Y., Manville, N. J., Chicago, Ill., Los Angeles, Calif., New Orleans, La., and Washington, D. C. The panels in the outdoor exposures were placed on racks at an angle of 45 degrees facing south. The seventh set of panels was subjected to an accelerated-weathering test which consisted in exposing the panels alternately to light from an inclosed carbon arc, water spray, and to sudden temperature changes.[6]

III. PHYSICAL PROPERTIES OF THE FILLERS

The physical properties of the fillers are listed in table 2. As shown in the table, fillers 14 to 19 were prepared from fillers 4, 5, and 13.

[5] The method of preparing the panels is fully described in a paper by O. G. Strieter, *Accelerated tests of asphalts*, BS J. Research **5**, 247 (1930) RP197; also in the *Proposed method for accelerated-weathering tests on bituminous materials*, Proc. Am. Soc. Testing Materials **33**, pt. I, 381 (1933).

[6] The accelerated weathering test is fully described in the *Proposed method for accelerated-weathering tests on bituminous materials*, Proc. Am. Soc. Testing Materials **33**, pt. I, 381 (1933).

TABLE 2.—*Physical properties of the fillers*

Filler number	Kind of filler	Particle size of filler			Specific gravity	Compacting weight	Fineness factor, *f*
		Passing No. 200 sieve	Passing No. 100, retained on No. 200 sieve	Retained on No. 100 sieve			
		Percent	*Percent*	*Percent*			
1	Slate flour—air-floated No. 000 grade	81	17	1	2.86	1.35	1.1
2	Dolomite	92	7	1	2.85	1.63	0.8
3	do	85	14	1	2.88	1.73	.7
4	Limestone	91	8	1	2.76	1.62	.7
5	Peach Bottom slate—No. 000 grade	79	16	5	2.98	1.40	1.1
6	Silica sand	2	13	85	2.69	1.74	0.6
7	Greenstone	65	24	12	3.08	1.66	.9
8	Hydrated lime	99	2	----	2.39	.83	1.9
9	Trap rock	97	3	----	2.94	1.52	0.9
10	Celite (Hy Flo Supercel)	100	----	----	2.52	.30	7.4
11	Mica	42	28	30	3.20	.51	5.3
12	Foliated talc	100	(a)	----	2.97	1.05	1.8
13	Silica dust	67	26	7	2.69	1.68	0.6
14	Silica dust (prepared from filler 13)	100	----	----	2.69	1.63	.7
15	do	----	100	----	2.69	(b)	----
16	Slate flour (prepared from filler 5)	100	----	----	2.98	1.30	1.3
17	do	----	100	----	2.98	(b)	----
18	Limestone (prepared from filler 4)	100	----	----	2.76	1.63	0.7
19	do	----	100	----	2.76	(b)	----

(a) Trace retained on No. 200 sieve.
(b) Insufficient material for test.

The specific gravities of the fillers were determined by means of a picnometer, using kerosene as the liquid. The details of the method have been described elsewhere.[7]

The compacting weight (weight of the filler occupying a volume of 1 ml when compacted) was determined in a 100 ml graduated cylinder. A quantity of filler judged to approximate a volume of 10 ml when compacted was placed in the cylinder and compacted by tapping the bottom of the cylinder against a padded table top. A distinctive, dull sound indicated when the filler was compact. This operation was repeated until a volume of 100 ml of compact filler was obtained. The weight of this filler divided by 100 was taken as the "compacting" weight.

Since the compacting weights of fillers with different specific gravities cannot be directly compared, the compacting weights were used to calculate a "fineness factor," f, according to the following formula.[8]

$$f = \frac{\text{density} - \text{compacting weight}}{\text{compacting weight}}$$

The finer a given filler has been ground, the larger is its fineness factor.

Table 3 shows the increases in the softening points of the asphalt due to the addition of filler. Examination of the data will show that the higher the fineness factor of the filler, the greater the increase in the softening point of the asphalt. It should be borne in mind, how-

[7] *Standard methods of test for specific gravity of pigments*, A. S. T. M. Designation D 153-27, Book of Standards, Am. Soc. Testing Materials, pt. II, 568 (1933).
[8] Franz Pöpel. Der Moderne Asphaltstrassenbau (Strassenbau-Verlag Martin Boerner, Halle, 1929).

TABLE 3.—*Effect of fillers on the softening point of the asphalt*

Kind of filler	Filler number	Filler by weight	Fineness factor *f*	Increase in softening point of asphalt due to addition of filler
		Percent		°C
Supercel	10	15	7.4	14.0
Mica	11	15	5.3	9.5
Hydrated lime	8	15	1.9	8.0
Foliated talc	12	15	1.8	3.5
Slate	16	35	1.3	7.0
Do	5	35	1.1	6.5
Green slate	1	35	1.1	5.5
Greenstone	7	35	0.9	5.0
Dolomite	2	35	.8	5.0
Limestone	4	35	.7	5.0
Silica dust	13	35	.6	4.5
Silica sand	6	35	.6	2.0

ever, that the increases in the softening points of an asphalt due to additions of filler follow a parabolic curve,[9] i. e., the first small additions of filler have only a slight effect, but with subsequent additions of small amounts of filler the softening point of the asphalt increases rapidly. The average void diameter of the fillers as present in the mixture can also be used to characterize the filler in place of the fineness factor, and instead of the increase in softening point the increase in absolute viscosity can be determined.[10]

IV. OUTDOOR EXPOSURES AND ACCELERATED TESTS

1. OUTDOOR EXPOSURES

Asphalts exposed outdoors weather characteristically, depending upon their composition and upon the weather peculiar to the locality of exposure. Thus there is a marked difference in appearance in the six series of panels exposed in the various localities. The outdoor panels, examined after 3 years of exposure, are described under the following headings.

(a) SURFACE OXIDATION

Asphalts exposed to the weather form a film of oxidized material on the surface, which may be readily rubbed off. The amount of such oxidized material formed depends upon the nature of the asphalt, the intensity of the sunlight, and the amount of moisture.

As regards the degree of surface oxidation of the coatings, the localities of exposure are rated in the following ascending order: Los Angeles, *L;* Chicago, *C;* Manville, *M;* Buffalo, *B;* Washington, *W;* and New Orleans, *N.*

(b) CRACKING

Asphalts crack upon continued exposure to the weather. This type of weathering is influenced by the composition of the coating and is also characteristic for each locality.

The *B* coatings cracked to the greatest degree but are followed closely by the *M* and *C* coatings. The *N* and *W* coatings cracked

[9] See footnote 8.
[10] R. N. Traxler, Ind. Eng. Chem. 29, 489–492 (1937).

less and the *L* coatings the least of all. As a rule, the *B*, *M*, and *C* coatings showed short cracks tending to form four-sided but irregular checks. The *W* coatings, as a rule, showed long, narrow cracks, whereas in the *N* coatings the cracks were much wider.

(c) CLASSIFICATION OF OUTDOOR EXPOSURES

The degree of cracking during outdoor exposure was made the basis for classifying the various coating mixtures. For this purpose the coatings in each outdoor exposure were arranged in order from best to poorest according to appearance and were subdivided into three groups, as shown in table 4, according to the following scheme:

TABLE 4.—*Order of durability of asphalt-filler mixtures*

Specimen number	Composition			Durability
	Amount	Kind of filler	Filler No.	
	GROUP I			
	Percent			*Cycles*
29	15	Mica	11	65+
30	35	Talc	12	65
31	25	do	12	65
42	35	Slate	16	65
45	35	do	17	65
13	35	do	5	65
1	35	do	1	62
14	25	do	5	62
46	25	do	17	65
43	25	do	16	51
32	15	Talc	12	48
	GROUP II			
51	35	Limestone	19	58
19	35	Greenstone	7	65
39	35	Silica	15	35
40	25	do	15	35
2	25	Slate	1	45
47	15	do	17	43
28	15	Supercel	10	40
20	25	Greenstone	7	46
36	35	Silica	14	35
44	15	Slate	16	43
25	35	Trap rock	9	43
16	35	Silica	6	28
17	25	do	6	28
41	15	do	15	28
52	25	Limestone	19	48
5	25	Dolomite	2	28
15	15	Slate	5	43
4	35	Dolomite	2	37
3	15	Slate	1	37
33	35	Silica	13	35
34	25	do	13	33
26	25	Trap rock	9	37
8	25	Dolomite	3	37
37	25	Silica	14	30
7	35	Dolomite	3	40
11	25	Limestone	4	37
48	35	do	18	45
10	35	do	4	43
21	15	Greenstone	7	40

TABLE 4.—*Order of durability of asphalt-filler mixtures*—Con.

Specimen number	Composition			Durability
	Amount	Kind of filler	Filler No.	
		GROUP III		
	Percent			*Cycles*
18	15	Silica	6	28
38	15	do	14	28
27	15	Trap rock	9	28
35	15	Silica	13	28
9	15	Dolomite	3	28
53	15	Limestone	19	28
54	----------	Asphalt, softening point 108° C	----------	28
55	----------	Asphalt, softening point 104° C	----------	28
56	----------	Asphalt, softening point 99.5° C	----------	28
57	----------	Asphalt, softening point 94° C	----------	28
49	25	Limestone	18	33
50	15	do	18	28
6	15	Dolomite	2	28
12	15	Limestone	4	33
24	15	Hydrated lime	8	28
23	25	do	8	28
22	35	do	8	28

No. I. Panels showing no cracks visible to the unaided eye, or, at most, showing faint cracks to the unaided eye.

No. II. Panels showing fair-sized cracks to the unaided eye.

No. III. Panels showing wide cracks to the unaided eye.

Such a method of classification can only approximate the true relative positions of the panels. The detailed descriptions of the coatings after 3 years of outdoor exposure in various localities are given in table 5. In this table, however, the same arrangement of the panels as listed in table 4 has been retained.

2. ACCELERATED-WEATHERING TESTS

The life or durability of the coatings in the accelerated-weathering tests is given in cycles (table 4). The results are the average of duplicate panels differing by not more than 3 to 5 cycles. The end point of the accelerated-weathering test was determined by measurement of electrical conductivity. In the "conductivity test," [11] the panel is placed in a circuit and covered with a template having 10 holes. The asphalt surface is then moistened through these holes with an electrolyte. If cracks through to the aluminum are present in the coating, the electrolyte will conduct electricity. The end point of the test is reached when at least 6 of the 10 holes in the template conduct current.

The results of the "conductivity test" on the outdoor exposure samples are shown in table 5.

[11] Method described in *Proposed method for accelerated-weathering tests on bituminous materials*, Proc. Am. Soc. Testing Materials 33, pt. I, 384-385 (1933).

n—No cracks on surface of panel visible to eye.
c—Cracks on surface of panel visible to eye.
i—No cracks on surface of panel visible to eye.

n=No cracks on surface of panel visible to eye.
c=Cracks on surface of panel visible to eye.
1=No cracks on surface of panel visible under magnifying glass (12×).
2=No cracks at side of panel visible under magnifying glass (12×).
3=No cracks at side of panel visible to eye.
4=No conductivity in the electrical conductivity test.
+=Although specimen has deteriorated in the manner stated, the deterioration is not marked.
v=Aluminum panel visible to eye through cracks in coating.

TABLE 5.—*Appearance of coatings after three years' exposure outdoors in various localities*

Specimen number	Composition			Exposures						
	Amount	Kind of filler	Filler number	L	W	M	C	B	N	A
				GROUP I						
	%									Cycles
29	15	Mica	11	n, 1, 2, 3, 4	n, 1, 2, 3, 4	n, 1, 2, 3, 4	n, 1, 2, 3, 4	n, 1, 2, 3, 4	n, 1, 2, 3, 4	[a] 65+
30	35	Talc	12	n, 1, 2, 3, 4	n, 1, 2, 3, 4	n, 1, 2, 3, 4	n, 1, 2, 3, 4	c, 2, 3	n, 1, 2, 3, 4	65
31	25	do	12	n, 1, 2, 3, 4	n, 1, 2, 3, 4	c+	c, 2, 3	c, 2, 3	n, 1, 2, 3, 4	65
42	35	Slate	16	n, 1, 2, 3, 4	n, 1, 2, 3, 4	c+	c	c, 2, 3	n, 2, 3, 4	65
45	35	do	17	n, 2, 3	n, 1, 2, 3, 4	n	n	c, 3	n, 2, 3	65
13	35	do	5	n, 1, 2, 3, 4	n, 1, 2, 3, 4	c+	c+	c, 3	n, 2, 3	65
1	35	do	1	c+, 2, 3	c, 2, 3	c	c	c+	c, 3	62
14	25	do	5	n, 2, 3, 4	c, 2, 3	c	c+	c++	c, 3	62
46	25	do	17	n, 2, 3	n, 3	c	c	c++	n, 3	65
43	25	do	16	n, 2, 3	c, 2, 3	c	c	c++	c, 3	51
32	15	Talc	12	c, 2, 3	c, 2, 3	c	c	c+	c, 2, 3	48
				GROUP II						
51	35	Limestone	19	c,	c	c	c	c	c	58
19	35	Greenstone	7	c, 3	c, 3	c	c	c	c, 3	65
39	35	Silica	15	c	c+	c	c	c	c	35
40	25	do	15	c	c+	c	c	c	c	35
2	25	Slate	1	c, 3	c, 3	c	c	c	c+	45
47	15	do	17	c, 3	c, 3	c	c	c	c	43
28	15	Supercel	10	c, 2, 3	c, 2, 3	c	c	c	c+	40
20	25	Greenstone	7	c, 3	c, 3	c	c	c	c	46
36	35	Silica	14	c, 3	c, 3	c	c	c	c+	35
44	15	Slate	16	c, 2, 3	c, 3	c	c	c	c+	43

[a] In this particular case the + means that the panel had not reached the end point of test after an exposure of 65 cycles.

n=No cracks on surface of panel visible to eye.
c=Cracks on surface of panel visible to eye.
1=No cracks on surface of panel visible under magnifying glass (12×).
2=No cracks at side of panel visible under magnifying glass (12×).
3=No cracks at side of panel visible to eye.
4=No conductivity in the electrical conductivity test.
+=Although specimen has deteriorated in the manner stated, the deterioration is not marked.
v=Aluminum panel visible to eye through cracks in coating.

TABLE 5.—*Appearance of coatings after three years' exposure outdoors in various localities*—Continued

Specimen number	Composition			Exposures						
	Amount	Kind of filler	Filler number	L	W	M	C	B	N	A
				GROUP II—Continued						
25	35	Trap rock	9	c, 3	c+	c	c	c	c	43
16	35	Silica	6	c	c	c	c	c	c	28
17	25	do	6	c	c	c	c	c	c	28
41	15	do	15	c	c+	c	c	c	c	28
52	25	Limestone	19	c	c	c	c	c	c	48
5	25	Dolomite	2	c, 3	c+	c (wide)	c	c	c	28
15	15	Slate	5	c	c+	c	c	c	c+	43
4	35	Dolomite	2	c, 2,3	c	c	c	c	c	37
3	15	Slate	1	c	c+	c	c	c	c	37
33	35	Silica	13	c	c+	c	c	c	c	35
34	25	do	13	c	c+	c	c	c	c	33
26	25	Trap rock	9	c (badly)*	c+	c	c	c	c	37
8	25	Dolomite	3	c (badly)	c+	c	c	c	c	37
37	25	Silica	14	c	c+	c	c	c	c	30
7	35	Dolomite	3	c, 2,3	c+	c	c	c	c	40
11	25	Limestone	4	c (badly)	c+	c	c	c	c	37
48	35	do	18	c (badly)	c	c	c	c	c	45
10	35	do	4	c, 2,3	c	c	c	c	c	43
21	15	Greenstone	7	c	c+	c	c	c	c (large)	40

* Indicates that the coating was badly cracked.

GROUP III

GROUP III

18	15	Silica	6	c	c	c	c	c	c	28
38	15	do	14	c	c	c	c	c	c (wide)	28
27	15	Trap rock	9	c (badly)	c	c	c	c	c (wide)	28
35	15	Silica	13	c	c	c	c	c	c	28
9	15	Dolomite	3	c	c	c	c	c	c (wide)	28
53	15	Limestone	19	c	c	c	c	c	c	28
54	----------	Asphalt, softening point 108° C	----------	c (v)	c	c (v)	c	c (wide)	c (wide)	28
55	----------	Asphalt, softening point 104° C	----------	c (v)	c	c	c	c (wide)	c (wide)	28
56	----------	Asphalt, softening point 99.5° C	----------	c (v)	c	c (v)	c	c (wide)	c (wide)	28
57	----------	Asphalt, softening point 94° C	----------	c (v)	c	c	c	c (wide)	c (wide)	28
49	25	Limestone	18	c	c	c	c (wide)	c (wide)	c (wide)	33
50	15	do	18	c (long)	c	c	c (wide)	c (wide)	c (wide)	28
6	15	Dolomite	2	c	c	c	c	c (wide)	c (wide)	28
12	15	Limestone	4	c	c	c	c	c (wide)	c (wide)	33
24	15	Hydrated lime	8	c (badly)	c (v)	c (v)	c	c (v)	c (v)	28
23	25	do	8	c (badly)	c (v)	c (v)	c (v)	c (v)	c	28
22	35	do	8	c (badly)	c (v)	c (wide)	c (v)	c (v)	c (v) lost adhesive properties.	28

V. DISCUSSION OF RESULTS

In general, the coatings failed in the same order in the outdoor as in the accelerated-weathering test. In the outdoor exposures the silica-filled coatings received higher ratings, when classified according to appearance, than in the accelerated tests. The conductivity test showed that the panels exposed to accelerated weathering were porous and absorbed the electrolyte readily, giving an end point of test, although their appearance was still excellent. The relatively poor adhesion of the silica particles to asphalt is the cause of this porosity.

Figures 2 to 22, inclusive, are actual-size photographs of sections of the test pieces exposed outdoors for 3 years. Some of the photographs are of coatings exposed for 65 cycles in the accelerated test.

Groups I, II, and III (table 4) are illustrated in figures 2 to 9, inclusive. Since the specimens within a group are arranged in the order from best to poorest, and since group II is large, photographs are shown which typify the most durable panels (figs. 4 and 5) and the least durable (figs. 6 and 7) in this group. Examination of these photographs will show differences in the durabilities of the coatings resulting from differences of composition and location of exposure.

Figures 10 and 11 show the unfilled coating asphalt, specimens 55 (table 4), in the outdoor and accelerated-weathering exposures. Comparison with figures 2 and 3 shows that a suitable filler greatly improves the durability of the asphalt.

In figures 12 and 13, 35, 25, and 15-percent of slate, respectively, are compared with one another and also with the unfilled coating asphalt. The specimens are shown in their exposures at Buffalo and New Orleans. These exposures were chosen because they differ widely in temperature and humidity. The coatings with the greatest amount of filler are the best, the unfilled coating asphalt is the worst.

The behavior of various fillers to outdoor exposure is shown in figures 14 and 15. These specimens are quite similar in durability, but are not as good as those shown in figures 2 and 3, or the 35-percent of slate shown in figures 12 and 13.

Figures 16 and 17 show specimens containing 25 percent by weight of limestone filler, but in various particle sizes. The one size was a finely cracked material practically all of which passed a No. 100 sieve and 91 percent a No. 200 sieve. The other two sizes consisted of the portions of the material which passed through and were retained on a No. 200 sieve, respectively. Figure 18 shows the same coatings after exposure to accelerated weathering. Figure 19 shows the Buffalo exposures and figure 20 the New Orleans exposures of a similar series of compositions, but using silica instead of limestone as a filler. Figures 21 and 22 show similar coatings with slate, however, only in amounts of 15 percent by weight instead of 25 percent. In each case, irrespective of the kind or amount of filler, the specimens containing fillers passing a No. 100 but retained on a No. 200 sieve have the best appearance. The specimens with filler passing a No. 200 sieve do not show up as well. However, final conclusions regarding the most suitable size of fillers cannot be drawn from those tests. More extensive testing is required to settle this question.

Fillers appear to affect asphalts in two ways, first, a stiffening effect, normal to all fillers and evidenced by a higher softening point, and, second, an effect shown mostly by the coarser fillers, which is actually the production of a rigid structure. This structure-giving property

of the coarser fillers is probably the reason for the better appearance of the specimens containing 100- to 200-mesh filler (see figs. 16 to 22). It is also the reason for the good appearance of those coatings containing silica, a structure-giving filler.

VI. SUMMARY

These weathering tests, outdoor and accelerated, show that the addition of fillers increases the durability of coating asphalts in varying degrees, depending upon the character, proportion, and particle size of the fillers.

The best results were obtained with coatings containing talc, mica, and Peach Bottom slate. Less positive results were obtained with coatings containing silica, trap rock, dolomite, and limestone in amounts of 15 percent by weight. Hydrated lime was the only filler tested that did not increase the durability of the coating.

Within the limits tested, and excepting the coatings containing hydrated lime, the higher the percentage of a given filler, the more durable was the coating. The coatings containing 35 percent by weight of hydrated lime lost their adhesive properties and separated from the aluminum panels.

The question of the most suitable particle size and distribution of the fillers was not settled by these tests. The tests do show, however, that fillers passing a No. 100 sieve, but retained on a No. 200 sieve, produce better coatings than fine filler, all of which passes a No. 200 sieve.

The data demonstrate the similarity between outdoor and accelerated exposures.

The author expresses appreciation to H. R. Snoke and to L. R. Kleinschmidt, both of the Bureau staff, for their assistance in many ways in this investigation.

WASHINGTON, November 26, 1937.

U. S. DEPARTMENT OF COMMERCE NATIONAL BUREAU OF STANDARDS

RESEARCH PAPER RP1074

Part of Journal of Research of the National Bureau of Standards, Volume 20, February 1938

MINOR CONSTITUENTS IN PORTLAND CEMENT CLINKER

By Herbert Insley and Howard F. McMurdie

ABSTRACT

The optical and structural properties of some minor phases in portland cement clinker as observed in thin sections, polished sections, and a new type of polished thin section are recorded. The similarity of such phases to those found in laboratory preparations is pointed out. Methods of determination of free CaO, free MgO, "light" interstitial material, and "dark" interstitial material are given. The "light" interstitial material is shown to be $4CaO \cdot Al_2O_3 \cdot Fe_2O_3$. There are three kinds of "dark" interstitial material which have the properties of: (1) glass; (2) $3CaO \cdot Al_2O_3$; and (3) a prismatic crystalline material. The prismatic crystalline material apparently is a compound of the alkalies with some of the other oxides in the clinker. Glass is found in the majority of portland cement clinkers. At present, it is impossible to calculate precisely the compound composition from chemical analyses because of lack of knowledge of cooling conditions, the effect of minor constituents on phase relations, and other variables.

CONTENTS

	Page
I. Introduction	173
II. Preparation of polished thin sections	174
III. Identification of free CaO and free MgO	174
1. Free CaO	174
2. Free MgO	175
IV. Identification of other interstitial constituents	176
1. The "light" interstitial phase	177
(a) Relations with MgO	177
2. The "dark" interstitial material	179
V. Discussion	182
VI. Summary	183
VII. References	184

I. INTRODUCTION

In a previous paper [1][1] the structural characteristics of some constituents of portland cement clinker were described and the deviations of these constituents from the pure compounds were pointed out. Studies investigating the nature and extent of these deviations were suggested. This paper presents the results of a similar study restricted to the minor constituents.[2]

As in the previous study, the petrographic and metallographic microscopes and the X-rays were used. In addition, a combination

[1] Figures in brackets refer to references at the end of the paper.

[2] The authors have arbitrarily defined "minor constituents" as those phases which never occur in amounts greater than 25 percent in commercial portland cement clinker.

of the petrographic and metallographic methods was employed, which is described later in the paper.

As material for the investigation of structures there were available not only the laboratory-prepared clinkers which were made from mixtures of the separate oxides (or carbonates) and heat treated in a small platinum resistance furnace, but also about 60 samples of commercial portland cement clinker, of which a large majority were obtained through the generous cooperation of Mr. Dalton G. Miller.[3]

Following common usage in technical reports on cement constitution, a system of abbreviations is used in referring to the compounds, thus: $3CaO.SiO_2=C_3S$; $4CaO.Al_2O_3.Fe_2O_3=C_4AF$; $8CaO.Na_2O.3Al_2O_3=C_8NA_3$, etc.

II. PREPARATION OF POLISHED THIN SECTIONS

A method of preparing mounts which could be observed both by transmitted and by reflected light was developed for the microscopic study of clinker. The clinker piece to be sectioned was heated in a resin having a high index of refraction[4] until the resin became tough but not brittle. After grinding one face to a plane with fine emery the piece was cemented to an object slide with the same resin used for impregnation and the other surface then ground down until the section was of the required thickness (15 to 20 microns). After fine grinding with fine emery and alcohol the exposed surface of the clinker was polished with a mixture of jeweler's rouge and alcohol on a canvas-covered rotating lap. The polished surface was then etched. With a vertical illuminator and objective corrected for use without cover glass, attached to the tube of a petrographic microscope, the specimen could be examined either in reflected or transmitted light without changing its position on the stage of the microscope.

III. IDENTIFICATION OF FREE CaO AND FREE MgO

1. FREE CaO

Although free CaO is not a constituent of properly proportioned, well-mixed and well-burned portland cement clinker, it is so commonly present in small amounts in commercial clinker that its easy determination, both qualitatively and quantitatively, is of great importance.

Of the many methods which have been devised for the determination of free CaO, three very commonly used are White's reaction, the ammonium acetate method, and the determination by optical properties. White's reaction, [2] which results in the formation of calcium phenolate crystals by interreaction of the free lime with phenol in nitrobenzene and water, gives qualitative results.

The ammonium acetate method [3] is quantitative. The fact that both White's reaction and the ammonium acetate method give positive results for calcium hydroxide as well as for free lime may sometimes be a disadvantage.

The microscopic identification by optical properties makes use of the isotropy and high index of refraction (1.83) of free CaO. In quantitative estimation in thin sections of cement clinker the amount of free CaO is very likely to be underestimated because of overlap of birefringent constituents.

[3] Senior Drainage Engineer, U. S. Department of Agriculture.
[4] Liquid Hyrax or Aroclor No. 4465 was found satisfactory.

Polished specimens prepared by the method described in the previous paper [1][5] are satisfactory for the observation of free CaO. A mixture of rouge and ethyl alcohol is substituted for the rouge-water mixture in polishing to avoid hydration of the free CaO. The specimen is then etched in a 1:1 water-alcohol mixture for 1 to 3 minutes, the shorter times being required at higher room temperatures. This method has been found to give more uniform results than Tavasci's method [4] of etching during polishing with a mixture of rouge, alcohol, and water. The etching treatment causes a decided darkening of the exposed surfaces of free CaO grains, probably because of formation of thin films of $Ca(OH)_2$.

Free CaO usually occurs as rounded grains, either singly or in aggregates (fig. 1). Aggregates appear to be the result of imperfect batch mixing. Single grains, which are often located at the centers of C_3S, are evidently the result of imperfect diffusion during reaction to form dicalcium and tricalcium silicates.

The qualitative determination of free CaO in polished section has some advantages over other methods. It is more rapid than any of the other methods except White's and it permits observation of the structural relations to other clinker constituents. By use of one of the integrating stages [5] the free CaO may be determined quantitatively. It is possible that a rapid quantitative method could be devised in which the polished sample to be determined could be compared with a set of standard polished specimens composed of individuals varying by some convenient step, say 5 percent. The standards would, of course, have to be kept in a dry atmosphere to prevent the hydration of the free lime.

2. FREE MgO

In completely crystallized portland cement clinker all or nearly all of the MgO occurs as crystalline MgO (periclase), commonly known as free magnesia [6]. In clinker which have been solidified so rapidly that some glass is present, varying amounts of MgO will be dissolved in the glass [7, 8] depending upon the cooling rate, the amount of MgO, etc.

Because evidence is accumulating that excessive expansions in concrete have been caused by the hydration of crystalline MgO, the identification of free MgO is of great importance. So far only two methods of identification have been described which can be regarded as at all satisfactory. By one method the free MgO is left as undissolved residue after solution of the cement in a mixture of HNO_3 and HF [8], but because it is slowly soluble in this reagent this method gives results which are low.

The second method of identification, by means of the petrographic microscope, is of qualitative value. Even qualitative distinction, however, is difficult because crystalline MgO is isotropic and has an index of refraction very close to that of other constituents. In thin sections free MgO may easily be overlooked because it usually occurs in very small grains and may be masked by overlapping, birefringent constituents.

[5] Besides the impregnating resins mentioned in the paper referred to, Bakelite resinoid 0014 has been used successfully. The specimens are immersed in the resinoid in small vials, subjected to vacuum produced by a faucet aspirator for 2 to 3 hours, heated overnight at 75 to 80° C and finally at 105 to 110° C for 24 hours. The vials are broken away from the hardened preparations before grinding and polishing.

A new method which, it is believed, gives better results than either of the preceding is the determination in polished specimens by reflected light. Free MgO observed by this method is found to occur in small, angular grains (fig. 2) with a reflectivity greater than that of other constituents except C_4AF. It can easily be seen in unetched sections or in sections etched with the milder reagents such as water and alcohol-water mixtures. Characteristics of free MgO in polished specimens were first observed in laboratory preparations in which MgO, the only crystalline phase determined by petrographic examination, was present in a glassy matrix. Failure, heretofore, to identify free MgO in polished sections was found to be caused by difficulty in proper polishing. Unless polished with extreme care, the edges of the MgO grains are fragmented and secondary scratches beginning from these fragmented areas cover the surface of the specimen. Crystalline MgO is known to have an unusually high thermal expansion. It seems probable that during cooling of the clinker the MgO crystals contract faster than the other constituents until they finally break away from the surrounding materials. During grinding and polishing the abrasive media collect in these peripheral cracks and widen them.

Free MgO occurs in commercial clinker almost without exception as inclusions in the interstitial constituents and is, therefore, one of the later phases to crystallize.

Like free CaO, it may be determined quantitatively in polished sections by the use of the integrating stage, and rapid quantitative methods perhaps could be developed which depend upon comparison of the unknown with standard specimens in which free MgO had already been determined with the integrating stage.

Quantitative microscopic determinations of free MgO have been made on a number of commercial clinker specimens, the results of which will be published in a forthcoming paper [10]. It was found in most of the samples that free MgO as determined microscopically was less than total MgO determined chemically. This is a confirmation of other evidence [6, 8] that when glass is present MgO is partially or wholly dissolved in the glass.

IV. IDENTIFICATION OF OTHER INTERSTITIAL CONSTITUENTS

Cement clinker of normal composition is never completely liquid at maximum kiln temperatures (1,400 to 1,475° C), but always contains crystalline C_2S, C_3S, or both [11]. The liquid, containing most, if not all, of the Al_2O_3, Fe_2O_3, MgO, and alkalies, as well as some CaO and SiO_2, solidifies during cooling and forms the interstitial material surrounding the C_2S and C_3S. Some C_2S, which occurs as granular fringes on the borders of C_3S crystals and as overgrowths on previously formed C_2S crystals, should strictly be considered as interstitial material, but since it retains the optical properties and etching characteristics of the coarse-grained C_2S, it will not be discussed here.

Polished sections of clinker which have been etched with a 1-percent alcoholic solution of HNO_3 [6] show two readily distinguishable forms of interstitial material [1, 4] which, for purposes of identification, are here called "light interstitial" and "dark interstitial."

[6] This reagent is made by adding 1 ml of HNO_3 (sp gr 1.42) to 100 ml of ethyl alcohol.

1. THE "LIGHT" INTERSTITIAL PHASE

The light interstitial phase may readily be distinguished from other constituents in polished sections by its higher reflectivity and greater resistance to most etchants. This constituent was identified by Tavasci [4] as C_4AF and all the observations made by us confirm his identification. Examination with reflected polarized light shows definitely that the constituent is anisotropic, and comparisons of this phase (in clinker sections where it is well developed) with pure C_4AF show that the degree of anisotropy and reflectivity is about the same. The compound C_2F ($2CaO.Fe_2O_3$), which might presumably exist in clinker under some conditions of cooling, has a higher reflectivity and a greater degree of anisotropy than the light interstitial phase so far observed in commercial clinker. Examination of clinker petrographically shows the presence of a birefracting, highly refractive constituent with the optical properties of C_4AF wherever the polished specimens of the same clinker contain the light interstitial constituent.

The crystalline habit of the light interstitial phase depends in part on the Al_2O_3/Fe_2O_3 ratio of the clinker and the cooling treatment to which it has been subjected. It is almost universally present as prisms. Where the Al_2O_3/Fe_2O_3 ratio is low and the cooling slow, the prisms tend to be large and broad. Where the Al_2O_3/Fe_2O_3 ratio is high the crystals are frequently very small, slender needles or are dendritic growths.

Optical properties determined either in transmitted or reflected light are not sufficiently precise to decide whether C_4AF exists in the pure form or whether it contains other material in solid solution. Indeed, quantitative microscopic determinations [10] on some clinker with low Al_2O_3/Fe_2O_3 ratios show more light interstitial material than can be accounted for by calculating all Fe_2O_3 as C_4AF. McMurdie [12] has shown that in the system CaO-Al_2O_3-Fe_2O_3, C_4AF may take into solid solution between 2.5 and 5 percent of C_3A and about 5 percent of C_5A_3.

The influence of other oxides such as MgO upon the optical properties, particularly color and pleochroism, of C_4AF has been noted by other observers [13]. Schwiete and zur Strassen [14] also noted the change in color and pleochroism produced by the presence of MgO, and attempted to determine the amount of solid solution of MgO in C_4AF by the presence and intensity of X-ray diffraction lines of MgO in mixtures with C_4AF heated to high temperatures, as compared with X-ray lines of mechanical mixtures of the two compounds. They found that in the system C_4AF-MgO the limit of solid solution of MgO in C_4AF was about 2 percent. As will be seen in the following brief study of the system C_4AF-MgO by the present authors, the limits of solid solution as defined by Schwiete and zur Strassen were not confirmed.

(a) RELATIONS WITH MgO

Equilibrium relations of C_4AF and MgO were outlined by a combination of heating curve and quenching determinations. Mixtures containing C_4AF crystallize rapidly during quenching. It was found possible to prevent this by pointing the lower end of the envelop containing the charge, thus permitting the charge to penetrate the surface of the mercury quenching bath when dropped from the furnace.

The system was found to be a simple eutectic one. The eutectic composition and temperature (6.5 percent of MgO : 93.5 percent of C_4AF, 1,347 ±3° C) were indicated by extrapolation of the two liquidus curves to the intersection. The temperature was confirmed by the temperature of the lowest break on the heating curve of a previously crystallized mixture of 90 percent of C_4AF : 10 percent of MgO, and both temperature and composition by quenching tests on a mixture of 6.5 percent of MgO : 93.5 percent of C_4AF. These results differ somewhat from those of Schwiete and zur Strassen, who located the eutectic at about 8 percent of MgO : 92 percent of C_4AF and about 1,370°C. The equilibrium diagram as determined by the present authors is shown in figure 3 and the results of the quenches are given in table 1.

TABLE 1.—*Results of the quenches in the system* MgO–$4CaO.Al_2O_3.Fe_2O_3$

Composition		Temperature	Phases present
MgO	C_4AF		
Percent	*Percent*	°C	
2.0	98.0	1355	C_4AF+glass
		1350	C_4AF+glass
		1310	C_4AF+MgO
4.0	96.0	1395	Glass only
		1385	C_4AF+glass
5.0	95.0	1370	Glass only
		1360	C_4AF+glass
		1350	C_4AF+glass
		1340	C_4AF+MgO
6.5	93.5	1352	Glass only
		1345	C_4AF+MgO
7.5	92.5	1410	Glass only
		1405	MgO+glass
10.0	90.0	1350	MgO+glass

In spite of the fact that the qualitative observations of previous workers were confirmed, namely, that the presence of MgO deepened the color and markedly increased the pleochroism of C_4AF, no other evidence of solid solution could be found in compositions containing 1 percent or more of MgO. Mixtures of 1 percent of MgO : 99 percent of C_4AF were heated to temperatures near the liquidus, cooled at rates less than 0.5°/min to 1340° C, a temperature just below that of the solidus, maintained at that temperature for ½ hour or longer, and quenched. Microscopic examination of these charges always showed a small amount of material with the optical properties of crystalline MgO (isotropic, n_D about 1.735) and X-ray patterns of such charges failed to show any perceptible shift in the lines of C_4AF as compared with those of the pure compound. Mixtures of 50 percent of MgO and 50 percent of C_4AF, held for periods up to 16 hours at about 1340° C, after very slow cooling from higher temperatures showed no shift in the X-ray lines of either C_4AF or MgO as compared with the pure compounds. Evidence from the studies reported here indicates, therefore, that in the system MgO–C_4AF, solid solution of MgO in C_4AF must be less than 1 percent.

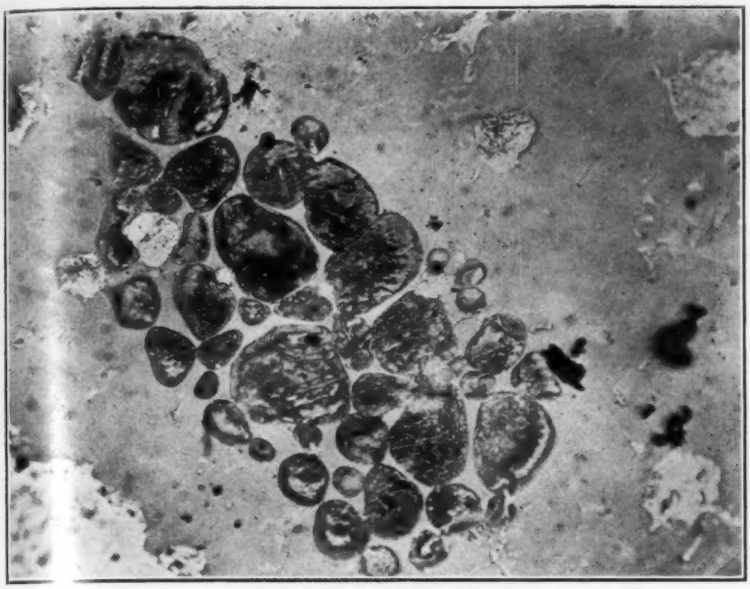

FIGURE 1.—*Free* CaO *in commercial portland cement clinker.*

Polished specimen, etched with 1 : 1 alcohol-water solution for 2 minutes. Reflected light. Magnification 1,000×.

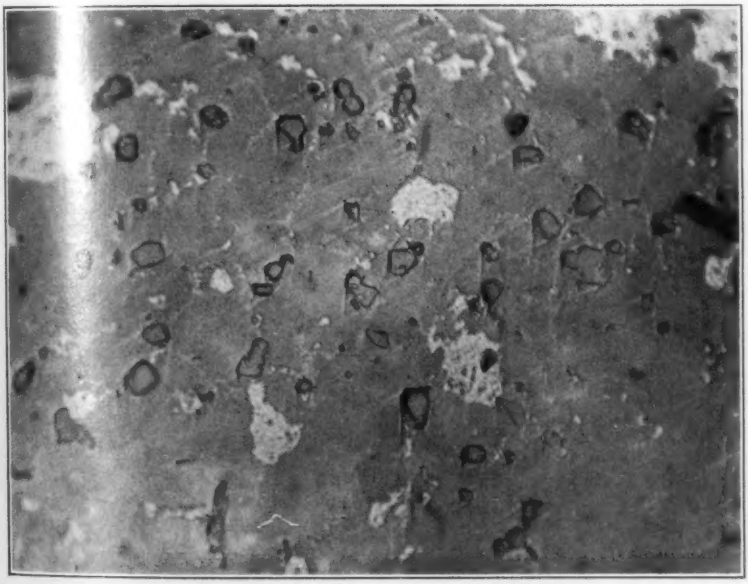

FIGURE 2.—*Free* MgO *in commercial portland cement clinker.*

Polished specimen, unetched. Reflected light. Magnification 500×.

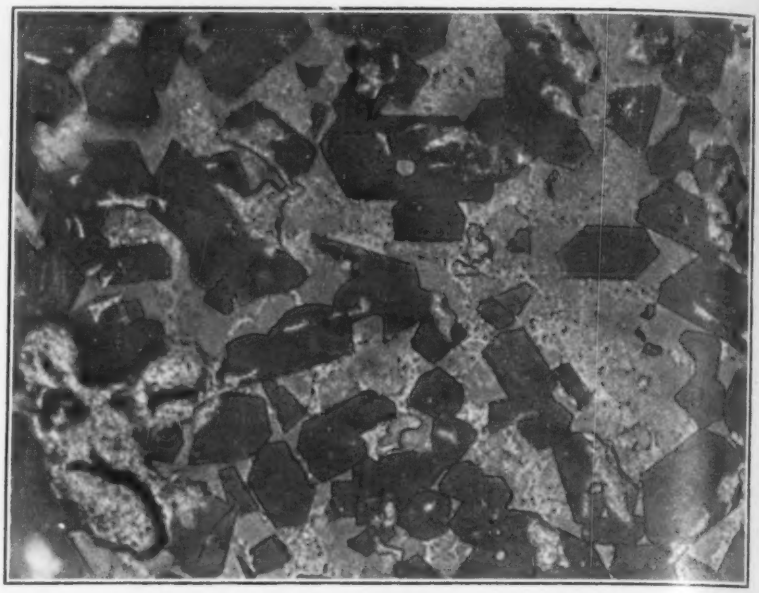

FIGURE 4.—*Amorphous type of dark interstitial material in commercial portland cement clinker.*

Polished specimen etched with water for 2 seconds followed by 1-percent HNO_3 in alcohol for 2 seconds. Reflected light. Magnification 500×.

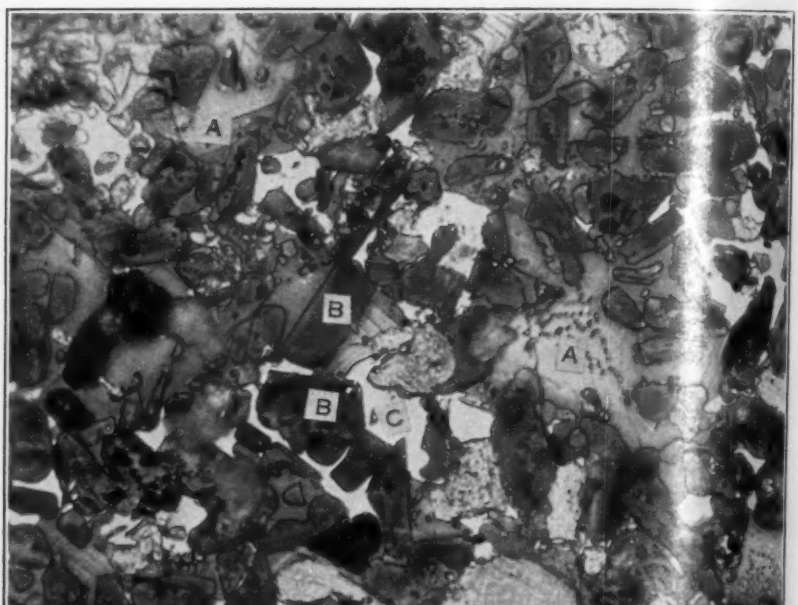

FIGURE 5.—*Rectangular type of dark interstitial material in commercial cement clinker.*

Polished specimen etched with water for 2 seconds followed by 1-percent HNO_3 in alcohol for 2 seconds. The rectangular interstitial material encloses $3CaO.SiO_2$ crystals, and in places contains regularly oriented minute inclusions. *A*, rectangular dark interstitial material; *B*, $3CaO.SiO_2$; *C*, light interstitial material. Magnification 500×.

2. THE "DARK" INTERSTITIAL MATERIAL

The dark interstitial material is so called because it has a number of characteristics in polished sections which distinguish it from the other constituents of clinker. It has a decidedly lower reflectivity than the light interstitial material and etches more readily in a 1 percent alcoholic solution of HNO_3. It lacks the internal structure of C_2S and the external hexagonal form of C_3S and it etches somewhat less readily than C_3S.

The dark interstitial material may be separated into three types on the basis of microscopic observations in both transmitted and

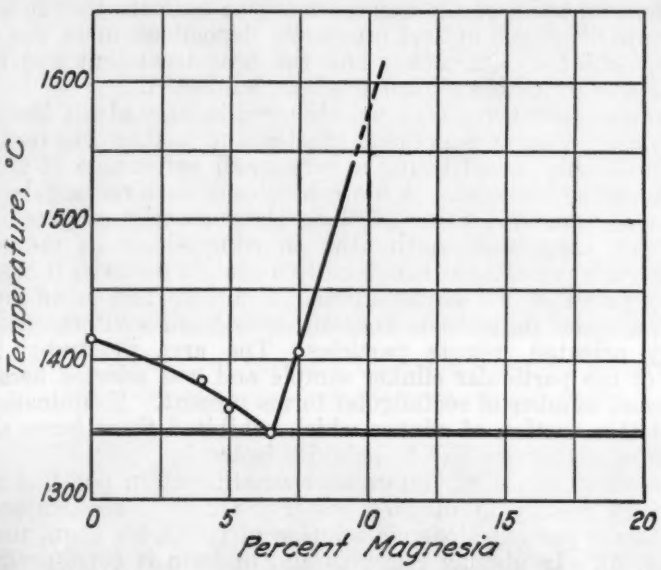

FIGURE 3.—*Equilibrium diagram of the system* $MgO\text{-}4CaO.Al_2O_3.Fe_2O_3$.

reflected light. These types are not always sharply delimited and distinction is sometimes difficult. They will here be called the amorphous, the rectangular and the prismatic types.

The amorphous type of dark interstitial material is the most abundant and most commonly occurring of the three types. Where observations can be made this phase is isotropic in microscopic preparations and its shape is imposed by surrounding constituents. In some other properties, notably index of refraction, it varies considerably. It etches readily in a 1 percent alcoholic solution of HNO_3. In distilled water [7] for 2 to 3 seconds this type etches somewhat less readily than the other two types of dark interstitial material but somewhat more readily than either C_2S or C_3S. Its color and index of refraction apparently depend upon the composition of the clinker and the cooling conditions. In most clinker having a low Al_2O_3/Fe_2O_3 ratio the amorphous dark interstitial material has no apparent color when viewed microscopically and has an index of refraction somewhat less than 1.70 [1], whereas in clinker with a high Al_2O_3/Fe_2O_3

[7] Dr. G. W. Ward, of the Portland Cement Association, suggested this etchant for distinguishing amorphous from other types of dark interstitial material. It is the most sensitive of any thus far tried.

ratio it has a green color in microscopic preparations viewed by transmitted light, and its index is generally greater than 1.74.

The clinker constituents associated with the amorphous type of dark interstitial material also vary somewhat. C_4AF is generally intimately associated with it (figure 4), but in a few clinkers large areas have been found in which interstitial material other than the dark amorphous is absent. Apparently rapid cooling is necessary to prevent the crystallization of C_4AF in small clinker pieces or in the outer layer of larger pieces. Amorphous material has been observed associated with the prismatic crystalline type and is sometimes present as outer irregular layers on the prisms.

All the properties of the amorphous type indicate that it is glass, with composition and optical properties dependent upon the chemical composition of the clinker and the heat treatment and cooling conditions to which the clinker has been subjected.

The rectangular type has been observed in only about four of the 70 samples of commercial clinker studied and in these four it occurred only sporadically, constituting a very small percentage of the total dark interstitial material. A few examples of such rectangular forms are seen in figure 5. Some of these show a series of parallel etch lines which suggest discontinuities in composition in the crystal. Although this constituent is evidently a matrix material it is seen to inclose crystals of the earlier-formed dicalcium and tricalcium silicates and some individuals contain, near their centers, groups of similarly oriented minute particles. The area illustrated is not typical of the particular clinker sample and was selected because of the unusual number of rectangular forms present. Examination of a polished thin section of clinker which exhibited these forms showed that the crystals were nearly or quite isotropic.

The rectangular, dark, interstitial constituent in polished section etches very readily in distilled water for 2 to 3 seconds and less readily in a 1 percent alcoholic solution of HNO_3 for about the same time (fig. 5). In etching relations and in form it corresponds very closely to well-crystallized preparations of C_3A. Although it is very difficult to detect with transmitted light in powdered clinker, material has been isolated which apparently corresponds to this constituent. It is isotropic or very nearly so with an index of refraction close to 1.72. All of the properties observed indicate that the rectangular type is very similar to C_3A, with index of refraction raised somewhat by the iron oxide [12, 15].

Brown [16] also identified an isotropic crystalline material as an interstitial (matrix) phase in portland cement clinker, but his observations differ from ours in that he found it to be a characteristic constituent occurring in grains 350 microns or more in diameter, whereas we can find it only as rare and localized crystals with a diameter never in excess of 70 microns.

A more abundant and characteristic constituent is the prismatic type of dark interstitial material. Of the 70 samples of commercial clinker examined, the type was found to some extent in at least 20 samples and of these 13 contained large amounts. It is noteworthy that in all 20 of these samples the Al_2O_3/Fe_2O_3 ratio was >1.8.

This constituent occurs as prismatic crystals which are etched readily by water (fig. 6) and somewhat less readily by HNO_3-alcohol solution (fig. 7). The crystals are usually associated with C_4AF in

FIGURE 6.—*Prismatic dark interstitial material in commercial cement clinker.*
Polished specimen etched with water for 2 seconds. Magnification 500×.

FIGURE 7.—*Same field as figure 6 etched with water for 2 seconds followed by 1-percent* HNO_3 *in alcohol for 2 seconds.*
Magnification 500×.

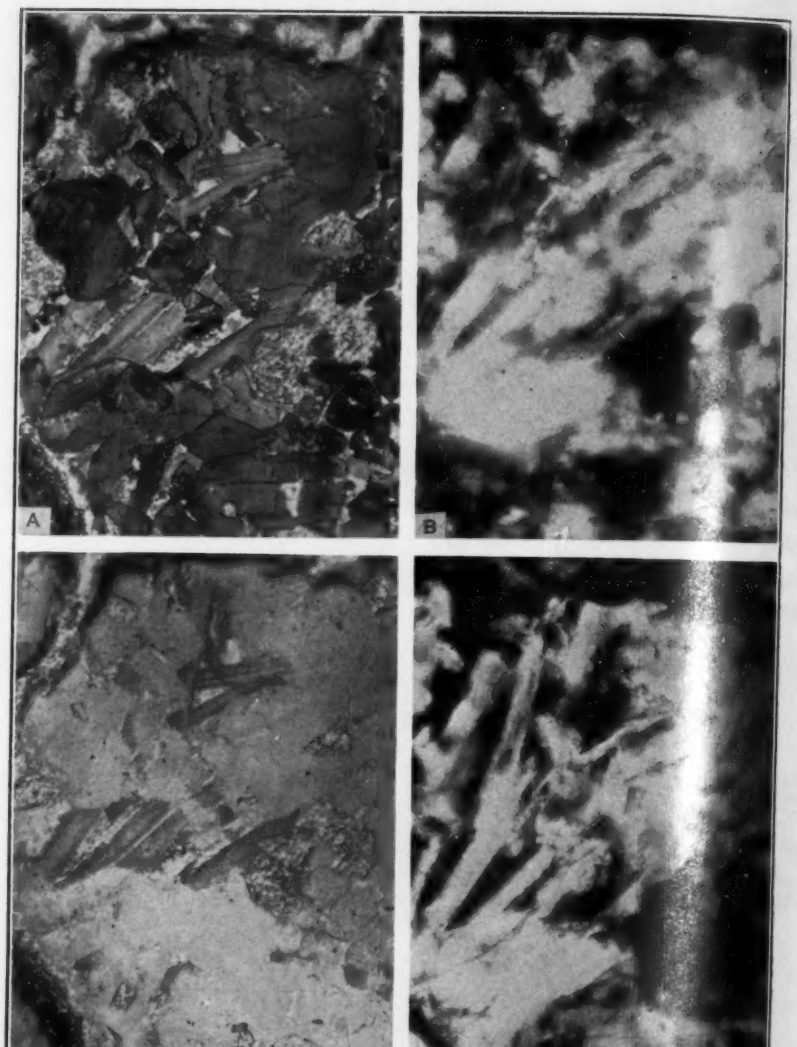

FIGURE 8.—*Polished thin section of portland cement clinker.*

A, With reflected light, after etching with water for 2 seconds, followed by 1-percent HNO_3 in alcohol for 2 seconds; *B*, same field as *A*, but viewed with transmitted light, crossed nicols; *C*, same field as *A* with reflected light after etching for 2 seconds to show prismatic dark interstitial material; *D*, same field as *A*, but viewed with ordinary transmitted light. Magnification 500×.

the matrix material, and sometimes prisms of the dark interstitial constituent alternate with prismatic crystals of C_4AF in parallel orientation. Examination of polished thin sections of clinker containing well-developed prismatic crystals shows that such crystals have a low but distinct double refraction with parallel extinction. Figure 8 shows photomicrographs of the same field of a polished thin section of commercial portland cement clinker; figure 8 (*A*) in reflected light after etching with distilled water followed with 1 percent HNO_3 in alcohol, figure 8 (*B*) in transmitted light with crossed nicols, figure 8 (*C*) in reflected light after etching with distilled water, figure 8 (*D*) in ordinary transmitted light. The etching characteristics and the double refraction of the prismatic dark interstitial crystals are clearly shown. Observation of a number of polished thin sections indicates that the double refraction is somewhat variable, but is of the same order as that of tricalcium silicate (0.005). Prismatic interstitial crystals identified microscopically in powdered clinker were found to have a mean index approximating 1.72. The similarity of many of the optical properties of this phase to those of C_3S affords an obvious explanation of failure to identify it by the usual petrographic methods. Etching characteristics of the two phases are so different, however, that distinction is easy in polished specimens (figs. 6 and 7).

In searching for the composition of the prismatic interstitial material attention was turned to the possible effect of alkalies, because cements are known to contain as much as 1.2 percent of Na_2O and 1.7 percent of K_2O. To determine experimentally the effects of these oxides, a laboratory preparation was made up containing CaO, Al_2O_3, Fe_2O_3, and SiO_2 in about the proportions in an average portland cement clinker. The mixture, on the ignited basis, contained 67.7 percent of CaO, 22.9 percent of SiO_2, 6.3 percent of Al_2O_3, and 3.1 percent of Fe_2O_3 and had a potential compound composition of 55 percent of C_3S, 24 percent of C_2S, 12 percent of C_3A, and 9 percent of C_4AF. Na_2CO_3 was added to one portion of this and K_2CO_3 to another portion, so that the resulting mixtures contained 1.5 percent of Na_2O, and 1.5 percent of K_2O, respectively. The alkali-free, the Na_2O-bearing and the K_2O-bearing, samples were then heated at 1,450° C for 15 minutes, cooled from 1,450 to 1,250° C at 10° per minute, and air-quenched from the latter temperature. Polished sections and powder preparations were made from each sample. The alkali-free sample when examined in reflected light (figs. 9 and 10) was seen to contain the irregular and rectangular types of dark interstitial material with no trace of prismatic crystals. In transmitted light the interstitial phase associated with C_4AF was isotropic with an index of refraction about 1.72.

The Na_2O-bearing and K_2O-bearing samples contained definite prismatic interstitial crystals (figs. 11 to 14, inclusive) which had the same etching characteristics as the corresponding prismatic type of dark interstitial material in portland cement clinker. In powder preparation, the prismatic crystals were associated with C_4AF in the interstitial materials, were definitely doubly refracting with extinction parallel to the prism axis, and both had mean indices of refraction near 1.72. No differences could be seen between the prismatic crystals in the Na_2O-bearing and those in the K_2O-bearing samples. Prismatic crystals with the same forms and optical properties were also produced in experimental clinker containing 0.7 percent

of alkalies and in another clinker containing 0.7 percent each of both Na_2O and K_2O (figs. 15, 16).

Brownmiller [17] in a study of the system CaO-Na_2O-Al_2O_3 discovered a compound which he described as having the composition $8CaO.Na_2O.3Al_2O_3$ with the following optical properties: $\alpha=1.702$, $\gamma=1.710$, biaxial (−), medium 2V. These properties, with the exception of somewhat lower indices of refraction, agree well with those of the prismatic material found in the Na_2O-bearing laboratory preparation and in the prismatic interstitial material in cement clinker. Experiments made by the present authors show that the laboratory-prepared compound in the presence of Fe_2O_3 also has increased indices which are practically identical with those of the prismatic crystals in commercial clinker. Preliminary work by the present authors has cast some doubt on the validity of the formula $8CaO.Na_2O.3Al_2O_3$. Further studies are being made to answer this question as well as to discover the composition of the prismatic crystals in preparations containing K_2O.

V. DISCUSSION

As Lerch [8] has pointed out, the behavior of portland cement in use depends to some extent upon the amount of glass present. Inevitably, also, the composition of the glass, as well as of the other interstitial phases, must play some part in the behavior of the cement. Characteristics of interstitial phases are dependent principally upon chemical composition of the clinker and the heat treatment, including cooling conditions, during and after clinkering. Lea and Parker [11] have shown that, in clinker composed only of CaO, Al_2O_3, Fe_2O_3 and SiO_2, the order of crystallization of C_3A and C_4AF is determined by the ratio Al_2O_3/Fe_2O_3 when cooled under conditions of complete equilibrium. When the ratio is greater than 1.38, C_3A crystallizes before C_4AF; when the ratio is less than 1.38, C_4AF precedes C_3A. In commercial clinker, which frequently contains small amounts of MgO, Na_2O, K_2O, TiO_2, Mn_2O_3, FeO, SO_3 and P_2O_5, quantitative microscopic determinations [10] as well as the structure of the interstitial phases indicate that the ratio at which C_4AF crystallizes last is somewhat higher than for the 4-component system.

Cooling conditions are at least as important as composition in determining the constitution of the interstitial phases. The almost universal presence of glass indicated by our own examinations, as well as by the indirect method of Lerch [8] shows that some glass is present in the great majority of clinker samples whatever the ratio of Al_2O_3 to Fe_2O_3, and that therefore sufficiently rapid cooling to arrest crystallization must have occurred some time during the progress of the clinker from the clinkering zone in the kiln to the storage pile.

In clinker with low Al_2O_3/Fe_2O_3 ratio, such as the "low-heat" cement clinker, C_4AF crystallizes as well developed prisms leaving the glassy interstitial phase low in iron and consequently with a fairly low index of refraction [1]. In clinker with a high Al_2O_3/Fe_2O_3 ratio, a partial crystallization of "dark interstitial" phases may produce a residual glass with a higher Fe_2O_3 content and consequently a deeper color and higher index of refraction. This appears to be true in spite of the fact that C_4AF has a high crystallization potential

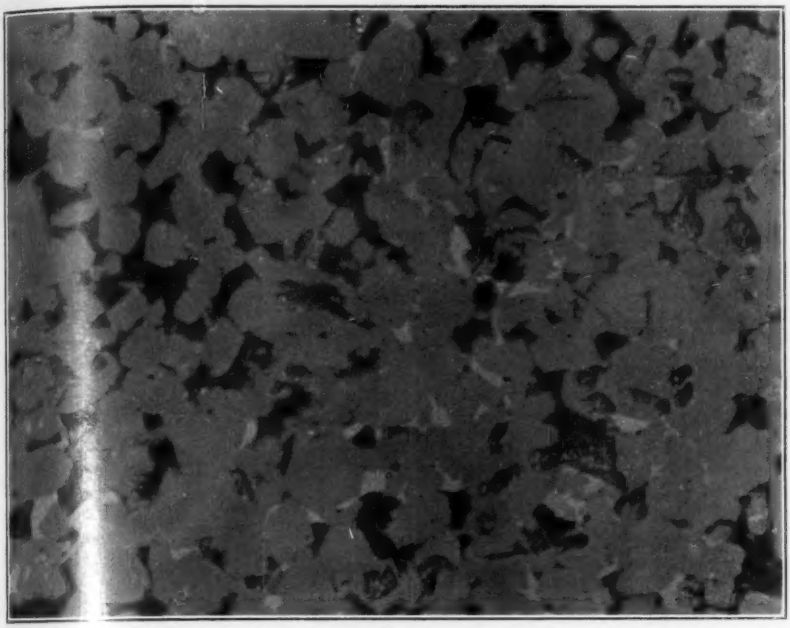

FIGURE 9.—*Laboratory-prepared cement clinker containing no alkalies.*
Polished sample etched with water for 2 seconds. Reflected light. Magnification 500×.

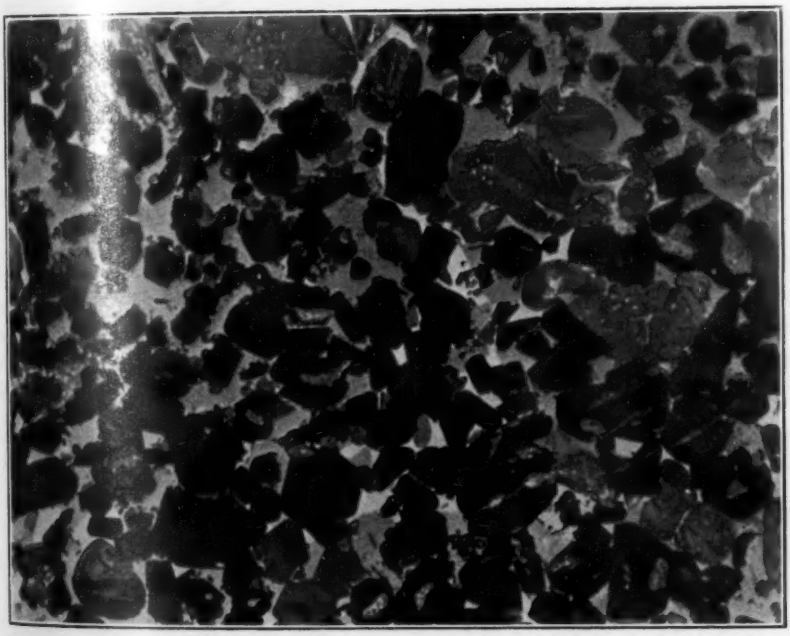

FIGURE 10.—*Same field as figure 12, but etched with water for 2 seconds followed by 1-percent* HNO_3 *in alcohol for 2 seconds.*
Reflected light. Magnification 500×.

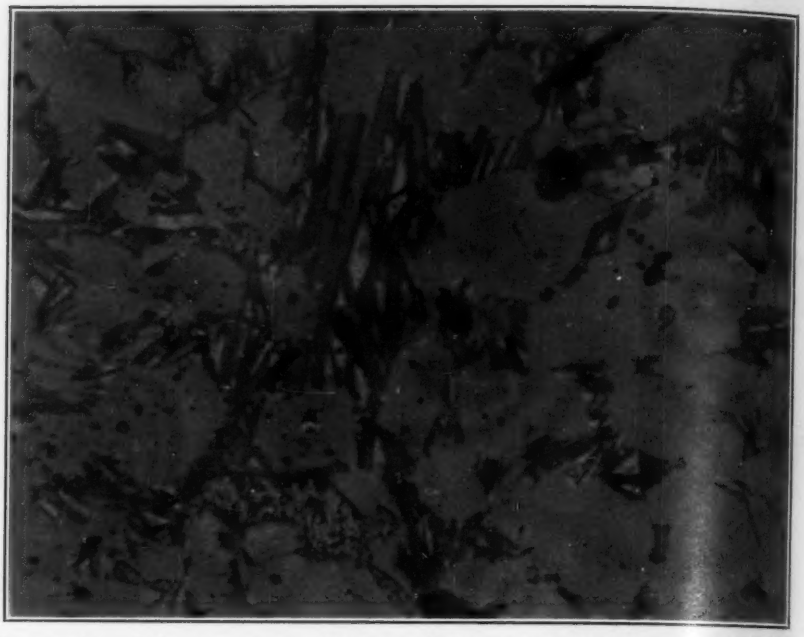

FIGURE 11.—*Laboratory-prepared cement clinker containing 1.5 percent of* Na_2O.
Polished sample etched with water for 2 seconds. Reflected light. Magnification 500×.

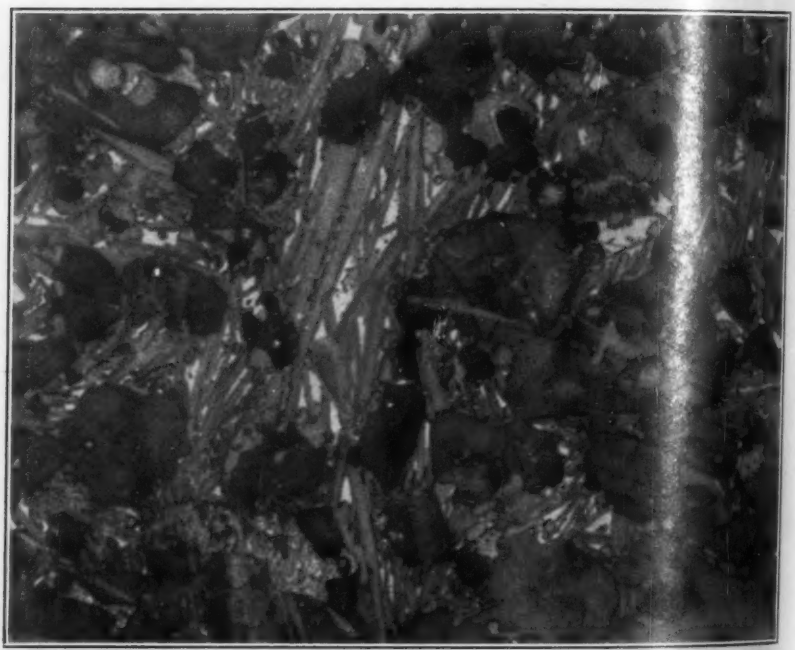

FIGURE 12.—*Same field as figure 14, but etched with water for 2 seconds followed by 1-percent* HNO_3 *in alcohol for 2 seconds.*
Reflected light. Magnification 500×.

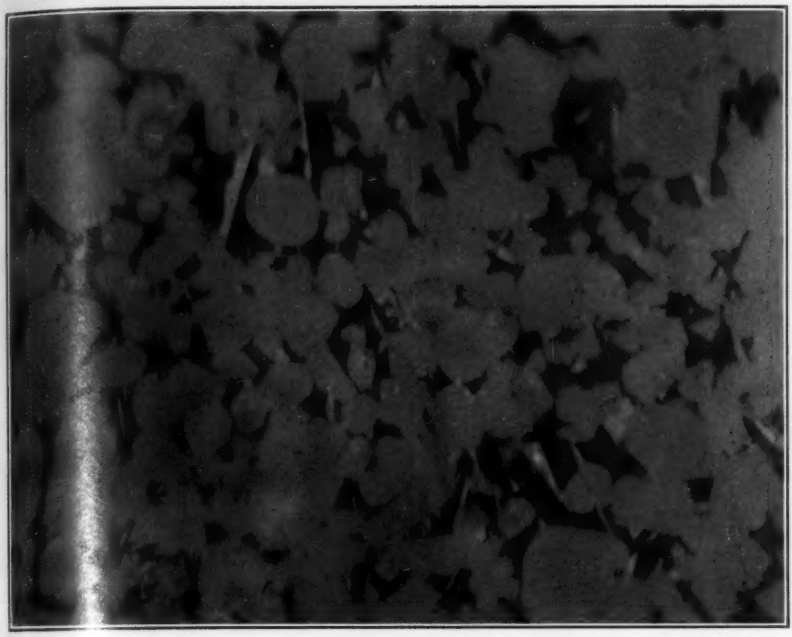

FIGURE 13.—*Laboratory-prepared cement clinker containing 1.5 percent of* K_2O.
Polished sample etched with water for 2 seconds. Reflected light. Magnification 500×.

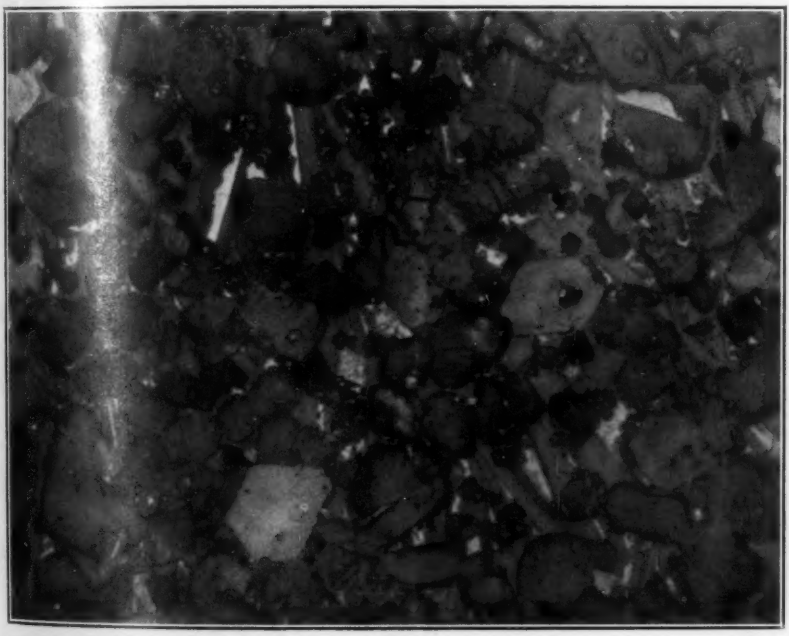

FIGURE 14.—*Same field as figure 16, but etched with water for 2 seconds followed by 1-percent* HNO_3 *in alcohol for 2 seconds.*

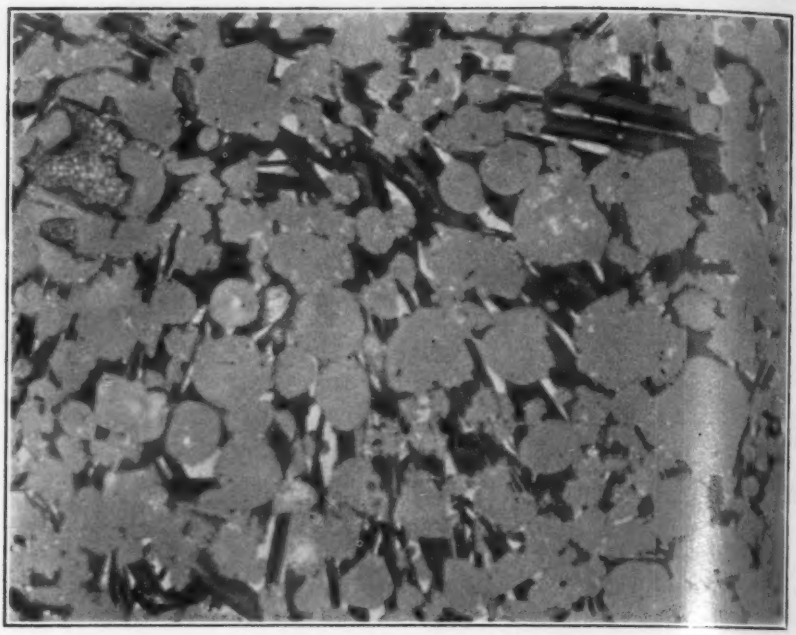

FIGURE 15.—*Laboratory-prepared cement clinker containing 0.7 percent each of* Na_2O *and* K_2O.

Polished sample etched with water for 2 seconds. Reflected light. Magnification 500×.

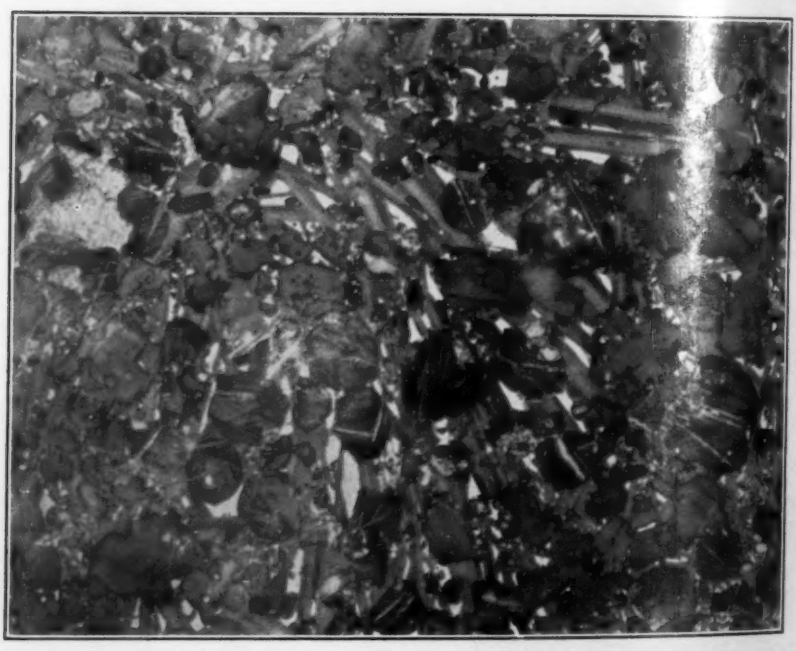

FIGURE 16.—*Same field as figure 18, but etched with water for 2 seconds, followed by 1-percent* HNO_3 *in alcohol for 2 seconds.*

Reflected light. Magnification 500×

and often crystallizes as extremely fine needles or dendritic forms, probably a product of devitrification of the glass.

The amount and composition of the glass also determine the amount of MgO crystallizing as the oxide. Quantitative microscopic analyses [10] show that the amount of free MgO is characteristically less than the total MgO in commercial clinker. As might be expected from phase relations [6], MgO is one of the last phases to crystallize in cement compositions, and therefore any glass formed will be saturated with MgO.

Crystalline interstitial materials other than C_4AF occur frequently in clinker with high Al_2O_3/Fe_2O_3 ratios, but are rarely if ever encountered in clinker with low ratios. Usually these crystalline interstitial compounds are prismatic in character and are apparently compounds of lime and alumina with alkalies. Their development depends upon cooling rates as well as composition, and wide variations may be observed in different pieces from the same clinker batch.

The precise computation of the actual compound composition of clinker from the chemical composition appears to be quite impossible without a more complete knowledge of the poly-component equilibrium system comprising the oxides in commercial clinker, and a determination of the temperatures in individual kiln installations at which crystallization is arrested and the formation of glass begins.

Quantitative microscopic methods using polished, etched specimens and reflected light are available, but at present lack precision, because: (1) the compositions of solid solution phases have not been accurately determined, and (2) no etching method permitting sharp distinction between crystalline and glassy dark interstitial material has been developed. Ward's [8] method of etching with distilled water to distinguish between the rapidly etched crystalline material and the slowly etched glassy material is promising, but further studies of etching time and temperature are necessary for adequate control. The lack of uniformity in structure of commercial clinker also complicates the quantitative determination of compounds. Even where distribution of the major constituents is fairly uniform, rapid chilling of the outer portion of a clinker piece may produce a glass quite different from the glassy or crystalline interstitial materials in the interior of the piece.

VI. SUMMARY

The minor constituents in commercial portland cement clinker and in laboratory preparations of similar composition have been studied by microscopic and thermal methods. The microscopic methods included the examination of powdered preparations and thin sections with transmitted polarized light, polished etched sections with reflected light, and a combination of reflected and transmitted light using polished, etched thin sections.

Free MgO may be identified in polished unetched sections of commercial clinker and free CaO in sections etched with alcohol-water mixtures. Both free CaO and free MgO may be determined quantitatively in such sections.

The light interstitial material in cement clinker is shown to be $4CaO.Al_2O_3.Fe_2O_3$. New determinations of the relations in the binary system $4CaO.Al_2O_3.Fe_2O_3$-MgO have been made. $4CaO.Al_2O_3.Fe_2O_3$ takes less than 1 percent of MgO into solid solution.

[8] See footnote 4.

The dark interstitial material consists of three types: amorphous, rectangular, and prismatic. The amorphous material is glass. Characteristics and associations of the glassy material are given. Glassy material occurs in most commercial portland cement clinker. The rectangular material is $3CaO.Al_2O_3$, and is found only rarely in commercial clinker. The prismatic interstitial material frequently observed in commercial clinkers is probably a compound of lime, alumina and alkalies with a small amount of $4CaO.Al_2O_3.Fe_2O_3$ in solid solution. Its close similarity to $3CaO.SiO_2$ in optical properties has prevented its identification by petrographic methods. It is readily distinguished from $3CaO.SiO_2$ in polished section by the use of suitable etchants. It is frequently found in commercial cement clinker with a moderately high Al_2O_3/Fe_2O_3 ratio. Laboratory-prepared clinker composed of CaO, Al_2O_3, Fe_2O_3 and SiO_2 when cooled at moderate rates, contains rectangular dark interstitial material, whereas the same preparation with small amounts of Na_2O, K_2O, or both, contains prismatic dark interstitial material. The K_2O compound forming the prismatic crystals has not been identified. The Na_2O compound has properties very like those of the compound to which the formula $8CaO.Na_2O.3Al_2O_3$ has been assigned by its discoverer.

Changes in composition of the minor constituents depending upon chemical composition and cooling condition of the clinker are discussed. Difficulties in quantitative determination of the compound composition of clinker are enumerated.

VII. REFERENCES

[1] H. Insley, J. Research NBS **17**, 353 (1936) RP917.
[2] A. H. White, Ind. Eng. Chem. **1**, 5 (1909).
[3] Wm. Lerch and R. H. Bogue, Ind. Eng. Chem. Anal. Ed. 2, 296 (1930.)
[4] B. Tavasçi, Giorn. Chim. Ind. Applicata **16**, 538 (1934).
[5] C. K. Wentworth, J. Geol. **31**, 228 (1923).
[6] H. F. McMurdie and H. Insley, J. Research NBS **16**, 467 (1936) RP884.
[7] Wm. Lerch and L. T. Brownmiller, J. Research NBS **18**, 609 (1937) RP997.
[8] Wm. Lerch, J. Research NBS **20**, 77 (1938) RP1066.
[9] Wm. Lerch and W. C. Taylor, Concrete **45**, 199, 217 (1937).
[10] H. Insley, E. P. Flint, and J. A. Swenson (in preparation).
[11] F. M. Lea and T. W. Parker, Dept. Scientific and Ind. Research, Bldg. Research Tech. Pap. 16 (1935).
[12] H. F. McMurdie, J. Research NBS **18**, 475 (1937) RP987.
[13] R. H. Bogue, Ind. Eng. Chem. Anal. Ed. **1**, 192, footnote (1929).
[14] H. E. Schweite and H. zur Strassen, Zement **23**, 511 (1934).
[15] W. C. Hansen, L. T. Brownmiller, and R. H. Bogue, J. Am. Chem. Soc. **50**, 396 (1928).
[16] L. S. Brown, Tricalcium aluminate and the microstructure of portland cement clinker, American Society for Testing Materials, Proc. **37**, pt. 2, 277 (1937).
[17] L. T. Brownmiller and R. H. Bogue, Am. J. Sci. **23**, 501 (1932).
[18] L. T. Brownmiller, Am. J. Sci. **29**, 260 (1935).

NOVEMBER 23, 1937.

U. S. DEPARTMENT OF COMMERCE NATIONAL BUREAU OF STANDARDS

RESEARCH PAPER RP1075

Part of Journal of Research of the National Bureau of Standards, Volume 20
February 1938

RADIOMETRIC MEASUREMENTS OF ULTRAVIOLET SOLAR INTENSITIES IN THE STRATOSPHERE

By R. Stair and W. W. Coblentz

ABSTRACT

A description is given of a photoelectric cell and filter type of ultraviolet-intensity meter [1][1] which is combined with an audio-frequency generator and radio transmitter and transported aloft by means of unmanned balloons.

The radio-frequency wave is modulated by the response of the photoelectric cell, the response being proportional to the intensity of the incident ultraviolet rays. The height of the balloons is indicated by a radio barograph. The radio signals giving the altitude of the apparatus and the ultraviolet intensities are received and recorded graphically at a ground station.

Six balloon ascensions were made during the latter part of June and the early part of July 1937. Altitudes up to about 80,000 ft (24 km) were attained, but owing to the weakness of the signal and the consequent interference by noise strictly quantitative data were obtained only to about 64,000 ft (19 km).

Below 14 km the transmissions of ultraviolet through the filters remain fairly constant, indicating but little change in the spectral quality of the shortest wave lengths. At a height of about 14 km the transmissions of the filters begin to decrease, indicating a selective increase in intensity of ultraviolet of the shortest wave lengths, as a result of a decrease in the amount of ozone above the apparatus.

Between 14 and 19 km the filters show an unmistakable decrease in transmission, indicating that the apparatus had passed through an appreciable portion of the ozone layer, variously estimated at 15 to 30 percent of the superposed ozone, the lower value being in good agreement with previous explorations (in 1934), taking into consideration the latitude and the season of the year.

At the highest altitudes attained the intensity of the ultraviolet radiation in the band of wave lengths shorter than 3132 A was about 3 times the value observed at sea level. This spectral band includes, of course, also wave lengths not observed at sea level.

CONTENTS

	Page
I. Introduction	186
II. Description of the ultraviolet-intensity meter and auxiliary apparatus	188
III. Description of the assembled apparatus	190
1. Description of the electric motor	192
2. Data on the filters and photoelectric cells	193
IV. Description of a balloon flight	194
1. Notes on the six flights	196
V. Evaluation of the ultraviolet-intensity measurements	198
1. Standardization of the audio-frequency response	199
2. Standardization of the radiation sensitivity of the stratosphere ultraviolet meter	200
(a) Determination of factor P	201
(b) Determination of factor G	203
3. Correction for variation in photoelectric response with angle of incidence of radiation	204
4. Evaluation of the data	206
VI. Discussion of the data	208
1. Calculation of the amount of ozone traversed	210
VII. References and notes	214

[1] Numbers in brackets refer to references and notes at the end of this paper.

I. INTRODUCTION

For some years the writers have made measurements of ultraviolet solar radiation, using a photoelectric cell and filter radiometer [1, 2]. By means of this device a measurement is obtained of the spectral quality (the spectral-energy distribution) and the total intensity of the radiation in the band of wave lengths shorter than 3132 A, which is recognized as having a therapeutic effect, at least in healing rickets.

It is well known that the spectral quality and total intensity of the ultraviolet solar radiation that comes to the earth's surface are determined largely by the amount and distribution of ozone in the stratosphere. This information has been obtained almost entirely by means of spectrophotography. While the results so obtained appear to be authentic, nevertheless, the photographic method has several shortcomings, the most noteworthy being that no strictly quantitative measurement is obtained of the intensity of the incident radiation at different heights above the earth's surface.

In a previous paper [4] there was given an outline of a proposed method of determining the spectral quality and the total intensity of the ultraviolet of short wave lengths in solar radiation at various heights above the earth's surface. The proposed device consists of a photoelectric cell, filter radiometer [2], and auxiliary apparatus for transmitting radio signals. It is transported aloft by means of sounding balloons. While the photoelectric cell and filter radiometer cannot compete with a spectroradiometer in recording fine details in spectral-energy distribution, it has proved adequate for the purpose for which it was designed [2, 3]; and, because of its light weight, it is easily adapted for transportation into the stratosphere by means of sounding balloons [23].

In this connection, it is interesting to note that within the past few years radio-wave transmitting and receiving instruments (like many other physical devices) have become a very useful auxiliary means of recording data obtained in remote or otherwise inaccessible places. In earlier researches, in which the measuring apparatus (thermometer, barograph, pyrheliometer, etc.) was transported in sounding balloons, the uncertainty of subsequently securing the data depended upon the additional hazard of recovering the balloons. Nowadays, the measurements of temperature, barometric pressure, humidity, and in the present instance, ultraviolet solar intensity, are transmitted from aloft by means of radio waves, which are received and recorded in a central station on the ground coincidently with the time of observation. No lives are hazarded and the observations are on record, even if the balloons and measuring instruments are not recovered.

In this respect the writers have been singularly fortunate. Using three sets of instruments, six flights were made, and, to date, only one instrument remains unrecovered. This particular instrument had made two previously successful flights, and each time it was recovered undamaged.

One unit remained hidden for more than a month between two large trees in an infrequently visited forest before it was recovered, undamaged. The recovery of this unit was especially important, because the photoelectric cell had ceased to function after attaining a height of 21,500 ft (6.5 km; the barometer signal indicated an ascent

to 78,000 ft; 23.8 km), and on recovery it was ascertained that it was the photoelectric cell and not the resistors that had become defective.

It is of course to be recognized that the herein-described radiometric procedure is still in an experimental stage of development. However, when we consider the fact that in this preliminary trial the apparatus was assembled from stock laboratory equipment which had many shortcomings (the photoelectric cells were not the most sensitive that can be made; the radio-wave transmitter was weak; and the radio-wave receiver was not the most sensitive obtainable), we regard the method feasible and highly promising for studying ultraviolet solar intensities in the stratosphere.

Aside from the scientific value of the data so obtained, from a purely utilitarian standpoint, the investigation of this problem is of importance because of the need of information on the spectral-energy distribution in the extreme ultraviolet of solar radiation used in heliotherapy.

Some experimenters have attempted to evaluate the ultraviolet in solar radiation by calculation, on the assumption that the spectral-energy distribution in the extreme ultraviolet of the sun, outside the earth's atmosphere, is similar to that of a black body at 6,000° K.

In a previous communication [4] attention was called to spectro-radiometric measurements by Pettit [6] and to photoelectric cell and filter measurements by the writers [3] showing that the solar spectral intensity, in the extreme ultraviolet, has an abrupt and continuous drop with decrease in wave length; and that the slope of this spectral-energy distribution outside the earth's atmosphere is closely represented by that of a black body at 4,000° K, or perhaps even lower.

The object of the present paper is to present the results of a preliminary attempt to determine radiometrically the spectral quality and total intensity of the ultraviolet solar radiation of short wave lengths, in the stratosphere, and thereby obtain a check on the spectrographic determinations of the distribution of ozone (made by Dobson, Goetz, Regener, and others), which are somewhat in disagreement in that in Regener's [8] balloon ascents a considerable portion of the ozone appeared to be diffused to somewhat lower elevations than recorded in the two ascents reported upon by O'Brien [11] and by Mohler [10]. As will be shown presently, both sets of observations may be correct. For example, in our flight 3, as the apparatus rose above the earth's surface there was an increase in the values of the filter transmissions with but little change in the total intensity, just as though the bulk of the ozone was increasing in amount during the flight and was situated at a much higher elevation than was attained by our apparatus on that date. Again, on two of our subsequent flights (4 and 5) there appeared to be a definite change in spectral quality and a rapid increase in total intensity, beginning at a much lower elevation than in flight 3, indicating a considerable penetration into the layer of ozone which seemed to extend to a much lower elevation on these dates.

Since the information in flights 3 and 5 was obtained with the same instrument, the differences in intensity of ultraviolet solar radiation at the same elevation, observed on widely different dates, may perhaps be ascribable to differences in formation or diffusion of ozone into the lower levels of the stratosphere, rather than to differences in instrumental equipment. However, as noted in section VI, until confirmatory data can be secured, the unexpected results obtained in

flight 3 are ascribed to unexplained changes in the instruments rather than to an increase in ozone during the flight, although varying meteorological conditions suggest such a possibility.

In this connection, reference is made to a discussion of atmospheric ozone and meteorology by Dobson and Meetham [13, 16], in which it is shown that the total amount of ozone varies with the latitude and the season, being a maximum in the local spring and a minimum in the local autumn; also that (in Europe) marked daily variations in ozone occur with varying meteorological conditions, the maximum amounts of ozone being generally observed in areas of low barometric pressure ("cyclonic regions") and the smallest amounts in areas of high barometric pressure ("anticyclonic regions") [16]. However, the association of this rise in ozone value with polar air currents, in the troposphere, does not seem to be the result of a simple transportation of ozone by air currents [19].

From the foregoing citations it appears that the position of the ozone layer, which is situated on the average at a height of 22 [9] to 24 km [8], is not stationary [16]. In fact, in addition to slow seasonal changes reported by others, there are irregularly occurring variations of short duration. For example, in the ultraviolet-intensity measurements made by one of the writers (W. W. C., in 1934) at Flagstaff, Ariz. (elevation 7,300 ft.; 2.2 km), on several days the filter transmission measurements indicated a conspicuously higher transparency (a lower ozone concentration) than the average value for the same season, the same air mass, and the same visual clearness of the atmosphere [2].

The data obtained in these preliminary explorations of ultraviolet solar intensities in the stratosphere are too meagre to warrant more than a brief consideration in connection with the relation that is known to exist between the variations in the ozone content and meteorological conditions. They are very suggestive, nevertheless, in indicating a quick method of exploring the extent and location of the maximum concentration of the ozone layer as a function of the season, barometric pressure, circulation of polar air currents, etc. [12, 13, 16].

II. DESCRIPTION OF THE ULTRAVIOLET-INTENSITY METER AND AUXILIARY APPARATUS

In the photoelectric cell and filter radiometer [1], as used by the writers on the earth's surface, the ultraviolet intensity is measured in terms of the scale reading of a microammeter. The intensity can be obtained also with a graphically recording meter.

For measuring the ultraviolet intensity in the stratosphere, it was necessary to introduce a very radical change in the design of this apparatus in order to reduce the weight. Instead of the balanced amplifier and microammeter, the photoelectric cell controls an audio-frequency generator which feeds into an amplifier.

For tests in the laboratory, the auxiliary apparatus used with this type of ultraviolet meter consists of telephone receivers (also a standard audio-frequency generator [17] for use in determining the audio frequency emitted by the ultraviolet meter) or a suitable electronic frequency meter.

For measurements in the stratosphere, the auxiliary apparatus used with our photoelectric ultraviolet meter [1, 4] is based on the radio-meteorograph method [7] developed by Diamond, Hinman,

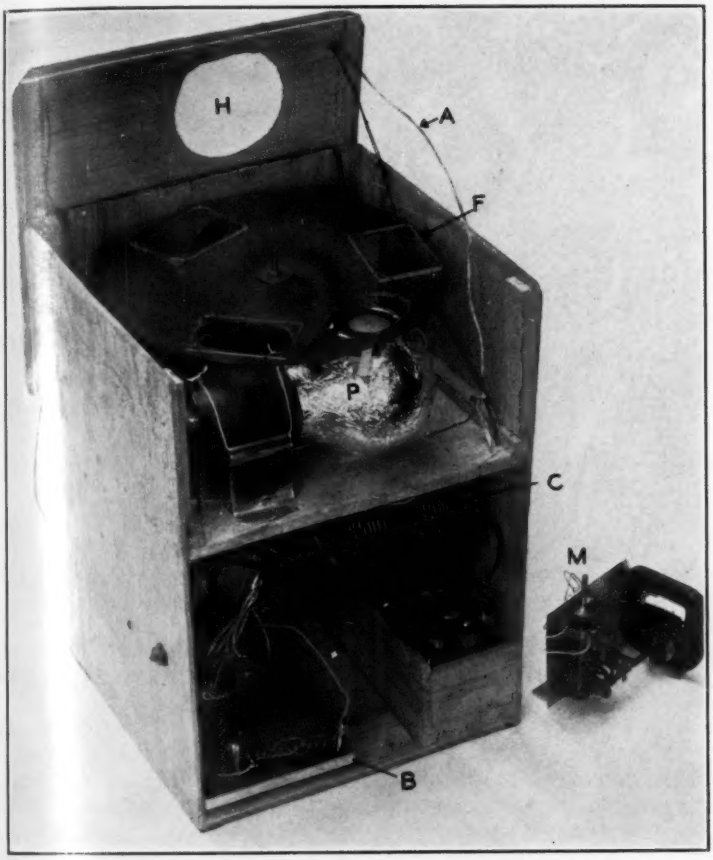

FIGURE 1.—*Assembled stratosphere ultraviolet meter, housed in balsa-wood box, open at the top and front, showing the photoelectric cell, P; glass filters, F; radio barograph, B; radio-frequency oscillator, C; antenna, A; sample motor, M; hole, H; and other accessories.*

and Dunmore of the radio section of this Bureau. It comprises (a) a radio transmitter, which, combined with the ultraviolet meter, is transported in the unmanned balloon; and (b) a ground-station receiving and graphically recording apparatus, consisting of a super-regenerative receiving set, an electronic frequency meter, an amplifier and electrical filter unit, and a recorder. The radio section made available to us a sample radio-meteorograph transmitter and a complete receiving setup, and assisted us in modifying, to meet our needs, the ingenious barometric-pressure element of the radio meteorograph [7] used for the purpose of indicating the altitude of the balloons.

An essential part of this barograph,[2] *B*, shown in the lower part of figure 1, consists of a number (about one-third the number used in

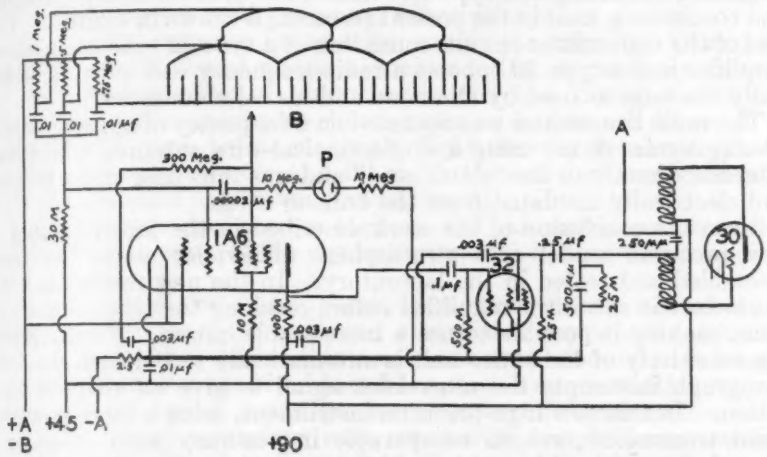

FIGURE 2.—*Electric-circuit arrangement of the photoelectrically controlled, P, audio-frequency generator, and, upper part, the radio barograph circuit, B.*

the radio meteorograph [7]) of thin electric-conducting strips, separated by thicker insulating strips. A contact point on a movable arm, operated by the pressure diaphragm of the barometer, closes an electric circuit as it crosses these metal strips; and, depending upon the resistance and capacitance connected in the grid circuit, a predetermined modulation frequency is produced, characteristic of a particular segment. By suitable connection of the segments, in groups of one and three (as shown at *B*, in fig. 2) having the same modulation frequency, identification is obtained of the height attained by the balloons. This barometric apparatus was calibrated for pressure (in absolute scale) by the aeronautic instruments section of this Bureau.

It should be noted (fig. 2) that the grid circuit of the relaxation oscillator contains a resistance of many megohms and an extremely small charging condenser in order to secure sufficient sensitivity for the type of photoelectric cell used. In order to reduce the effects of the capacitance of the electrodes, a high resistance (10 megohms) is connected on each side of the photoelectric cell. The circuit is essentially voltage-controlled.

[2] Manufactured by Julien P. Friez & Sons, Inc., Baltimore, Md. [7]. One of the modifications consisted in cutting the contact arm near its end and connecting it (suitably insulated) directly to the control grid in order to reduce its capacitance

It is to be noted also that the photoelectric cell functions by an emission of electrons, on exposure to ultraviolet radiation, and not as a variation in resistance [7] as the oscillating circuit is commonly used. Upon irradiation of the photoelectric cell, the liberated electron current changes the potential of the control grid, thus changing the frequency of the audio oscillation. It is necessary to keep a potential of some 45 v on the negative electrode (the photosensitive surface) in order to properly operate the photoelectric cell. It is, therefore, difficult to build a stable oscillator, directly controlled by a relatively insensitive photoelectric cell. The circuit arrangement described in the previous paper [4], represented a first step in the evolution of a suitable photoelectrically controlled audio oscillator. The audio oscillator, consisting of a type 1A6 radio tube with suitable resistances and condensers, used in the present research, is shown in figure 2. The rest of the transmitter circuit, consisting of a type 32 tube as an audio amplifier and a type 30 tube as a radio-frequency oscillator, is essentially the same as used by Diamond and his collaborators [7].

The radio transmitter was operated on a frequency of approximately 50 megacycles (6 m) using a single vertical-wire antenna, which was attached directly to the "shock cord" and was thus held under tension and electrically insulated from the balloon cords.

Since the conclusion of the work described in the present paper, a new precision model of a stratosphere ultraviolet meter has been assembled and tested in the laboratory. In the new instrument the photoelectric current is amplified before reaching the relaxation oscillator, making it possible to use a more stable circuit. Furthermore, the sensitivity of the entire unit is automatically tested each time the barograph interrupts the ultraviolet signal to give an altitude indication. In this new high-precision instrument, using a more powerful radio transmitter, results comparable in accuracy with those at a ground station should be obtainable.

III. DESCRIPTION OF THE ASSEMBLED APPARATUS

In figure 1 is shown the ultraviolet meter. This consists of a photoelectric cell and filters and a photoelectrically controlled audio-frequency generator; also the auxiliary radio-transmitting apparatus, assembled in its housing of balsa wood, temporarily open at the top and front for purposes of exposition [23]. The dimensions of the box are 16 by 16 by 22 cm.

When all adjustments have been made, the apparatus is completely inclosed, except the hole, *H*, in the top to admit sunlight to the photoelectric cell. The sides and bottom are then wrapped with cotton batting and covered with a black cloth. The total weight is about 1.6 kg (3.5 lb).

Referring to figure 1, and beginning the description at the top, an essential part of the apparatus is a cardboard disk (boiled in ceresin wax to exclude moisture) with four elliptical openings (25 by 37 mm), three of which are covered with glass filters, *F*, having the spectral transmissions shown in figure 3. This disk is rotated by a small electric motor, *M* (shown at the lower right of fig. 1), operated on 0.009 amp from two small flashlight batteries.

The speed of rotation of this disk ranged from 1 revolution in about 40 sec (about 60 sec in fig. 4) to 2 min in the different flights. In the slower rotations the momentary shadows cast on the photoelectric

cell by the suspension threads, as the instrument rotated about its axis, are clearly indicated by indentations in the graphical record (fig. 4).

The cadmium photoelectric cell, *P*, is a General Electric type FJ-135, spherical bulb, with the base removed and the glass covered with aluminum foil to exclude stray light and to remove possible electrostatic charges. This type of cell, which responds to radiation of wave lengths extending from 2600 to 3250 A, is eminently adapted to this type of ultraviolet measurement. The top of the cell is covered with a diffusing window of Corex *A* glass (40 mm in diameter and 2 mm thick) molded to fit the spherical bulb, and fine ground on both faces. Over this window, which is highly transparent to 2500 A in the ultraviolet, is placed a black-paper cover with an opening 17 mm in diameter, as shown in figure 1. This combination is secured to the photoelectric cell by means of adhesive tape.

The spectral response for an equal-energy stimulus (fig. 3), and the sensitivity for different angles of incidence (fig. 5), were determined for each combination of photoelectric cell and Corex *A* diffusing window before mounting, as shown in figure 1. As will be noted on a subsequent page, before making a flight the complete unit (photoelectric ultraviolet meter and its radio transmitter) was calibrated against a standard of ultraviolet radiation [5].

In the lower part of the box is shown the barometric switching unit (*B*, to the left), some of the dry batteries, and *C*, the radio-frequency oscillator coils.

The box containing this apparatus is suspended from its corners by strong (waxed) linen threads and a stranded copper-wire antenna, *A*, 1.5 m in length. Above this is a "shock cord" about 3 m in length, consisting of six strands of rubber ribbon, each 3 mm in width.

Some of the earlier ascensions were made with three balloons in a cluster, and later ascensions were made with four balloons tethered at different lengths (5 to 20 m) from a common meeting point, from which the box of apparatus was suspended (on a cotton cord) at a total distance of about 25 m below the balloons, which was sufficient to prevent possible shadowing by the balloons when fully expanded. The ascensions were made in relatively still air, and there was practically no drifting of the box of instruments which hung vertically below the balloons as they ascended.

The balloons were sufficiently inflated with hydrogen to exert a pull of 1¾ to 2¼ lb (800 to 950 g) each, as determined by a small spring balance. One balloon was inflated more than the others in order to have it burst before the others, which acted as parachutes to retard the descent and prevent injury to the instruments.

In order to secure a radiometric record of the ultraviolet intensity near the earth's surface, when there was no strong wind, the balloons were released by means of a cord drawn through a metal ring attached above the rubber "shock cord," by means of which the whole device could be held in leash, thus permitting the instrument box to swing freely some 5 m above the ground.

When all was in readiness, and the recorder was working properly, one end of this launching cord was released, the pull of the balloons caused the cord to slip through the ring without difficulty, and the ascension of the apparatus proceeded without further interruption. Six exploratory flights were made in this manner.

The ascensions of the apparatus were made at the Bureau's radio field station at Meadows, Md., some 25 km from Washington. In the preliminary part of the work we had the valuable experience and assistance of W. S. Hinman, Jr., and, later on, E. G. Lapham, both from the radio section of this Bureau.

Several ascensions were made through cloudy skies. Judging from the cleanness of the filters after recovery of the apparatus, if any moisture was condensed on the filters while passing through the clouds its effect was only temporary. There are some indications that the temperature of the disk rose to 55° C, or perhaps higher, during the flight.

A notice was attached to the instrument box stating that a reward would be paid for the return of the instruments, intact as found; and the finder was requested to write us, describing the recovery—how many balloons had burst, etc. These descriptions of recovery of the apparatus proved interesting and instructive. In one instance, the balloons and apparatus must have traveled some 500 km; and, at 5 o'clock on the morning following the flight, two balloons, carrying the instrument box about 10 m above the ground, were discovered floating above a cornfield, some 50 km south of Raleigh, N. C.—a distance of some 450 km in direct line from their starting point. The apparatus ("camera") was returned unbroken and made two subsequent flights. In another instance the instruments (motor still running) and two unexploded balloons descended, and were recovered unharmed during a rain and lightning storm near Allentown, Pa., a distance of some 200 km. Aside from the interest in the monetary reward, the finders seemed interested and cooperative in returning the apparatus.

1. DESCRIPTION OF THE ELECTRIC MOTOR

One of the preliminary problems in the development of the stratosphere ultraviolet meter was a means of temporarily placing the glass filters, in succession, over the window of the photoelectric cell. A small electric motor was decided upon as best adapted for this purpose. But since no commercial motors having the proper power and weight were available, it was necessary to construct a suitable unit to rotate a disk supporting three filters. After a few trials a model (see fig. 1) was constructed which operated on about 9 ma at a potential of 3 v, and yet had sufficient power to rotate the disk. This motor with the reduction gearing (800 to 1) weighed only 3 oz.

The field poles are constructed of tool steel and measure over-all approximately 1¾ by 1¾ by 3/16 in. The armature, which is ⅞ in. in diameter and 3/16 in. in thickness, is wound with four coils (about 3,500 turns) through eight slots (0.2 in. diameter) near the circumference of the armature.

The silver commutator and brushes, and the reduction gears were obtained from d-c watthour meters,[3] and were remodeled to give a desired speed of rotation of the filter disk, which was about 1 rpm (revolution per minute).

Since the relaxation oscillator was operating in an extremely sensitive manner it was necessary to locate the motor relative to the transmitter coils, photoelectric cell, and relaxation oscillator circuits,

[3] The commutators and gearing from a number of replaced d-c watthour meters were kindly supplied to us by the Potomac Electric Power Co., of this city.

so that the electromagnetic effect of the rotation of the armature of the motor was a minimum. In this position, the field through the motor was at right angles to that through the radio-frequency oscillator coils.

In the first flights, motor troubles were encountered because the small dry cells (type *Z*) which were used did not have sufficient capacity to maintain the proper voltage to operate the motor at the low temperatures encountered. In one case, there was evidence of a breakdown in the motor winding, resulting in excessive battery drain. For the later flights, large cells (standard flashlight type) were employed and gave practically uniform motor speed throughout the records (see fig. 4).

2. DATA ON THE FILTERS AND PHOTOELECTRIC CELLS

Supplementing the foregoing general information on the radiometric equipment, it is relevant to include the following details regarding the spectral transmissions of the filters and the spectral responses of the photoelectric cells depicted in figure 3.

The three glass filters (fig. 3) were selected to have suitable transmissions in order to give three bands of radiation of approximately the same increments of intensity and to secure a good tracing on the recorder sheet. The samples of Helioglass (*H*) and barium-flint (*Ba-1*) were ground and polished to a suitable thickness. The sample of lantern-slide glass (*LS*) was selected to meet our filter-transmission requirements. Sufficient material of each kind of glass was provided in order to have a reserve for a number of ultraviolet meters, thus saving work in determining the transmissions and simplifying the calculations in the reduction of the data.

Since completion of this preliminary exploration, it appears that the Helioglass (*H*) filter is too transparent (fig. 7) to suppress the incidental errors of observation and to show the expected change in transmission with altitude. Hence, in the future, a more opaque filter will be used.

The spectral responses of the Cd photoelectric cells, covered with the Corex *A* diffusing glass, are depicted in figure 3. They are practically insensitive to wave lengths longer than about 3250 A and have a maximum response in the region of 2850 A. Hence, they are well adapted for measuring the slight increase in intensity in the ultraviolet at 2880 to 2900 A, which becomes perceptible at high altitudes.

The spectral range of the photoelectric response coincides closely with the numerous important absorption lines of ozone in the region of 3227 A and shorter wave lengths [14].

While this narrow spectral response makes the measurement more nearly in terms of homogenous radiation, nevertheless, it would have been desirable to use a cell with a wider spectral response in order to secure a more powerful action in the radio transmitter and thus furnish a more stable sending device. However, with the new instrument proposed for future work, the stability of the relaxation oscillator and transmitter are independent of the sensitivity of the photoelectric cell.

From the data thus far obtained, it appears that when more is known about ultraviolet intensities in the stratosphere it may be possible to dispense with the filters as a means of determining the spectral quality of the incident radiation. This will reduce the

weight, and will make it possible to attain higher altitudes with the equipment now used. Furthermore, a larger part of the photoelectric cell can then be exposed and intensities at lower solar altitudes can be measured. By suitable standardization [5] before the ascent, it may be possible to explore the ozone layer from day to day without these filters to determine the spectral quality.

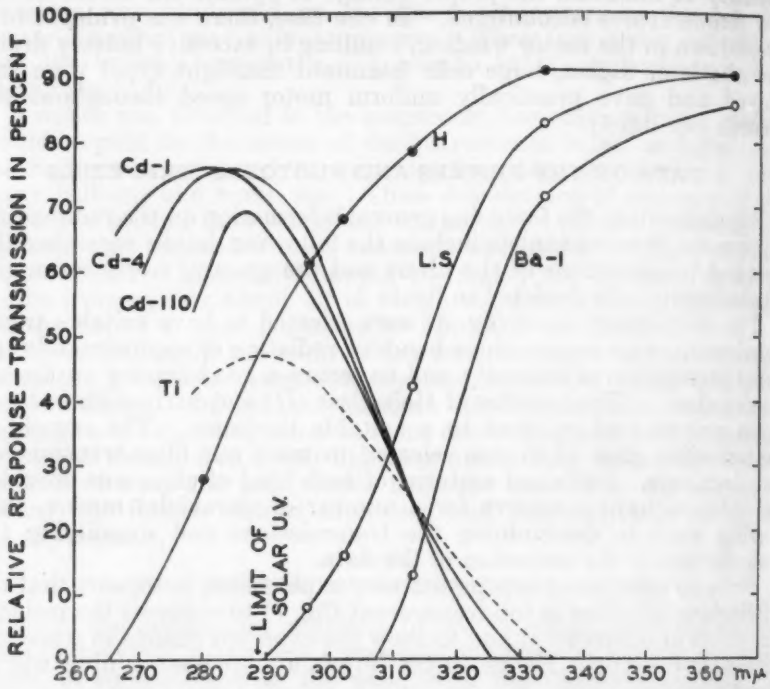

FIGURE 3.—*Graphs showing the spectral response of the various cadmium photoelectric cells; also the spectral-transmission curves of the filters*

IV. DESCRIPTION OF A BALLOON FLIGHT

As already mentioned, the ground-station receiving and recording equipment was a duplicate of the apparatus described and illustrated in figure 10 of the paper published by Diamond, Hinman, and Dunmore [7]. The recorder and its auxiliary amplifier failed to depict frequencies proportional to the change in intensities of ultraviolet radiation.[4] The recorder was therefore used merely as an indicator of the time scale and for identification of the altitude signals. The values of the audio frequencies, emitted by the transmitter, were therefore read directly on the dial of the electronic-frequency meter and written in pencil on the corresponding graphical record. This saves time in subsequent calculations.

In figure 4 are shown two parts of a graphic record of an exploratory flight (4) made with our apparatus on July 2, 1937.

Referring to figure 1, it may be noted that, as the disk rotates, the two opaque spaces between the glass filters, *F*, act as a shutter to

[4] The cause of this defect was subsequently located in the auxiliary amplifier.

exclude radiation from the photoelectric cell, and the lowest audio frequencies recorded (along the lower horizontal line marked 1.0, fig. 4), are reference frequencies, analogous to a graphic laboratory record of the zero scale reading of a galvanometer.

When the oblong open space in the disk is over the window of the photoelectric cell, as shown in figure 1, the maximum audio-frequency

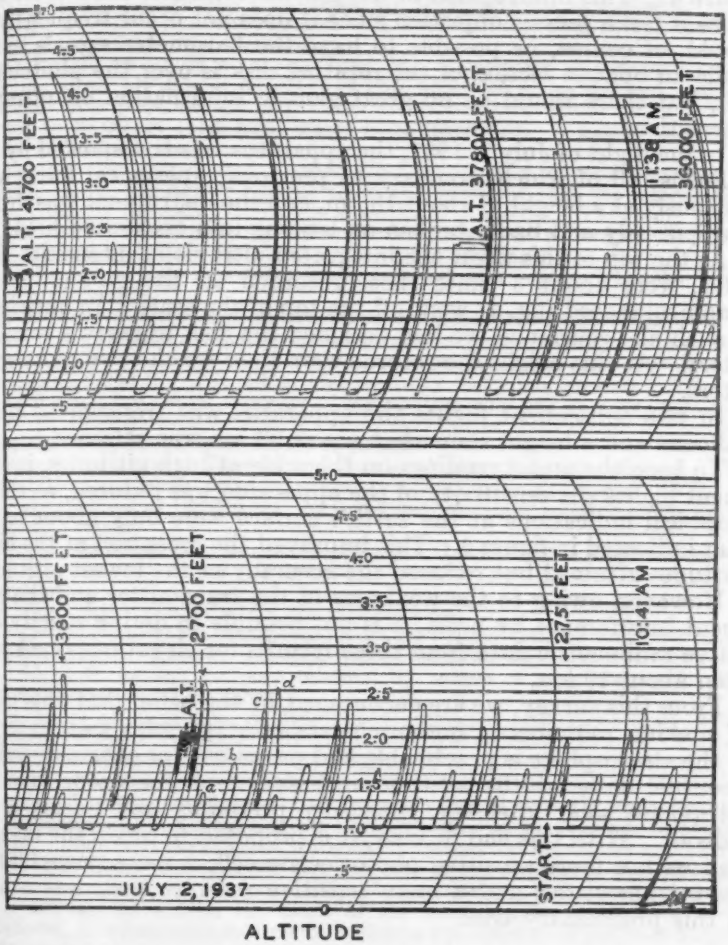

FIGURE 4.—*Reproduction of two parts of a graphic record of the ascension of a stratosphere ultraviolet solar intensity meter, showing the change in frequency (ordinates) with change in intensity of ultraviolet radiation transmitted through the filters (a, b, c) as a result of change in altitude; also audio-frequency signals, ALT, of the radio barograph.*

note is emitted, the maximum deflection is read on the dial of the electronic frequency meter, and the maximum deflection of the recorder arm is inscribed on the graphical record, as shown in figure 4.

As the disk continues to rotate, the three filters, *F*, which are arranged in order of decreasing transparency to ultraviolet radiation, pass in succession over the window of the photoelectric cell; and cor-

respondingly smaller deflections are successively read on the frequency meter and are traced on the graphical record.

With change in elevation of the apparatus, the movable arm of the barometric-pressure apparatus crosses the metal contacts on the pressure switching element (B, in figs. 1 and 2) and an entirely different audio-frequency note is emitted, as indicated at the points *ALT*, figure 4. This interruption in the graphic record of ultraviolet intensities is not a serious objection since it does not occur frequently. It would, of course, be possible to have the barometer signals emitted while an opaque section of the rotating disk is over the photoelectric cell, but there would be no great gain in information on ultraviolet intensities.

In the flight of July 2, 1937, the apparatus was transported by three balloons, all of which, contrary to previous experience, burst simultaneously at a height of about 18 km, and the instrument was dropped precipitously and badly broken on landing in a cultivated field.

At the top of this flight the integrated ultraviolet intensities, for no filter, were about 3 times those recorded on the ground, and the graphical record (fig. 4) went off the top of the scale. In anticipation of such an occurrence, we had designed the disk to carry a number of filters. At this height the records were clear for the two most opaque filters.

In two subsequent flights the apparatus was transported by four balloons and a height somewhat above 23 km was attained.

To keep the meter readings on the scale at high altitudes, in subsequent flights the sensitivity of the apparatus was reduced, so that the graphical indications at the earth's surface were only about one-half that indicated in figure 4. This improved the reception at the highest altitudes attained but reduced the accuracy at the lowest altitudes.

However, owing to the weakness of the transmitter and the consequent interference by noise, it is not possible to derive strictly quantative radiometric data from these records for elevations much higher than about 19 km.

From this survey, we are encouraged in the belief that this method of making radiometric measurements of ultraviolet solar intensities in the stratosphere is practicable and promising for obtaining valuable scientific data on the altitude and extent of the ozone layer, and ultraviolet solar intensity, especially preceding and during a radio fadeout. With this end in view, it is proposed to renew the investigation with a more sensitive photoelectric cell, a more powerful radio-wave transmitter, and a more sensitive receiver than was available in this preliminary trial.

1. NOTES ON THE SIX FLIGHTS

In view of the interest these observations may have in other fields of research, as they already have in the case of radio-wave fadeouts, a few details are given regarding each flight. In all the flights latex balloons, model 350, made by the Dewey and Almy Chemical Co. were used.

Flight 1.—Cd-1 photoelectric cell and auxiliary apparatus transported aloft by means of three balloons joined in a cluster. Strong NNW wind; a few fleeting fractocumulus clouds but none near the apparatus.

Ascent started at 11:22 a. m., EST, on June 22, 1937. Ultraviolet record terminated at 12:14 p. m. at an elevation of 33,500 ft (10 km), when the motor

ceased rotating the filters, leaving the photoelectric cell covered with the opaque-filter mounting. On recovery it was observed that the heat of the sun had melted the ceresin wax in the filter mounting, showing a rise in temperature to 55° C. Total height attained was 69,000 ft (21 km). Apparatus recovered in good condition on June 25 at Bishop's Head, Md.

For comparative purposes, simultaneous observations of ultraviolet solar intensities were made with NBS standard ultraviolet meter and *Ti-1* photoelectric cell [1] from 10:40 a. m. to 1:40 p. m.; sky free from dust after several rainy days.

Good radio intensity reported by the radio section of this Bureau.

Flight 2.—Cd-110 apparatus transported by three balloons in a cluster. Sky thick, hazy; no wind; balloons released with cord through ring, which method permitted observations near the earth.

Ascent started at 11:06 a. m. on June 24. Ultraviolet record terminated 11:59 a. m., at an altitude of 29,900 ft (9 km) when the motor stopped, leaving the *LS* filter over photoelectric cell, which furnished observations of ultraviolet intensities to 38,000 ft (11.5 km), where noise interfered. A maximum height of 60,000 ft (18 km) was attained.

At the start this unit drifted E, then ENE at 11:10 a. m. and disappeared from sight. Later the signals became stronger, indicating that the instruments were again near by (probably drifting in a southerly direction). They were found at 5 a. m. the following morning floating over a cornfield at Angier, N. C., a distance of some 260 miles (435 km) south of the starting point.

Poor radio record and a possible radio fade-out was reported by the radio section of this Bureau.

Flight 3.—Cd-110 apparatus, for second time, transported by three balloons in a cluster. Sky was thick and partly covered with fractocumulus clouds. Balloons disappeared between clouds at 3,000 ft; were again visible at 5,000 ft and disappeared at 6,000 ft. The ultraviolet intensity increased between 6,000 and 10,000 ft (3 km.), indicating exposure of the photoelectric cell to solar radiation. At 12,000 ft the apparatus entered a second cloud layer from which it emerged quite rapidly at an elevation of 13,000 ft (4 km).

This ascent was made on June 30 and the signaling period extended from 11:08 a. m. to 1:15 p.m., when noise interfered. A maximum altitude of 52,250 ft (16 km) was attained at 12:07 p.m. In this flight the motor interfered somewhat with the radio signal.

This apparatus descended, uninjured, during a thunderstorm, near Allentown, Pa., and was recovered, motor still running, about 2:30 p.m., soon after the radio signal was lost.

Good radio intensity reported by the radio section.

Flight 4.—Cd-1 apparatus transported aloft for second time by means of three balloons in a cluster. The sky was clear except for a few scattered fractocumulus clouds. Light W breeze; balloons released by means of ring and cord. No drift of apparatus behind ballons.

Ascent started at 10:42 a.m., on July 2 and continued until 12:34 p. m., when all three balloons burst simultaneously at an altitude of 60,500 ft (18 km). During the descent the barograph signals were received in rapid succession, indicating a rate of fall of 100 mph (miles per hour) at the start to 85 mph in the lower atmosphere. The box containing the instruments landed squarely on its bottom (under the barograph) in a cornfield near Chestertown, Pa., where it was recovered on July 15. Aside from breakage of the radio tubes and one glass filter and injury to the barograph and photoelectric cell, the rest of the apparatus was salvaged intact. In order to avoid the possibility of one bursting balloon affecting the others (which may have been the cause of the simultaneous bursting of these three balloons), in subsequent ascents the balloons were leashed at different heights from the apparatus.

In this flight an excellent graphical record (fig. 4) was obtained, except above 50,000 ft (15 km), where noise interfered with the recording of the full ultraviolet intensity (I_0) when no filter intervened.

The radio section reported more absorption in the radio signal (less ozone). This is also indicated by higher ultraviolet intensities, figure 9.

Flight 5.—Cd-110 apparatus used for third time, transported by four balloons, staggered and less highly inflated than in preceding trials in order to attain a higher altitude. Sky relatively clear at start. Balloons passed through clouds at an elevation of about 2,000 ft. Light W breeze. In rising, the balloons drifted slowly ENE, then NE, then possibly S, after reaching an altitude of 8,000 to 10,000 ft (radio signal alternately faded, indicating the apparatus was almost directly overhead).

Ascent started at 10:37 a. m. on July 7, and the ultraviolet record continued until 12:46 p. m. The maximum altitude of 64,000 ft (19.4 km) was attained at 12:27 p. m., after which an interesting barograph record was obtained of the first part of the descent (also ultraviolet, except for noise).

The radio section observed a large radio fade-out beginning at 1:47 p. m. and lasting 15 min. Unfortunately, our ultraviolet record ceased at 12:46 p. m. Judged from flights 4 and 5 (see fig. 9), the ultraviolet intensity preceding the fade-out was lower (in flight 5) than in flight 4. Of the three sets of instruments used in the six flights, only this one remains unrecovered.

Flight 6.—Cd-1 apparatus transported aloft by four staggered balloons. Sky overcast, no direct sunlight below 3,000 ft. Strong breeze and windy, but no lag of apparatus behind the balloons.

Ascent started at 10:36 a. m. on July 12, and the ultraviolet record continued until 11:12 a. m., at 21,600 ft, when the photoelectric cell ceased to function. The instruments attained an altitude of 78,000 ft (23.6 km) and landed in an infrequently visited woods near Hollywood, Md. (some 30 miles (50 km) from the starting point), where the apparatus was found, uninjured, over a month later. It was then found, as surmised at the time of the ascent, that the photoelectric cell and not the resistors in that part of the circuit had failed.

V. EVALUATION OF THE ULTRAVIOLET-INTENSITY MEASUREMENTS

Since the spectral-response curves of the photoelectric cells and the transmissions of the filters used in this work are similar to those employed in our previous investigations, the procedure used in evaluating the measurements of ultraviolet solar radiation of wave lengths shorter than 3132 A in the stratosphere is the same as that employed in calculating the data secured with our standard photoelectric intensity meter at a ground station [3].

In these calculations use is made of the spectral response data of the photoelectric cell (covered with the diffusing window of Corex *A* glass) for an equal energy spectrum; also the data on the spectral transmissions of the glass filters. Furthermore, since, in the stratosphere flights, the angle of incidence of the rays on the photoelectric cell varies with the solar height it is necessary to determine also the sensitivity (the response) for different angles of incidence of radiation upon the window of the photoelectric cell. Since, as will be shown presently, this factor is small, the errors resulting from a change in angle of incidence with rotation of the ultraviolet meter around the suspension cord as an axis and with the slow (conical pendulum) swaying of the apparatus during the flight (the latter is indicated by periodic variations in the audio-frequency signals, see fig. 5) seem to be outweighed by other larger, also unavoidable, instrumental errors that enter into the measurements.

These errors would be most effective in determining the absolute value of the full intensity (I_0) at a given height. This is different from the determination of the percentage transmission of the filters in which a knowledge of the full intensity I_0 is unnecessary; the chief requirement being that there is no marked change in intensity while securing the two intensity measurements (filter and no filter, I_s, and I_0, respectively).

The rotation of the filters is so rapid that the change in intensity on the photoelectric cell with a slow (conical pendulum) swaying of the apparatus, while passing from one filter to an adjoining filter, is of secondary importance. Hence, the variation in the percentage transmission of a filter as a result of swaying of the apparatus container would be largest for the filter opposite to the uncovered opening in

the disk and could be detected and corrected by comparing the relative transmissions of two adjoining filters, or the percentage transmissions of the two filters adjoining the unobstructed opening (I_0) in the disk. This is evident in the sequence of rotations *A*, *B*, *C*, *D*, in figure 5, where all the points lie on the average curve (*A* and *C*) or some points do not fall on the average curve (in *B* and *D*).

In this survey no corrections of this type are undertaken, partly because the ascensions were made in relatively still air, and there was practically no swaying of the apparatus, at least while it remained in sight. Furthermore, there are no marked indentations in the records

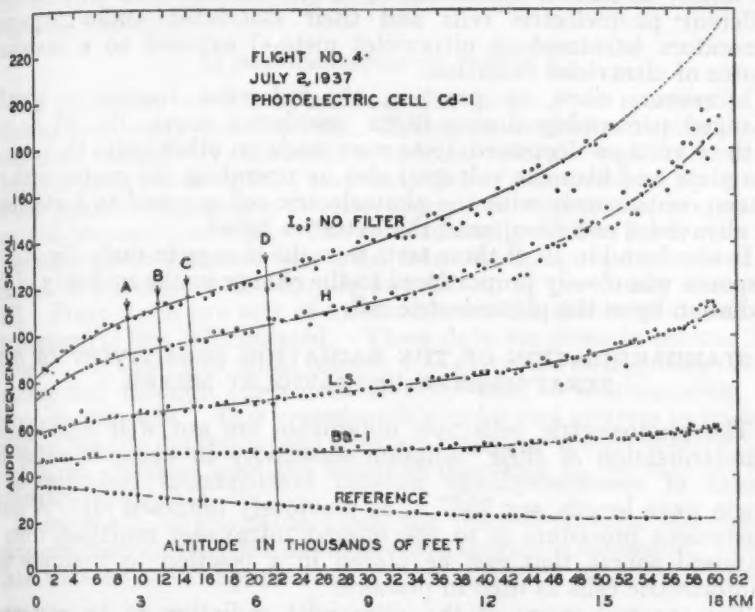
FLIGHT NO. 4
JULY 2, 1937
PHOTOELECTRIC CELL Cd-I
I_0; NO FILTER
H
L.S.
BB-I
REFERENCE
A
B
C
D
AUDIO FREQUENCY OF SIGNAL
ALTITUDE IN THOUSANDS OF FEET
0 2 4 6 8 10 12 14 16 18 20 22 24 26 28 30 32 34 36 38 40 42 44 46 48 50 52 54 56 58 60 62
0 3 6 9 12 15 18 KM

FIGURE 5.—*Variation in ultraviolet intensity (audio-frequency signal) with altitudes as observed through the three glass filters.*

Data taken from the complete graph, of which figure 4 is a part.

of ultraviolet intensities caused by shadowing of the radiometer window as the result of marked swaying of the apparatus in the stratosphere where the measurements are of the greatest importance. The momentary shadowing of the window of the photoelectric cell by the antenna (and to a lesser extent, by the suspending threads) during rotation of the instrument container produces a sharp indentation in the tracing of the stylograph pen (fig. 4). However, the errors resulting from this interruption in the record seem negligible.

1. STANDARDIZATION OF THE AUDIO-FREQUENCY RESPONSE

In the operation of the ultraviolet meter, it is important to know the relation between the audio-frequency response and the intensity of radiation upon the photoelectric cell.

It is to be noted that in this instrument a frequency of 40 to 60 cycles (the lowest depression in fig. 4 and the lowest line in fig. 5) is generated when the photoelectric cell is not illuminated. This

"reference frequency" is determined primarily by the values of the high resistance (300 megohms) and the small capacitance (0.00002 μf) in the control grid circuit of the type 1A6 relaxation oscillator tube (see fig. 2). The sensitivity of the meter is likewise determined by these units.

Upon exposure of the photoelectric cell to ultraviolet radiation, the control grid becomes more and more positive as the radiation is increased, resulting in an increased frequency of audio oscillation.

The proportionality of this increase in audio frequency with increase in intensity of ultraviolet radiation was tested by means of a group of filters, of known transmission, used in connection with several different photoelectric cells and their associated audio-frequency generators (stratosphere ultraviolet meters) exposed to a standard source of ultraviolet radiation.

Moreover, since, in practice, the reference frequency usually changed perceptibly during flight (see lower curve, fig. 5) as the battery voltages decreased, tests were made on other units by varying the plate and filament voltages; also by operating the meter with its filters, continuously with the photoelectric cell exposed to a standard of ultraviolet radiation, until the batteries failed.

It was found in all of these tests that the change in audio-frequency response was closely proportional to the change in the intensity of the radiation upon the photoelectric cell.

2. STANDARDIZATION OF THE RADIATION SENSITIVITY OF THE STRATOSPHERE ULTRAVIOLET METER

The photoelectric cells now obtainable are not well adapted for standardization of their radiation sensitivity in absolute value by means of spectroscopically isolated homogeneous radiation of a single wave length, say 2967 A, as previously proposed [5]. A more convenient procedure is to use filtered ultraviolet radiation from a standard source that can be placed in a position to irradiate the photoelectric cells as used in practice.

The spectral range of the ultraviolet radiation to be measured extends from about 2900 to 3250 A—that is, from the short wave-length limit of the solar spectrum to the long wave-length limit of the response of the photoelectric cells used in this research. Hence, it is important to obtain calibration factors only for this spectral band.

By means of a screen of Corex *D* glass (see table 1, col. 4), which is opaque to wave lengths shorter than about 2800 A, the radiation from the standard quartz mercury-arc lamp [5], effective on the photoelectric cell, is confined practically to the strong emission lines at 2967, 3024, and 3132 A. This is found to be a convenient and reliable source for standardizing the radiation sensitivity of the photoelectric ultraviolet meter, including the audio-frequency generator, in absolute units. However, since the 60-cycle fluctuations in light intensity of the new type of alternating-current quartz mercury-arc lamp (having Wehnelt electrodes) caused interference in the audio-frequency generator circuit, the first described [5] form of direct-current quartz mercury-arc lamp was used to standardize the stratosphere ultraviolet-intensity meter. This source irradiates the interior of the photoelectric cell closely in the same manner as when it is exposed to solar radiation. This eliminates small corrections for variation in sensitivity of different parts of the photosensitive surface of the cell.

Since the photoelectric cell is selective in its spectral response it is necessary to incorporate in the calibration of the ultraviolet meter two radiation sensitivity constants, or factors.

One of these factors, designated factor P, associates the absolute spectral intensities of the standard of ultraviolet radiation with the relative spectral response of the photoelectric cell and the total response of the ultraviolet meter (the audio frequency generated) when the cell is exposed to this standard.

The other factor, G, associates the relative spectral emission of the source measured (in this case the sun) with the same relative spectral response of the photoelectric cell as used in calculating the factor P. The method used in obtaining these two factors is outlined in the two following captions:

(a) DETERMINATION OF FACTOR P

The procedure used in calculating the factor P, is practically the same as previously described [3]. If the standard of radiation [5] has been used extensively, the relative spectral intensities of the mercury emission lines between 2537 and 3342 A are redetermined by means of an achromatic quartz-fluorite spectroradiometer, calibrated for spectral transmission [15]. The total intensity of this band of radiation, at a given distance (say 1 m) from the lamp, is determined by means of a balanced thermopile and filters, as previously described [15]. From these two sets of measurements the absolute intensity of each spectral line is calculated. These data are given in column 2 of table 1. In this same table, column 4, is given the energy (in $\mu w/cm^2$) transmitted through the Corex D filter used in standardizing the photoelectric cells. This procedure is simpler and appears to be more reliable than to determine the absolute intensity of each spectral line, at a given distance from the lamp, as measured at the exit slit of a spectroradiometer [3, 18].

In column 5 of the same table, the relative spectral response of photoelectric cell *Cd-1* for different wave lengths is tabulated. These data were obtained by placing the cell (covered with the Corex A

TABLE 1.—*Standard mercury lamp calibration of the stratosphere-ultraviolet meter used for flight 4*

[Determination of the factor P for evaluating the observed data.]
On exposure of the stratosphere-ultraviolet meter (*Cd-1*, flight 4) to the standard of ultraviolet radiation, the observed audio-frequency meter scale reading was 895. The factor P is 198.7÷895=0.222 for flight 4.

1	2	3	4	5	6
Wave length	Energy of Hg arc lamp	Transmission, Corex *D* screen	Energy through Corex *D*	Relative response, *Cd-1*	Energy times relative response
A	$\mu w/cm^2$		$\mu w/cm^2$		
3132	408.0	0.790	322	0.250	80.5
3024	17.1	.686	117	.495	57.9
2967	85.5	.585	50	.610	30.5
2890	37.6	.425	16	.720	11.5
2804	65.3	.245	16	.760	12.2
2750	21.4	.140	3	.750	2.3
2700	27.0	.075	2	.710	1.4
2650	125.0	.032	4	.600	2.4
Total			530		198.7

diffusing glass window as used in sunlight) at the exit slit of a spectrometer and comparing the photoelectric responses with those of a thermopile. Each wave length is diffused over the surface of the cell in much the same manner, so that any effect of unequal surface sensitivity should be minimized.

From the products of the relative responses of the photoelectric cell (col. 5 of table 1) and the spectral distribution of energy of the quartz mercury-arc lamp, radiated through the Corex *D* glass screen (col. 4) a calculated total response index (198.7) is obtained for the photoelectric cell *Cd-1* when exposed to the standard of ultraviolet radiation (see col. 6, table 1).

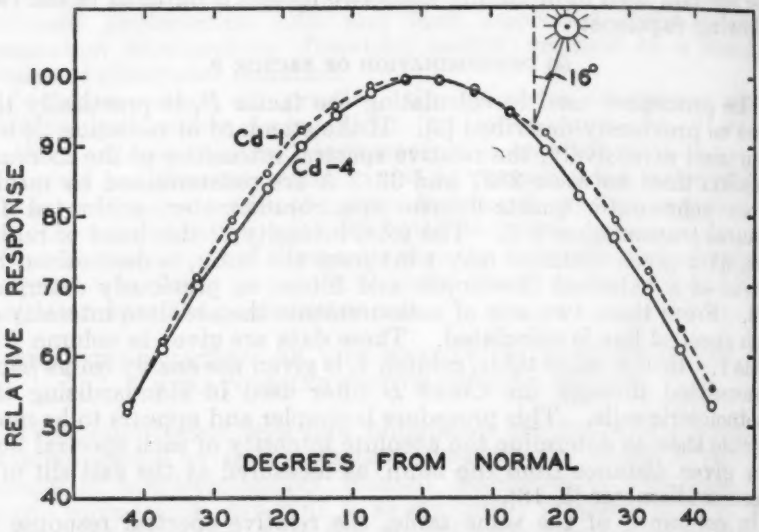

FIGURE 6.—*Variation in sensitivity of the photoelectric cell with variation in angle of incidence of radiation on the diffusing window*

The photoelectric cell is now placed in the audio-frequency ultraviolet meter and, upon exposure to the standard of ultraviolet radiation, the resulting change in audio frequency is recorded. For example, using cell *Cd-1* in the instrument outfit of flight 4, a change of 895 in the scale reading of the frequency meter was obtained. (It is to be noted that in the tables the frequency meter scale reading, which is 5 times the actual audio frequency has been used throughout for convenience.) The ratio of the two values ($198.7 \div 895 = 0.222$) is known as the factor P for photoelectric cell *Cd-1* in its associated ultraviolet meter. This factor, $P = 0.222$, was used in evaluating the intensity of ultraviolet radiation of sunlight during flight 4.

The factor P depends, of course, on the kind of photoelectric cell and the constants of the relaxation oscillator circuit. For example, in flight 1, using the same photoelectric cell, *Cd-1*, the numerical value of this factor was $P = 0.191$.

In practice, the latter part of this calibration (namely, the standardization of the change in audio frequency upon exposure to the standard mercury arc lamp) is made when the apparatus is completely assembled and adjusted, shortly before launching.

(b) DETERMINATION OF FACTOR *G*

In order to determine the factor G used in evaluating the ultraviolet solar radiation of wave lengths shorter than 3132 A (relative to the total range of wave lengths intercepted by the photoelectric cell), a knowledge of the relative spectral intensities in this spectral range is required.

The method used in determining the spectral-energy distribution by the photoelectric cell and filter method is described in detail in a previous publication [3].

Briefly stated, the first requisite is a series of ultraviolet-filter transmissions observed for various solar altitudes (air masses); or, in this case, for various elevations of the ultraviolet meter. These are obtained from the audio-frequency values observed at any altitude.

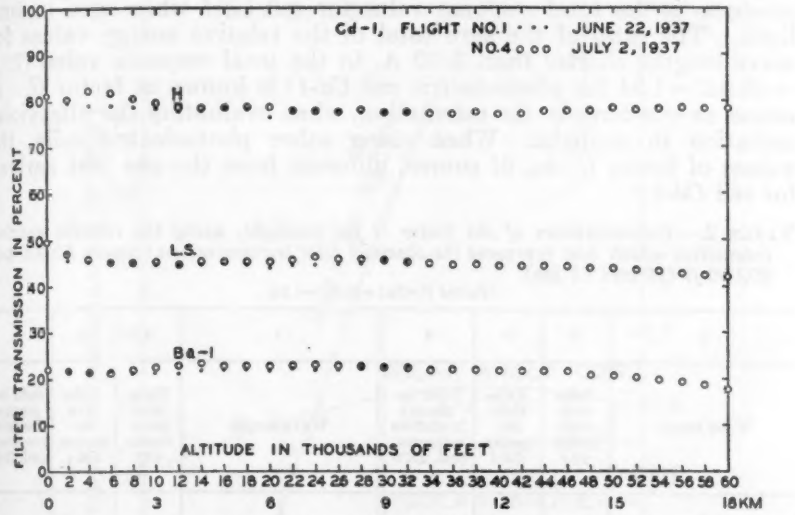

FIGURE 7.—*Percentage transmissions of the glass filters used in the stratosphere ultraviolet meter*

Data calculated from the curves of observations depicted along the lines *A*, *B*, *C*, *D*, etc. of figure 6.

For example, referring to line *A*, figure 5, at an elevation of 10,000 feet (3 km) the percentage transmission of the *Ba-1* filter is the height of the ordinate of *Ba-1* above the reference frequency divided by the height of the ordinate I_0, similarly above the reference frequency.

In this manner, the percentage transmissions of the three filters are calculated for the various flights. The calculations of the transmissions for flight 4 are depicted in figure 7, from which it may be noted that at an elevation of 10,000 ft. (3 km) these filters, when used with photoelectric cell *Cd-1*, had a transmission of 22, 45, and 79 percent, respectively.

In this connection, it is to be emphasized that, using smooth curves drawn through the observations, as indicated in figure 5, the calculations of two persons, working independently, were in agreement within 1 percent. Hence, no attempt was made to calculate each observation independently.

As may be noted in figure 7, there is but little change in the transmissions of these filters (i. e., the spectral-energy distribution) in ascending from 10,000 to 60,000 ft (3 to 18 km). Hence, within the limits of experimental errors, the factor G is calculated for a single spectral-energy curve that best represents the filter measurements at the highest altitudes. The data for this spectral-energy distribution are given in column 2 of table 2.

Referring to table 2, in the calculations involving the spectral energy, a wave-length interval of 10 A is used. The wave length (col. 1) associated with each band, is at the center of this 10 A interval.

In column 3, the photoelectric response data are given for cell *Cd-1* as read from the smooth curve in figure 3. In column 4 is tabulated the product of the relative solar energy and the relative photoelectric response for the different wave-length intervals. The sum of these products is the total response value for cell *Cd-1* when used in sunlight. The ratio of the sum total of the relative energy values for wave lengths shorter than 3132 A, to the total response value ($79.1 \div 58.957 = 1.34$ for photoelectric cell *Cd-1*) is known as factor G. It enters as one term in the calculation, when evaluating the ultraviolet radiation in sunlight. When using other photoelectric cells, the values of factor G are, of course, different from the one just derived for cell *Cd-1*.

TABLE 2.—*Determination of the factor G for sunlight, using the relative spectral intensities which best represent the observed filter transmissions between 50,000 and 60,000 ft (15 and 18 km)*

[Factor $G = 79.1 \div 58.957 = 1.34$]

1	2	3	4	1	2	3	4
Wave length	Relative solar intensity	Relative response, *Cd-1*	Solar intensity ×relative response, (col. 2×3)	Wave length	Relative solar intensity	Relative response, *Cd-1*	Solar intensity ×relative response, (col. 2×3)
A				A			
2935	0.25	0.665	0.166	3135	10.0	.235	2.350
2945	.45	.650	.293	3145	11.1	.215	2.386
2955	.70	.630	.441	3155	12.3	.190	2.337
2965	.95	.615	.584	3165	13.6	.175	2.380
2975	1.20	.600	.720	3175	14.9	.160	2.384
2985	1.50	.580	.870	3185	16.3	.140	2.282
2995	1.75	.560	.980	3195	17.8	.125	2.225
3005	2.20	.540	1.188	3205	19.2	.110	2.112
3015	2.6	.515	1.339	3215	21	.095	1.995
3025	3.0	.495	1.485	3225	22	.085	1.870
3035	3.7	.470	1.739	3235	24	.070	1.680
3045	4.3	.450	1.935	3245	26	.055	1.430
3055	4.8	.425	2.040	3255	27	.045	1.215
3065	5.4	.405	2.187	3265	29	.035	1.015
3075	6.0	.380	2.280	3275	31	.025	.775
3085	6.6	.355	2.343	3285	33	.015	.495
3095	6.9	.330	2.277	3295	35	.005	.175
3105	7.4	.310	2.294	Total			58.957
3115	8.3	.280	2.324				
3125	9.1	.260	2.366	Total shorter than 3132 A	79.1		

3. CORRECTION FOR VARIATION OF THE PHOTOELECTRIC RESPONSE WITH THE ANGLE OF INCIDENCE OF RADIATION

In view of the fact that the sun is never directly overhead in this latitude and varies in altitude with the time of the day and of the year, it is necessary to have a knowledge of the variation of photo-

electric response with the angle of incidence of solar radiation upon the Corex A diffusing window (fig. 1).

In figure 6 data are given on this variation of response with variation in incidence of radiation, through an angle of 40° from the normal, for cells *Cd-1* and *Cd-4*. In this illustration each curve is the average of data taken by rotating the cell in two different planes

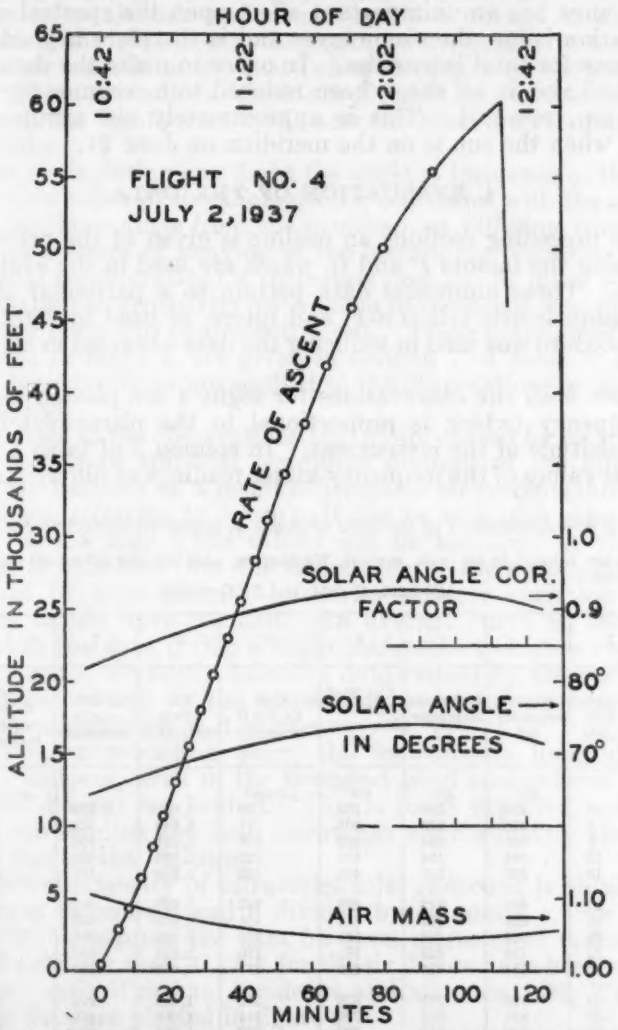

FIGURE 8.—*Graph showing rate of ascent, solar-angle, and air-mass data used in the calculations described in the text for flight 4.*

at right angles to each other and observing the response at intervals of 5° in the four directions from the normal position.

It is to be noted that within an angle of 20° (which includes the solar angle during most of the stratosphere flights) the correction is relatively small. Nevertheless, a correction is made in the evaluation of the data for the slightly reduced response resulting from the angular deviation of the incident radiation from normal (see fig. 8) on the cell.

Associated with the (angular) change in the height of the sun during the measurements is the change in air mass (see the lower curve in fig. 8) which occurs as the result of the solar rays coming through the atmosphere at varying angles during the different times of the day. This is not to be confused with another change in air mass as the result of increasing altitude of the balloons and apparatus, which change has an unimportant effect upon the spectral quality of the radiation below the ozone layer and is therefore neglected in the calculations for total intensities. In order to make the data comparable, they have, in all cases, been reduced to a common air mass for Washington, $m=1.04$. This is approximately the minimum value attained when the sun is on the meridian on June 21.

4. EVALUATION OF THE DATA

In two preceding sections an outline is given of the procedure for determining the factors P and G, which are used in the evaluation of the data. These numerical data pertain to a particular ultraviolet meter, photoelectric cell (*Cd-1*) and filters, as used in flight 4. The same procedure was used in reducing the data obtained in all the other flights.

In figure 5 all the observations for flight 4 are plotted in terms of audiofrequency (which is proportional to the ultraviolet intensity) and the altitude of the instrument. In column 2 of table 3 are given numerical values of the frequency-meter readings at different altitudes.

TABLE 3.—*Evaluation of the data of flight 4, using photoelectric cell, Cd-1*

[Intensities are reduced to air mass, $m=1.04$, Washington, with the sun at normal incidence to the photoelectric cell.]

[$P=0.222$; $G=1.34$; and $P\times G=0.2975$]

1	2	3	4	5	6	7	8
Altitude in feet ÷1,000	Signal frequency, ×5	Reference frequency, ×5	Col. 2−3 corrected frequency, ×5	Col. 4×P×G intensity	Air-mass correction	Solar-angle correction	Col. 5×6+7 corrected intensity
	c/s	c/s	c/s	μw/cm²			μw/cm²
0	410	180	230	68	1.061	0.823	88
4	478	173	305	91	1.049	.838	114
8	526	164	362	108	1.041	.850	132
12	564	154	410	122	1.035	.861	147
16	593	148	445	132	1.029	.871	156
20	624	142	482	143	1.023	.881	166
24	653	134	519	154	1.019	.890	176
28	681	130	551	164	1.015	.897	185
32	716	125	591	176	1.012	.903	197
36	751	121	630	187	1.010	.909	208
40	793	117	676	201	1.008	.914	222
44	834	113	721	214	1.007	.919	235
48	890	111	779	232	1.005	.922	253
52	959	109	850	253	1.005	.923	275
56	1,047	110	933	278	1.006	.922	303
60	1,163	110	1,053	313	1.007	.921	342

As noted elsewhere, the vertical lines A, B, C, and D, in figure 5 indicate the sequence of the frequency-meter readings, in succession, as the different filters rotated over the window of the photoelectric cell.

From these frequency-meter readings is deducted the reference frequency (zero of the scale, col. 3) giving the corrected frequency (col. 4). The product of these values and the factors P and G gives the intensity of the ultraviolet radiation (col. 5) of wave lengths less than 3132 A incident upon the photoelectric cell, at various elevations.

Since during any flight (for example, flight 4; see fig. 8) there is a variation in solar altitude and consequently a change in air mass through which the rays reach the earth, a correction is made for variation of air mass from $m=1.04$ (when the sun is on the meridian, June 21). These corrections which are given in col. 6 of table 3, are small since all the flights were made near the noon hour and near the summer solstice.

Moreover, since during any flight the angle of incidence of the solar rays upon the window of the photoelectric cell varies with the altitude of the sun (the hour angle from the meridian, as differing from small variations, as a result of swaying of the instrument container, which require special consideration) a correction (see fig. 8) must be made also for variation in sensitivity with angle of incidence (see fig. 6) of the solar rays upon the photoelectric cell. These corrections to the data obtained in flight 4, are given in column 7 of table 3; and, of course, similar corrections are applied to the observations obtained on the other flights.

The variations in the observations (fig. 5) are caused by an irregular swinging (circular or elliptical pendulum motion) of the apparatus relative to the balloons as a result of irregular air currents during the ascent. Hence, referring to figure 6, it can be seen that some of the points will be too high while others will be too low. A study of figures 5 and 6 indicates that the magnitude of the swing never exceeded about 5° from normal, otherwise a larger variation in the observations should have resulted. An average curve is, therefore, drawn through the data, giving a slight preference to higher values to compensate for the obviously defective data caused by the shadowing of the photoelectric cell by the suspension cords and antenna at the corners of the instrument as it rotates.

As noted on a preceding page, the instruments hung directly beneath the balloons, even in the strongest wind encountered (15 to 20 mph) and did not lag behind. This is to be expected, since the air stream surrounding the instrument has approximately the same velocity as that at the balloons.

The corrected intensity of ultraviolet solar radiation is obtained as the product of columns 5 and 6 divided by column 7. (See col. 8, table 3.) In this manner the data for total intensity of radiation of wave lengths shorter than 3132 A for the six flights have been reduced to a common basis of normal incidence and air mass 1.04, Washington. These data are plotted in figure 9.

Based upon observations made with a receiver of small angular opening at Washington and at Flagstaff and upon measurements of scattered radiation by Pettit [6] and the authors, an estimated curve (dotted curve in fig. 9) for direct sunlight has been plotted basing the higher altitude values upon those of flight 5.

In table 4, meteorological data as observed by the United States Weather Bureau are tabulated for 11:00 a. m. on the days on which the six flights were made. These data may prove of interest in show-

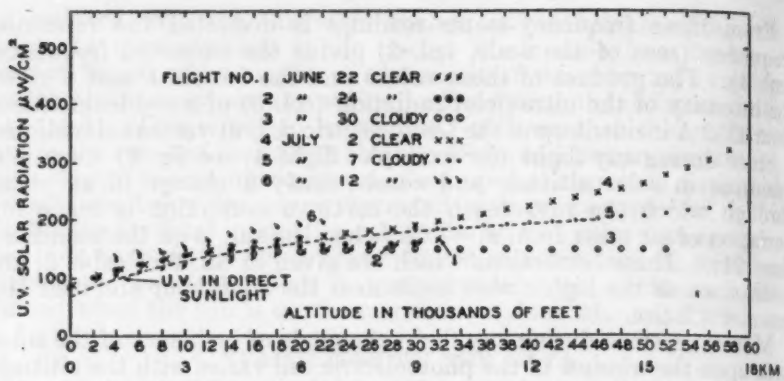
U.V. SOLAR RADIATION μW/CM²
500
400
300
200
100
0
FLIGHT NO. 1 JUNE 22 CLEAR
2 " 24 "
3 " 30 CLOUDY
4 JULY 2 CLEAR
5 " 7 CLOUDY
6 " 12 "
U.V. IN DIRECT SUNLIGHT
ALTITUDE IN THOUSANDS OF FEET
0 2 4 6 8 10 12 14 16 18 20 22 24 26 28 30 32 34 36 38 40 42 44 46 48 50 52 54 56 58 60
0 3 6 9 12 15 18KM

FIGURE 9.—*Ultraviolet solar and sky radiation at various altitudes above the earth's surface*

ing a possible relation between movements of cold masses of air and intensity of ultraviolet radiation as affected by an increase in ozone.

TABLE 4.—*Meteorological data on the days of the six stratosphere flights as reported by U. S. Weather Bureau*

Date (1937)	Radiation (g cal/cm²/day)		Temperature	Wind		Sunshine	Indicated air mass
	Actual	Normal		Direction	Velocity		
			°F		mph		
June 22	736	496	78	NW	14	Clear	NPC
24	790	501	80	WNW	7	do	NPC
30	322	520	78	SW	5	Cloudy	NPC+NPA.
July 2	770	512	73	WSW	5	Clear	NPC
7	598	502	86	NW	6	Cloudy	TA, possibly NP
12	660	493	87	NW	10	do	TA

VI. DISCUSSION OF THE DATA

In taking an inventory of the results obtained in this investigation of ultraviolet solar intensities in the stratosphere it is to be noted that, unfortunately, our observations cease at an elevation of about 19 km, above which the information sought promises to be the most interesting.

As already noted, the results obtained are too meagre to attempt an extensive calculation of the two main factors that reduce the ultraviolet intensities of short wave lengths in the directly incident beam. These factors are: (a) molecular (Rayleigh) scattering by the air, which theoretically should vary inversely as the 4th power of the wave length, and (b) selective absorption by ozone, which, beginning at about 3200 A, increases rapidly in absorption with decrease in wave length, attaining a maximum in the region of 2500 A [21, 22]. Below elevations of about 7,000 ft the intensity of ultraviolet solar radiation is further reduced by absorption and scattering by smoke and dust, especially in the vicinity of cities.

From our measurements at Flagstaff, Ariz. (elevation 7,300 ft, 2.2 km) the effect of sky radiation was found to be extremely small; averaging about 0.3 percent of the total ultraviolet intercepted through

an angular opening of 23° [2]. In the present investigation the angular opening to the interior of the photoelectric cells was about 68°, from which the calculated sky radiation entering this type of radiometer, at an elevation of 7,000 to 10,000 ft (2.1 to 3 km) amounts to 3 or 4 percent of the total. This appears to be negligible in comparison with other far greater errors that enter into the present measurements.

In the relatively narrow band of wave lengths intercepted by the photoelectric cell, the selective increase in intensity of ultraviolet solar radiation, of the shortest wave lengths relative to the longer wave lengths, as the result of Rayleigh scattering at high altitudes, is small [11]. Hence, the effect upon the filter transmissions is of a second order in determining the spectral quality of the directly incident ultraviolet solar radiation. Incidentally, this effect would produce a less rapid decrease in the filter transmission (a less rapid decrease in the apparent amount of ozone overhead) than the true value.

Since the spectral range of the response of the photoelectric cell is so narrow (less than 250 A) but little change in transmission of the filters with altitude is to be expected, unless there is a marked change in the amount of superimposed ozone. For this reason in future ascents a filter that is considerably more opaque to the ultraviolet than *H*, in figure 7, is to be used.

It is desirable to obtain data on different dates, using the same apparatus. In this manner operating conditions will be the same, and any marked variations in the observations may be ascribed presumably to differences in meteorological conditions.

In this connection, the data on ultraviolet intensities (fig. 9) and filter transmissions obtained on flights 2, 3, and 5 are of especial interest, because they were obtained on widely different dates, using the same photoelectric cell, *Cd-110*, and the same filters.

The observations obtained on flight 3 are inconsistent in that there was a continuous increase in the values of the transmissions of the filters with altitude, up to the highest altitudes (16 km) attained. Coincidently, there was practically no increase in the total intensity (I_o) with increase in altitude (fig. 9). On this date meteorological conditions were so unsteady that, until confirmatory data can be obtained showing that during an ascension the apparatus can drift under or into an increasing mass of cold air (see table 4) containing a larger mass of ozone [13, 16], this inconsistency is to be ascribed to an unexplained temporary defect in the instruments.

On the other hand, in flight 5, using the same instruments, the measurements are consistent with similar data obtained in flight 4 (using another instrument, see figs. 7 and 9), and they are consistent with expectations based upon known physical conditions of the atmosphere, showing a gradual increase in total intensity (I_o) and a decrease in the transmissions of the filters, with increase in altitude.

Using the data obtained in flights 4 and 5, it is of interest to obtain a rough estimate of the ozone layer traversed in these two ascents. In order to eliminate the effect of dust and smoke, in the present calculations the lowest elevation taken into consideration is 30,000 ft (9 km), although, as shown in figure 7, there is but little change in the filter transmissions between 10,000 ft (3 km) and this elevation.

At a height of about 14 km the transmissions of the filters begin to decrease, indicating a decrease in ozone. This is in good agreement with the results reported by O'Brien [11] and by Mohler [10]

who, on two ascensions in manned balloons (in 1934 and 1935), found but little ozone below the 15-km level.

For elevations above 14 to 19 km (46,000 to 64,000 ft), where our quantitative measurements cease, the two filters, *Ba–1* and *LS*, show a gradual decrease in transmission (the high-transmission filter, *H*, ordinarily varies but little in transmission [3]), indicating a spectrally selective increase in intensity in ultraviolet of the shortest wave lengths, relative to the longer wave lengths intercepted, as the result of an appreciable decrease in the amount of ozone above the apparatus.

This is in good agreement with the results reported by Mohler [10], in which the amount of ozone above the exploring balloon changed appreciably in rising from a height of 16 to 22 km (53,000 to 72,000 ft), indicating a decrease of over 20 percent in the superposed ozone. This variation in ozone concentration with height was more abrupt than that found by the Regeners [8] and by Goetz, Dobson, and Meetham [9].

1. CALCULATIONS OF THE AMOUNT OF OZONE TRAVERSED

As already mentioned, in passing through the upper regions of the earth's atmosphere ultraviolet solar radiation is reduced in intensity (a) by molecular scattering and (b) by ozone absorption.

In order to obtain an estimate of the amount of ozone traversed, it is necessary to eliminate the effect of molecular (Rayleigh) scattering, which varies as the inverse 4th power of the wave length.

Data on the reduction in intensity (based upon the optical density of 1 atmosphere) at given wave lengths by Rayleigh scattering are taken from a paper by O'Brien [11]. To simplify our calculations, these data are transformed into transmissions for tenths of atmospheres and plotted in figure 10.

From these spectral transmissions and the calculated spectral values of solar intensity times the relative response of the photoelectric cell (see col. 4, table 2) and the spectral transmission of filter *Ba-1* (see fig. 3) is calculated the change in transmission of the filter as a function of altitude. This change (scattering correction) is given in figure 11. The difference between the observed filter transmissions and the correction for Rayleigh scattering ($A-B$) gives the change in transmission associated with the amount of ozone penetrated (curve *C*, fig. 11).

In order to translate this change in filter transmission into depth of the ozone layer penetrated, a knowledge of the spectral transmission of ozone is essential. From the published data of Fabry and Buisson [21] the spectral transmissions of hundredths of a centimeter of ozone (ntp) have been calculated and plotted in figure 10.

The effect of change in ozone thickness upon the filter (*Ba-1*) transmission is calculated in the same manner as outlined above for scattering. The spectral values in each of the transmission curves for hundredths of a centimeter of ozone are multiplied by the product of the photoelectric-cell response and the relative spectral solar intensities (see col. 4, table 2). This gives a total calculated response value for the photoelectric cell for different thicknesses of ozone in intervals of 0.01 cm. The maximum of this response corresponds to a wave length of approximately 3125 A. Next, a product is obtained

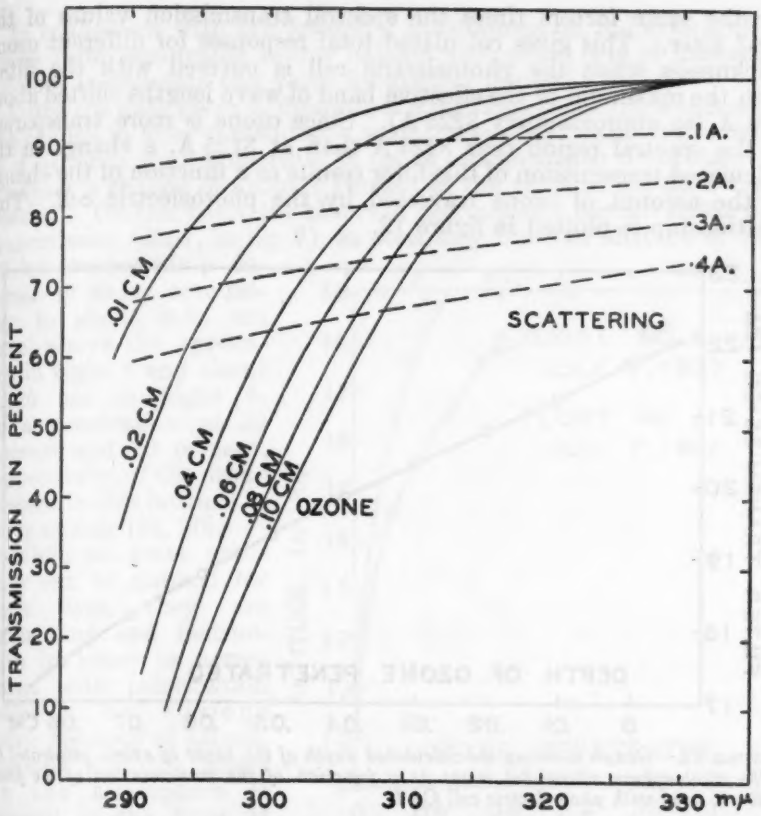

FIGURE 10.—*Graphs showing the spectral transmission of the air as affected by molecular (Rayleigh) scattering and by ozone absorption.*

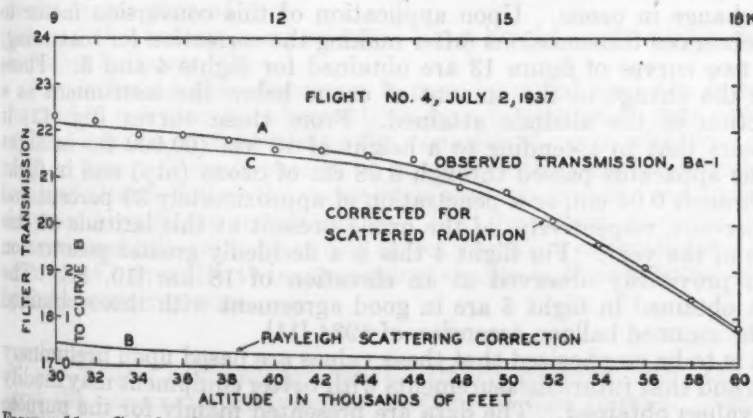

FIGURE 11.—*Graphs showing the observed transmissions of the filter* Ba-1 *at various altitudes (curve A) and the corrected transmissions (curve C) after correction for molecular (Rayleigh) scattering (curve B).*

for the same factors times the spectral transmission values of the *Ba-1* filter. This gives calculated total responses for different ozone thicknesses when the photoelectric cell is covered with the filter, with the maximum of the effective band of wave lengths shifted about 100 A (to approximately 3225 A). Since ozone is more transparent in the spectral region near 3225 A than at 3125 A, a change in the calculated transmission of this filter results as a function of the change in the amount of ozone traversed by the photoelectric cell. This relationship is plotted in figure 12.

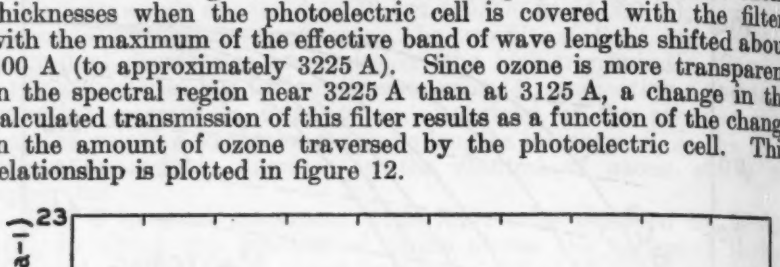

FIGURE 12.—*Graph showing the calculated depth of the layer of ozone penetrated by the stratosphere ultraviolet meter as a function of the transmission of the filter, Ba-1, used with photoelectric cell Cd-1.*

For a change in thickness of about 0.1 cm (ntp) in the layer of ozone, this curve approximates a straight line, for which a change in filter (*Ba-1*) transmission of 1 percent corresponds closely to 0.02 cm change in ozone. Upon application of this conversion factor to the observed transmissions (after making the correction for scattering) the two curves of figure 13 are obtained for flights 4 and 5. These give the change in the amount of ozone below the instrument as a function of the altitude attained. From these curves (fig. 13) it appears that in ascending to a height of 18 km (60,000 ft) in flight 4, the apparatus passed through 0.08 cm of ozone (ntp) and in flight 5, through 0.04 cm, or a penetration of approximately 30 percent and 15 percent, respectively, of the ozone present at this latitude at this time of the year. For flight 4 this is a decidedly greater penetration than previously observed at an elevation of 18 km [10, 11]. The data obtained in flight 5 are in good agreement with those obtained in the manned balloon ascension of 1934 [11].

It is to be emphasized that these values are based upon preliminary data and that future measurements with better equipment may modify the values obtained. The data are presented mainly for the purpose of illustrating a new method of determining the distribution of ozone at high altitudes.

In connection with the foregoing calculations on the extent of the ozone layer penetrated in our balloon ascensions, it is of interest to attempt to estimate this value by another method.

Using the data given in figure 7, of a previous paper [2], which shows the change in filter transmission with the seasonal variation in ozone, it is deduced that a decrease in ozone amounting to 0.013 cm (ntp) produces a change of about 1 percent in the value of the filter transmission. On this basis, the observed decrease of 4 percent in the filter transmission (*Ba-1*, in fig. 7), in ascending from an altitude of 14 to 19 km, represents a decrease in ozone amounting to about 0.05 cm (ntp) above the apparatus in flight 4 and about 0.025 cm in flight 5, or a penetration of 20 percent and 10 percent, respectively, of the ozone present in this latitude in June to July [13, 20].

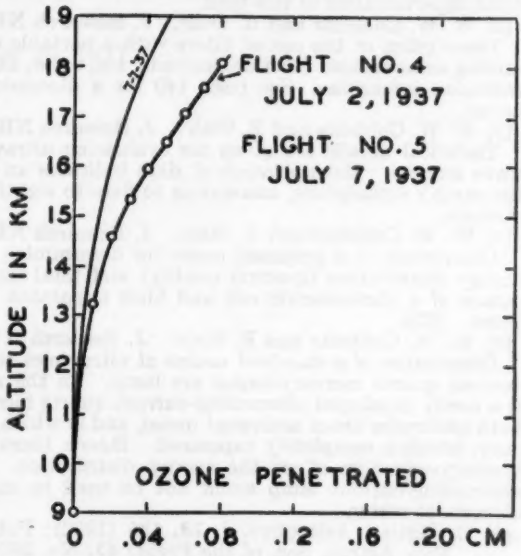

FIGURE 13.—*Graphs showing the depth of the ozone layer penetrated by the stratosphere ultraviolet meter in flights 4 and 5.*

While no great accuracy can be claimed for such data, they are interesting and instructive in being in agreement with information obtained by various other methods of attack, showing that the ozone in the atmosphere is present in the form of a definite layer, presumably having an appreciably higher concentration in the center than at the top and the bottom, and situated at a height easily attainable by sounding balloons.

In concluding this discussion it may be noted that the foregoing method of reducing the observations may be applied to data obtained at land stations in determining the variation of ozone with time of the day or year. Thus it should be possible with a single photoelectric cell and filter to follow the ozone cycle through the year and from year to year through the sunspot cycle. It is important, however, to use a number of cells (at least two or three) which are calibrated and intercompared frequently to insure against change in their spectral or total photoelectric response.

The writers acknowledge the assistance received from the radio and the aeronautic instruments sections of this Bureau. Acknowledgment is also made to the National Academy of Sciences for a grant from the Joseph Henry Fund, which was used in defraying part of the expense of this investigation.

VII. REFERENCES AND NOTES

The publications of the National Bureau of Standards are obtainable only through the Superintendent of Documents, U. S. Government Printing Office, Washington, D. C., prepaid, at the prices indicated.

[1] W. W. Coblentz and R. Stair. BS J. Research **12**, 231 (1934) RP647 (5¢).
Description of a portable ultraviolet-intensity meter consisting of a balanced amplifier, photoelectric cell, and microammeter. A novelty in this device is a means of testing its sensitivity at any moment—an item apparently overlooked by some experimenters in this field.

[2] W. W. Coblentz and R. Stair. J. Research NBS **15**, 123 (1935) RP816 (5¢).
Description of the use of filters with a portable ultraviolet meter [1] in determining some factors (altitide, latitude, fog, snow, sky) affecting ultraviolet solar-radiation intensities. See page 140 for a discussion of a low concentration of ozone.

[3] W. W. Coblentz and R. Stair. J. Research NBS **16**, 315 (1936) RP877 (10¢).
Technical details are given for evaluating ultraviolet solar radiation of short wave lengths. Extrapolation of data indicates an ultraviolet intensity, outside the earth's atmosphere, amounting to five- to eightfold that observed at sea-level stations.

[4] W. W. Coblentz and R. Stair. J. Research NBS **17**, 1 (1936) RP899(5¢).
Description of a proposed meter for determining the ultraviolet solar spectral-energy distribution (spectral quality) and total intensity in the stratosphere by means of a photoelectric cell and filter apparatus transported by sounding balloons. [23].

[5] W. W. Coblentz and R. Stair. J. Research NBS **16**, 83 (1936), RP858 (5¢).
Description of a standard source of ultraviolet radiation consisting of a direct-current quartz mercury-vapor arc lamp. In the most recent setup, the source is a newly developed alternating-current quartz mercury-vapor arc lamp in which both electrodes are of activated metal, and in which there is only a globule of mercury, which is completely vaporized. Hence, there is no change in density of the mercury-vapor to effect the energy distribution. Because of interference, the alternating-current lamp could not be used in calibrating the audio-frequency ultraviolet meter.

[6] E. Pettit. Astrophys. J. **75**, 185 (1932); Pub. No. 445, Mt. Wilson Obs.; Pub. Astron. Soc. of the Pacific **47**, No. 280 (December 1935).

[7] H. Diamond, W. S. Hinman, Jr., and F. W. Dunmore, Bul. Am. Meteorolog. Soc. **18**, 73 (1937); J. Aeronaut. Sci. **4**, 241 (1937).

[8] Erich Regener and Victor Regener. Physik. Z. **35**, 788 (1934).
They used a small spectograph, transported by two sounding balloons. Three flights were made and attained heights of 21, 20, and 31 km, respectively. At 30 km they estimated that 70 percent of the ozone layer was below the apparatus.

[9] F. W. P. Goetz, A. R. Meetham, and G. M. B. Dobson. Proc. Roy. Soc. (London) [A] **145**, 149 and 416 (1934).

[10] F. L. Mohler. J. Wash. Acad. Sci. **26**, 487 (1936).
Vertical distribution of ozone, using a spectograph transported in a manned balloon (*"Explorer"*).

[11] Brian O'Brien, F. L. Mohler, and H. S. Stewart, Jr. Nat. Geographic Soc. Contrib. Tech. Papers, Stratosphere Series, No. 2, p. 71 (1936; and Brian O'Brien, *Vertical distribution of ozone in the atmosphere*, p. 49.

[12] F. W. P. Goetz. Beitr. Geophys. **31**, 119 (1931).
See p. 137 for seasonal variation in the amount of ozone at different latitudes.

[13] G. M. B. Dobson. Proc. Roy. Soc. (London) [A] **129**, 411 (1930).
Data and graphs are given on the amount of ozone in the earth's atmosphere as a function of the latitude and the season of the year. Supplementary data by H. H. Kimball and by E. Kidson.

[14] Fowler and Strutt. Proc. Roy. Soc. (London) [A] **93**, 577 (1917).

[15] W. W. Coblentz, R. Stair, and J. M. Hogue. BS J. Research **7**, 723 (1931) RP370 (10¢).

[16] G. M. B. Dobson and A. R. Meetham. J. Roy. Meteorolog. Soc. **60**, 265 (1934).
Discussion of atmospheric ozone and meteorology.

[17] E. G. Lapham BS J. Research **7**, 691 (1931) RP367 (10¢).

[18] Report of the Illum. Eng. Soc. Subcommittee on Measurement and Evaluation of Ultraviolet Radiation, Trans. Illum. Eng. Soc. **28**, 684 (1933).

[19] E. Kidson. Proc. Roy. Soc. (London) [A] **129,** 421 (1930).
Relation between weather and the amount of ozone in the earth's atmosphere above Christ Church, New Zealand.
[20] Rudolf W. Ladenburg. J. Opt. Soc. Am. **25,** 259 (1935).
Symposium survey of light absorption and the distribution of atmospheric ozone.
[21] Ch. Fabry and H. Buisson. J. phys. [5] **3,** 196 (1913); Astrophys. J. **54,** 297 (1921).
[22] A. Läuchli, Z. Physik **53,** 92 (1929).
[23] W. W. Coblentz and R. Stair. Bul. Am. Meteorolog. Soc. **18,** 345 (1937); Radiologica **1,** 12 (1937).

A brief description of a radiometric method of measuring ultraviolet solar-radiation intensities in the stratosphere; also an account of some preliminary results obtained.

WASHINGTON, November 20, 1937.

U. S. Department of Commerce National Bureau of Standards

RESEARCH PAPER RP1076

Part of Journal of Research of the National Bureau of Standards, Volume 20, February 1938

FIRE TESTS OF TREATED AND UNTREATED WOOD PARTITIONS

By Clement R. Brown

ABSTRACT

Fire-endurance tests were made of 13 wood partitions 4 ft square and of four partitions 10 ft high and 16 ft wide. Some of the smaller partitions were of untreated longleaf pine, while the others were made of longleaf pine impregnated with various amounts of monoammonium phosphate up to 17 percent by weight. They were built either of one, two, or three plies of ¾-in. boards, or of a 1¾-in. core with 5/16-in. veneers, giving a total thickness of 2⅛ in. The large partitions were of the latter design and were made of treated birch. The results of the tests of the small panels are compared with results of fire-tube and flame-penetration tests made on specimens representative of each panel.

CONTENTS

	Page
I. Introduction	217
II. Fire-endurance tests	218
1. Material and treatment	218
2. Construction	218
(*a*) Small panels	218
(*b*) Large panels	219
3. Fire tests and results	222
(*a*) Mounting of panels	222
(*b*) Method of testing	223
(*c*) Observations and results	223
1. Small panels	223
2. Large panels	226
(*d*) Discussion of results	227
III. Supplementary tests and results	230
1. Specimens	230
2. Fire-tube tests	231
3. Flame-penetration tests	232
IV. Comparison of results	236
V. Summary and conclusions	238
VI. References	238

I. INTRODUCTION

Recent interest in the use of fire-retardant treated wood has revived the demand for reliable methods of classifying such material both in terms of its resistance to fire and its fire hazard compared to that of untreated wood. As a result, several testing methods have been studied during the past few years by the Forest Products Laboratory, U. S. Department of Agriculture [1][1]; by Hartman, Williams, and

[1] Numbers in parentheses indicate the references at the end of this paper.

Bastress [2]; and by the National Bureau of Standards. That part of the Bureau's investigation dealing principally with the extent to which the fire-tube and flame-penetration tests indicate the tendency of wood to spread fire, has been reported in a paper published in 1935 [3].

The fire resistance of structural elements is usually determined by tests of relatively large specimens according to procedures similar to that described in ASA Standard A2–1934 [4], which formed the basis of the present tests. These tests indicate the performance, under specified test conditions, of a given type of construction in terms of ability to sustain a load when exposed to fire, to prevent the occurrence of unduly high temperatures on the unexposed side, and to retard the passage of flame or hot gases through the construction. Although this and similar testing procedures have been occasionally applied to floors, partitions, and doors constructed of treated wood [5], the tests usually have not been carried to failure of the structure, nor have they permitted direct comparisons between treated and untreated wood.

The present paper gives the results of fire-endurance tests on thirteen 4-ft-square partitions built of longleaf pine and varying in thickness, design, and concentration of treatment, and of four 10- by 16-ft treated birch partitions. In addition, fire-tube and flame-penetration tests were made on specimens from the same lots of material, carefully selected and prepared so as to be representative of the particular panels. The results of these three types of tests have been compared to determine the value and limitations of each test for indicating the fire-retarding properties of treated wood.

II. FIRE-ENDURANCE TESTS

1. MATERIAL AND TREATMENT

All of the small partitions, except Nos. 6 and 7 (table 1), were constructed of longleaf pine obtained from the Forest Products Laboratory of the Department of Agriculture. Panels 6 and 7 were built of untreated shortleaf and longleaf pine from our own stock. The treated wood was prepared by the Forest Products Laboratory, using monoammonium phosphate under pressure, with kiln drying after treatment.

The four large partitions were constructed of fire-retardant treated birch by a commercial woodworking and treating concern, the treatment being applied under pressure, followed by kiln drying. The actual concentration of treatment, although unknown, is believed to be relatively high.

2. CONSTRUCTION

(a) SMALL PANELS

The small fire-test panels were all approximately 4 ft square. Panels 1 to 10, inclusive, were constructed in our own shop, using ⅞-in. boards, 60 in. long, and from 2½ to 6 in. wide. The amount of treatment being known for each board, they were carefully selected and distributed in each panel so as to obtain about the same average amount of treatment throughout the panel. As noted in table 1, all of the boards in the first 10 panels were vertical, except the core boards of panel 3. The boards were planed to ¾ in. thickness, jointed,

and grooved. The ¼- by ½-in. splines fitted tightly into the grooves and no glue was used in the joints or between the plies. The plies were fastened together with several rows of nails on each side, and batten strips were nailed across the side unexposed to fire.

Figure 1 indicates the construction of panels 2 and 3. Chromel-alumel thermocouples (23 and 26 gage) were placed between the plies of the two- and three-ply panels, one couple in each of two opposite corners 12 in. from the adjacent sides, and one at the center of each panel, as shown in figure 1.

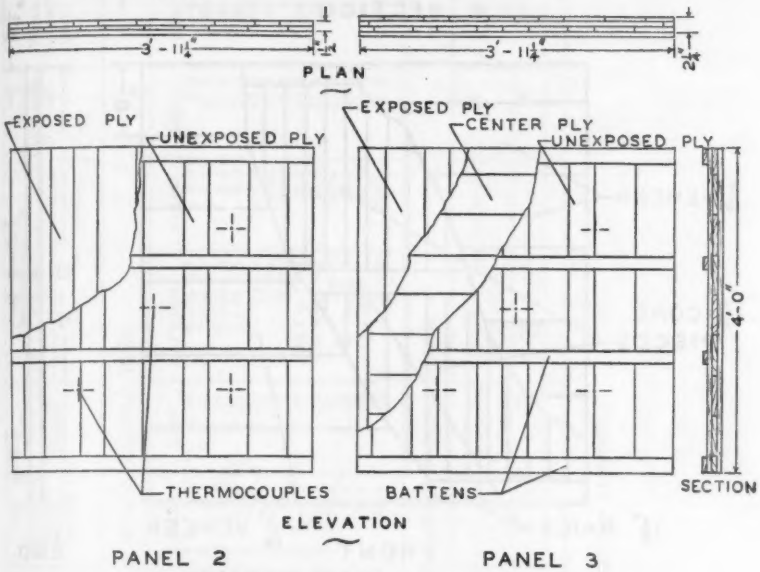

FIGURE 1.—*Construction of panels 2 and 3.*

Panels 11, 12, and 13 were constructed, as shown in figure 2, by a commercial woodworking concern according to our specifications, from the same lots of material used in panels 8, 9, and 10. All joints were glued, the veneer pieces being glued to the core under pressure. No thermocouples were placed in the interior of these three panels.

(b) LARGE PANELS

The large panels were built by a commercial concern from wood treated in its own plant. The panels were 10 ft high and 16 ft long and were constructed in sections, each from 2 ft 6 in. to 3 ft 2 in. wide. They were tongued and grooved on the edges so as to form smoke-tight joints when erected for the fire test. Figure 3 shows the construction of a section of panel *A*, which is typical for the large panels. The crossbanding of these panels corresponds structurally to the veneers in panels 11, 12, and 13. All joints in the core were tongued and grooved and were glued together under pressure. The crossbands were about 6 or 7 in. wide and were glued to the core under pressure. The thicknesses of core and crossbanding used in the different panels were varied slightly in order to obtain the desired variation in total thickness of the panel. Table 1 also gives density

data for two of the large panels but the moisture content at time of test was not definitely known for any of these panels.

Panels *A*, *B*, and *C* were very similar in construction, but in panel *D*, a flush-type door was substituted for one of the sections. This door, 2⅛ in. thick, was similar in construction to the rest of the panel

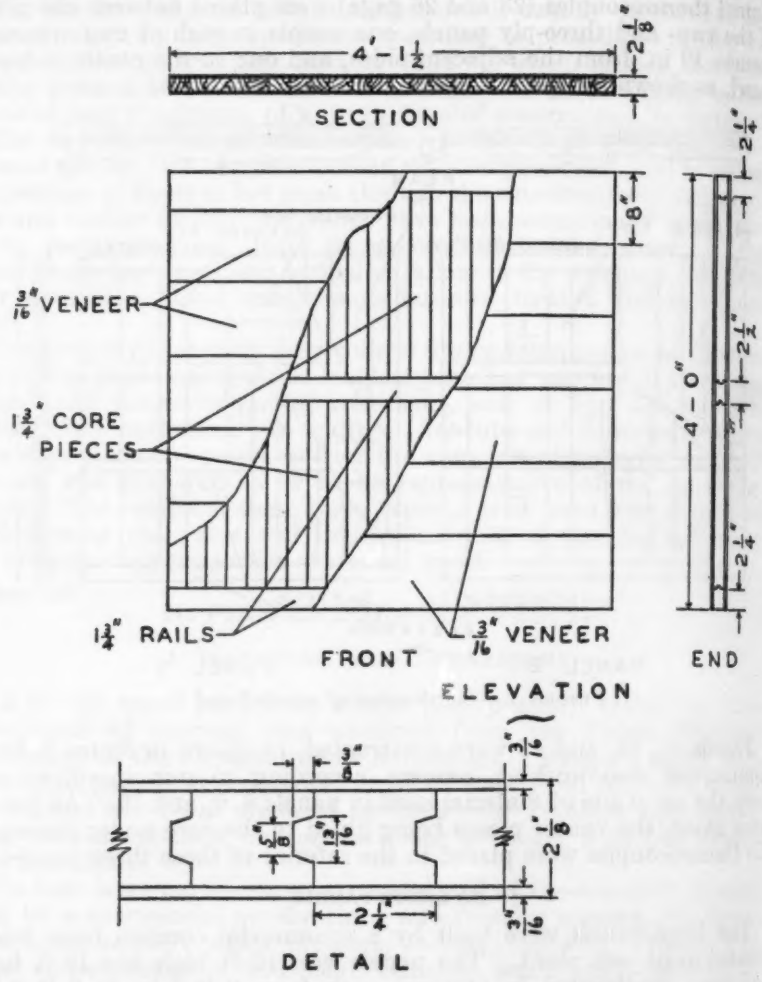

FIGURE 2.—*Construction of panels 11, 12, and 13.*

and hung to open toward the side to be exposed to fire. The edges of the door were beveled and the beveled door jambs were tongued on the back so as to fit into corresponding grooves in the adjacent panel sections. The clearance around the door on the exposed side varied from 0 to 0.05 in. and between door and stop on the unexposed side, from 0 to 0.09 in. The door fittings were of bronze and the hinge pins projected on the side of the panel to be exposed to fire.

TABLE 1.—*Description of partitions and results of fire-endurance tests*

Panel number	Description	Total thickness	Moisture content when tested	Apparent density	Concentration of treatment [1]		Light seen through panel	Flame through panel	Limiting temperature reached	Failure by—
					Range	Average				
	(A) SMALL PANELS, PINE									
		In.	*Percent*	*g/cm³*	*Percent*	*Percent*	*Min.*	*Min.*	*Min.*	
1	One-ply, boards vertical	¾	8.8	0.64	8.1 to 8.3	8.2	7.2	9.4	11.0	Flame.
2	Two-ply, boards vertical	1½	9.1	.63	7.6 to 8.9	8.2	27.4	29.5	28.3	Temperature.
3	Three-ply, outside boards vertical	2¼	8.6	.61	7.6 to 9.0	8.3	37.8	40.5	41	Flame.
4	Two-ply, boards vertical	1½	8.3	.65	6.6 to 7.3	6.9	29.0	31.1	30.5	Temperature.
5	Three-ply, all boards vertical	2¼	9.7	.62	[2] 4.1 to 11.0	8.6	42.2	45.3	45.4	Flame.
6	Two-ply, boards vertical	1½	9.4	.61	None	None	28.5	29.4	----------	Do.
7	One-ply, boards vertical	¾	8.1	.61	None	None	8.3	8.9	----------	Do.
8	Two-ply, boards vertical	1½	7.8	.57	13.6 to 18.9	15.9	30.0	34.5	31.5	Temperature.
9	----do	1½	8.8	.58	13.4 to 19.2	15.9	31.5	34.5	36.3	Flame.
10	----do	1½	10.2	.57	None	None	30.0	32.7	32.3	Temperature.
11	1¾-in. core, 3/16-in. veneers	2⅛	8.4	.57	13.3 to 22.2	17.0	59.2	62.9	63.6	Flame.
12	----do	2⅛	8.4	.58	13.2 to 23.2	17.2	68.4	72.1	----------	Do.
13	----do	2⅛	11.4	.60	None	None	63.3	69.2	67.0	Temperature.
	(B) LARGE PANELS, BIRCH									
A	1 13/16-in. core, ¼-in. veneers	2 1/16	----------	----------	Unknown, but believed to be high.		62	62	63	Glow.[3]
B	1¾-in. core, 7/32-in. veneers	2 3/16	----------	0.79	----do	----------	----------	64.5	----------	Flame.
C	1¾-in. core, 3/16-in. veneers	2⅛	----------	.77	----do	----------	61	61.5	----------	Do.
D	----do	2⅛	----------	----------	----do	----------	----------	----------	----------	None.

[1] Ratio of dry salt to air-dry wood, by weight.
[2] Only a few pieces of material with this low concentration, the rest being above 7.3 percent.
[3] Glow on surface.

3. FIRE TESTS AND RESULTS

(a) MOUNTING OF PANELS

The small panels were mounted in a 50-in.-square concrete frame, which was placed in front of the Bureau's small gas-fired wall furnace [6], the spaces between the panel and frame being filled in with asbestos, fire clay, and narrow strips of treated wood, where necessary.

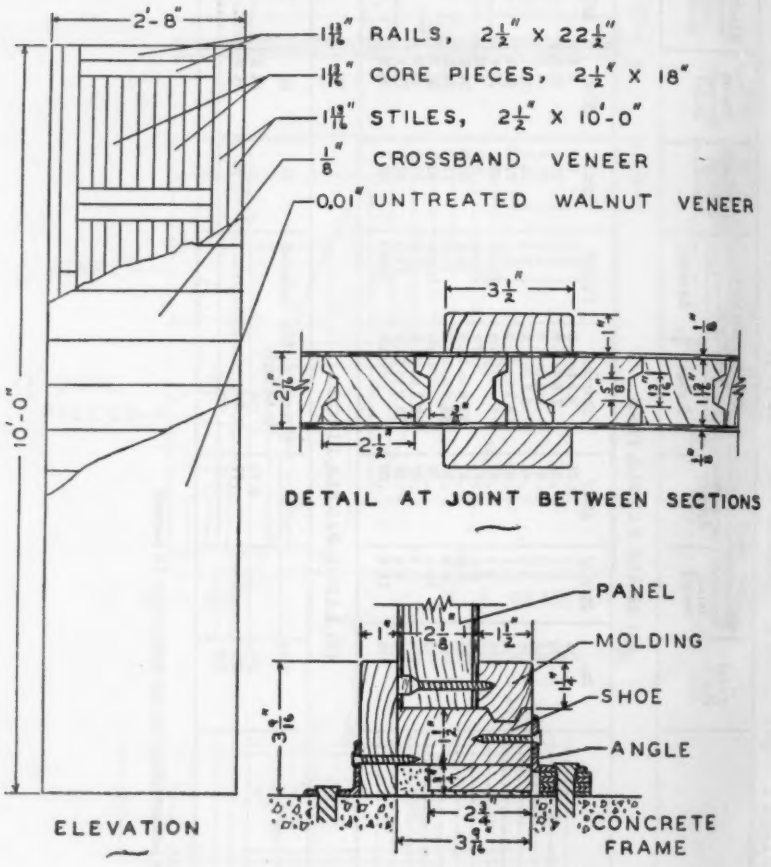

FIGURE 3.—*Construction of large panels.*

The panels were fastened to angles attached to the frame. Pieces of wood, ¾ by 1¾ in., were nailed along the sides of the first 10 panels and all around the edges of panels 11, 12, and 13, in order to make a reasonably tight joint between panel and frame.

The four large panels were erected in sections in a large steel and concrete frame having an inside opening of 10 ft 1 in. by 16 ft. Panels *A* and *B* were held in place by means of 2- by 2½-in. marginal strips of treated birch, which were fastened to the concrete frame with angles and expansion bolts. The special marginal frame shown in figure 3 was used for panels *C* and *D*. All openings between the

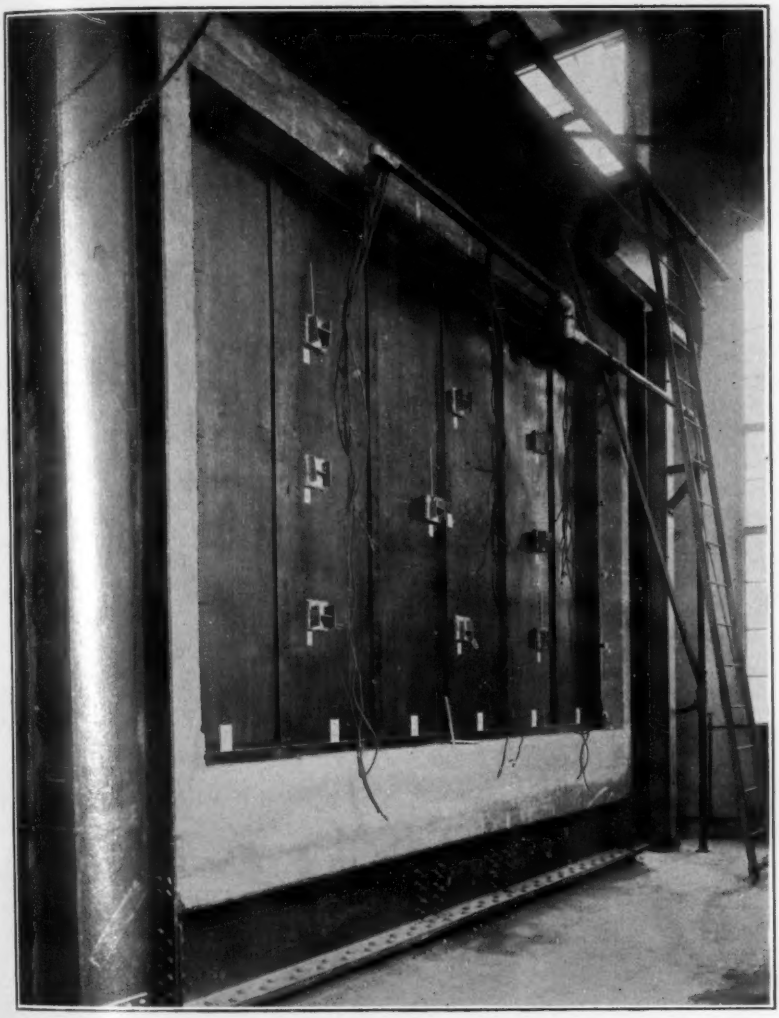

FIGURE 4.—*Panel B mounted in furnace ready for test.*

FIGURE 7.—*Unexposed side of panel B after fire exposure.*

panel and the frame were filled with asbestos cement. The joints between the sections of all panels were covered with 1- by 3½-in. batten strips, also of treated birch.

(b) METHOD OF TESTING

The tests were conducted in accordance with the specifications for fire tests of building construction and materials of the American Standards Association [4]. Temperatures in the furnace were measured with 18-gage chromel-alumel thermocouples, six being used in the small furnace and nine in the large furnace. Except for the test of panel *B*, the furnace exposure was controlled so as to give indicated furnace temperatures approaching as nearly as possible those given by the reference time-temperature curve. In the case of panel *B*, the average furnace temperature followed the reference curve for the first half hour and was then increased more rapidly in an attempt to obtain an average exposure of 1,700°F for the last half hour.

Temperatures on the unexposed surface of the small panels were measured with five fine-wire chromel-alumel thermocouples placed under 6- in.-square felted-asbestos pads 0.4 in. thick. One couple was located at the center and one in each of the four corners, 12 in. from the edges of the panel. Thermometers were placed under three of the pads. As already mentioned, fine-wire thermocouples were placed between the plies of panels 2 to 6 and 8 to 10, inclusive.

Nine fine-wire chromel-alumel thermocouples were placed under pads on the unexposed surface of the large panels, but no couples were placed between the plies. The surface thermocouples were located at or close to the intersection of the lines dividing the panel surface vertically and horizontally into quarters. Thermometers were placed under three of the pads on these panels also.

Deflection measurements relative to stationary vertical wires were taken on the large panels at points close to the thermocouple pads. Figure 4 shows panel *B* in place in front of the furnace before test.

In conducting the test the criterion of failure was taken as any one of the following: An average temperature rise of 139°C (250°F) above the initial, as shown by the surface thermocouples; a maximum temperature rise of 181°C (325°F) above the initial at any one thermocouple location; or the appearance of flame on the unexposed surface. The test was discontinued shortly after any one of the above endpoints was reached.

All of the tests were fire-endurance tests except that on panel *D*, which was a fire test for ½ hr, immediately after which the panel was removed and a hose stream applied to the exposed surface for 2.4 minutes.

(c) OBSERVATIONS AND RESULTS

1. *Small Panels.*—The temperature records for 6 of the 17 fire tests are given in figures 5 and 6. *F* max, *F* avg, and *F* min denote the time-temperature curves for the furnace maximum, average, and minimum, respectively. The control of the furnace was based on the curve marked "Reference Curve." Maximum and average temperatures indicated by the surface thermocouples are denoted by *C* max and *C* avg, respectively, while *T* denotes the surface tem-

peratures, as indicated by the thermometers, and *R* indicates the room temperature during test. For the two-ply panels, the curves marked 1 are the average temperatures indicated by the fine-wire

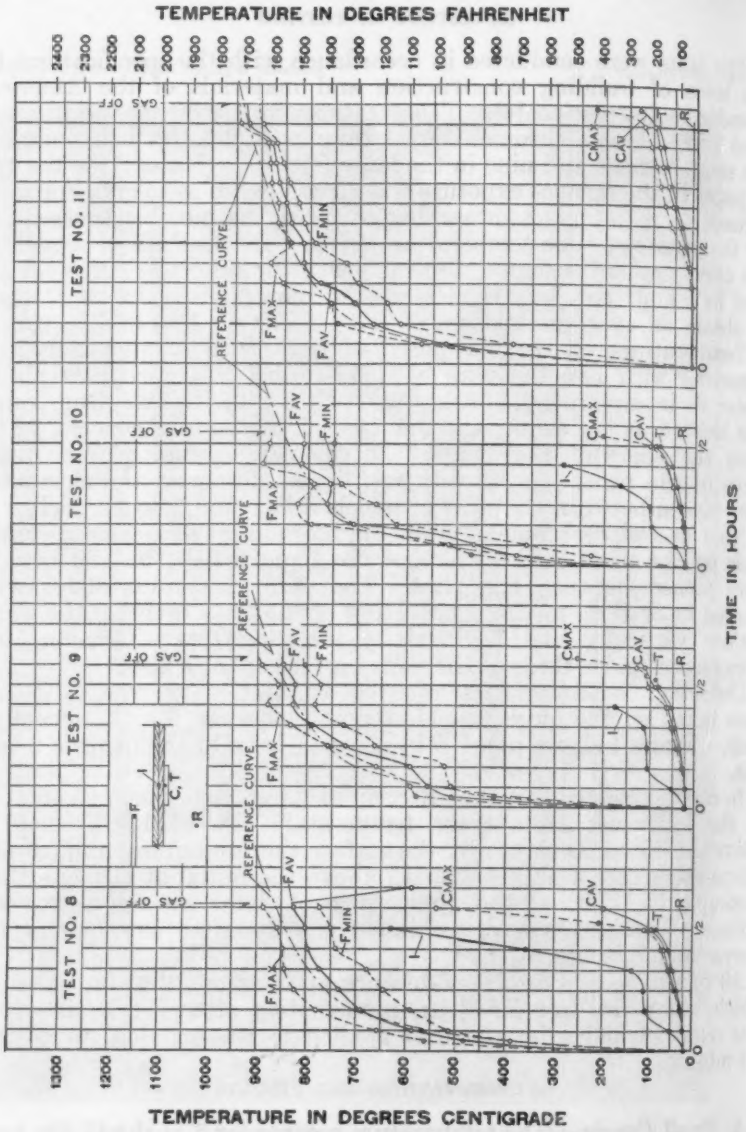

FIGURE 5.—*Temperature records for fire tests of panels 8, 9, 10, and 11.*

couples between the plies, while for the three-ply panels the curves marked 1 refer to the interior location nearest the exposed side, and those marked 2, the location closest to the unexposed side.

The principal results of the tests are given in table 1. The behavior of panels 1 to 10, inclusive, was very similar except for the amount and character of flaming. The exposed surface was charred and began

checking within the first 2 min, and the joints in the ply nearest the fire began opening at from 9 to 18 min. Short pieces of the boards of this ply began falling off the panel at from 21 to 25 min, and most

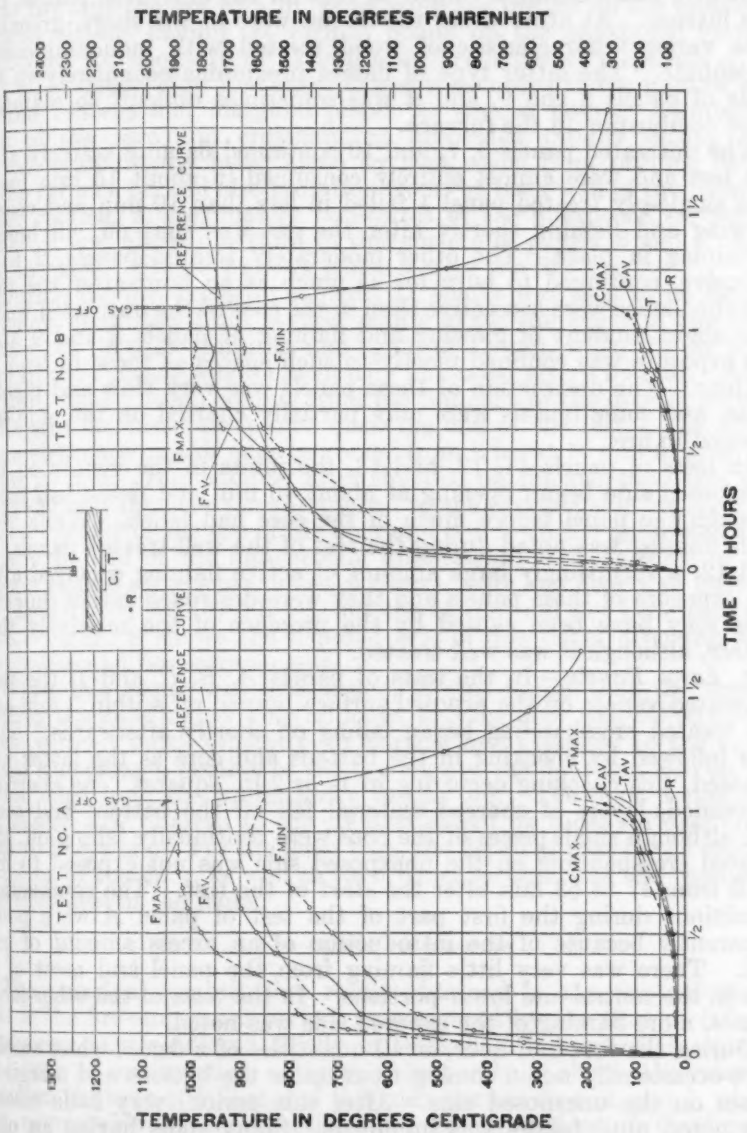

FIGURE 6.—*Temperature records for fire tests of panels A and B.*

of this ply had fallen off within the next 5 or 6 min. This was followed by warping and opening of joints in the adjacent ply. In the case of the three-ply panels, 3 and 5, the core boards began falling off at 34 and 36 min, respectively. The time at which the joints in the unexposed ply had opened sufficiently to permit light from the furnace to be seen is given in table 1.

For the untreated panels, periods of vigorous, active flaming alternated with periods of subdued flaming during fire exposure. The flaming during the exposure of the moderately treated panels, 1 to 5, inclusive, was sometimes similar to that for the untreated panels, but less intense. At other times the flames were of the short, greenish-blue variety characteristic of wood treated with monoammonium phosphate. The latter type of flames predominated entirely in the tests of panels 8 and 9, and it was sometimes difficult to maintain good combustion in the furnace.

The untreated panels 6, 7, and 10 continued flaming actively after the test and were almost entirely consumed in about 15 min more. The single-ply treated panel 1 failed in less than 10 min and ceased glowing and flaming shortly after the gas was shut off, all boards remaining in place. The other moderately treated panels, 2 to 5, inclusive, continued to burn for as much as an hour after the test, but the flames were less active than in the case of the untreated wood. The slight amount of glowing and flaming of panels 8 and 9 after fire exposure was confined mostly to such spaces as those in back of battens. The destruction of these panels was very slow and incomplete, and some boards were only partially charred on the side not exposed to fire.

In tests of panels 11, 12, and 13, the joints in the veneer on the unexposed side began opening at about 40 min and flame had come through the panel before much of the core had fallen. While very little flaming was noted during the test of the well-treated panels, 11 and 12, a surprisingly large amount of active flaming occurred after fire exposure of these panels and they were destroyed rather quickly. This may have been caused by the presence of the relatively thin veneer, although it was well treated.

2. *Large Panels.*—In the tests of panels *A*, *B*, *C*, and *D* the thin untreated veneer on the exposed surface burned off within 2 min and the treated crossbanding began falling off shortly afterwards. This was followed by checking in the battens and core as the latter was exposed, this checking occurring in 1- or 2-in. squares. As charring proceeded, layers of charred material fell off the battens and core, and although small pieces of the core were continually falling off, the treated crossbanding on the unexposed side was not exposed to fire until from 47 to 63 min after the start of the test. The combustion conditions during the first part of the test of panel *A* were poor; apparently because of the introduction of an excess amount of gas fuel. There was very little flaming from the panel and most of it was in the central and lower portions. In the tests of the other large panels, more flaming of the exposed side was noted.

During the first half-hour, small quantities of a dense, white smoke were occasionally noted coming from under the battens and marginal pieces on the unexposed side. After this period, very little smoke was noted until failure was imminent. Shiny spots having an oily appearance began to show on the unexposed surface after 35 min. Warping of this surface and apparent buckling of the panel were first noted at about 45 min. Failure by flame penetration was preceded by the appearance of a blister on the unexposed surface, which soon turned black and then cracked, glow or flame appearing a few minutes later. In the case of panel *A*, glow appeared on the surface at 62 min, and as a cotton pad in contact with the glowing surface was

ignited, this time was taken as failure, although flame did not appear until several minutes later.

The deflection of the large panels was relatively small, varying from ⅛ in. towards the fire to ⅜ in. away from the fire for all the panels.

Intermittent flaming at various points on the unexposed surface continued for about 10 or 12 min after fire exposure of panels *A*, *B*, and *C*, although glow and short flames were noted in the interior and behind battens and marginal pieces for several hours. Disintegration of the core and crossbanding proceeded rapidly during this period, undoubtedly being aided by heat rising from burning debris in the furnace pit and also radiation from the back wall of the furnace. After cooling, approximately two-thirds of the unexposed surface of panel *A*, and about one-third of this surface of panels *B* and *C*, were still in place. Figure 7 shows panel *B* after the fire test.

During the fire exposure of panel *D*, smoke was seen to be issuing in small quantities from several points along the edges of the door within the first few minutes, and again at 12 min, when the air pressure in the furnace was momentarily increased above normal. After 22 min, smoke began coming from the top edge of the door in regular puffs and increased in volume until the end of the test. The maximum clearance on this edge increased from ¼ in. at 19 min to nearly ½ in. at 26 min. Immediately after shutting off the gas, the panel was removed and the hose stream applied to the exposed side for 2.4 min. Water came over the top of the door and ran down the unexposed side before the end of the hose-stream application, and the force of the stream caused some loose pieces of charred core and nearly all battens on the exposed side to fall off, but the stream did not penetrate the core. Figure 8 shows the exposed side of this panel after the fire-endurance and hose-stream test.

When this panel was dismantled, it was found that the screws holding the door hinges were all loose, and the door was pulled out of place without much difficulty. Charring had extended to the unexposed side along a portion of the top edge of the door and also on the inside edge from the upper hinge to the top. The door jambs and stops were also charred to the greatest extent on those surfaces adjacent to hardware. For the most part, the depth of char in the central portions of the door, as well as each panel section, was less than half the thickness of the panel.

(d) DISCUSSION OF RESULTS

The principal quantitative result obtained in the fire-endurance test is the fire-endurance period, as measured by the time of failure. The small panels differed chiefly in thickness, amount of treatment, and type of construction. Figure 9 (upper half) shows the relation between the time of failure and thickness for panels 1, 2, and 5, which are comparable in construction and concentration of treatment. This relation is practically linear, differing in this respect from the behavior found for incombustible walls and partitions, the fire endurance of which increases approximately with the square of the thickness. From the lower half of figure 9 it is evident that concentration of treatment has very little (if any) effect on the time of failure in this particular type of test, at least in the range from 0 to 16 percent. Also, the untreated core and crossband panel 13 developed nearly the same fire endurance as the average for the heavily treated panels 11

and 12 of similar construction. This may not necessarily hold for other species of wood or other treatments. On the other hand, the type of construction is an important factor. Table 1 shows that the performance of the core and crossband panels 11, 12, and 13 was much

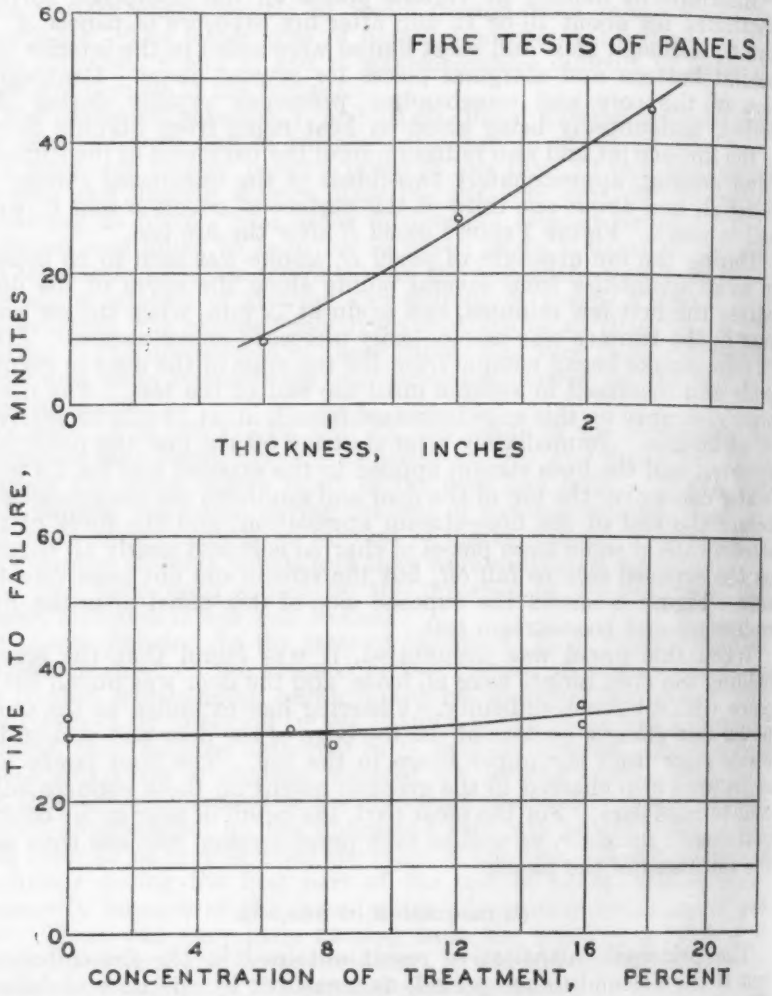

FIGURE 9.—*Influence of thickness of panel and concentration of treatment on time of failure, in fire tests of partitions.*

Data in upper half are from tests of panels 1, 2, and 5. Data in lower half are from tests of panels 2, 4, 6, 8, 9, and 10.

better than that of the ply panels 3 and 5, even though the latter had slightly greater thickness.

The large panels differed too little to permit a study of such factors as thickness and type of construction. They were similar in construction and thickness to small panels 11, 12, and 13, and although they differed from the latter in wood species and treatment details, there was very little difference between the results of the tests of these

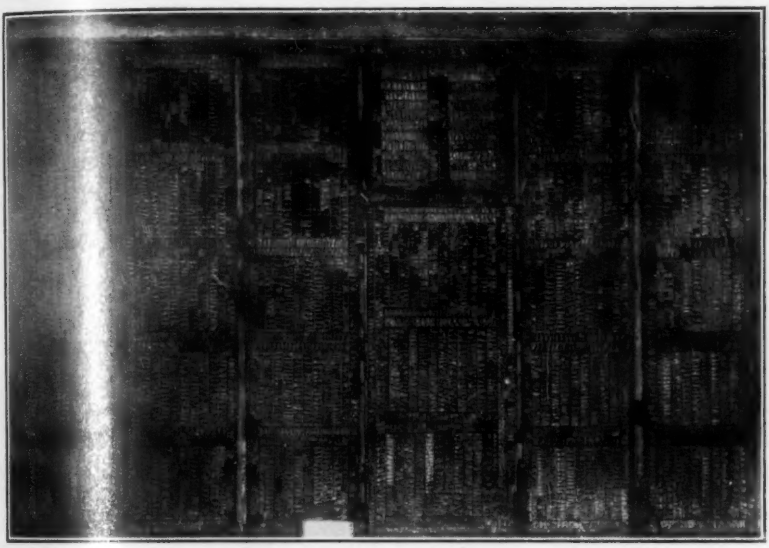

FIGURE 8.—*Exposed side of panel D after fire exposure and hose-stream application*

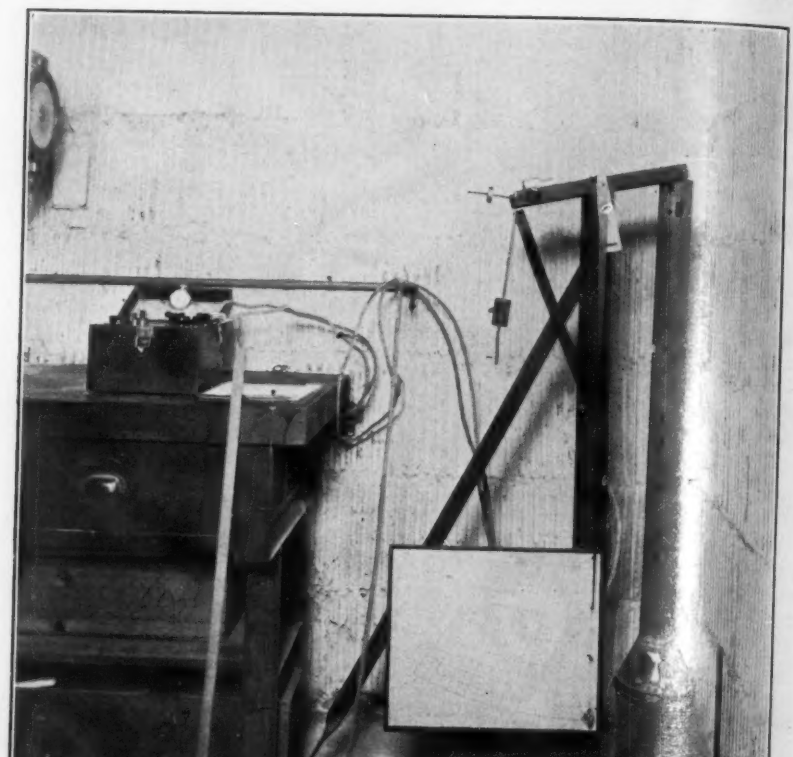

FIGURE 10.—*Fire-tube apparatus.*

large and small panels. Considering also the relatively small deflections of the large panels, it appears that size of specimen in the range included does not greatly affect the fire endurance of wood partitions of the given type of construction. This point might be definitely decided by tests of panels of identical materials and construction.

The standard fire-test specification [4] states that assemblies which burn freely during fire exposure or continue flaming after the furnace is shut off shall be termed "combustible." Of the 13 small panels tested, the untreated and moderately treated panels can be said to have burned freely, at least at times, during fire exposure. While some flaming was observed during the fire tests of panels 8, 9, 11, and 12, it was not the active flaming characteristic of untreated wood and therefore these might be classed as not "burning freely." The large partitions behaved similarly to the latter during fire exposure. All partitions, however, continued flaming after fire exposure, although in varying extent, depending upon concentration of treatment. In view of the latter fact, it appears that all of the 17 panels tested would be classed as "combustible" under the standard fire-test specification.

The standard fire-endurance test [4] used in the present work is based on the application of temperatures on one side of the partition which increase with time according to a prescribed schedule. In the case of a partition made up entirely of incombustible materials, all of the heat required to maintain these temperatures is necessarily supplied by the gas or other fuel used in the furnace. In the case of partitions built wholly or in part of combustible materials, however, some heat is supplied by the combustion of these materials. Consequently, in maintaining the same exposure temperatures, the amount of furnace fuel is reduced to compensate for this amount of heat supplied to the furnace by the burning of the partition itself. It is to be noted that, insofar as the latter forms a significant portion of the total exposure, the tests of partly or wholly combustible partitions differ from the tests of entirely incombustible partitions. Also under this test procedure the exposure given the combustible type of partition is less severe relative to that given the incombustible partition than it would be if the test required a definite amount of furnace fuel to be burned in a given time rather than the maintenance of a certain time-temperature relationship.

In the present tests, failure of both treated and untreated wood partitions was obtained in approximately equal periods of time, but probably with the supply of greater amounts of gas fuel in the tests of the treated wood partitions. Again, the amount of fuel used in a number of comparable tests of incombustible partition constructions was definitely greater than in the tests of treated wood partitions in the present series. In evaluating the performance to be expected from partitions such as these in an actual fire, the relative amounts of fuel supplied to maintain the same temperature rise within the furnace may be significant.

Whether or not these considerations are of importance in the present tests, attention is called to them as a precaution in the application of the results of fire-endurance tests of combustible or partly combustible partitions. In the design of buildings, the fire-resistance ratings of the different members are determined by the expected severity of fires that can occur in the given location. Hence, in

estimating such fire severities, account should be taken of any combustible content of the partition selected as a barrier to fire, as well as the amount of combustibles within the building, such as furniture and other contents, and in other building members.

III. SUPPLEMENTARY TESTS AND RESULTS

1. SPECIMENS

For each of the small panels tested, three specimens for the flame-penetration test and five or six specimens for the fire-tube test were prepared from the material remaining after construction of the panel. Several fire-tube specimens representative of the treated birch used in the large panels were also obtained at the time of construction of the latter. The specimens for the flame-penetration test were about 10 in. square and of the same thickness and type of construction as the corresponding panel, being made from the ends of boards and splines cut off during the construction of the latter. The specimens for panels 11, 12, and 13 were made at the plant where the panels were constructed.

In the case of the small panels, the fire-tube specimens were ⅜ by ¾ in. and from 42 to 48 in. in length and were cut from unused boards, spline material, pieces ripped from end boards, rails, etc., of the material selected for the particular panel. For the large panels, some of the fire-tube specimens were selected at random by the manufacturer from his supply of treated birch and others were selected from boards to be used in the construction of certain parts of panel *D*.

TABLE 2.—*Descriptive data for supplementary test specimens*

Panel number	Fire-tube specimens						Flame-penetration specimens					
	Number	Moisture as tested	Apparent density	Concentration of treatment			Number	Thickness	Moisture as tested	Apparent density	Concentration of treatment	
				Minimum	Maximum	Average					Minimum	Maximum	Average
		Percent	g/cm³	*Percent*	*Percent*	*Percent*		*In.*	*Percent*	g/cm³	*Percent*	*Percent*	*Percent*
1	3	6.6	0.63	------	------	8.2	3	¾	8.8	0.60	8.1	8.3	8.2
2	6	7.0	.56	7.6	8.8	8.4	3	1 13/16	9.1	.57	7.6	8.9	8.2
3	6	6.1	.58	7.6	8.6	8.0	3	2¼	8.6	.58	7.6	9.0	8.2
4	6	6.9	.62	6.8	7.6	7.0	3	1½	8.3	.61	6.6	7.3	7.0
5	6	9.9	.61	4.1	9.4	8.4	3	2¼	9.7	.59	4.1	11.0	8.5
6	3	8.6	.60	------	------	0	3	1 15/16	9.4	.59	------	------	0
7	3	7.8	.60	------	------	0	3	¾	8.1	.61	------	------	0
8	6	7.4	.69	13.6	18.9	15.8	3	1 13/16	8.2	.63	14.3	17.6	15.8
9	6	7.4	.68	14.5	18.3	16.0	3	1½	8.4	.66	14.1	18.3	16.2
10	6	8.6	.62	------	------	0	3	1 15/16	9.6	.57	------	------	0
11	5	9.3	.62	15.0	17.6	16.2	3	2 1/16	8.7	.64	------	------	17.0
12	5	8.9	.64	14.9	15.6	15.2	3	2 1/16	10.2	.66	------	------	17.2
13	5	10.3	.66	------	------	0	3	2⅛	11.4	.58	------	------	0
A	------	------	------	------	------	------	------	No specimens.			------	------	------
B	------	------	------	------	------	------	------	Do.			------	------	------
C	3	------	.78	------	------	------	------	Do.			------	------	------
D	7	10.3	.64	------	------	------	------	Do.			------	------	------

Moisture samples representative of the respective panels were selected from unused material at the time of construction of the small panels. These also served as moisture samples for the corresponding flame-penetration specimens. For the fire-tube specimens the mois-

ture samples were taken from the pieces cut off the ends of the sticks when cutting to length at the time of test. These were weighed immediately, dried at 105° C for 24 hr, and then reweighed. All specimens and samples were stored with the panels so as to be subjected to the same atmospheric conditions, and the material had been stored in buildings long enough to have reached moisture equilibrium. The principal descriptive data for the supplementary specimens are given in table 2.

2. FIRE-TUBE TESTS

The fire tube, developed by the Forest Products Laboratory, U. S. Department of Agriculture, consists of a sheet-metal tube about 50 in. long, which is suspended from one arm of a balance beam (fig. 10). The lower end of the tube is enlarged and has screened sides and a solid bottom. Adjustable weights are placed on the other end of the beam to counterbalance the weight of the tube and specimen before test. A pointer attached to the center of the beam indicates the loss in weight on an adjustable scale during the test. Temperatures are measured at the top of the tube by means of a 14-gage chromel-alumel thermocouple. A slot in the lower end of the tube permits the insertion of a low form of bunsen burner. The flame of this burner with its tall indistinct inner cone is adjusted to give a temperature of 180° C at the top of the tube.

In conducting a test, the beam weights and scale are adjusted so that the pointer indicates 0-percent loss with the specimen in place and 100-percent loss when the tube is empty. After a preliminary heating of the tube, the specimen, ⅜ by ¾ by 40 in., previously conditioned and weighed, is suspended centrally in the tube. The bunsen burner is then inserted about 1 in. below the lower end of the specimen and readings of temperature and loss in weight are taken at frequent intervals. The burner is removed at the end of 4 min and the readings are continued until 2 min after all flaming has ceased. Subsequently, the temperature and weight-loss data are plotted against time, from which derived results, such as the area under the time-temperature curve, are obtained.

TABLE 3.—*Average results of fire-tube tests*

Specimens for panel	Treatment	Temperature		Duration of flaming[1]	Total weight loss			Maximum rate of weight loss		
		Max	Area under temperature curve		Percentage		Actual			
					Range	Avg	Avg	Min	Max	Avg
	Percent	° C	° C–min	min	*Percent*	*Percent*	g	g/min	g/min	g/min
1	8.2	708	1,055	4.3	49 to 65	59	68.6	24.7	28.5	26.7
2	8.4	387	465	4.2	27 to 67	44	45.2	8.9	26.6	16.1
3	8.0	390	335	4.4	24 to 62	40	42.7	9.0	20.3	14.0
4	7.0	460	594	4.3	28 to 69	49	56.2	9.8	28.7	19.4
5	8.4	306	292	4.3	29 to 69	38	42.8	9.9	20.7	13.2
6	0	724	1,816	5.1		83	91.5	28.3	30.5	29.4
7	0	743	1,630	4.9		83	91.4	31.0	32.9	31.9
8	15.8	183	(2)	4.0	14 to 28	19	23.4	5.3	11.1	7.5
9	16.0	174	(2)	4.0	14 to 23	18	22.8	5.4	9.7	7.2
10	0	731	1,697	4.9	82 to 84	83	95.4	27.4	35.5	31.8
11	16.2	179	(2)	4.0	14 to 23	19	22.0	4.7	8.4	7.0
12	15.2	180	(2)	4.0	13 to 28	18	21.8	4.7	10.6	7.0
13	0	707	1,888	5.5	82 to 85	84	105.1	29.7	36.8	32.6
C		163		4.0	11 to 18	14	20.6	4.4	8.4	6.2
D		192	13	4.0	21 to 33	26	30.4	7.9	15.5	10.6

[1] Includes time of burner application.

[2] Some specimens exceeded 180° C, but not all.

The results of the fire-tube tests are given in table 3. Average, minimum, and maximum values are given for the total weight loss in grams and the maximum rate of weight loss in grams per minute, while only averages are given for other figures although similar variations were also obtained in the latter results. The "maximum temperature" is the average of maximums recorded in individual tests and the area under the temperature curve, measured above the 180° Cline, is given in "° C-min" units. The actual weight loss was calculated from the original weight of the specimen and the loss in weight (in percent) indicated by the pointer at the end of the test. The maximum rate of weight loss was calculated on the basis of the greatest loss in weight for a single minute occurring during the test.

Because of the nature of the specimen used, the concentration of treatment is the only factor studied in the fire-endurance tests which could possibly affect the results of the fire-tube tests. The relations between some of the results obtained in the fire-tube test, and the concentration of treatment for the specimens tested, are given in figure 11. The data for panel 1 have been omitted from figure 11 since they represented specimens from only a single board. The dashed portions of the curves have been drawn to correspond in general shape to that established by other tests [1, 3] since the present data are insufficient in the region of low concentration of salt. Similar relations hold between the concentration of treatment and other results obtained in the fire-tube tests, thus showing the distinct effect of treatment, particularly above 8 percent. The results are more consistent at higher concentrations, and it is significant that none of the specimens in the latter class continued flaming after burner removal.

3. FLAME-PENETRATION TESTS

In the flame-penetration test the specimen is supported in a horizontal position so that its center is 3 in. above the tip of a ⅜-in. tirrill burner. For the specimens representative of panels 1 to 7, inclusive, the rate of gas flow was adjusted so that the burner was producing about 2,800 Btu/hr, and for the remaining tests this rate was increased to 3,000 Btu/hr, but the difference is not considered significant as far as the results are concerned. Having adjusted the gas flow, the burner flame was adjusted by starting with a tall inner cone and increasing the air supply until the inner cone has just reached a minimum. With the gas used in this laboratory, a flame having an outer cone of about 7 in. and an inner cone of nearly 2 in. is obtained by the above procedure. A thermocouple is located at the center of the top surface of the specimen and temperature readings are taken at frequent intervals. Other data taken include time for light to come through any crack, time of flame penetration, time of ignition on the top surface, duration of flaming, and loss in weight. If ignition does not occur within 5 min after flame penetration, the burner is then removed.

The average results of these tests are given in table 4. The rate of weight loss is found by dividing the total loss in weight by the sum of the time of burner application, plus the duration of flaming after burner removal. In order to place the weight-loss results on a comparable basis, the loss in weight in percent has been calculated for a specimen 10 in. square having the same loss in grams as the actual

specimen. The resulting figure is termed the nominal loss and is thus corrected for departures in dimensions from the nominal size of 10 in. square.

The flame-penetration specimens were varied in the same respects as the panels, that is, in thickness, concentration of treatment, and

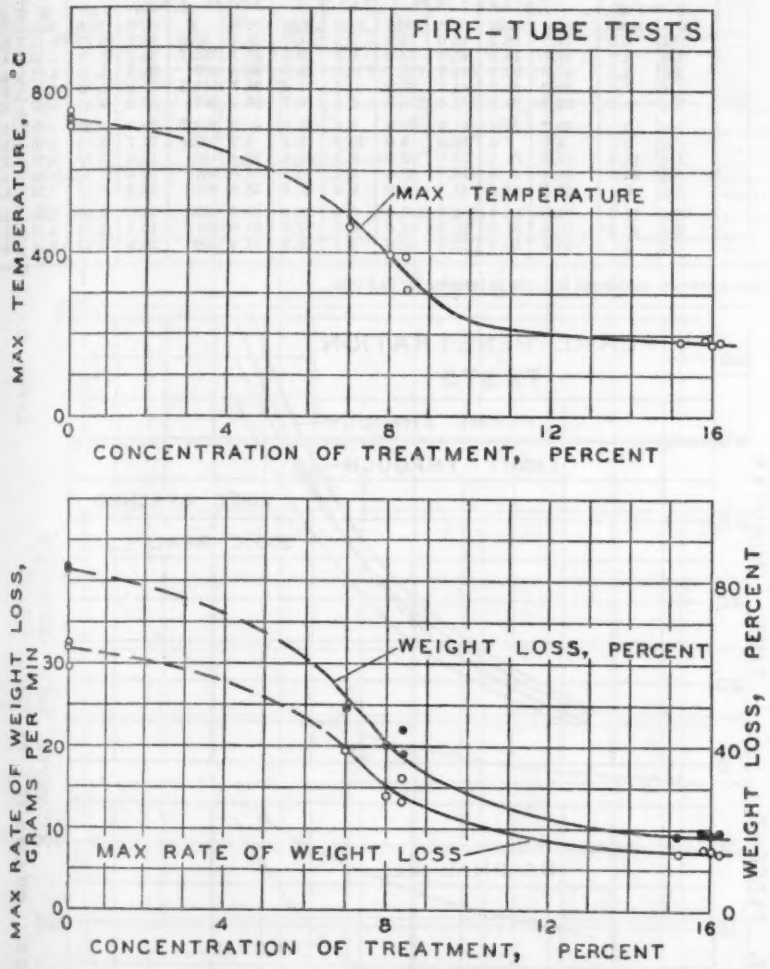

FIGURE 11.—*Influence of concentration of treatment on maximum temperature, weight loss, and maximum rate of weight loss, in fire-tube tests.*
Data from tests of panel 1 have been omitted.

type of construction. Referring to figure 12, it is seen that all of the results based on time (upper half) and the loss in weight figures (lower half) increase rapidly as thickness of the specimen increases, for panels 1, 2, and 5, which are comparable in amount of treatment and construction. Apparently, however, the rate of weight loss of these built-up specimens is affected very little, if at all, by thickness (see table 4). The time to flame penetration (see fig. 13), and other time data as well, do not appear to be greater for moderately treated

TABLE 4.—*Average results of flame-penetration tests*

Specimens for panel	Thickness	Treatment	Time of light through specimen	Time of flame penetration or ignition			Duration of flaming	Time to reach		Loss in weight		Rate of weight loss		
				Min	Max	Avg		100° C	200° C	Actual	Nominal	Min	Max	Avg
	in.	*Percent*	min	min	min	min	min	min	min	g	*Percent*	g/min	g/min	g/min
1	¼	8.2	12.7	16.2	18.0	17.2	0.3	11.0	15.1	86.0	11.8	3.58	4.15	3.83
2	1½	8.2	35.0	34.2	47.5	40.6	0.3	29.8	37.1	195.7	13.7	3.40	6.29	4.39
3	2¼	8.2	95.6	95.5	142.7	113.7	[1] 12.5	76.8	98.5	469	21.8	3.10	3.82	3.52
4	1½	7.0	36.2	33.7	48.2	41.8	0.5	31.5	38.7	162.3	10.9	3.12	4.24	3.64
5	2¼	8.5	92.2	92.7	115.3	101.2	5.1	75.7	86.1	371	17.2	3.11	3.62	3.33
6	1¼	0	40.7	29.0	51.9	42.8	8.0	33.8	40.2	293.3	20.5	5.22	7.31	5.98
7	¾	0	8.0	7.9	10.0	9.0	10.5	7.2	8.7	109.6	14.7	5.58	5.70	5.62
8	1½	15.8	56.2	50.5	79.0	62.3	0.8	43.8	55.4	195	12.6	2.63	3.13	2.90
9	1½	16.2	56.4	51.6	75.4	63.5	1.2	44.7	57.6	201	12.4	2.58	3.26	2.92
10	1¾	0	36.3	34.5	47.1	38.9	9.5	27.5	33.8	341	24.3	6.37	7.54	6.98
11	2⅛	17.0	93.6	95.6	109.1	100.6	0.4	77.2	89.0	310	14.0	2.88	2.99	2.92
12	2⅛	17.2	90.4	87.6	99.3	95.0	0.7	77.6	86.9	361	15.8	2.93	4.15	3.61
13	2⅛	0	55.6	50.4	75.5	60.6	6.1	48.4	55.0	422	20.9	5.02	8.54	6.48

[1] One specimen continued flaming in interior for 34.8 min.

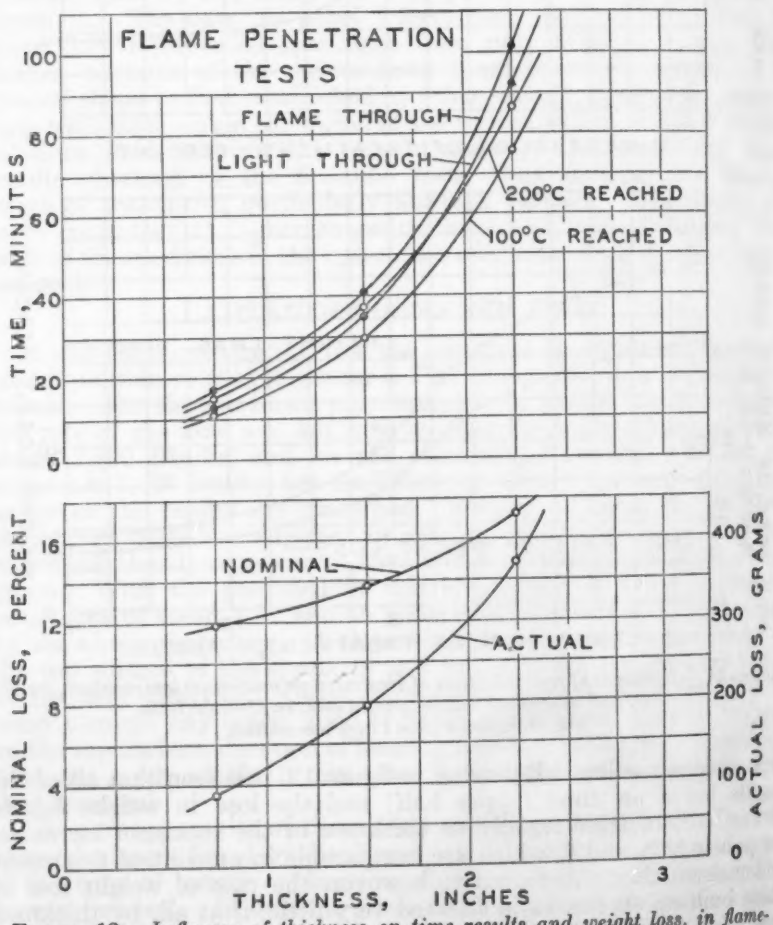

FIGURE 12.—*Influence of thickness on time results and weight loss, in flame-penetration tests.*

Data from tests of panels 1, 2, and 5.

specimens than for untreated specimens, but are much greater for the well-treated specimens. On the other hand, the rate of weight loss decreased more rapidly with increasing amount of treatment in the range of low concentration than in the range of high concentration,

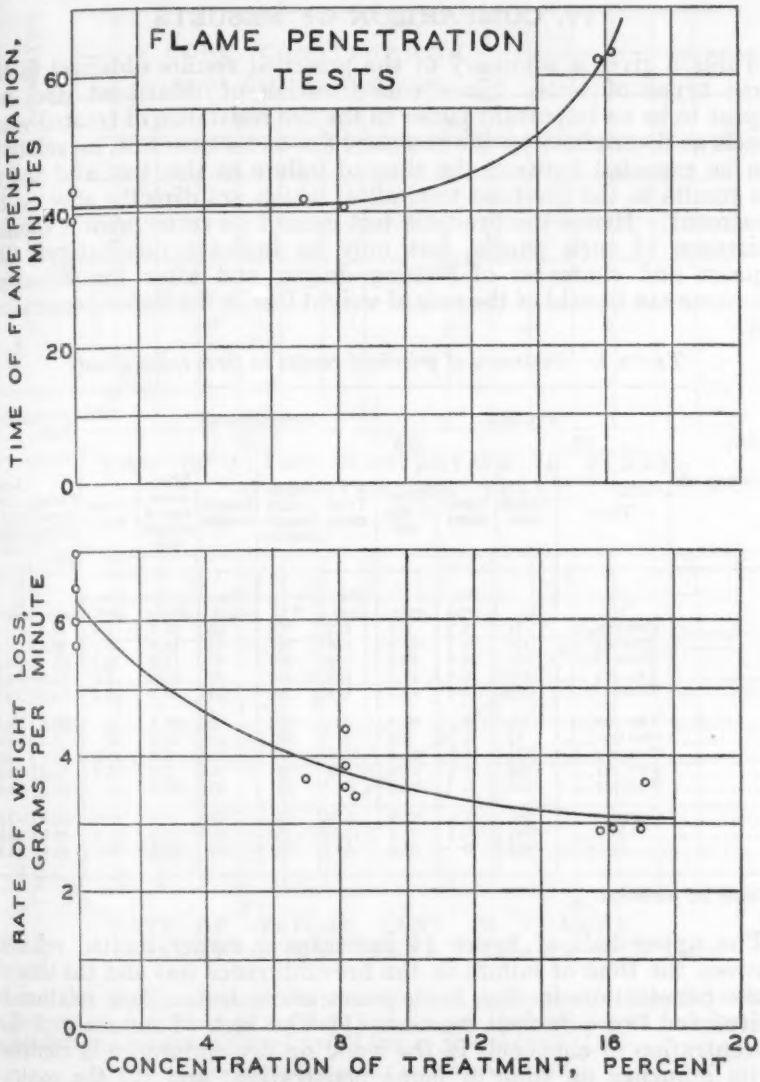

FIGURE 13.—*Influence of concentration of treatment on time of flame penetration and rate of weight loss, in flame-penetration tests.*

Data in upper half from tests of panels 2, 4, 6, 8, 9, and 10. Data in lower half from tests of all panels.

as seen in the lower half of figure 13. Regarding the effect of type of construction, the specimens for panels 11 and 12 did not show the increased resistance to flame penetration over those for panels 3 and 5, to be expected from the increased concentration of treatment and type of construction, although the average weight-loss results

were lower. This might be attributable to the fact that there was always a joint in the core at the center of the specimens for panels 11 and 12, and hence directly over the burner flame, while such was seldom the case for the 2¼-in., three-ply specimens.

IV. COMPARISON OF RESULTS

Table 5 gives a summary of the principal results obtained in the three types of tests. Since concentration of treatment does not appear to be an important factor in the fire resistance of treated-wood panels as determined by the standard fire-endurance test, no relations can be expected between the time of failure in this test and any of the results in the fire-tube test, all of which are directly affected by treatment. Hence the fire-tube test cannot serve to predict the fire resistance of such panels, but only to indicate qualitatively the amount and character of flaming during and after fire exposure. The same can be said of the rate of weight loss in the flame-penetration test.

TABLE 5.—*Summary of principal results in three types of tests*

Panel number	Fire tests				Fire-tube tests				Flame-penetration tests		
	Type	Thickness	Treatment	Time to failure	Treatment	Maximum temperature	Loss in weight	Maximum rate of weight loss	Treatment	Flame penetration	Average rate of weight loss
		in.	*Percent*	min	*Percent*	°C	*Percent*	g/min	*Percent*	min	g/min
1	One ply	¾	8.2	9.4	8.2	708	59	26.7	8.2	17.2	3.83
2	Two ply	1½	8.2	28.3	8.4	387	44	16.1	8.2	40.6	4.39
3	Three ply [1]	2¼	8.3	40.5	8.0	390	40	14.0	8.2	113.7	3.52
4	Two ply	1½	6.9	30.5	7.0	460	49	19.4	7.0	41.8	3.64
5	Three ply	2¼	8.6	45.3	8.4	306	38	13.2	8.5	101.2	3.38
6	Two ply	1½	0	29.4	0	724	83	29.4	0	42.8	5.98
7	One ply	¾	0	8.9	0	743	83	31.9	0	9.0	5.62
8	Two ply	1½	15.9	31.5	15.8	183	19	7.5	15.8	62.3	2.90
9	Two ply	1½	15.9	34.5	16.0	174	18	7.2	16.2	63.5	2.92
10	Two ply	1½	0	32.3	0	731	83	31.8	0	38.9	6.08
11	Core	2⅛	17.0	62.9	16.2	179	19	7.0	17.0	100.6	2.92
12	do	2⅛	17.2	72.1	15.2	180	18	7.0	17.2	95.0	3.61
13	do	2⅛	0	67.0	0	707	84	32.6	0	60.6	6.48

[1] Center ply horizontal.

The upper half of figure 14 indicates a rather limited relation between the time of failure in the fire-endurance test and the time of flame penetration in the flame-penetration test. This relation is limited for two principal reasons: (1) The lack of influence of the concentration of chemicals in the wood on fire endurance in contrast to its influence on time of flame penetration; and (2) the contradictory influence of the type of construction on these two results. In comparing these two types of test, certain differences in the nature of the exposure should be noted. In the fire-endurance test, practically the entire surface of one side of a very large specimen is exposed to furnace temperatures. The fuel supplied to the furnace is constantly adjusted so that the furnace temperatures follow a definite curve. The exposure is severe, and any part of the structure having poor fire resistance can hardly escape the test and is most likely to be the

place of failure. On the other hand, only a small portion of a small sample is subjected to the direct flame of a burner in the flame-penetration test. The fuel is supplied at a constant rate, but the exposure temperature is influenced by the combustibility of the

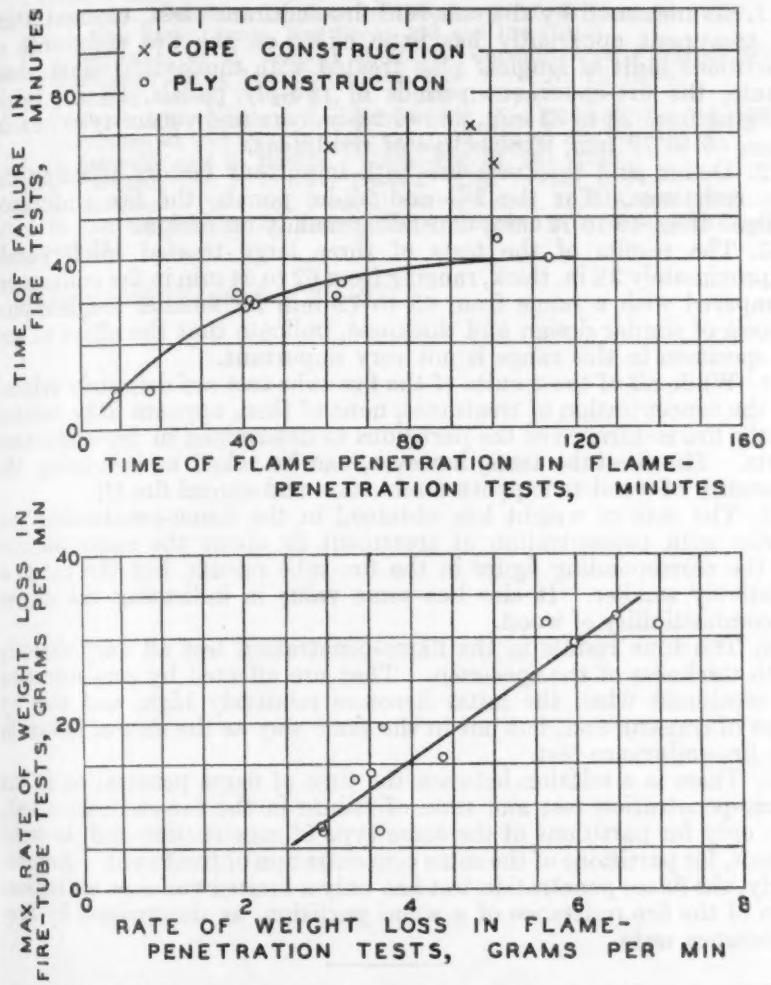

FIGURE 14.—*Relations between (a) time of flame penetration in flame-penetration tests and time of failure in fire tests, and (b) rate of weight loss in flame-penetration tests and maximum rate of weight loss in fire-tube tests.*

Data from tests of panel 1 omitted in lower half.

material being tested. The exposure is not as severe as in the fire test, and even with the use of several samples, the poorest parts of the structure, such as joints, may not be tested. These differences in the two tests may explain the differences in the results.

Finally, there is apparently a general relation between the maximum rate of weight loss obtained in the fire-tube test and the average rate of loss obtained in the flame-penetration test, as shown in the lower half of figure 14.

V. SUMMARY AND CONCLUSIONS

The principal conclusions to be drawn from the fire tests of partitions, the flame-penetration, and the fire-tube tests on representative specimens of the same materials are:

1. As measured by the standard fire-endurance test, concentration of treatment apparently has little effect on the fire endurance of partitions built of longleaf pine treated with monoammonium phosphate, the fire-endurance periods of two-ply panels, 1½ in. thick, ranging from 28 to 35 min, and of 2⅛-in. core and veneer-type panels, from 63 to 72 min, irrespective of treatment.

2. Design and thickness are both important factors affecting the fire resistance. For the 2⅛- and 2¼-in. panels, the fire endurance ranged from 40 to 72 min, depending mainly on design.

3. The results of the tests of three large treated birch panels approximately 2⅛ in. thick, ranging from 62 to 64 min in fire endurance, compared with a range from 63 to 72 min for smaller longleaf-pine panels of similar design and thickness, indicate that the effect of size of specimen in this range is not very important.

4. While all of the results of the fire-tube test are definitely related to the concentration of treatment, none of them appears to be related to the fire endurance of the partitions as determined in fire-endurance tests. The fire-tube tests, however, can be taken as indicating the tendency of wood to support combustion and spread fire [3].

5. The rate of weight loss obtained in the flame-penetration test varies with concentration of treatment in about the same manner as the corresponding figure in the fire-tube results, but the range is relatively smaller. It also has some value in indicating the degree of combustibility of wood.

6. The time results in the flame-penetration test all vary directly with thickness of the specimen. They are affected by concentration of treatment when the latter becomes relatively high, and also by type of construction, but not in the same way as the time of failure in the fire-endurance test.

7. There is a relation between the time of flame penetration in the flame-penetration test and time of failure in the fire-endurance test, but only for partitions of the same type of construction and, to some extent, for partitions of the same concentration of treatment. Accordingly, the flame-penetration test has only a limited value as an indication of the fire resistance of a wood partition, as determined by fire-endurance tests.

The author's acknowledgements are made to S. H. Ingberg for advice in the planning of the tests, and to N. D. Mitchell, F. M. Hoffheins, A. C. Hutton, and C. R. Beahm for aid in conducting the fire tests.

VI. REFERENCES

[1] T. R. Truax and C. A. Harrison. Proc. Am. Soc. Testing Materials **29**, pt. II, 973 (1929).

T. R. Truax and C. A. Harrison. Trans. Am. Soc. Mech. Engrs. **52**½(No. 17) 33 (May-Aug. 1930).

G. M. Hunt, T. R. Truax, and C. A. Harrison. Proc. Am. Wood Preservers' Assn. **26**, 130, 159 (1930).

T. R. Truax., Proc. Nat. Fire Protection Assn. **35**, 189 (1931); Safety Eng. **62**, 179 (1931).

[2] E. F. Hartman, A. S. Williams, and R. C. Bastress. Proc. Am. Soc. Testing Materials **34**, pt. II, 754 (1934).
[3] C. R. Brown. Proc. Am. Soc. Testing Materials **35**, pt. II, 674 (1935).
[4] *Standard specifications for fire tests of building construction and materials (C19–33)*, Am. Soc. Testing Materials Book of Standards, pt. II, 254 (1933). ASA Standard A–2–1934.
[5] Anonymous. Southern Lumberman **136** (No. 1762) 63 (Aug. 15, 1929).
British Fire Prev. Comm. Red Books 193 and 194 (1914).
H. Riegelmann, et al. Report of Special Committee on Fireproof Wood (Multiple Dwelling Law Committee, New York, N. Y., 1930).
A. T. North. Arch. Forum **54**, pt. 2, 247 (1931).
F. P. Cartwright, Southern Lumberman **142** (No. 1795) 39 (Jan. 15, 1931); Timberman **32** (No. 3), 116 (Jan. 1931); **32** (No. 4) 32 (Feb. 1931).
C. G. Schwalbe and K. Berling. Chem.-Ztg. **57**, 881 (1933).
E. F. Hartman. N. Y. Lumber Trade J. Dec. 1, 1933, p. 14.
E. F. Hartman. Proc. Am. Wood-Preservers' Assn. **31**, 218, 225 (1935).
[6] S. H. Ingberg and H. D. Foster. BS J. Research **2**, 1 (1929) RP37. (See page 33).

WASHINGTON, November 29, 1937.

38682—38——10

U. S. DEPARTMENT OF COMMERCE NATIONAL BUREAU OF STANDARDS

RESEARCH PAPER RP1077

Part of Journal of Research of the National Bureau of Standards, Volume 20, February 1938

EVALUATION OF CREASE-RESISTANT FINISHES FOR FABRICS

By Herbert F. Schiefer

ABSTRACT

Certain flexural characteristics of representative woven fabrics before and after the application of commercial crease-resistant finishes were measured using three different methods, namely, the creasing angle, flexometer, and modified compressometer methods. Specimens of paper, Cellophane, cotton, rayon, worsted, and rubber, which are recognized to vary in resistance to creasing over a great range, were also measured by the three methods and the results used for comparison.

The crease-resistant finishing treatments increased the energy required to deform the cloth specimens, that is, increased the stiffness of the cloths. This increase exceeded 100 percent for some of the cloths. The energy of recovery was also increased by these treatments, the increase ranging from 20 to 100 percent. Neither of these two quantities can be taken individually as a measure of crease resistance. However, the ratio of the latter to the former, here termed "resilience," is related to the resistance to creasing. The resilience of nearly all of the cloths, as determined by each of the three test methods, was increased by the crease-resistant finishing treatments.

The three test methods described can be used to evaluate the improvement given by crease-resistant finishes, using the measurements on the cloths before treatment as the basis of comparison. The methods should be valuable in systematic studies of the effect of different finishing treatments and in determining the effects of relative humidity, temperature, and other factors on the different finishes. Method 1, however, does not give a critical measure of stiffness, a property that is greatly affected by crease-resistant finishes and should be measured. The resilience as determined by these methods is dependent upon the testing conditions, as for example, the magnitude of the maximum load in method 3. It may be found necessary in test methods of this type to vary the maximum load with the thickness or weight of the fabric to be tested.

CONTENTS

	Page
I. Introduction	241
II. Materials and test methods	242
1. Samples	242
2. Creasing-angle method	242
3. Flexometer method	243
4. Compressometer method	244
III. Results and discussion	245

I. INTRODUCTION

Most textiles fibers are deficient in natural resilience. Articles made from them tend to become wrinkled and to lose their shape and desired appearance. It has been found possible in recent years to im-

prove the resilience of textiles by chemical processing, and crease-resistant fabrics are now available. The "anticrease" process of Tootal, Broadhurst, Lee, Ltd., which is being applied in the United States as well as in England, was the first to attract attention. In it the fabric is impregnated with a synthetic resin. This development in the industry has led to a need for a quantitative method for evaluating the improvement of the product and of the resilience of fabrics in general. The work reported in this paper was undertaken to determine the flexural characteristics of woven fabrics before and after the application of commercial crease-resistant finishes. The results are compared with the flexural characteristics of a series of samples which have not had crease-resistant treatments, but which are recognized to vary in resistance to creasing over a considerable range.

The flexural characteristics of the samples were measured by three different methods. The results are presented and discussed in this paper.

II. MATERIALS AND TEST METHODS

1. SAMPLES

Representative woven fabrics ranging from light-weight voile to heavy suiting cloth, before and after the application of crease-resistant finishing treatments, were furnished for the work by several manufacturers. These fabrics were made from cotton, rayon, and linen. Specimens of paper, Cellophane, cotton, rayon, worsted, and rubber, having crease resistances varying over a great range, were added to the list of samples for comparison. Specimens of the materials were conditioned by exposure for several days in an atmosphere of 65-percent relative humidity and a temperature of 70° F, and they were tested under these conditions.

2. CREASING-ANGLE METHOD

The specimens tested were 2 inches long and ½ inch wide with the long dimension in the warp or in the filling for tests in these respective directions. Each specimen was folded by bringing the two ends into coincidence, thereby forming a loop at the middle. The two ends were held together with a pair of tweezers and the loop of the specimen was inserted between two parallel plates and placed under a load of 1.00 pound. The load was removed at the end of 3 minutes, and the specimen was picked up with the tweezers and suspended freely at the middle over a horizontal wire of small diameter, approximately 1 mm. At the end of 3 minutes the horizontal distance between the two ends was measured and the angle at the vertex, where the specimen was folded, was calculated. An angular scale, graduated in degrees, placed directly back of the test specimen, is a convenience in reading the angle directly. A device of this kind, developed by Barnard, is shown in figure 1. Eight specimens can be suspended on it at a time. The disk on which the specimens are suspended can be rotated by means of a crank to bring any one of the eight specimens into position for measurement, that is, to align one edge of the specimen with the zero-angle line and the other edge to indicate the magnitude of the creasing angle.

In this test method the ends of the specimens droop an amount which depends not only upon the magnitude of the load and the time it is applied to the fold, but also upon the weight, thickness, and type

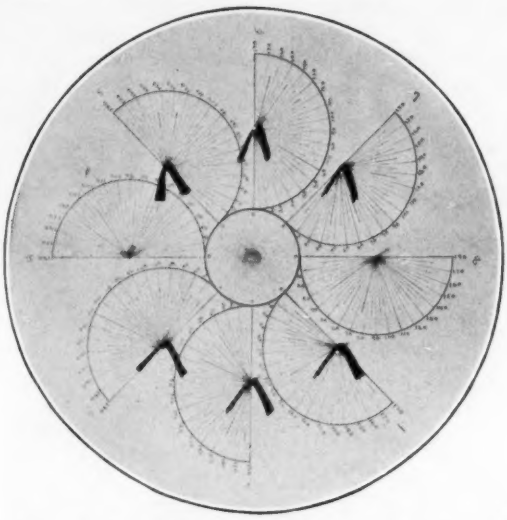

FIGURE 1.—*Multiple protractor for measuring the creasing angle.*

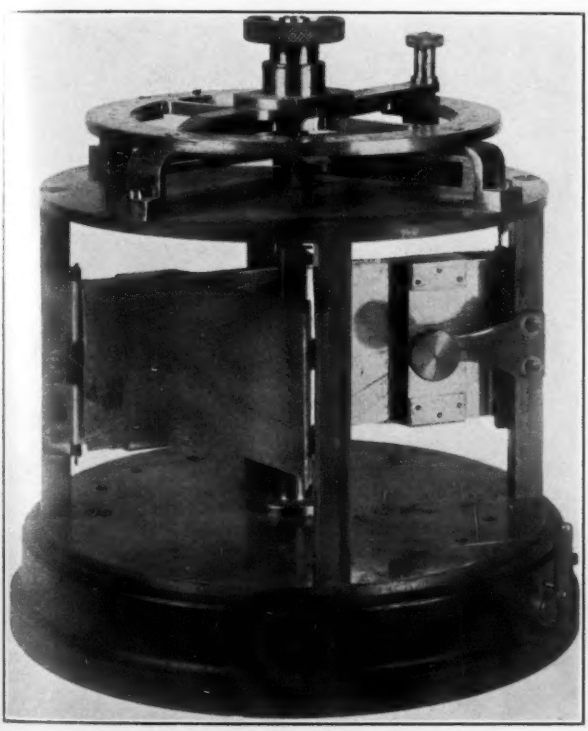

FIGURE 2.—*Flexometer.*

UNIV. OF MICH.

of construction of the cloth. The angular deflections of the ends of the various specimens tested vary over a great range because of these inherent differences between the cloths. For example, the ends of a specimen of a thin sheet of rubber which shows no crease after the application of the load, droop more, even before the load is applied to the specimen, than the ends of a specimen of an easily creased cotton fabric after the application of the load to the fold. To take account of this natural drooping of the ends of each specimen, the angular deflection was determined both before and after the application of the load to the fold. The ratio of the angle at the vertex of a specimen after the load is applied to the fold to the angle before the application of the load is here designated the "resilience ratio."

Various modifications [1] of this method for measuring the effect of crease-resistant treatments have been reported in the literature. In one arrangement the specimen is folded as already described and then compressed by a dead weight for several minutes, after which the specimen is placed on edge, with the fold in a vertical position, on the surface of mercury. The angle of the fold is measured after a specified period. The result by this method is influenced by the condition of the mercury surface. Also, it is not possible to determine the effect of the treatment on the stiffness of the cloth. Since the stiffness is greatly affected by the treatments and should be evaluated, the procedure of floating the creased specimen on mercury was not used in this investigation.

3. FLEXOMETER METHOD

Two specimens, each 4 inches long and 1¾ inches wide with the long dimension in the warp or in the filling for tests in these respective directions, were mounted in opposite angles formed by the two intersecting vertical plates of the flexometer [2] shown in figure 2. One of these plates is cut along the intersecting axis and each half is fastened to the frame of the instrument. The other plate is attached to a spindle and can be rotated freely about the axis of intersection of the two plates. The top of the spindle carries six calibrated cantilever springs mounted radially 60 degrees apart. A hub having six spokes, which can be rotated by means of a knob, is located above the six springs. By placing a pin in a spoke and rotating the hub the spring located directly below the spoke is deflected. The deflection of the spring exerts a torque on the spindle and causes the plate to rotate. The magnitude of this torque is equal to the torque exerted by the pair of test specimens as they resist being folded between the two plates. The magnitude of the applied torque is ascertained from the deflection of the calibrated cantilever spring. Readings were taken at definite angles between the plates, first for decreasing and then for increasing angles, according to the procedure described in Bureau Research Paper RP555. Successive readings were taken as rapidly as possible, the time required for one reading being about 15 seconds. The energy expended in folding the specimens through a given angle is equal to the product of the average torque and the

[1] C. Amick. *Crease-resisting fabrics*, Am. Dyestuff Reptr. **24**, 554–557, 662–664, 645–648, and 665 (1935).
W. Matthaes. *Lilienfeld rayon: Crease resistance*, Kunstseide **18**, 292–293 (1936).
Society of Dyers and Colourists, **52**, No. 1, 38; **52**, No. 8, 117 (1936).
Crease-resistant textiles without resins, Silk and Rayon, **11** p. 46 (January 1937).
K. Quehl. *Staple fibre fabrics: Crease-resistance*, Melliand Textilberichte **18**, 241–242 (1937).

[2] Herbert F. Schiefer. *The flexometer, an instrument for evaluating the flexural properties of cloth and similar materials*, BS J. Research **10**, 647–657 (1933) RP555.

change in the angle between the two plates. The total energy expended in folding the specimens to a minimum angle between the plates was determined, as well as the energy recovered when the specimens were allowed to unfold. The minimum angle to be employed was calculated from the thickness of the material using the equation $\beta=430\ h$, where β is the angle in degrees and h is the thickness in inches measured with a gage having a circular foot 1 inch in diameter and exerting a pressure of 1 lb/in^2. The ratio of the energy recovered to the energy expended is here termed the "flexural resilience."

The work recovered after keeping the specimens folded at the minimum angle for 5 minutes, and the work done and recovered in refolding and unfolding the specimens after they were allowed to remain unfolded for 5 minutes were also measured. These data did not contribute to the evaluation of crease resistance and accordingly are not reported here. Apparently, 5 minutes was too short a period of time to allow for readjustments in the specimens.

4. COMPRESSOMETER METHOD

A very sensitive modified compressometer, illustrated in figure 3, was designed and used for measuring the flexural properties of lightweight woven fabrics. The instrument has a circular presser foot, 1 inch in diameter, which is fastened to the top of a helical spring through a ball-and-socket connection. The foot may be lowered or raised by means of a rack and pinion, thereby increasing or decreasing the load which the presser foot exerts upon a specimen placed on an anvil beneath it. This load is indicated by the dial indicator which registers the elongation of the calibrated helical spring. The vertical displacement of the rack is indicated on the scale engraved upon the circumference of a disk which is fastened to the axis of the pinion. The vertical displacement of the foot is equal to the displacement of the rack minus the elongation of the spring. The rack and pinion must be uniform, because any irregularities in them produce nonuniform vertical displacements and necessitate either engraving a nonuniform scale on the disk or applying a correction.

The specimens tested were 3 inches long and 2 inches wide, with the long dimension in the warp or in the filling for tests in these respective directions. Two rows of three holes each were punched in each specimen. The holes were spaced 1 inch apart in the long direction and 1½ inches in the short direction. The specimen was mounted through these holes in an accordion fashion consisting of two loops on a special support, as illustrated in figure 3. An aluminum plate weighing 0.02 pound was placed on this specimen. The support and specimen were placed underneath the presser foot of the compressometer. The height, in inches, of the accordion loops was determined first for increasing loads up to 0.60 pound and then for decreasing loads, readings being taken at 0.05, .10, .15, .20, .30, .40, and .60 pound. Successive readings were taken as rapidly as possible, the time required for one reading being about 10 seconds. The energy, in inch-pounds, expended during loading and that recovered during unloading were calculated, using the expression $0.025\ (3a+2b+2c+3d+4e+6f-20g)$, where a, b, c, d, e, f, and g are the heights of the accordion loops at the above loads, respectively. The ratio of the energy re-

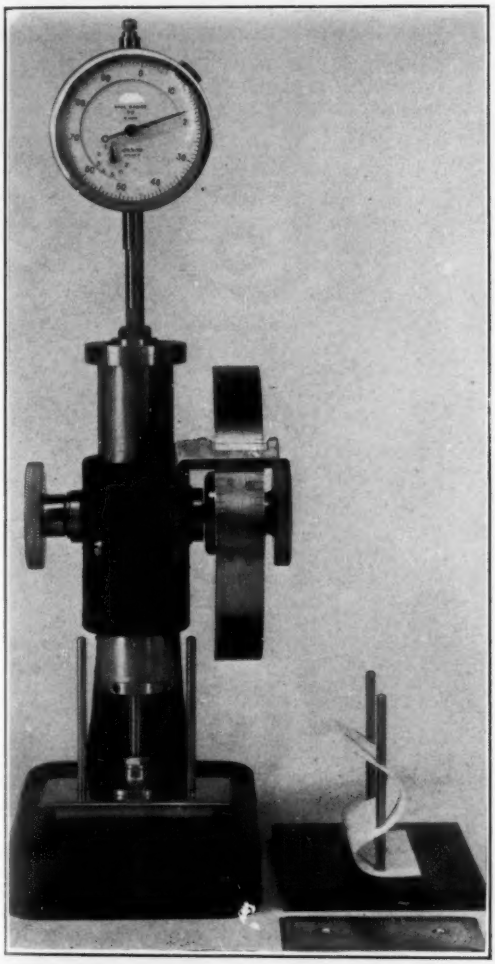

FIGURE 3.—*Modified compressometer.*

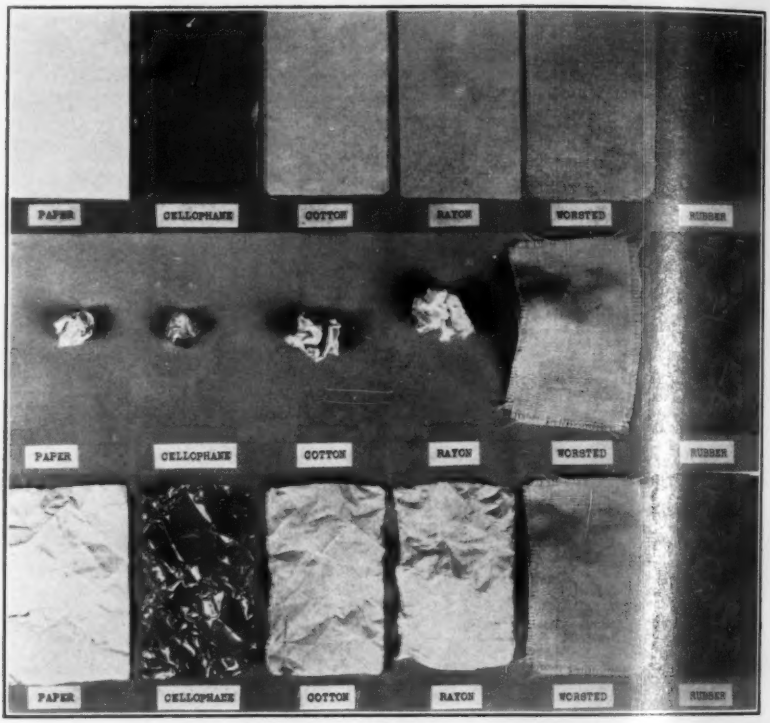

FIGURE 4.—*Specimens having crease resistances varying over a great range.*

Top row. Appearance of specimens before wrinkling.
Middle row. Appearance of specimens after being compressed and crushed into a small ball.
Bottom row. Final appearance of specimens after being straightened out.

covered to the energy expended is here termed the "compressometer flexural resilience."

The data obtained after allowing the specimen to remain compressed for 5 minutes at the maximum load of 0.60 pound and after allowing it to remain uncompressed for 5 minutes did not contribute to the evaluation of crease resistance, agreeing with the flexometer method in this respect. However, the time of application of the load of deformation may be as important as the magnitude of the load. For example, a sample of worsted cloth in which the loops were compressed continuously for 3 months by a load of only 0.02 pound showed more pronounced creases of a more permanent nature, judged by visual appearance, than the creases produced by a load of 0.60 pound acting for only 5 minutes.

A method in which the test specimen is folded in a series of accordion loops and compressed by a dead weight has been used by Sommer.[3] The height of the loops under a small initial load, the height of the loops when compressed by a dead weight, and the final height of the loops after the weight was removed were used in evaluating a fabric. The value obtained decreased nonlinearly with the magnitude of the dead weight used. Specific details regarding this method and the time of application of the dead weight are not given.

III. RESULTS AND DISCUSSION

The results of the tests are given in table 1.

[3] *Textilprüfung auf neuen Wegen.* Abstract of a paper delivered at a meeting of the German Engineering Society, by Prof. H. Sommer, Director, Fibrous Division, National Institute for Testing Material, Berlin, on September 25, 1936.

TABLE 1.—*Effect of crease-resistant finishing treatments on cloths measured by three methods*

[Specimens 12 to 17, inclusive, are a series having crease resistances varying over a great range. *W* and *F* indicate the warp and filling directions, respectively. The units for work in methods 2 and 3 are different, to conform with those previously used for the flexometer and compressometer]

Specimen	Thickness	Designation	Treatment	Direction	Method 1			Method 2			Method 3		
					Angle		Resilience ratio	Work done	Work recovered	"Flexural resilience"	Work done	Work recovered	"Compressometer flexural resilience"
					Before applying the load	After applying the load							
					(1)	(2)	(3)	(1)	(2)	(3)	(1)	(2)	(3)
	Inch				*Degrees*	*Degrees*	*Percent*	*Ergs*	*Ergs*	*Percent*	In.-Lb.	In.-Lb.	*Percent*
1	0.007	Cotton voile	Not treated	*W*	148	39	26	43×10^3	18×10^3	41	34×10^{-4}	9×10^{-4}	26
			do	*F*	128	45	35	39	19	48	33	10	30
			Treated	*W*	152	71	47	59	28	48	51	16	31
			do	*F*	148	85	57	62	36	57	53	18	34
2	.008	Cotton voile	Not treated	*W*	144	63	44	44	22	50	63	26	42
			do	*F*	137	50	36	48	21	44	70	28	40
			Treated	*W*	134	81	60	64	35	55	100	32	32
			do	*F*	129	70	60	58	35	60	91	34	37
3	.009	Cotton-warp and rayon-filling dress fabric	Not treated	*W*	137	46	34	74	39	53	111	36	32
			do	*F*	144	55	38	80	47	59	119	32	27
			Treated	*W*	137	70	51	109	65	60	131	48	37
			do	*F*	128	74	58	109	76	70	138	45	33
4	.012	Spun-rayon dress fabric	Not treated	*W*	121	60	50	82	52	64	129	38	30
			do	*F*	103	46	45	63	38	60	114	34	30
			Treated	*W*	180	123	68	187	103	55	197	70	35
			do	*F*	110	65	59	76	53	70	119	52	44
5	.015	Spun-rayon dress fabric	Not treated	*W*	134	57	43	94	55	58	189	41	22
			do	*F*	108	63	58	67	41	61	144	44	31
			Treated	*W*	152	87	57	240	122	51	245	84	35
			do	*F*	128	81	63	109	72	66	159	73	46
6	.026	Cotton plaid	Not treated	*W*	157	59	38	106	47	44	178	41	23
			do	*F*	152	55	36	125	52	41	144	43	30
			Treated	*W*	180	80	44	193	88	45	218	60	28
			do	*F*	180	79	44	178	79	44	176	55	31
7	.005	Rayon dress fabric	Not treated	*W*	180	61	34	181	68	36	142	29	20
			do	*F*	140	45	32	85	35	41	96	28	29

7	.005	Rayon dress fabric	Not treated	W	180	61	34	181	68	38	142	29	20
			do	F	140	45	32	85	35	41	96	28	29
			Treated	W	164	106	65	171	104	61	197	67	34
			do	F	130	75	58	111	75	67	130	39	30
8	.016	Rayon suiting	Not treated	W	137	72	53	125	74	60	190	57	30
			do	F	140	72	51	179	100	56	210	70	33
			Treated	W	148	79	53	154	93	60	202	72	36
			do	F	148	84	57	241	138	57	234	85	40
9	.013	Rayon jacquard	Not treated	W	180	87	48	203	113	55	279	49	18
			do	F	128	93	73	69	46	66	134	56	42
			Treated	W	180	131	73	454	203	66	386	179	46
			do	F	180	128	71	174	69	55	215	69	32
10	.020	Spun-rayon suiting	Not treated	W	162	54	34	168	80	48	304	50	16
			do	F	144	49	33	225	107	48	321	79	25
			Treated	W	144	80	56	315	156	49	278	109	39
			do	F	162	92	57	408	203	50	398	136	34
11	.019	Linen suiting	Not treated	W	180	55	30	511	164	32	399	79	20
			do	F	180	47	33	414	122	29	325	64	20
			Treated	W	157	60	55	413	251	61	371	141	38
			do	F	152	59	47	231	144	62	268	105	39
12	.003	Bond typewriting paper	Not treated	A	180	19	11	1360	273	20	567	137	24
			do	B	180	26	15	800	179	22	513	113	22
13	.002	Cellophane[9]	Not treated	A	180	26	14	274	84	31	265	36	14
			do	B	180	29	16	211	95	45	262	25	11
14	.005	Cotton lining	Not treated	W	180	65	36	302	108	34	255	33	13
			do	F	180	57	32	259	91	25	214	29	14
15	.004	Rayon lining	Not treated	W	180	78	43	96	47	49	189	28	15
			do	F	180	81	45	74	42	57	111	26	23
16	.018	Worsted necktie lining	Not treated	W	180	123	68	286	221	77	323	208	64
			do	F	180	140	78	287	244	85	322	230	71
17	.012	Sheet-rubber dental dam	Not treated	----	61	55	90	78	61	79	138	125	91

Specimens 1 to 11, inclusive, are a representative group of cotton, rayon, and linen cloths ranging from light to heavy weight. Measurements were made on these cloths before and after crease-resistant finishing treatments. The results on these cloths indicate the effect of the crease-resistant treatment. Specimens 12 to 17 included paper, Cellophane, cotton, rayon, worsted, and rubber, which have not had crease-resistant treatments but which have crease resistances varying over a great range, as can be judged from the appearance of these specimens in figure 4. They also vary in stiffness over a great range. The measurements on them serve as a criterion of the relative crease resistance of the cloths before and after treatment. The data in table 1 serve as a basis in comparing the three test methods used.

The values reported for each test method in the columns numbered (1) are related to the stiffness of the cloths; those in columns numbered (2) are related to the energy of recovery; and those in columns numbered (3) are related to the resilience.

The data in table 1 are plotted in figure 5 to show the over-all effect of the crease-resistant treatments and for a comparison of the three test methods. The results for method 1 are plotted in the first column; those for method 2 are plotted in the second column; and those for method 3 are plotted in the last column. The values reported in the columns numbered (1) in table 1 are plotted in the top row of figure 5; those in columns numbered (2) are plotted in the second row; and those in columns numbered (3) are plotted in the bottom row. The values for the treated specimens are plotted as abscissas and those for the specimens before treatment are plotted as ordinates. The 45-degree diagonal is drawn in each plot to indicate whether or not the treatment increased or decreased the quantity plotted, a point falling below or above the diagonal indicating an increase or a decrease, respectively. A point which falls on the diagonal indicates that the treatment had no effect on the quantity plotted. The data for specimens 12 to 17, which have not had crease-resistant treatments, are plotted on the 45-degree diagonal for ease of comparison with the results for the specimens before and after the crease-resistant treatment.

With only a few exceptions, the treatments increased the energy required to deform the cloth specimens, that is, increased the stiffness of the cloths. This increase exceeded 100 percent for some of the cloths. Specimen 11, a linen fabric, is an exception.

Since the stiffness of the cloth is greatly affected by the crease-resistant treatments, the evaluation of this characteristic may be very important, at least for some of the uses for which these cloths may be intended. Method 1 does not give a critical measure of stiffness. Many of the specimens which are known to vary greatly in stiffness, in particular specimens 12 to 16, inclusive, are not differentiated by this method. This is a disadvantage of the method.

The energy of recovery of each fabric, including the linen specimen 11, was increased by the crease-resistant treatments. The increase ranged between 20 and 100 percent. The percentage increase in the energy of recovery of the treated to the untreated specimens of the same cloth is no doubt a measure of the improvement resulting from the treatment. The magnitude of the angle after creasing, method 1, which has been used as a criterion of the resistance to creasing, is not necessarily a measure of crease resistance. According to such a cri-

terion, specimen 17, which is a thin sheet of rubber and has practically no tendency to assume a permanent crease under a load, would be considered very poor compared to many of the other specimens which actually show a marked crease after the application of a load. For the same reason, the magnitude of the energy recovered in method 2 or 3 cannot be taken as a criterion of the resistance to creasing of woven fabrics.

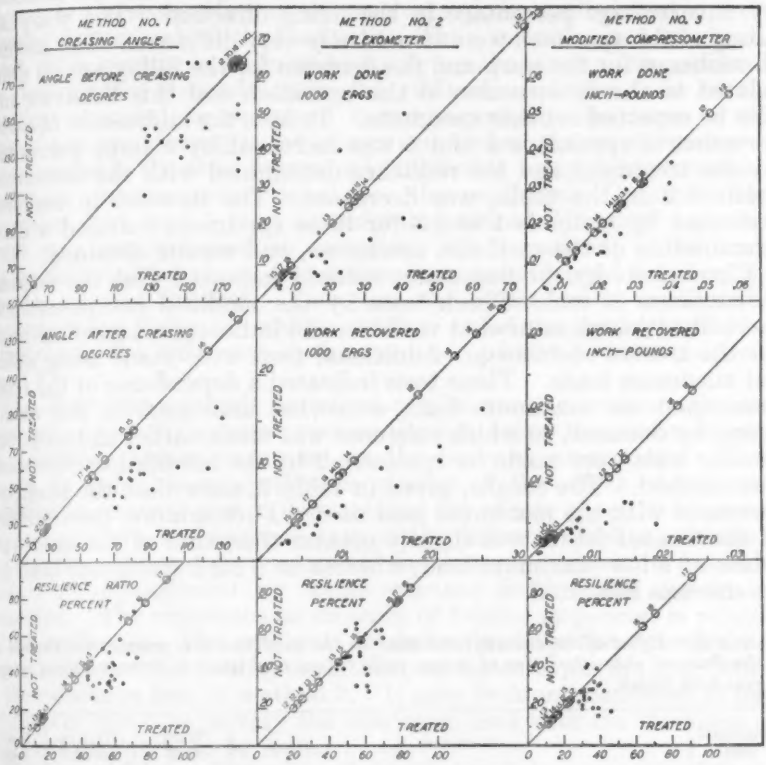

FIGURE 5.—*Effect of crease-resistant treatments on cloths as measured by three test methods.*

Solid points indicate specimens 1 to 11 before and after treatment. Open circles, specimens 12 to 17, are plotted on the 45-degree diagonal for ease of comparison and indicate the fabrics having crease resistances varying over a great range without a treatment.

The ratio of the energy of recovery to that expended, designated "resilience," is related to the resistance to creasing. For example, specimens 12, 13, and 14, having low crease resistances, were found to have low values of resilience, whereas specimens 16 and 17, having high crease resistances, were found to possess high values of resilience. Using the resilience of these specimens as a criterion, the specimens 1 to 11 as a group, are superior to specimens 12, 13, and 14, but inferior to 16 and 17. Although the resilience of nearly all of the fabrics, as determined by each of the three test methods, was increased by the crease-resistant finishing treatments, as a group these fabrics are inferior to fabrics made from fibers having high natural resilience. These conclusions were also borne out by visual observation of the appearance of these specimens after the various tests. The general

improvement in resilience imparted by the crease-resistant finishing treatments is well established, however, and still greater improvement may be expected to result from more extensive researches.

A closer examination of the results for resilience given in table 1 indicates that the finishing treatments did not increase the resilience of all fabrics. The value for specimen 9 tested in the filling direction is a notable exception. The stiffness of this specimen was increased by a very large percentage in the filling direction. The warp and filling of this specimen were structurally very different. The increase in resilience for the warp and the decrease for the filling are no doubt related to the construction of this specimen and this behavior may also be expected in other specimens. In fact, the stiffness in the warp direction of specimens 4 and 5 was increased by a large percentage by the treatment and the resilience determined with the flexometer, method 2 in the table, was decreased. The increase in resilience indicated by methods 1 and 3 for these specimens justified a closer examination of the methods, specimens, and results obtained.

Check tests by the flexometer method indicated that the decrease in resilience is real. Check tests by the modified compressometer method, although somewhat variable, still indicated a higher resilience for the treated specimens. Additional tests were made using different maximum loads. These tests indicated a dependence of the resilience upon the maximum load, somewhat analogous to the results found by Sommer, to which reference was made earlier in this paper. Similar tests were made for specimen 2 by the modified compressometer method. The results, given in table 2, show that the resilience increased with the maximum load used. Furthermore, the resilience of the treated fabric was slightly greater than that of the untreated fabric at a low maximum load, whereas at a high maximum load the reverse was indicated.

TABLE 2.—*Effect of maximum load used in the modified compressometer method on the flexural characteristics of cotton voile before and after treatment with a crease-resistant finish.*

Maximum load	Specimen	Work done	Work recovered	Resilience
lb		in.-lb	in.-lb	*Percent*
0.30	Not treated	32×10^{-4}	5×10^{-4}	16
	Treated	46	8	17
.40	Not treated	41	8	20
	Treated	66	15	23
.50	Not treated	47	14	30
	Treated	80	18	23
.60	Not treated	63	26	42
	Treated	100	32	32

These results show that the reversal in resilience between methods 2 and 3 may be attributed to the difference in their testing conditions. In methods 1 and 3 the specimens are compressed by a constant maximum load, regardless of the weight or thickness of the specimens. In method 2, however, the specimens are folded to a minimum angle of such magnitude that equal stresses are produced in the extreme

fibers of homogeneous isotropic specimens. Although fabrics cannot be considered as homogeneous isotropic specimens, the testing procedure in method 2 of folding the specimens to a minimum angle, which is determined from the thickness of the specimen, is more rational than applying a constant maximum load to all the specimens as in methods 1 and 3. For in deforming a specimen by a series of increasing loads, as in method 3, the total work expended on the specimen is equal to the summation of the products of the applied load and the distance through which the load acts. Thus, in testing two specimens which differ greatly in stiffness by applying the same maximum load, the deformation depends upon the stiffness, and the ratio of the energies expended or recovered is not necessarily the same as the ratio of the energies expended or recovered when these two specimens are deformed to the same degree, as in method 2, by applying a variable maximum torque proportional to the stiffness. Unfortunately, specimens 2, 4, and 5 were considerably wrinkled during shipment. Great care was exercised in sampling, but variations, which could not be detected by visual inspection, may have existed between the samples selected for test. Therefore, the variations in resilience by methods 2 and 3 for the specimens 2, 4, and 5 cannot be attributed definitely to the difference in the condition of test between methods 2 and 3.

The three test methods described can be used to evaluate the improvement given by crease-resistant finishes, using the measurements on the cloths before treatment as the basis of comparison. They should be valuable in systematic studies of the effect of different finishing treatments and in determining the effects of relative humidity, temperature, and other factors on the different finishes. Method 1, however, does not give a critical measure of stiffness, a property that is greatly affected by crease-resistant finishes and should be measured. The resistance to creasing of fabrics in general is related to the resilience. The resilience as determined by these methods is dependent upon the testing conditions, as for example the magnitude of the maximum load in method 3. It may be found necessary in test methods of this type to vary the maximum load with the thickness or weight of the fabric to be tested.

The user of fabrics, however, who probably judges crease resistance primarily by the changes in the appearance of the fabrics, is not concerned so much with the effects of finishing treatments on a particular fabric as with the resistance to creasing of different fabrics regardless of the treatment they may have received in the course of manufacture. Although the test methods described in this paper indicate whether or not an improvement in crease resistance results from a finishing treatment, they may not clearly indicate the relative merits of the fabrics of different compositions and constructions from the viewpoint of the user. For this there appears to be needed first a standard procedure for subjecting fabrics to creasing forces in a manner and under conditions that can be correlated with normal use of the fabrics, and second, a method for evaluating the changes in appearance the fabrics undergo in this treatment. Work on the development of an optical method of test for this purpose is being undertaken in the Textile Section of the National Bureau of Standards.

The author acknowledges his indebtedness to Mr. Kenneth Barnard of the Pacific Mills and chairman of the Committee on test methods for crease resistance and permanent finishes, of the American Association of Textile Chemists and Colorists, and to Dr. D. H. Powers, who is also a member of the committee, for suggestions and interest in this work. Grateful acknowledgment is also made to Röhm & Haas Co., Pacific Mills, and Tootal, Broadhurst, and Lee, Limited, for furnishing material for testing.

WASHINGTON, December 4, 1937.